Performance Evaluations of Sediment Barrier Practices and Unmanned Aircraft System Mapping Technologies

by

Jarrell Blake Whitman

A dissertation submitted to the Graduate Faculty of
Auburn University
in partial fulfillment of the
requirements for the Degree of
Doctor of Philosophy

Auburn, Alabama
December 15, 2018

Keywords: sediment barrier, stormwater management,
unmanned aircraft systems

Approved by

Wesley C. Zech, Chair, Professor of Civil Engineering
Wesley N. Donald, Research Fellow IV of Civil Engineering
Xing Fang, P.E., Professor of Civil Engineering
Mark Dougherty, P.E., Associate Professor of Biosystems Engineering

ABSTRACT

Sediment barriers are sediment control practices typically installed along the perimeter of construction sites that are intended to intercept, capture, and temporarily contain sheet to shallow concentrated flows prior to site discharge. In doing such, transported sediment is retained within the limits of the site, thus preventing polluted stormwater runoff from adversely affecting the surrounding environment. This dissertation explores improvements made in the design, selection, and application of sediment control technologies through full-scale performance testing of sediment barrier practices (e.g., silt fence, manufactured silt fence systems, sediment retention barriers, and manufactured sediment barrier products) and small-scale performance testing of geotextile fabrics (e.g., nonwoven and woven) used as the filtering component of silt fence installations.

Full-scale performance evaluations of various nonwoven, wire-backed silt fence installation designs suggested that an offset 24 in. (61.0 cm) fence with 1.25 lb./ft (1.9 kg/m) T-post spaced 5 ft (1.5 m) on-center resulted in the best overall improvement, retaining an average of 93% of sediment and deflecting only 0.18 ft (0.05 m) over the course of three 2-yr, 24-hr simulated storm events. Additionally, the implementation of a dewatering mechanism within a silt fence installation proved to be an effective means for controlled dewatering. Effluent flow rates calculated from the dewatering board installation were 6.2 times greater than flows calculated for installations without a dewatering board. Increased effluent flows reduced

dewatering time from +24 hours (w/o dewatering board) to 4 hours (w/ dewatering board). Water quality analyses indicated that the inclusion of the dewatering board had little to no effect on water turbidity.

Full-scale performance evaluations of innovative and manufactured sediment barrier practices indicated that a major failure mode was undermining. Performance based comparisons of sediment retention rates, maximum impoundment heights, effluent flow rates, and treatment efficiencies were determined for each practice. Longevity tests were conducted to evaluate how each of these parameters changed over multiple storm events. Overall performance evaluations indicated practices which achieve impoundment depths between 1 and 1.5 ft (0.3 and 0.46 m) achieved sediment capture rates of at least 90% and reduced impoundment surface turbidity up to 60% when compared to turbidity along the bottom of the impoundment.

Small-scale performance evaluations of geotextiles used in silt fence applications indicated that effluent flow rates observed during the 30-minute test period for nonwoven geotextiles were on average 43% lower than woven materials. Sediment retention evaluations indicated that on average nonwoven geotextiles (97% retention) outperformed woven geotextiles (91% retention). Water quality analyses suggested that the primary means for turbidity reduction was sedimentation during the 30-minute test periods (46% reduction) and geotextile filtration during the 90-minute dewatering periods (19% reduction).

Stormwater pollution prevention plans (SWPPP) are used to communicate erosion and sediment control (ESC) designs and installation instructions to construction personnel. Accurate topographic depictions are critical to insure proper functionality of ESC practices. Thus, an evaluation of unmanned aircraft system (UAS) mapping technologies used in the development of

triangular irregular network (TIN) surface models was completed. Vetical accuracy analyses indicated elevation differences between 9 TIN surface models and known ground surface points from a single test site were within the range of -0.62 ft (-0.19 m) and +0.72 ft (+0.22 m) for data collected at flight altitudes of 100 feet above ground level (AGL) and -0.65 ft (-0.20 m) and +1.57 ft (+0.48 m) for flight altitudes of 300 feet AGL.

ACKNOWLEDGEMENTS

I would like to extend my gratitude to Dr. Wesley C. Zech for his support, mentorship, and academic guidance throughout my time at Auburn. Additionally, I would like to thank Dr. Wesley Donald, Dr. Xing Fang, Dr. Mark Dougherty, Dr. Eve Brantley, and Dr. Jeffrey LaMondia for their time and guidance throughout this research effort. I would also like to thank the Alabama Department of Transportation, Auburn University Highway Research Center, and the National Center for Asphalt Technology for their support. This work would have not been possible without the assistants of Mr. Guy Savage and the numerous undergraduate research assistants who put countless hours into laboratory testing. I am most grateful to my family for their love, unending support, and sacrifices made throughout my endeavor.

TABLE OF CONTENTS

LIST OF FIGURES

LIST OF TABLES

LIST OF ABBREVIATIONS

AASHTO – American Association of State Highway and Transportation Officials

ADEM – Alabama Department of Environmental Management

AGL – Above Ground Level

ALDOT – Alabama Department of Transportation

AL HB – Alabama Handbook

ANOVA – Analysis of Variance

AOS – Apparent Opening Size

AU-ESCTF – Auburn University – Erosion and Sediment Control Testing Facility

BMP – Best Management Plan

CAD – Computer Aided Design

CGP – Construction General Permit

CN – Curve Number

CP – Check Point

DEM – Digital Elevation Model

DOT – Department of Transportation

DSM – Digital Surface Model

DTM – Digital Terrain Model

ESC – Erosion and Sediment Control

FAA – Federal Aviation Administration

GCP – Ground Control Point

GDOT – Georgia Department of Transportation

GNSS-RTK – Global Navigation Satellite System-Real Time Kinematic

GSD – Ground Site Distance

GSWCC – Georgia Soil and Water Conservation Commission

LiDAR – Light Detection and Ranging

MFPP – Multi Filament Polypropylene

HDPE – High Density Polyethylene

MD – Machine Direction

PAC – Project Advisory Committee

PVC – Polyvinyl Chloride

RMSE – Root Mean Square Error

SB – Sediment Barrier

SRB – Sediment Retention Barrier

SRSF – Stage Release Silt Fence

SWMP – Stormwater Management Plan

SWPPP – Stormwater Pollution Prevention Plan

TIN – Triangular Irregular Network

TLS – Terrestrial Laser Scanning

UAS – Unmanned Aircraft System

USDA – United States Department of Agriculture

USEPA – United States Environmental Protection Agency

XMD – Cross Machine Direction

LIST OF CONVERSIONS

1 ft = 0.3048 m

1 ft^2 = 0.0929 m^2

1 ft^3 = 0.0283 m^3 = 28.32 L = 7.481 gallon

1 inch = 2.54 cm

1 lb. = 0.4536 kg

1 lb./ft = 1.49 kg/m

1 $oz./yd^2$ = 33.9 g/m^2

1 acre = 0.4047 hectare

1 ft^3/s = 0.0283 m^3/s = 448.83 gallon/min = 1,699 L/min

CHAPTER ONE:
INTRODUCTION

1.1 BACKGROUND

Construction activities can create unstabilized areas near stormwater runoff conveyances and bodies of water. Runoff emanating from these disturbed areas takes the form of sheet, shallow concentrated, and concentrated flows. The result of these flows is soil loss and transport in the form of interrill, rill, and gully erosion. Sheet and shallow concentrated flows are either collected by diversions and conveyance channels, or by perimeter controls. If intercepted and collected by perimeter controls, these sediment control devices become the final treatment practice prior to discharge of stormwater beyond construction boundaries.

The United States Environmental Protection Agency (USEPA) construction general permit (CGP) requires one of the following three alternative scenarios for protecting adjacent water bodies beyond required erosion and sediment control (ESC) practices: (1) provide and maintain a 50 ft (15.2 m) undisturbed natural vegetative buffer, (2) provide and maintain an undisturbed natural buffer that is less than a 50 ft (15.2 m) buffer and is supplemented by ESC practices that achieve, in combination, the sediment load reduction equivalent to a 50 ft (15.2 m) undisturbed natural buffer, and (3) if no buffer can feasibly be maintained, ESC practices must be implemented to create an equivalent sediment removal efficiency of a 50 ft (15.2 m) natural buffer (*USEPA 2017*). The CGP further states that the buffer does not replace typical ESC practices

and that sediment controls are also required around the downslope perimeter of the site disturbance (*USEPA 2017*). The USEPA provides tables for determining sediment removal efficiencies of 50 ft (15.2 m) buffers, but leaves determining the amount of sediment removal efficiencies for the supplemental erosion and sediment control practices to the designer. This can be accomplished by using a number of available modeling programs or calculators. These modeling programs typically do not provide exact reductions for specific products, installation practices, or new practices that have not been included in the program database, thereby limiting feasible options for designers. Due to the lack of scientific data available within industry for determining performance expectations of various perimeter control practices, a need exists for conducting evaluations and quantifying performance capabilities of common perimeter control practices, as well as, innovative sediment retention devices emerging within industry.

1.2 PURPOSE OF EROSION & SEDIMENT CONTROLS

ESC practices [i.e., diversion swales, erosion control blankets, sediment basins, sediment barriers (SBs), etc.] are used to minimize erosion and sediment-related pollution. Controlling erosion and sediment transport on construction sites has been deemed a top priority for environmental agencies such as the USEPA and the Alabama Department of Environmental Management (ADEM). The most critical environmental problem facing the construction industry is the impairment of nearby water bodies caused from sediment-laden stormwater discharges off-site (*USDA 2006*). Sediment transport increases when erosion rates are accelerated by rainfall impacts on unprotected and unvegetated areas disturbed during earthwork activities. This problem can be compounded by soil compaction, which reduces infiltration, increases runoff volume, and increases flow velocities thereby increasing erosion potential. Untreated

stormwater discharged from construction sites can increase turbidity of nearby waterways causing degradation of water quality by preventing sunlight from penetrating the water, inhibiting aquatic plant growth, and adversely affecting the aquatic ecosystem (*USDA 2006*). Sedimentation in waterways and storm sewers can decreases flow capacity, increase flooding potential, stifle vegetative growth, and destroy fish spawning areas (*USDA 2006; Willet 1980*). Sediment particles can also transport other pollutants (i.e., hydrocarbons, phosphates, metals etc.) that originate from construction equipment and fertilizer used to establish vegetative cover, further increasing the importance for controlling sediment transport. Impacts of sediment-laden stormwater discharge and the need to implement preventative measures was recognized as a serious pollution problem by the U.S. Congress with the enactment of the Clean Water Act of 1972 and the Water Quality Act of 1987 (*U.S. Congress 1972; U.S. Congress 1987*). Thus, it is important to understand the effectiveness of ESC practices when it comes to intercepting, treating, and discharging construction site stormwater runoff.

1.3 RESEARCH OBJECTIVES

This research was divided into five main components associated with the design, evaluation, and improvement of SB practices.

The specific objectives of this research are as follows:

(1) Develop a full-scale testing methodology, protocol, and apparatus for evaluating SB practices that improve upon current industry testing standards;

(2) Identify installation deficiencies and provide structural improvements to achieve the most effective nonwoven, wire-backed silt fence installation configuration;

(3) Provide performance-based comparisons between selected innovative and manufactured SB practices;

(4) Identify the effectiveness of common geotextiles used as the filtration component of silt fence perimeter controls; and

(5) Assess the elevation accuracy of triangular irregular network (TIN) models commonly used in stormwater pollution prevention plan (SWPPP) development that are derived from unmanned aircraft systems (UAS) imagery.

The project was divided into the following tasks to satisfy the defined research objectives as follows:

(1) Identify, describe, evaluate, and critically assess pertinent literature on the state-of-the-practice regarding SBs used by state agencies located in the southeastern United States;

(2) Design and construct a full-scale SB testing apparatus at the Auburn University – Erosion and Sediment Control Testing Facility to conduct full-scale testing on SB practices;

(3) Develop an applicable methodology and testing protocol for performance-based evaluations of SBs based upon an Alabama 2-yr, 24-hr design storm and current ASTM testing methods and technology;

(4) Conduct a series of iterative full-scale experiments on selected nonwoven, wire-backed silt fence installations and analyze the resulting structural, hydraulic, sediment, and water quality data collected to establish the most effective installation design;

(5) Conduct full-scale experiments on innovative and manufactured SB practices and analyze the resulting structural, hydraulic, sediment, and water quality data collected to identify the stormwater treatment effectiveness of each practice;

(6) Conduct small-scale experiments on common geotextiles used in silt fence applications and analyze the resulting hydraulic, sediment, and water quality data collected to determine in-field performance capabilities of each geotextile;

(7) Generate multiple TIN models of a single site using UAS images gathered at various altitudes over multiple days and analyze their elevation variations to determine surface model elevation accuracy.

1.4 EXPECTED OUTCOMES

The expected outcomes of this study are to provide ALDOT and the ESC industry with the knowledge, resources, and educational outreach opportunities needed to maintain design proficiency to conform to evolving stormwater regulations. Scientifically backed results from this study enable new and improved guidelines for properly designing and installing SB practices based on quantifiable data. Additionally, results provide controlling agencies with a platform to guide and govern designers, inspectors, and contractors. This research will provide a comprehensive understanding and knowledge base on in-field performance capabilities and limitations of SB practices. Additional research efforts should emanate from this project allowing further opportunities for increasing knowledge on ESC practices implemented on construction projects.

1.5 ORGANIZATION OF DISSERTATION

This dissertation is divided into eight chapters that organize, illustrate, and describe the steps taken to meet the defined research objectives. Following this chapter, Chapter Two: *Sediment Barrier Literature Review,* provides an overview of common SB practices used within industry, current testing methodologies, and previous research studies performed to further develop the body of knowledge. Chapter Three: *Full-Scale Sediment Barrier Test Apparatus Design and Testing Methodology*, outlines the testing apparatus, experimental design, testing methods, and procedures developed for preparing and conducting full-scale SB experiments. Chapter Four: *Performance Evaluations of Silt Fence Installations*, details alternative silt fence installation strategies and results of performed experiments. This chapter includes data, observations, and analyses aimed to improve the functionality of the standard ALDOT silt fence installation. Results from this chapter have been published in the Transportation Research Record: Journal of the Transpotation Research Board (doi: 10.1177/0361198118758029). Chapter Five: *Performance Evaluations of Innovative and Manufactured Sediment Barrier Practices*, details design characteristics, installation guidelines, and experimental findings of each innovative and manufactured SB practice evaluated as part of this study. Results from this chapter have been submitted to the Transportation Research Record: Journal of the Transpotation Research Board for publication consideration. This manuscript is currently under its second review. Chapter Six: *Small-Scale Performance Evaluations of Geotextiles used in Silt Fence Applications*, outlines the design of a small-scale SB test apparatus and presents the efficiency of geotextiles used in perimeter control applications. Results from this chapter have been submitted to the Journal of Geotextiles and Geomembranes for publication consideration.

Chapter Seven: *Statistical Evaluation of Multiple TIN Surfaces Constructed from Unmanned Aircraft System Imagery,* is a case study on TIN model elevation variations resulting from altitude changes over multiple days of image acquisition. Chapter Eight: *Conclusions and Recommendation*, provides a summary of the tasks accomplished through this study and identifies areas in which further research can be conducted to advance this body of knowledge.

CHAPTER TWO:
SEDIMENT BARRIER LITERATURE REVIEW

2.1 DEFINITION AND PURPOSE OF SEDIMENT BARRIERS

Sediment barriers (SBs) are sediment control practices typically installed along the perimeter of construction sites that are intended to intercept, capture, and temporarily contain sheet to shallow concentrated flows prior to site discharge. SBs are categorized as sediment retention devices (SRDs) due to the removal of sediment primarily through sedimentation and, to a lesser degree, filtration (*ASTM Standard D7351 2013*, *Barrett et al. 1998*). SB practices primarily reduce eroded soil transport through impounding stormwater runoff upstream of the practice and allowing for suspended particles to settle. Sediment capture is also achieved when flow passes through the SB and particles become lodged within the porous medium; however, this method of sediment removal is commonly less effective. The filtration efficiency of SB material is based upon, and is limited by, the size of the pore passages often resulting in small soil particles passing through void spaces within the material medium (*Barrett et al. 1998*). In addition, the flow-through capacity of materials degrade over time as pores become clogged with sediment, thereby increasing impoundment potential (*Haan et al. 1994*).

2.2 COMMON SB PRACTICES

Various state manuals on ESC practices provide installation details and recommendation

on different perimeter control practices. Troxel (*2013*) conducted an online review of 49 Department of Transportation (DOT) best management practices (BMPs) manuals and compiled a summary of the different types of SB detailed within the documents. As shown in Figure 2.1, all of the reviewed DOT manuals specify silt fence as a viable perimeter control practice. In addition, DOTs commonly referenced straw or hay bales, earth berms or diversion ditches, wattles, and filter socks to be used as sediment barriers. Each of these practices have inherent limitations and perform differently due to differing dimensions, component materials, and installation methods.

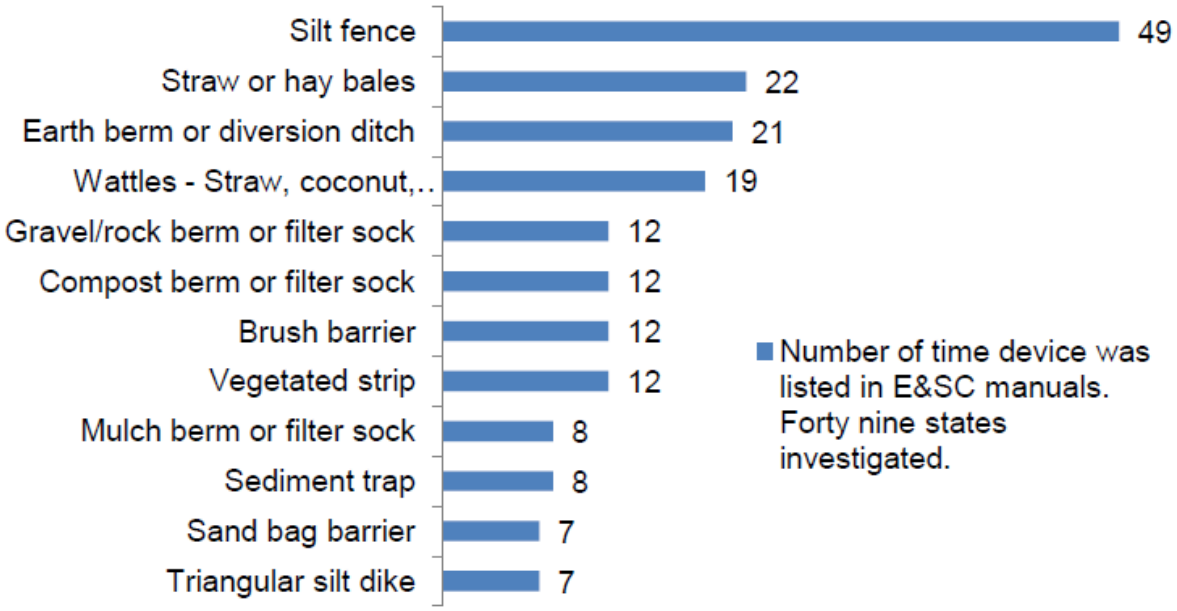

Figure 2.1. SB specified by U.S. states (*Troxel 2013*).

2.2.1 SILT FENCE

Silt fences essentially consist of a geotextile supported vertically by wooden or steel posts. Geotextiles used in silt fence applications generally fall into one of two categories, woven and nonwoven. Figure 2.2(a) and (b) illustrate typical silt fence installations observed along the perimeter of construction sites. Silt fences are available as pre-assembled systems ready for

installation or kits that require assembly during the installation process. In order for a silt fence to contain runoff, the geotextile must be secured into the soil by trenching or mechanical slicing and compacting. In areas of high runoff flows or velocities, geotextile reinforcement in the form of woven-wire or polypropylene netting may be required (*AL-SWCC 2014*, *GSWCC 2016*).

(a) nonwoven geotextile (b) woven geotextile

Figure 2.2. Silt fence installations.

2.2.2 Straw & Hay Bales

Straw bales are agricultural byproducts typically created from waste generated during wheat crop harvesting. On the other hand, hay bales are products created from agricultural grass that are typically used as livestock feed. The primary difference between the two is that straw bales only contain the stalk of the plant where hay contains the stalk and the seed heads of the plant. When used as a sediment control practices, bales are tightly abutted together in an attempt to intercept overland flows and reduce velocities to promote particle settlement. Properly installed bales should be buried, staked, and overlay one another. A common issue observed when implementing bales is rapid decay, which can cause bale clumps to wash into storm sever inlets resulting in clogging (*Harbor 1999*). Many state DOTs, as well as the U.S. Environmental Protection Agency (USEPA), do not recommend using bales for sediment control

because of their inferior sediment removal capabilities when compared to silt fences (*Troxel 2013*).

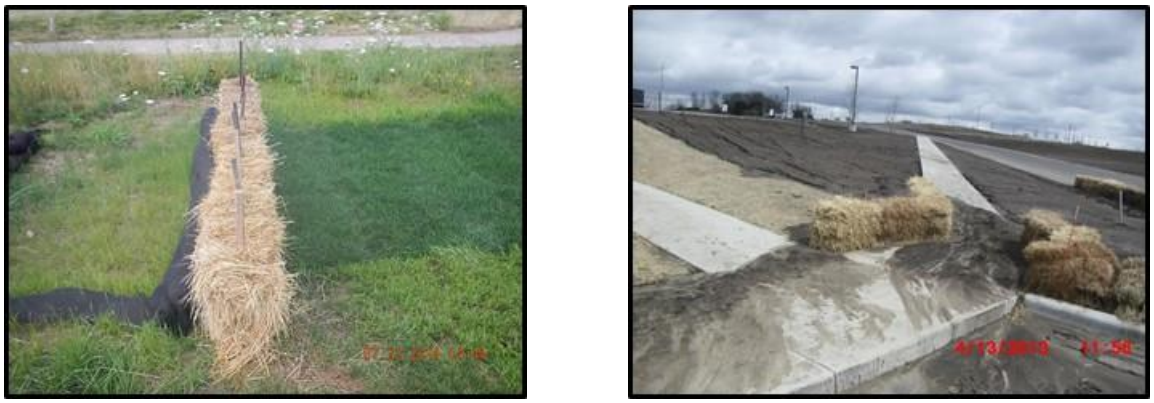

(a) typical installation (b) poor installation

Figure 2.3. Bale sediment control application. (*City of Madison 2018*)

2.2.3 DIVERSIONS

Diversions are water conveyance systems design to intercept and redirect overland flows to protect downslope areas from erosion, sediment accumulation, and flooding. Diversions are typically constructed by excavating a channel, compacting a soil ridge, or a combination of the two. If designed correctly, flow velocities within diversions are generally minimal and closely mimic natural flow patterns. Diversion can be constructed as temporary or permanently conveyances. In either case, adequate vegetation should be established as soon as possible in order to stabilize the channel. Flow exiting a diversion should be discharged to a stable outlet at non-erosive velocities.

(a) compacted diversion (*AL-SWCC 2014*)

(b) excavated diversion (*GSWCC 2016*)

Figure 2.4. Stormwater diversion systems.

2.2.4 TUBULAR SBS

Tubular SBs are manufactured ESC products that consist of an outer containment system (e.g., netting) that are filled with materials such as straw, excelsior, coir, compost, wood chips, synthetic fibers, or recycled rubber (*Donald et al. 2013*). Tubular SBs are typically available in diameters ranging from 8 to 20 in. (20 to 51 cm) and lengths between 10 to 40 ft (3 to 12 m). Installations of tubular SBs typically consist of trenching, staking, pinning, or a combination of these methods to secure the product in-place. These products are popular within the construction industry because they are easy to install and can be applied in various ESC scenarios (e.g., perimeter controls, inlet protection, ditch checks, etc.).

(a) straw wattle

(b) compost sock

Figure 2.5. Tubular sediment barriers.

2.2.5 BRUSH BARRIERS

Brush barriers are constructed from woody debris gathered during site clearing and grubbing operations by wind-rowing and compacting the material along the perimeter of the site. In certain scenarios, a geotextile fabric can be placed on the upstream face of the barrier to facilitate impoundment. Typically, brush barriers need to be constructed with a base width of at least 5 ft (1.52 m) but no wider than 10 ft (3.05 m). The height of the barrier should be between 3 and 5 ft (0.91 and 1.52 m) (*GSWCC 2016*). Brush barriers should only be used on sites that allow for barrier removal upon project completion without significantly damaging established permanent vegetation. Figure 2.6 illustrates a brush barrier installation detail.

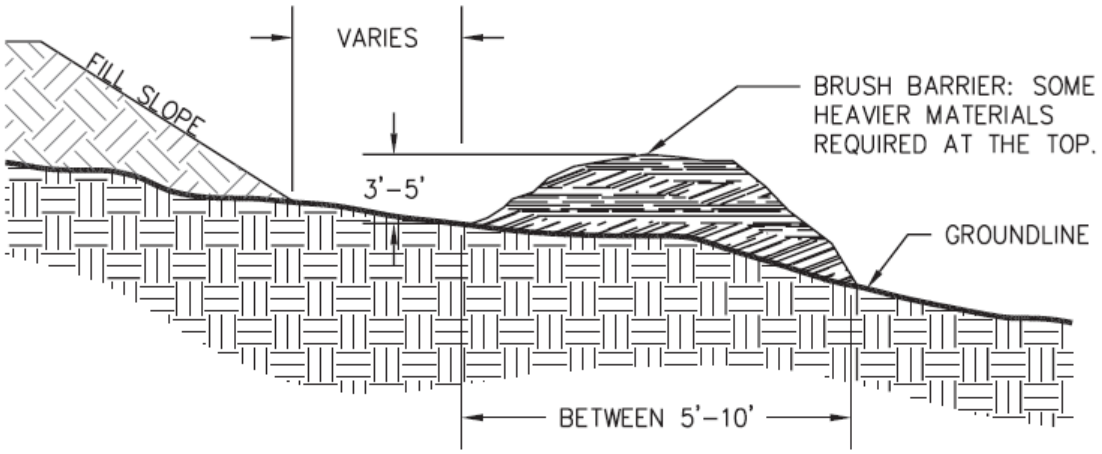

Figure 2.6. Brush barrier installation detail. (*GSWCC 2016*)

Each of these practices has inherent limitations (i.e., structural stability, porosity, impoundment capability, etc.) and performs differently due to differing dimensions, component materials, and installation methods.

2.3 SB IMPLEMENTATION

When used as a perimeter control, SBs should be installed prior to major clearing and grubbing actives and remain in place until final site stabilization occurs. Depending on the project

area, minor clearing activities may need to be completed in order to facilitate effective perimeter control installations. In such instances, soil disturbance should be limited to the width of the clearing mechanism and all debris removed should be windrowed upstream of the SB installation location to aid in sediment control and minimize potential SB damage during successive clearing activities. SB installation should immediately follow perimeter clearing activities and all perimeter controls should be installed prior to large-scale clearing and grubbing activities. This approach establishes clearing limits and prevents unnecessary land disturbance beyond the project area.

2.4 SB DESIGN CRITERIA

According to the USEPA (*2012*), most construction sites use silt fence, installed along the perimeter, as a SB. Since the use of silt fence as a perimeter control is so common, the USEPA and state environmental regulatory agencies have published criteria for the design and installation of this practice. However, limited design guidance exists for the application of other SBs. Design guidance that exists is typically based on rules-of-thumb or manufacturer installation recommendations, which can vary widely.

Though design criteria for silt fence are much more prevalent than other SBs, silt fence specifications are inconsistent across regulatory jurisdictions. Design and installation criteria for silt fence are critical to ensure effective performance in field applications. Factors to consider include the contributing drainage area, gradient (% slope), and slope length up-gradient from the practice. These design factors affect stormwater runoff volumes, flow rates, and corresponding sediment loads. Additional silt fence design specifications include minimum installed height, maximum post spacing, minimum trenching depth, geotextile material properties (i.e., flow

through, puncture resistance, tensile strength, etc.), and reinforcement. Table 2.1 shows a summary of the maximum design criteria used for determining appropriate contributing drainage area, slope gradient, and slope length for the proper application of silt fence as a perimeter control from the USEPA and ten southeastern states. The states presented in Table 2.1 were selected because each has a Revised Universal Soil Loss Equation (RUSLE) rainfall energy (*R)* value of 250 or greater. When compared to rest of the U.S., these states have the greatest potential for erosion due to higher *R* values. In addition, these states are also comprised of soils that are highly erodible, thus further signifying their need for effective sediment control practices (*Pitt et al. 2007*).

Table 2.1. Design Criteria for Silt Fence Sediment Barrier Applications (*Bugg et al. 2017*)

Agency	Criteria	Source(s)
USEPA	EPA-833-F-11-008 "rule of thumb": 10,000 ft^2 (929 m^2) of area per 100 ft (30.5 m) of silt fence or ≈ ¼ ac (0.10 ha) per 100 ft (30.5 m) of silt fence EPA-833-R-06-004 states ¼ ac (0.10 ha) per 100 ft (30.5 m) of silt fence	*USEPA 2012*; *USEPA 2007*
Alabama	¼ ac (0.10 ha) per 100 ft (30.5 m) unreinforced silt fence ½ ac (0.20 ha) per 100 ft (30.5 m) reinforced silt fence	*AL-SWCC 2014*
Arkansas	¼ ac (0.10 ha) per 100 ft (30.5 m) of silt fence Maximum upgrade slope perpendicular to the fence line ≤ 1*H*:1*V*	*AHTD 2009*
Florida	1 ac (0.41 ha) per 100 ft (30.5 m) of silt fence SB defined as two rows of silt fence, 4 to 6 ft (1.2 to 1.8 m) apart silt fence should allow a flow through rate of 70 gal/min/ft^2 (753.5 L/min/m^2)	*FDOT and FDEP 2013*
Georgia	¼ ac (0.10 ha) per 100 ft (30.5 m) of silt fence	*GSWCC 2016*
Louisiana	¼ ac (0.10 ha) per 100 ft (30.5 m) of silt fence Maximum slope gradient perpendicular to the fence is 2*H*:1*V*	*LA DOTD 2007*
Mississippi	¼ ac (0.10 ha) per 100 ft (30.5 m) unreinforced silt fence ½ ac (0.20 ha) per 100 ft (30.5 m) reinforced silt fence	*MDEQ 2011*
North Carolina	Drainage area should be ≤ ¼ ac (0.10 ha) per 100 ft (30.5 m) of silt fence Silt fence should be stable for the 10-yr peak design rainfall event runoff Depth of impounded water shall not exceed 1.5 ft (0.6 m) behind fence Silt fence shall not be used alone below graded slopes > 10 ft (3.0 m) in height	*NC-SCC, DNER, NC-AES 2013*
South Carolina	Max. slope length upslope of the silt fence is 100 ft (30.5 m) Max. slope gradient perpendicular to the fence is 2*H*:1*V* Sheet flow should not exceed 0.25 ft^3/s (7.08 L/s) Max. % slope and length: 3-5%, 100 ft (30.5 m) max.; 5-10%, 75 ft (22.9 m) max.; 10-20%, 50 ft (15.2 m) max.; 20-50%, 25 ft (7.6 m) max.	*SCDOT 2014*
Tennessee	The maximum drainage area for a continuous fence without backing (unreinforced) shall be ¼ ac (0.10 ha) per 100 ft (30.5 m) of fence length, up to a max. area of 2 ac (0.81 ha). The max. slope length upslope of the fence on the upslope side should be 110 ft (33.5 m) (as measured along the ground surface) The max. drainage area for a continuous silt fence with backing (reinforced) shall be 1 ac (0.41 ha) per 150 ft (45.7 m) of fence length. The slope length above the silt fence with backing should be no more than 300 ft (91.4 m)	*TNEC 2012*
Texas	¼ ac (0.10 ha) per 100 ft (30.5 m) of silt fence Steel posts required Woven wire backing required	*TxDOT 2012*

In addition to the design and installation criteria contained in Table 2.1, Alabama, Georgia, Mississippi, North Carolina, and Tennessee also use the design criteria summarized in Table 2.2, which stipulates the maximum slope length allowed upslope of the silt fence.

Table 2.2. Maximum Slope Length Criteria for Silt Fence (*Bugg et al. 2017*)

Criteria Reference	Slope	Max. Slope Length, ft (m)	Source
AL | GA | MS | NC | TN	<2%	100 (30.5)	*AL-SWWC 2014*; *GSWCC 2016*; *MDEQ 2011*; *NCSCC, DENR, NCAES 2013*; & *TNEC 2012*
	2 to 5%	75 (22.9)	
	5 to 10%	50 (15.2)	
	10 to 20%	25 (7.6)	
	>20%	15 (4.6)	

Another design and installation consideration is that silt fence perimeter control applications must be limited to areas experiencing only sheet flow. Richardson and Middlebrooks (*1991*) state that sheet flow is maintained for flow velocity less than 1.0 ft/s (0.3 m/s). They also state that this velocity can be maintained when the slope length is a maximum of 100 ft (30.5 m) and the slope steepness is less than 2.0%. The flow velocity of surface water is a function of slope gradient, slope length, and surface roughness. By making a conservative assumption that the ground is smooth, the flow velocity of surface water can be limited by reducing the allowable upstream slope length as the inclination of the slope increases. This principle is the basis for the various state design criteria shown in Table 2.2. Using this criteria, the drainage area is limited to less than ¼ ac (0.10 ha) per 100 ft (30.5 m) of silt fence. This is, therefore, the maximum contributory area allowed per 100 ft (30.5 m) of silt fence, provided the slope is less than 2.0%. The drainage area becomes much smaller as the slope gradient increases. Nevertheless, a drainage area of ¼ ac (0.10 ha) per 100 ft (30.5 m) of silt fence has become a widely adopted design criteria by the USEPA and most southeastern states regardless of the slope gradient and length upstream of the installed silt fence. Some states, (i.e., Alabama and Mississippi) allow up to ½ ac (0.20 ha) per 100 ft (30.5 m) of silt fence if it is reinforced with a wire backing.

2.5 EXISTING TESTING STANDARDS

Determining the performance capabilities and effectiveness of various SB practices is challenging when evaluating in-field installations on construction sites. The challenge lies within uncontrollable weather patterns and inconsistent site conditions, which makes field replicated experiments difficult to perform (*McLaughlin et al. 2001*). To achieve replicable performance evaluations of SB practices, several parameters need to be monitored during SB installation and throughout the experimental process.

Currently, ASTM recognizes two standards for testing SB performance: (1) ASTM D5141, *Standard Test Method for Determining Filtering Efficiency and Flow Rate of the Filtration Component for a Sediment Retention Device (SRD)* and (2) ASTM D7351, *Standard Test Method for Determination of Sediment Retention Device (SRD) Effectiveness in Sheet Flow Applications*.

2.5.1 ASTM D5141 TEST METHOD

ASTM D5141 describes the procedures for conducting small-scale flume experiments to determine sediment removal efficiency and flow through rates of geotextile fabrics. The development of this test method was a direct result of the work done by Wyant (*1981*), where he evaluated multiple nonwoven geotextile fabrics within a laboratory setting. As shown in Figure 2.7(a), the test apparatus consists of a 49.2 in. (125 cm) long by 33.5 in. (85 cm) wide flume with an 8% slope. Sediment-laden flow is introduced using a 19.8 gallon (75 L) container equipped with a mechanical stirrer to facilitate soil suspension. Wyant (*1981*) observed average sediment removal efficiencies of 92% for silty soil and 97% for sandy soil and flow rates ranging from 0.0004 to 3.5 $m^3/m^2/min$ (0.0013 to 11.5 $ft^3/ft^2/min$). Henry and Hunnewell (*1995*) also used this standard test method to evaluate nonwoven polyester and polypropylene geotextiles

using dredged sediment that mainly consisted of silt and clay. Results indicated sediment removal efficiencies of 45.5% and 72.8%, respectively, and flow rates ranging from 0.063 to 0.026 $m^3/m^2/min$ (0.206 to 0.085 $ft^3/ft^2/min$). Risse et al. (*2008*) performed sediment removal tests on the Silt-Saver® Belted Strand Retention Fence™ (BSRF) and the Georgia Soil and Water Conservation Commission Type-C silt fence using the standard test method, as well as a modified version. As shown in Figure 2.7(b), the modified version increase the slope of the flume from 8% to 58% to product increased hydraulic head on the geotextile. Results indicated that under standard sediment loading conditions the BSRF and Type-C silt fence reduced turbidity by 61% and 46%, respectively, and had effluent flow rates of 0.0149 and 0.0084 $m^3/m^2/min$ (0.0488 and 0.0276 $ft^3/ft^2/min$), respectively. As shown, this method allows for the evaluation of geotextile performance properties under sediment-laden flows. Nonetheless, it does not provide a means for evaluating installation improvement strategies, structural integrity, or full-scale performance capabilities.

(a) standard testing (*Sprague 2006*)

(b) modified testing (*Risse et al. 2008*)

Figure 2.7. ASTM D5141 test apparatus.

2.5.2 ASTM D7351 TEST METHOD

ASTM D7351 describes the procedure for conducting a full-scale experiment and quantifying a SRB's ability to retain soil eroded by sheet flow conditions. As shown in Figure 2.8, sediment-laden flow is generated by mixing 5,005 lb. (2,270 kg) of water and 300 lb. (136 kg) of sediment within a tank equipped with an internal agitator. The tank is positioned on a scale and the weight of the tank is monitored at regular intervals while discharging sediment-laden water at a constant flow rate of 176.8 lb./min (80 kg/min) during a 30-minute test. Test conditions are designed to simulate the peak 30 minutes of a 10-yr, 6-hr storm event in the mid-Atlantic region that produces 4 in. (10.1 cm) of rainfall. The flow and sediment load were determined by assuming 25% of the rainfall from the 10-yr, 6-hr storm occurs in the peak 30 minutes of the storm event and that 50% of the precipitation infiltrates into the ground. The associated sediment load resulting from erosion was calculated using the Modified Universal Soil Loss

Equation (MUSLE) (*Williams and Berndt 1977*), which allows the calculation of a storm specific quantity of sediment yield. The sediment-laden flow is directed down an impervious 3*H*:1*V* slope to the 20 ft (6 m) wide impervious test area where the SRD is installed. The flow passing through the SRD is collected and directed toward a collection tank where effluent weight is measured using a scale. Though the tanks provide a measurement of the amount of sediment-laden runoff discharged and collected, the flow rate for the 30-minute test is limited by the capacity of the tank. In addition, the scales only provide the total weight of sediment-laden water and does not have the ability to differentiate between the composition of sediment and water.

Figure 2.8. ASTM D7351 test apparatus. (*Troxel 2013*)

Troxel (*2013*) evaluated six sediment control devices using ASTM D7351: Type-A silt fence (polypropylene monofilament woven fabric with wooden stakes), Type-C silt fence (polypropylene monofilament heat bonded fabric with 4 in. [10 cm] square steel wire mesh and steel fence posts), mulch berm, straw bales, and two compost socks with diameters of 18 in. (45 cm) and 12 in. (30 cm). Results indicated TSS removal efficiencies of 98.4%, 97.6%, 95%, 91.2%, 92.9% and 88.2%, respectively. However, due to the upstream sampling point being located at the tank discharge, no determination could be made if the reduction was a result of sedimentation in the upstream impoundment generated by the device, or filtration.

A proposed modification to the standard test method incorporated a rainfall simulator that generates rainfall induced erosion on earth embankments while also being able to simulate different rainfall intensities. As shown in Figure 2.9, TRI/Environmental Inc. constructed a modified version of the proposed test standard published by Sprague and Sprague (*2012*). The plot is 8 ft (2.4 m) wide by 27 ft (8.2 m) long with a 33% slope. The apparatus uses rainfall simulation to mimic the natural erosion of embankments while also generating sediment-laden runoff. SB practices are installed along the toe of the slope to intercept and treat the runoff. A collection system is installed downstream of the installation to channel effluent into a collection tank. This method of SB evaluation introduces a series of variables that are difficult to control such as (1) sediment generation during the erosion process, (2) rainfall intensity, and (3) wind speed and direction. Additional factors that can impact the amount of soil eroded from the test bed during simulated rainfall events include moisture content, compaction, and surface roughness. Preparing the test bed so that moisture content and soil compaction remain

consistent over a large number of testing cycles requires considerable effort and is critical to producing meaningful test results that are repeatable and comparable.

Figure 2.9. Modified ASTM D7351 test apparatus. (*Sprague and Sprague 2012*)

2.5.3 TILTING TEST BED & RAINFALL SIMULATOR

The most widely recognized design criteria for unreinforced silt fence is ¼ ac (0.10 ha) drainage area per 100 ft (30.5 m) of installed fence, as illustrated in Table 2.1. Using this criterion, the length of the drainage area upstream of the installed fence is 108.9 ft (33.2 m). SB research performed to date (*Sprague and Sprague 2012*, *Dubinsky 2014*, *Gogo-Abite and Chopra 2013*) using rainfall simulators have only considered a fixed slope scenario, which limits the representative size and slope of the drainage area that can be used to subject a SB to field-like runoff conditions. Some researchers have overcome this slope limitation by using a tilting test bed for SB performance evaluations (*Dubinsky 2014*; *Gogo-Abite and Chopra 2013*). As shown in Figure 2.10, the developed test bed is 8 ft (2.4 m) wide by 30 ft (9.1 m) long and capable of

simulating a maximum slope of 2*H*:1*V*. Nonetheless, the maximum drainage basin area this test apparatus can simulate is limited to 240 ft^2 (22.3 m^2). This drainage area is much smaller than the criteria for maximum allowable area specified by many regulatory agencies. This inherent drainage area limitation of current rainfall simulator test apparatuses prevents realistic evaluations based on specified design criteria outlined within many ESC design manuals.

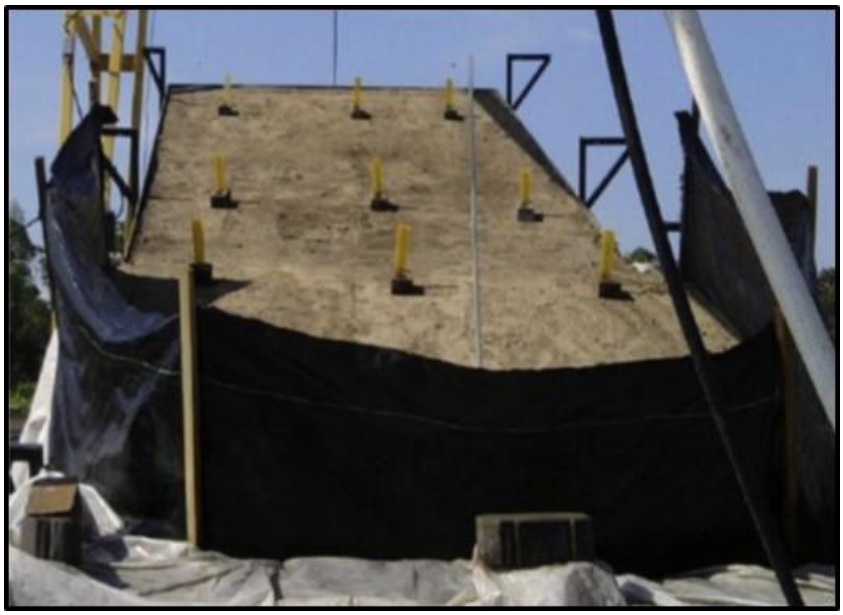

Figure 2.10. Tilting Test Bed & Rainfall Simulator (*Gogo-Abite and Chopra 2013*).

2.6 SB FAILURE MODES

Breaches in SBs are often common on construction sites; however, possible modifications to traditional installation practices may result in increased performance. Installation details and guidelines provided by government agencies and manufacturers are typically based on rules-of-thumb, field evaluations, and trial-and-error (*Bugg et al. 2017*). As shown in Figure 2.11, common failure modes observed when implementing these installation guidelines include unearthed fabric, undermining, scouring, overtopping, flow bypass, structural deflection, sag, detachment, and decomposition (*Stevens et al. 2004*). As a result, a need exists to evaluate current SB

practices and identify possible installation improvement strategies to minimize failure on future projects and gain an understanding of individual aspects affecting overall performance.

(a) unearthed fabric

(b) uncontrolled discharge

(c) flow bypass

(d) undermining

(e) sediment accumulation

(f) overtopping

Figure 2.11. Common SB failure modes.

2.7 SUMMARY

This chapter provides an overview of common SB practices used within the construction industry as well as common failure modes. Numerous SB design criteria were discussed from several regulatory agencies and ESC manuals. Current ASTM testing methods were outlined, as well as modified tests methods presented in published studies. Limitations of the testing methods were evaluated to develop a better understand of the needs throughout future testing efforts.

To date, little research has been published that scientifically analyses the effectiveness of SB practices and a number of issues can be found in the work that has be done (*Cooke et al. 2015*). As shown in the time line summary of the SB testing efforts (Table 2.3), most studies have focused on evaluating the performance of silt fence geotextiles (*Wyant 1981*, *Fisher and Jarrett 1984*, *Barrett et al. 1998,* *Britton et al. 2000*, *Robichaud et al. 2001*, *Keener et al. 2007*, *Risse et al. 2008*, *Troxel 2013*, *Gogo-Abite and Chopra 2013*). Because of this, there is a need for peer-reviewed research that broadens the understanding of erosion and sediment control technologies (*Kaufman 2000* and *Chapman et al. 2014*).

Table 2.3. Literature Review Summary

Study	Test Type	Materials Tested	Major Findings
Wyant 1981	small-scale flume	15 geotextiles	development of ASTM D5141
Fisher and Jarrett 1984	small-scale constant head filter fabric test apparatus	6 geotextiles	geotextiles retained all sands, removed various amounts of coarse silt, and were ineffective at removing silt-clay
Crebbin 1988	small-scale flume	4 geotextiles	geotextile apparent opening size (AOS) does not accurately predict filtering efficiency
Kouwen 1990	small-scale flume	geotextile fabrics	excessive ponding is due to geotextile blinding
Henry and Hunnewell 1995	ASTM D5141	nonwoven polyester and polypropylene geotextiles	Observed Flow Rates: 0.063 to 0.026 $m^3/m^{3/}min$ Observed Sediment Removal Rates: 45.5 to 72.8%
Barrett et al. 1998	small-scale flume and field observation	geotextile fabrics	Sediment removal is not achieved by filtration Lab Results: TSS removal rates of 68 to 90% Field Results: Little to no improvement in turbidity
Britton et al. 2000	small-scale flume	tight and open weave geotextiles	increasing impoundment volume improves sediment removal
Robichaud et al. 2001	full-scale	silt fence	observed sediment removal rates of 93% after one year and 92% after two years
Keener et al. 2007	small-scale flume	silt fence and Siltsoxx™	Siltsoxx's are less likely to overtop than silt fences
Risse et al. 2008	ASTM D5141 and Modified ASTM D5141 [conducted at UGA]	nonwoven BSRF and GDOT type-c	Turbidity Reduction: BSRF = 58 – 82% GDOT type-c= 25 – 58% each had similar flow rates
Troxel 2013	ASTM D7351	GDOT type-a, GDOT type-c, mulch berms, compost sock, straw bales	TSS Removal Efficiency: 98.4, 97.6, 95.0, 92.9, and 91.2%, respectively. Turbidity Removal Efficiency: 92.8, 92.3, 73.8, 64.9, and 49.2%, respectively.
Gogo-Abite and Chopra 2013	full-scale tilting test bed [conducted at UCF]	nonwoven BSRF and woven monofilament	Turbidity Reduction: nonwoven: 52% woven: 14% Sediment Removal: nonwoven: 56% woven: 23%
Chapman et al. 2014	created a weighted % efficiency by analyzing literature	silt fence and filter socks	Sediment Removal Efficiency: silt fence = 80.22% filter sock = 56.94%

CHAPTER THREE:
FULL-SCALE SEDIMENT BARRIER TEST APPARATUS DESIGN AND TESTING METHODOLOGY

3.1 INTRODUCTION

This chapter describes the sediment barrier (SB) test apparatus design, testing methodology, and data collection process developed for the large-scale testing of SBs. The testing apparatus and methodology developed in this study are based on current industry testing methods, as well as an in-depth literature review on SB performance evaluations. The apparatus was constructed to mimic typical grade conditions upstream of SB installations on Alabama Department of Transportation (ALDOT) projects. It also provides means for introducing accurate flow rates and sediment loads associated with a 2-yr, 24-hr design storm for the state of Alabama. The methodology aims to identify and quantify performance characteristics of SB practices such that comparisons between various practices can be conducted. Additionally, the methodology allows installation improvement strategies to be tested under identical loading conditions, which provides a means for assessing slight changes in installation techniques and material properties.

3.2 SEDIMENT BARRIER TEST APPARATUS DESIGN

Based on information gathered from literature and testing needs of ALDOT, a SB performance evaluation strategy was developed and an apparatus was designed and constructed at the Auburn University – Erosion and Sediment Control Testing Facility (AU-ESCTF).

Performance evaluation of SBs are based on structural integrity, sediment retention, hydrodynamics, water quality properties, and statistical analyses. A schematic design of the test apparatus is shown in Figure 3.1 and consists of the following features: (1) water and sediment introduction pad, (2) concrete curbing, (3) impervious *3H*:1*V* slope, (4) diversion vanes, (5) earthen test area, (6) removable steel access doors, and (7) catch basin.

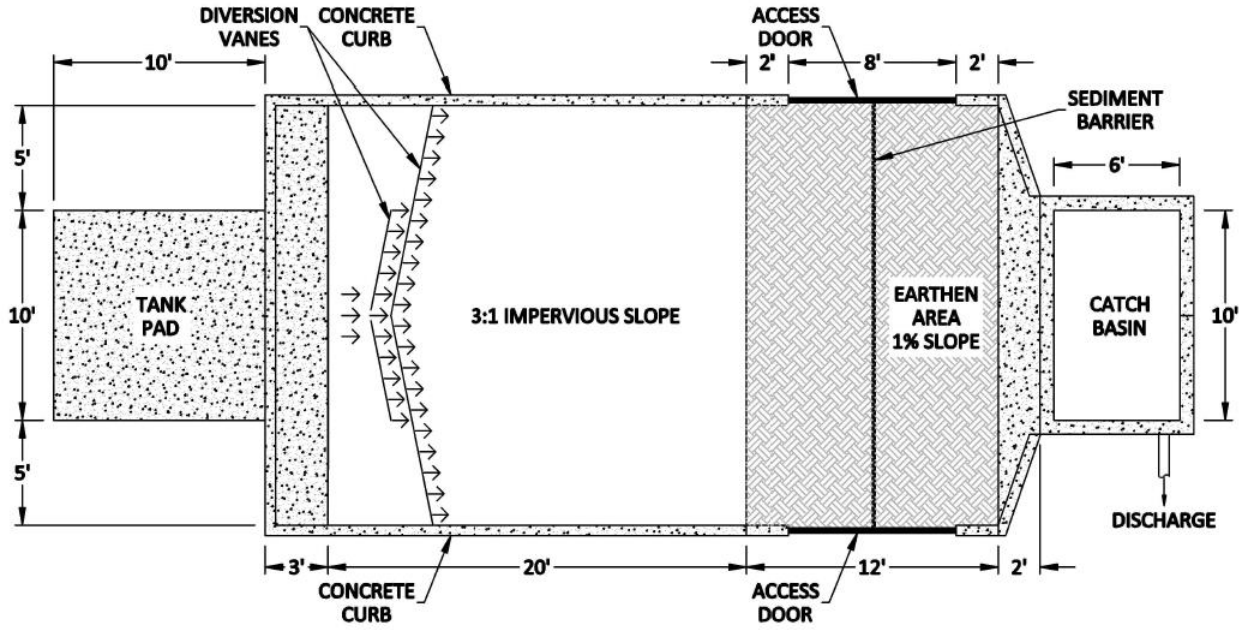

(a) plan view

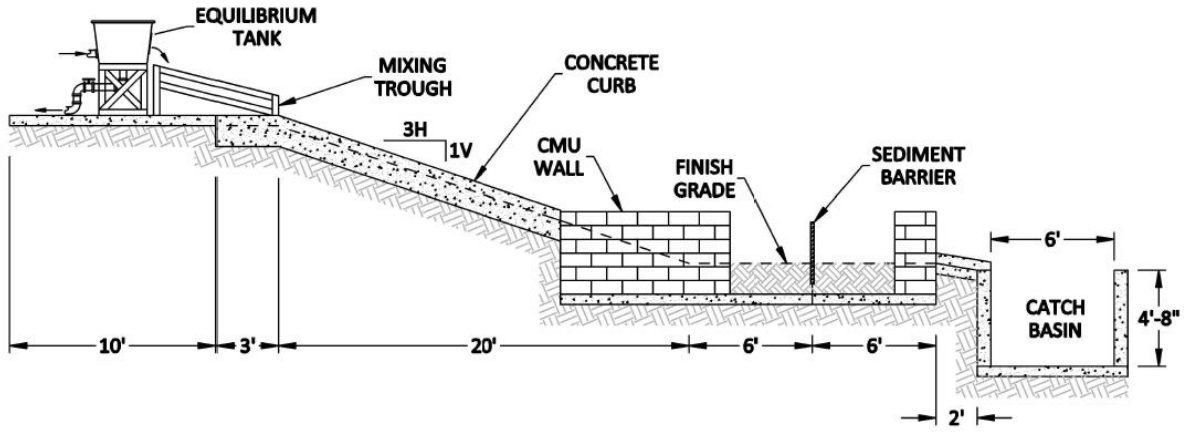

(b) profile view

Figure 3.1. SB test apparatus.

3.3 WATER AND SEDIMENT INTRODUCTION SYSTEM

Simulated flow is introduced to the system with a 3 in. (7.62 cm) trash pump that draws water from a supply pond. Water is pumped into a 300 gallon (1,135 L) water equilibrium tank [Figure 3.2(a)] that uses a series of valves and orifices to control flow over a calibrated weir prior to entering a mixing trough. The calibrated weir is monitored with a pressure tube that indicates flow rate across the weir. Adjustments to weir flow rates are accomplished via water tank discharge lines fitted with gate valves. The weir discharges into a mixing trough where sediment is introduced at a controlled rate and mixed with highly turbulent flowing water [Figure 3.2(b)].

Sediment introduction is accomplished using a steel hopper equipped with a hydraulic driven conveyor chain that allows sediment to be metered at a constant rate of 37.6 lb./min (16.9 kg/min) into the mixing trough. The conveyor chain is calibrated to assure the desired sediment introduction rate is achieved. After mixing has occurred, the sediment-laden water enters the top of the 3*H*:1*V* impervious slope of the test apparatus. The concentrated flow exiting the bottom of the mixing trough is converted to sheet flow using slotted diversion vanes mounted to the impervious slope.

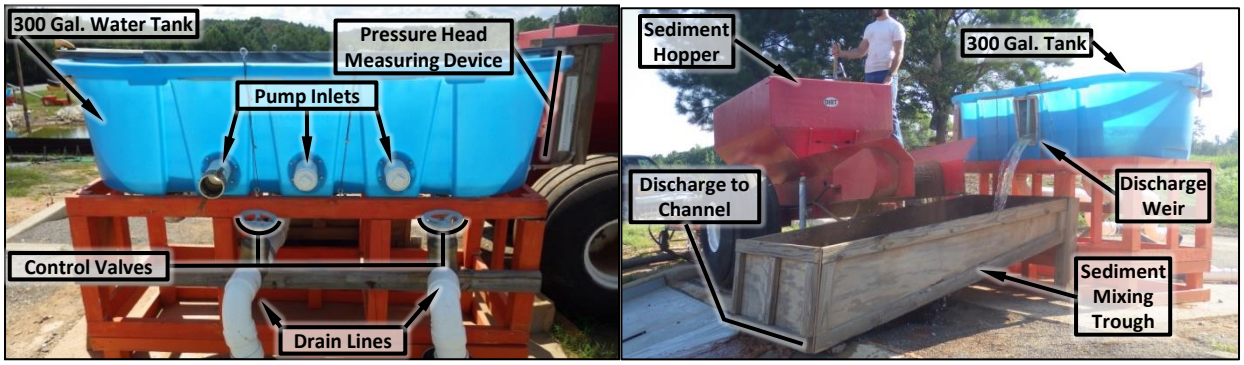

(a) water equilibrium tank (b) water/sediment introduction

Figure 3.2. Water/sediment introduction system.

3.4 TEST SLOPE

The test slope [Figure 3.3(a)] that conveys flow to the test area is 20 ft (6.1 m) wide and has a gradient of 3*H*:1*V*. This width allows field-like installations of SBs as found on construction site. This width also allows test scalability to simulate the design criteria for drainage areas of ¼ to ½ ac (0.10 to 0.20 ha) per 100 ft (30.5 m) of installed non-reinforced or wire reinforced SBs. The impervious slope is constructed of a 14 gage (2.0 mm) galvanized sheet metal lining and is removable. This lining allows the introduction of a controlled, consistent amount of water and sediment flow across the width of the test apparatus. The slope is bordered by an 8 in. (2.03 cm) tall concrete curb. Slotted diversion vanes are installed at the top of the slope to spread the sediment-laden flow evenly across the entire width of the test apparatus, creating sheet flow conditions. The upstream diversion vane has 1.0 in. (2.5 cm) wide, 2.0 in. (5.1 cm) tall openings cut 12 in. (30.5 cm) on center and extends 5 ft (1.5 m) on either side of the centerline of the impervious slope. The downstream diversion vane has 1.0 in. (2.5 cm) wide, 2.0 in. (5.1 cm) tall openings cut 6.0 in. (15.2 cm) on-center and extends across the entire width of the impervious slope. The combination of the slope length, gradient, and the diversion vanes ensure consistent delivery of sediment-laden sheet flow across the slope to the test area.

3.5 EARTHEN TEST AREA

The earthen test area is 20 ft (6.1 m) wide, perpendicular to the flow and 12 ft (3.7 m) long longitudinally, in the direction of flow. The area is bordered by a 4.0 ft (1.2 m) tall concrete filled concrete masonry unit (CMU) walls. The width of the test area allows for the installation of a representative section of a SBs including hardware and reinforcement (i.e. posts, stakes, wire reinforcement, etc.). CMU wall height is sufficient in that common SBs overtop due to upstream

impoundment prior to an impoundment depth equal to wall height. The earthen test area can accommodate the installation of a single SB or a series of SBs. The test area is equipped with water-tight, steel access doors that are 8 ft (2.4 m) wide [Figure 3.3(b)] that can be removed to accommodate tractor-pulled silt fence slicing machines, as well as other SBs requiring additional installations lengths.

(a) impervious slope and test area (b) removable access door

Figure 3.3. Test apparatus features.

3.6 CATCH BASIN

Flow passing a SB is discharged into a catch basin that is 10 ft (3.0 m) wide by 6 ft (1.8 m) long by 4.67 ft (1.5 m) deep, downstream of the test area. Water depth measurements within the basin are recorded throughout testing. The collection tank is fitted with a discharge pipe and inline valve, allowing controlled discharge of flow from the basin.

3.7 EARTHEN SOIL PREPARATION

Prior to testing, the earthen portion of the test area is prepared using standardized earthwork preparation, compaction, and monitoring practices to ensure repeatability. Soil is added to the earthen test area and tilled using a rear tined tiller to produce a homogenous mixture with in-place soil [Figure 3.4(a)]. The test area is graded on a 1% slope in the direction of flow and is level perpendicular to the direction of flow. Final grading is achieved using an

aluminum screed [Figure 3.4(b)] supported by wooden depth gages [Figure 3.4(c)] on either end to account for soil compaction. Final compaction is accomplished using an upright jumping-jack with a compaction plate of 14 by 11.5 in. (35.6 by 29.2 cm), blow count of 600 blows/min., and compaction force of 2,700 lb. (1,225 kg) [Figure 3.4(d)]. Once compaction is complete, soil density is determined using ASTM D3937 *Standard Test Method for Density of Soil in Place by the Drive-Cylinder Method* [Figure 3.4(e)]. For each installation, density samples are collected randomly within the earthen test area and weighted [Figure 3.4(f)]. Once weights are recorded, representative samples are collected from within each drive cylinder and processed in accordance with ASTM D2216 *Standard Test Method for Laboratory Determination of Water (Moisture) Content of Soil and Rock by Mass*. Once the desired density is obtained, the SB practices is installed and tested

(a) rear tined tiller

(b) aluminum screed

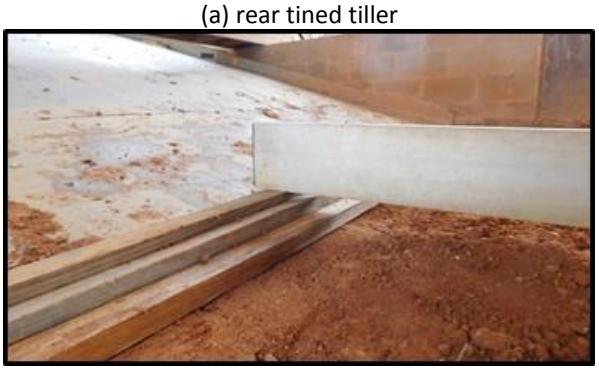

(c) wooden depth gages

(d) jumping jack compaction plate

(e) obtaining density sample

(f) weighting density sample

Figure 3.4. Earthen soil preparation.

3.7.1 SOIL PARAMETERS

Soil used throughout testing was acquired from a local source in Opelika, AL. Stockpiled soil was sieved through a 0.5 in (1.3 cm) mechanical sieve to remove large aggregate and organic material before use. A particle size distribution analysis and compaction test was conducted to characterize the soil properties. The average particle size distribution of four sieve analysis and two hydrometer analysis is shown in Figure 3.5. Based on the USDA soil texture triangle, the stockpiled soil corresponds to a sandy loam.

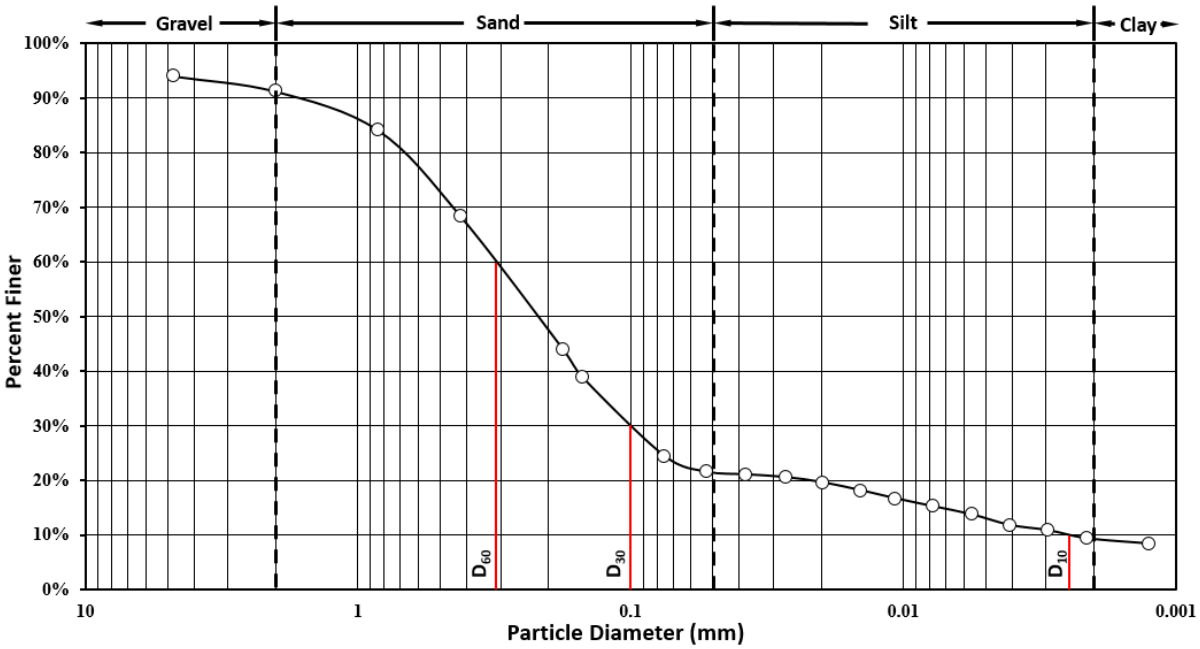

Figure 3.5. Particle size distribution for stockpile soil.

The soil was also analyzed for maximum achievable density. Based on the results of ASTM D698 *Standard Test Method for Laboratory Compaction Characteristics of Soil Using Standard Effort*, the maximum dry unit weight was determined to be 113.1 lb./ft^3 (1811 kg/m^3) with an optimum moisture content (OMC) of 15.0%. The developed proctor curve is shown in Figure 3.6. The acceptable dry density range selected for this research study was 95% of maximum, which corresponds to a minimum dry unit weight of 107.5 lb./ft^3 (1722 kg/m^3) with a moisture content ranging between 11.5 and 18.0%.

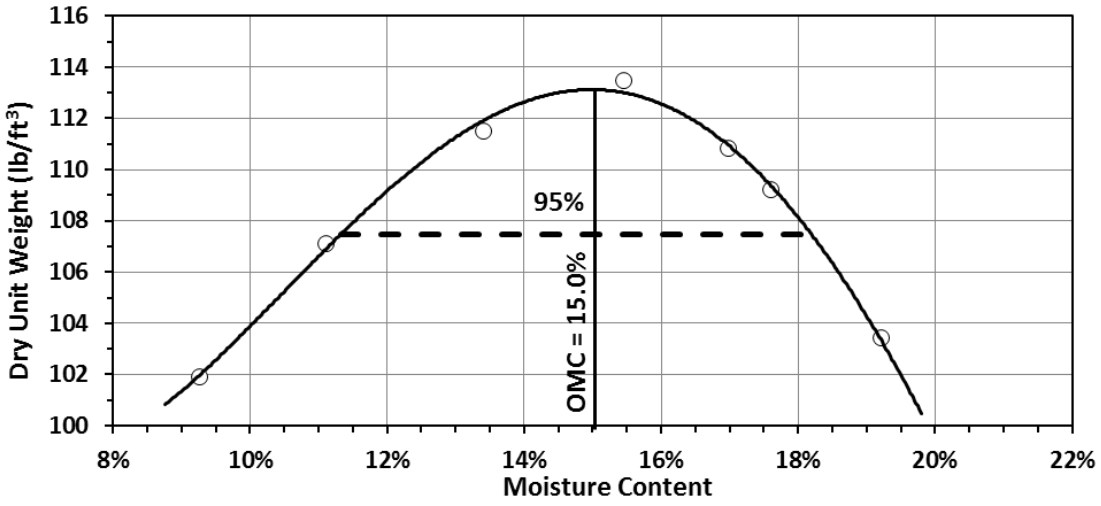

Figure 3.6. Compaction curve for SB test soil.

3.8 TESTING METHODOLOGY

To develop a testing methodology that replicates flow and sediment transport conditions similar to field-like conditions, emphasis was applied in determining a representative flow rate and sediment introduction rate used throughout testing.

3.8.1 THEORETICAL FLOW INTRODUCTION RATE

Test flow rate was determined based on the current design requirement for the State of Alabama that states SBs are to contain eroded sediment onsite that result from a 2-yr, 24-hr rainfall event (*ADEM 2016*). The design criteria applicable to silt fence for the State of Alabama (*AL-SWCC 2014*) are summarized below:

- The drainage area shall not exceed ¼ ac (0.10 ha) or ½ ac (0.20 ha) per 100 ft (30.5 m) of non-reinforced or wire reinforced silt fence, respectively
- The maximum slope length above the fence for slopes greater than 20% is 15 ft (4.6 m).

ALDOT requires that silt fence, reinforced with 14 gauge (2.0 mm) steel wire mesh, be installed on each construction project (*ALDOT 2016*). Thus, ALDOT design criterion for reinforced

silt fence was used to design the initial experimental protocol. The maximum slope length of the drainage area up-gradient of the silt fence based on the design criterion was calculated to be 217.9 ft (66.4 m). The maximum allowable drainage area of ½ ac (0.20 ha) per 100 ft (30.5 m) of wire reinforced silt fence was scaled down to an equivalent for the 20 ft (6.1 m) width of the test apparatus resulting in a drainage area of 0.10 ac (0.04 ha). The profile of the theoretical basin used to calculate test flow rate and sediment load for the initial SB testing protocol is shown in Figure 3.7. A 3*H*:1*V* slope directly up-gradient of the SB was selected as it is representative of typical road embankments and cut/fill areas where earthwork is required on construction sites. The remainder of the slope was assumed to be 5% as this is considered the worst case scenario while still maintaining sheet flow conditions up-gradient of the 3*H*:1*V* slope.

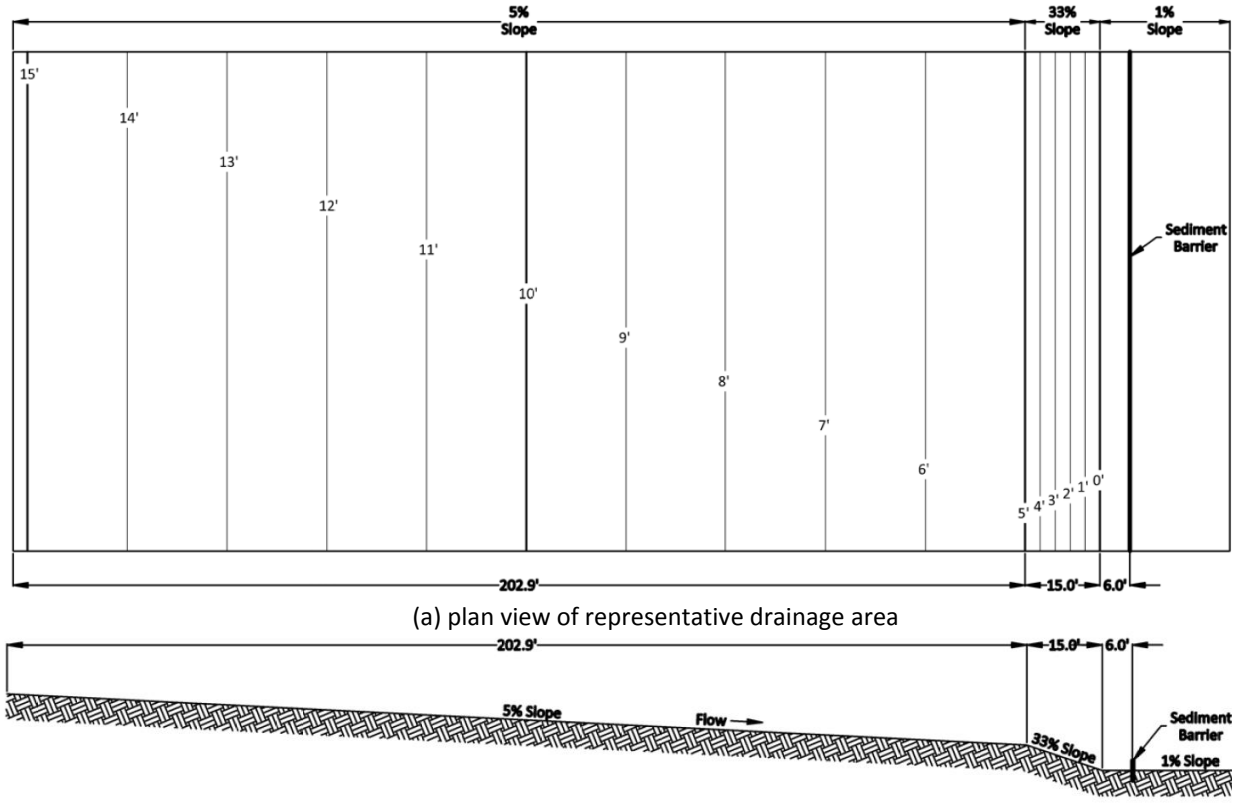

(a) plan view of representative drainage area

(b) profile of representative drainage area

Figure 3.7. Plan and profile of representative drainage area.

The flow rate for testing was calculated using Bentley® PondPack™ for the average 2-yr, 24-hr rainfall event for Alabama, which has an average precipitation depth of 4.43 in. (11.7 cm). The curve number (*CN*) used in the calculations was 88.5, which is the average *CN* for newly graded areas for Alabama based upon GIS analysis (*Perez et al. 2015*). The time of concentration for a disturbed area 20 ft (6.1 m) wide with a flow length of 217.9 ft (66.1 m) was estimated to be 5 minutes. Based on this information, the peak 30 minutes average flow rate for a 2-yr, 24-hr design rainfall event was calculated to be 0.20 ft^3/s (0.006 m^3/s), as shown in Figure 3.8.

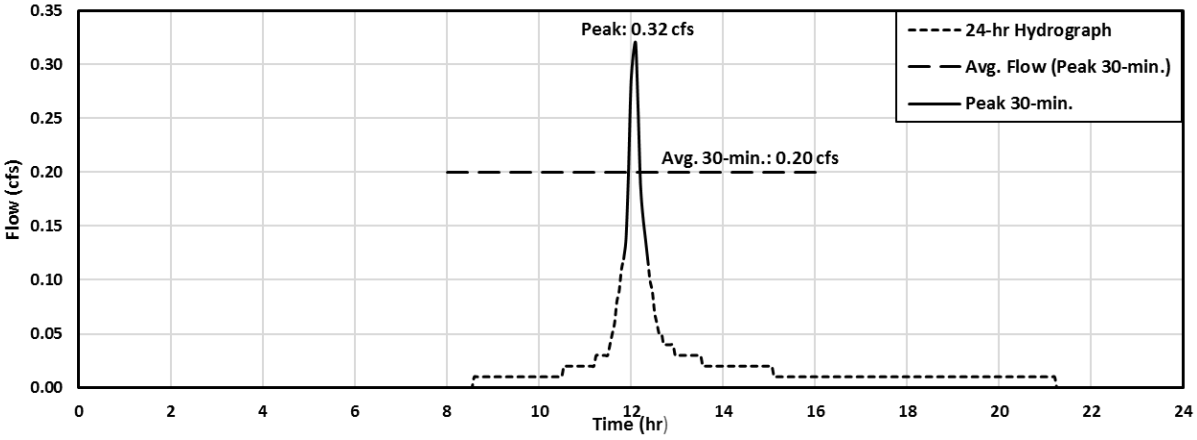

Figure 3.8. Hydrograph for 0.10 acre (0.04 ha) representative drainage area.

Essentially, flow will be introduced at a rate of 0.20 ft^3/s (0.006 m^3/s) for 30 minutes during SB testing. A summary of the theoretical areas, flow rates, and volumes for SB testing is shown in Table 3.1.

Table 3.1. Summary of Theoretical Flow Values for SB Testing

Representative Drainage Area ac (ha)	Scaled-Down Drainage Area ac (ha)	Peak Flow ft^3/s (m^3/s)	Avg. Flow for 30 Min Peak ft^3/s (m^3/s)	Total Vol. 30 Min Test ft^3 (m^3)	Total Vol. 30 Min Test Gal (L)
0.50 (0.20)	0.10 (0.04)	0.32 (0.01)	0.20 (0.0062)	360 (10.2)	2,693 (10194.1)

Note: Average 2-year, 24-hour storm for Alabama = 4.43 inches. NRCS Type III rainfall distribution. Average CN = 88.5 for Alabama; 1 ac = 0.4 ha; 1 ft^3/s = 0.028 m^3/s; 1 ft^3 = 0.028 m^3; 1 gal = 3.79 L

3.8.2 THEORETICAL SEDIMENT INTRODUCTION RATE

The quantity of sediment required for SB testing was calculated using the modified universal soil loss equation (MUSLE). The equations determines total sediment yield resulting from specific storm runoff volumes and peak flow rates. The use of runoff variables rather than erosivity enables the MUSLE to estimate sediment yields for individual rainfall events. The empirical version of the MUSLE equation is shown in Equation 3.1 (*Williams and Berndt 1977*):

$$S = 11.8(Qq_p)^{0.56}*K*LS*C*P \quad \text{(Eq. 3.1)}$$

Where:

S = sediment yield from an individual storm (metric ton)

Q = volume of runoff (m^3)

q_p = peak flow (m^3/s)

K = erodibility factor

LS= length-slope factor

C = cover management factor

P = erosion practice factor

Based upon flow calculations conducted for the state of Alabama, the MUSLE was applied to the peak 30 minutes of the design 2-yr, 24-hr rainfall event, which produces 360 ft^3 (10.2 m^3) of runoff with a peak flow (q_p) of 0.32 ft^3/s (0.006 m^3/s). From Pitt et al. (*2007*), a *K* factor of 0.15 for a *loamy sand, loamy fine sand, sandy loam, loamy, silty loam* was used. To account for the geography of the drainage area, an *LS* factor of 1.04 was used for a 15 ft (4.6 m) slope length at a 33% grade and a 202.8 ft (61.8 m) slope length at a 5% grade. *C* and *P* factors of 1.0 were

assumed for bare ground, no cover, and no conservation practices (e.g., contouring, strip-cropping, terracing, etc.) upstream of the installed SB. The total resulting sediment load for a 30-minute test was calculated to be 1,127.8 lb. (511.6 kg) of soil. Dividing this soil weight by 30-minutes, a sediment introduction rate of 37.6 lb./min (17.1 kg/min) was calculated. Based upon this rate, the sediment introduction concentration was calculated to be 3.1 lb./ft^3 (50,000 mg/L) as flow enters the testing apparatus. Table 3.2 summarizes the MUSLE values used for calculating this sediment yield.

Table 3.2. Summary of Theoretical Sediment Yield for SB Testing

Drainage Area (ac)	Q ft^3 (m^3)	q_p ft^3/s (m^3/s)	K	LS	C	P	S (Metric Tons)	S (U.S. Tons)	S (lb.)
0.10	360 (10.2)	0.32 (0.009)	0.15	1.04	1	1	0.51	0.56	1127.8

Note: MUSLE equation was used to calculate sediment expected resulting from the average 2-year, 24-hour storm for Alabama for 0.10 acres; 1 ft^3/s = 0.028 m^3/s; 1 Metric Ton = 1.10 U.S. Ton = 2,204.6 lb.

3.9 TESTING REGIME

A series of full-scale experiments introducing sediment-laden flow at a constant rate for 30 minutes were conducted to evaluate the performance of each SB tested. Three performance evaluations (i.e., I1, I2, and I3) were performed on each SB practice. One performance evaluation (i.e., I1) consists of installing a SB practice and run three iterative tests (i.e., P1, P2, and P3) on the installation. This allows performance data to be collected for new SB installations, as well as installations that have been subjected to sediment laden-flows. Using the data collected from each of these tests, performance degradation over time can be analyzed. In total, nine tests were conducted on each SB practices. The performance based testing regime that outlines the SB testing process is shown in Figure 3.9.

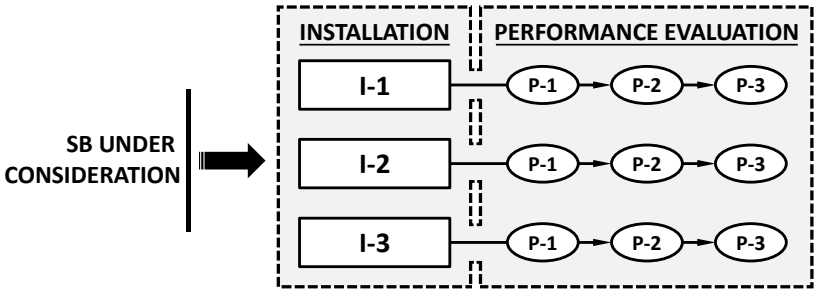

Notes: 1. Three installations (I1, I2, and I3) are performed to obtain replicate data sets and show reproducibility.

2. Three performance tests (P1, P2, and P3) are conducted sequentially per installation to evaluate the performance and longevity of a SB.

3. Nine total tests per sediment barrier are performed.

Figure 3.9. SB performance based testing regime (*Bugg et al. 2017*).

3.10 DATA COLLECTION

The evaluation of SB performance is based on data and observations collected throughout the duration of the experiment. These parameters are used to assess the overall performance of SB practices and allows comparisons between various SB practices.

3.10.1 STRUCTURAL PERFORMANCE

Photographs were taken prior, during, and post-testing from the locations shown in Figure 3.10. These photographs are used to document test conditions and changes to the SB practices due to sediment and hydraulic loading. Video documentation is collated throughout testing so that structural failures can be analyzed to identify modes of scouring, overtopping, and/or structural instabilities. A string line is installed across the test area [Figure 3.10] to measure the deflection of the SB support structures as loading occurs. This data is used to evaluate the structural performance of SB practices, as well as to identify avenues to improved performance.

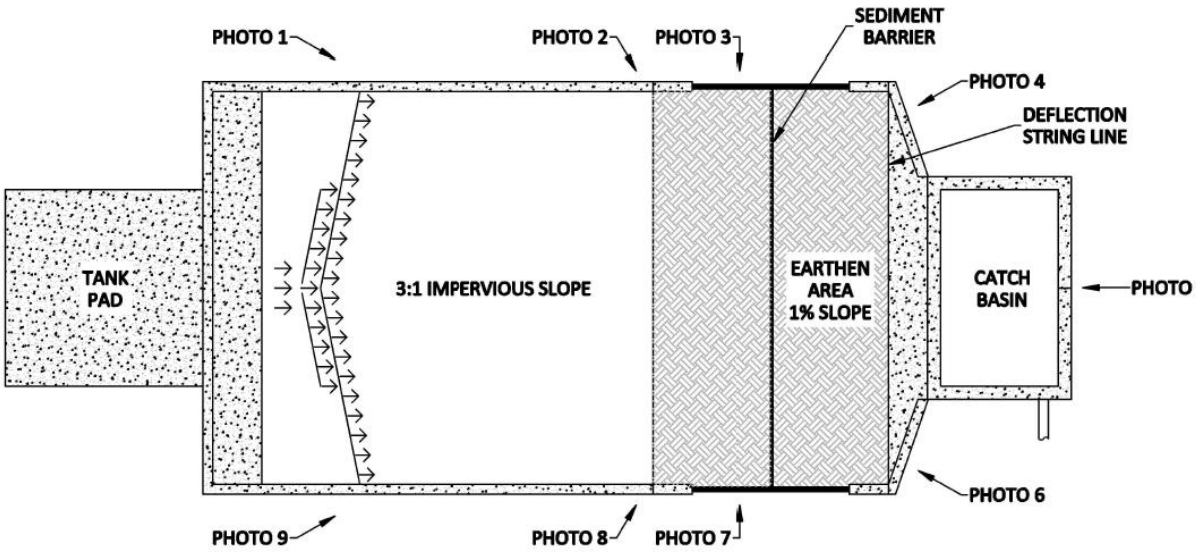

Figure 3.10. Sediment barrier data acquisitions locations.

3.10.2 SEDIMENT RETENTION

Complete topographical surveys of the test area were conducted pre- and post-test to quantify sediment retention. The surveys are performed using a Trimble® robotic total station [Figure 3.11] and analysis of the topographic data is conducted using computer-aided design software. This software converts raw data points into a triangular irregular network for a three-dimensional representation of the test area surface which allows for a comparison of the pre- and post-test channel topography, as shown in Figure 3.12.

Figure 3.11. Robotic total station setup and survey.

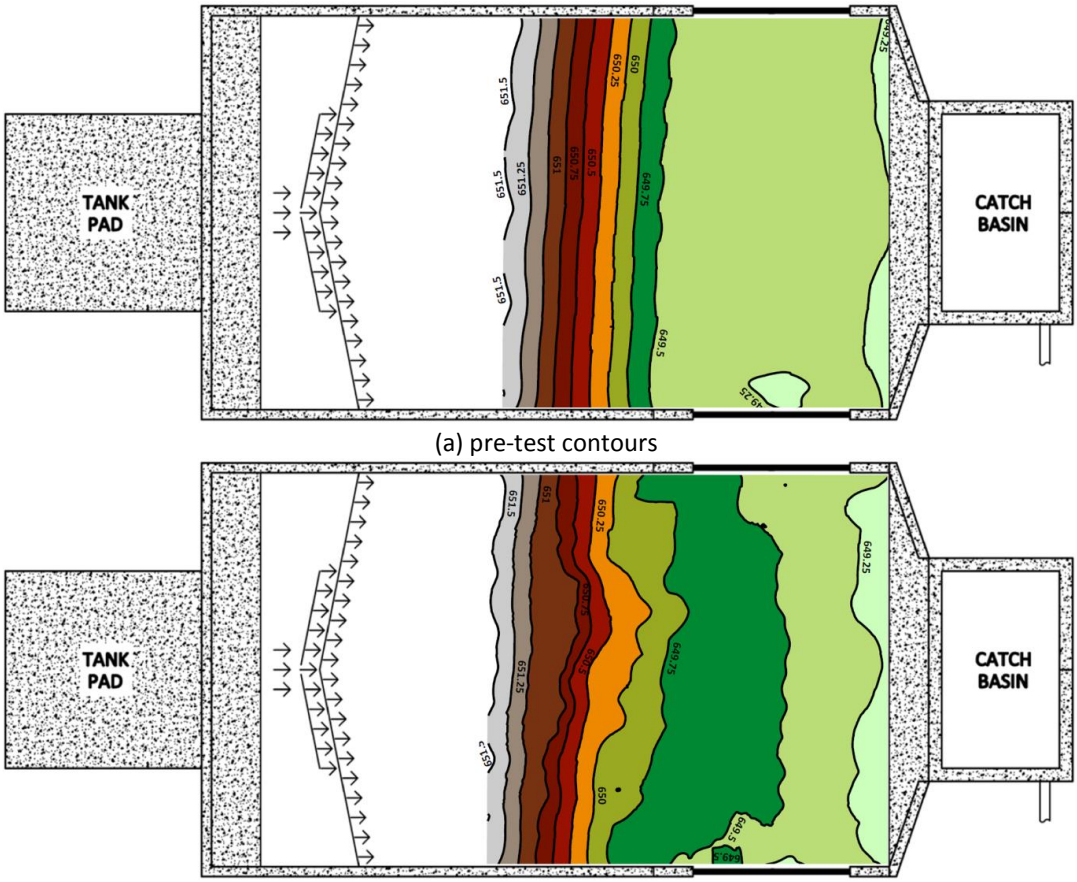

(a) pre-test contours

(b) post-test contours

Figure 3.12. Three-dimension representation of surveyed sediment deposition.

Note: Colored regions between contour intervals are intended to aid visual representations of elevation change from pre to post test

3.10.3 HYDRAULIC PERFORMANCE

Water ponding depth, pool length, and discharge flow rates were monitored and recorded during testing. Ponding depth and pool length were measured using a depth gauge at five-minute intervals for the 30-minute test duration and continuing after the test at five-minute intervals for 15 minutes; at 15 minute intervals for the following 15 minutes; and at 30 minute intervals for the final 60 minutes. Maximum depth and pool length were confirmed by monitoring, marking, and measuring the high water marks at the conclusion of each test. Catch basin water depth was also measured at the same intervals detailed above. The collection of this data allowed for the evaluation of a SB's ability to impound water and for the quantification of flow rate passing through the SB when subjected to sediment-laden flow.

3.10.4 TURBIDITY AND TOTAL SUSPENDED SOLIDS (TSS)

Water quality data was obtained from numbered 8.0 oz. (240 mL) grab samples [Figure 3.13(a)] collected throughout testing. Samples were collected every five minutes at five sample locations: (1) along the impervious slope (i.e., SL1), (2) upstream of SB on the surface of the impoundment (i.e., SL2), (3) upstream of SB along the bottom of the impoundment via sampling pump (i.e., SL3), (4) downstream of the SB (i.e., SL4), and (5) as water discharged into the catch basin (i.e., SL5). Figure 3.14 illustrates each of these sampling locations. The grab samples were processed and analyzed to determine turbidity and total suspended solids (TSS). Turbidity was measured using a Hach® 2100Q Portable Turbidimeter [Figure 3.13(b)] that measures water transparency in nephelometric turbidity unit (NTU). TSS was reported in mg/l and is determined by passing a well-mixed 25 mL (0.85 oz.) water sample through a membrane filter and determining the quantity of solids captured by the filter [Figure 3.13(c)], thereby quantifying the

amount of suspended solids in the sample. A comparison of turbidity and TSS at locations SL1 and SL2 was used to determine the effect on water quality due to rapid settling. Comparisons between locations SL2 and SL3 demonstrates the effects on water quality resulting from upstream impoundment and comparisons between locations SL3 and SL4 indicate the change in water quality due to geotextile filtration. Finally, SL4 and SL5 indicate the effects on water quality as flow travels over bare soil after being treated by the SB practices and leaves the construction site.

(a) grab sample container (b) turbidity meter (c) TSS filtering apparatus

Figure 3.13. Water quality measuring equipment.

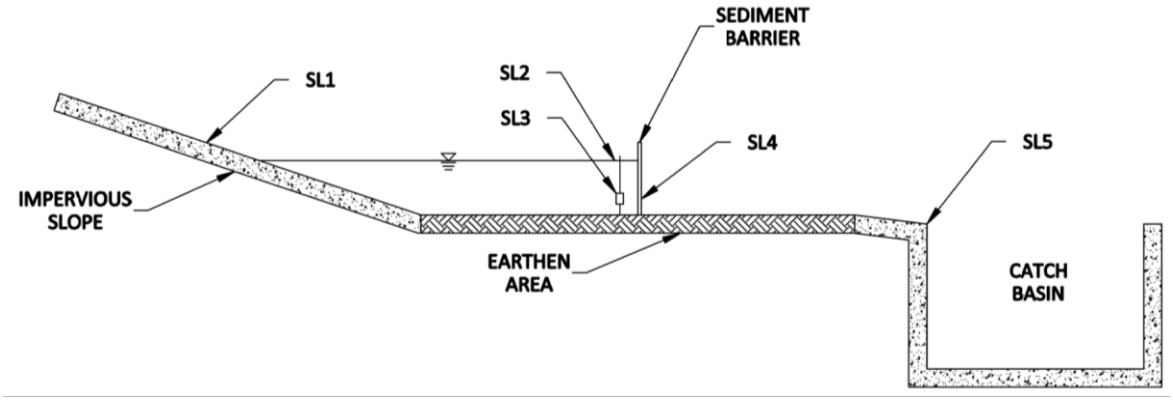

Figure 3.14. Water sampling locations.

3.11 SUMMARY

This chapter provides an overview of the SB test apparatus design, experimental methodology, and data collection processes developed for evaluating SB practices as part of this research. A comparison of existing SB test methods identified in the literature and the test method developed at the AU-ESCTF are shown in Table 3.3.

Table 3.3. Comparison of Various Test Methods and Test Requirements (*Bugg et al. 2017*)

Study	Focus	Design Storm	Drainage Basin ac (ha)	Flow Rate ft^3/s (m^3/s)	Sediment Load lb. (kg)	Test Duration (min)
TRI/Environmental ASTM D7351	Performance	10-yr, 6-hr	0.05 (0.02)	0.04 (0.001)	300 (136.1)	30
Gogo-Abite, Chopra UCF	Performance	1.0– 5.0 in./hr (25.4-127 mm/hr)	0.005 (0.002)	0.0071- 0.0283 (0.0002 - 0.0008)	N/A	30
ASTM D5141	Filtering Efficiency and Flow Rate	N/A	N/A	0.177 (0.005)	0.33 (0.15)	0.17
AU-ESCTF Full-Scale Testing	Performance & Longevity	2-yr, 24-hr	0.50 (0.20)	0.22 (0.006)	1,127.8 (511.6)	30

Note: 1 ac = 0.4 ha; 1 ft^3/s = 0.028 m^3/s; 1 lb. = 0.45 kg

The full-scale test apparatus developed and constructed at the AU-ESCTF can introduce a wide range of flow rates and sediment loading scenarios that SB practices may intercept thought out their life cycle on a roadway construction site. Currently, this SB testing process is the only one that allows for full-scale testing under realistic field-like conditions.

CHAPTER FOUR:
PERFORMANCE EVALUATIONS OF SILT FENCE INSTALLATIONS

4.1 INTRODUCTION

This chapter evaluates nonwoven silt fence sediment barrier installations, as well as alternative installation methods that focus on improving structural stability. The research presented exhibits the performance characteristics of Standard ALDOT silt fence installations and the effects small design and installation changes have on structural performance of silt fence when exposed to a replicable 2-yr, 24-hr design storm. A statistical analysis was conducted on T-post deflection data to determine individual aspect functionality as it relates to structural performance. Sediment retention rates, water quality analyses, and an effective means for dewatering impounded stormwater is also presented.

4.2 SILT FENCE INSTALLATION MATERIALS

The following outlines the materials used during performance testing.

- *filter fabric:* 3.5 oz./yd^2 (119 g/m^2), nonwoven, 48 in. (121.9 cm) wide fabric that conform to the American Association of State Highway and Transportation Officials (AASHTO) M288 standard (*AASHTO 2017*). Fabric was attached along the top of wire reinforcing using c-ring clips approximately 2 ft (0.61 m) on-center. Fabric was placed into a 6 in. by 6 in. (15.2 cm by 15.2 cm) trench and backfilled.

- *wire reinforcing:* 17 gauge (1.14 mm) steel woven wire reinforcement with maximum vertical spacing of 6 in. (15.2 cm) and horizontal spacing of 12 in. (30.5 cm). Wire reinforcing was used to support filter fabric.
- *studded T-post:* 5 ft (1.5 m) and 4.3 ft (1.3 m) studded T-post, 0.95 lb./ft (1.4 kg/m) and 1.25 lb./ft (1.9 kg/m), driven into ground 24 in. (61 cm), spaced 10 ft (3.0 m) and 5 ft (1.5 m) on-center. T-posts were used as vertical supports for reinforcing wire and filter fabric.
- *wire ties:* three 6.5 in. (15.6 cm), 11 gauge (3.175 mm), aluminum wire ties were used to attach reinforcing wire to each studded t-post.
- *c-ring clips:* 11/16 in. (1.75 cm), 16 gauge (1.29 mm), galvanized steel c-ring clips were used to secure filter fabric to reinforcing wire.

To accurately evaluate the performance of each silt fence installation configuration, the filter fabric manufacturer (DDD Erosion Control 3D 3.5 NW) and weight (3.5 oz./yd^3) were kept consistent throughout testing.

4.3 STANDARD ALDOT SILT FENCE INSTALLATIONS

The ALDOT standard wire-reinforced, nonwoven, trenched and sliced silt fence configuration, as illustrated in the ALDOT Standard Drawing ESC-200-4 (*ALDOT 2017*) (Figure 4.1) was evaluated. Results established the performance baseline for which installation modifications were compared. The standard ALDOT silt fence installation specifies constructing a silt fence that is: (1) a minimum of 32 in. (81.3 cm) above the ground surface, (2) supported by studded metal T-posts spaced 10 ft (3 m) on-center, and (3) entrenched 6 in. by 6 in. (15.2 cm by 15.2 cm) or sliced 8 in. (20.3 cm) into the ground.

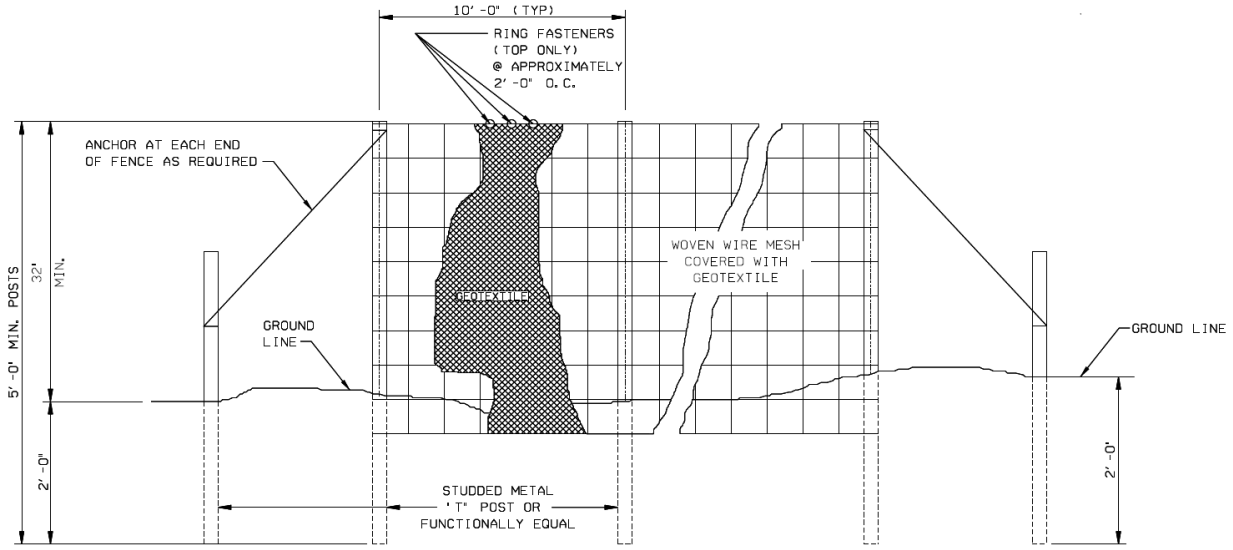

(a) ALDOT Type A– front elevation view

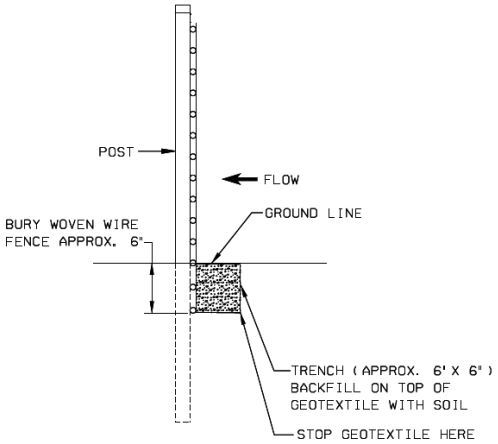

(b) ALDOT Type A – Trenched

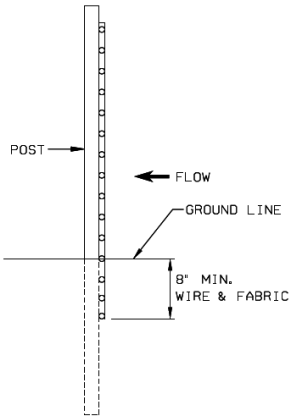

(c) ALDOT Type A - Sliced

Figure 4.1 ALDOT standard silt fence installation (*ALDOT 2017*).

4.4 NONWOVEN SILT FENCE INSTALLATION TESTS

The SB test apparatus was prepared in accordance with the experimental specifications outlined in Chapter 3 for each installation configuration to minimize inconsistencies between tests. Two standard installations and eight alternative installation configurations were evaluated to determine overall performance. Each standard installation was installed per the design drawings and each alternative trenching installation was installed in the same manner as the standard ALDOT installation but minor modifications were implemented, as noted below.

- *Standard ALDOT Trenched (STD-T):* 32 in. (81.3 cm) fence height, 10 ft (3.0 m) T-posts spacing, 0.95 lb./ft (1.4 kg/m) T-posts, and entrenched 6 in.by 6 in. (15.2 cm by 15.2 cm)
- *Standard ALDOT Sliced (STD-S):* 32 in. (81.3 cm) fence height, 10 ft (3.0 m) T-posts spacing, 0.95 lb./ft (1.4 kg/m) T-posts, and sliced 8 in. (20.3 cm)
- *Modification 1 (M1):* 0.95 lb./ft (1.4 kg/m) T-posts were replaced with 1.25 lb./ft (1.9 kg/m) T-posts.
- *Modification 2 (M2):* 0.95 lb./ft (1.4 kg/m) T-posts spacing was reduced from 10 ft (3.0 m) on-center to 5 ft (1.5 m) on-center.
- *Modification 3 (M3):* 0.95 lb./ft (1.4 kg/m) T-posts were replaced with 1.25 lb./ft (1.9 kg/m) T-posts and T-posts spacing was reduced from 10 ft (3.0 m) on-center to 5 ft (1.5 m) on-center.
- *Modification 4 (M4):* fence height was reduced from 32 in. (81.3 cm) to 24 in. (61.0 cm).
- *Modification 5 (M5):* fence height was reduced from 32 in. (81.3 cm) to 24 in. (61.0 cm) and T-post spacing was reduced from 10 ft (3.0 m) on-center to 5 ft (1.5 m) on-center.
- *Modification 6 (M6):* fence height was reduced from 32 in. (81.3 cm) to 24 in. (61.0 cm) and 0.95 lb./ft (1.4 kg/m) T-posts were replaced with 1.25 lb./ft (1.9 kg/m) T-posts.
- *Modification 7 (M7):* fence height was reduced from 32 in. (81.3 cm) to 24 in. (61.0 cm), 0.95 lb./ft (1.4 kg/m) T-posts were replaced with 1.25 lb./ft (1.9 kg/m) T-posts, and T-post spacing was reduced from 10 ft (3.0 m) on-center to 5 ft (1.5 m) on-center.
- *Modification 8 (M8):* mimics Modification 7; however, T-post were offset 6 in. (15.2 cm) downstream of the trench.

A summary of the variations between each installation configuration is provided in Table 4.1 and installation details for each modification are illustrated in Figure 4.2(a) through (h).

Table 4.1. Summary of Silt Fence Installations

Installation	Fence Height in. (cm)	T-Post Weight lb./ft (kg/m)	T-Post Spacing ft (m)	Embedment in. x in. (cm x cm)
STD-T	32 (81.3)	0.95 (1.4)	10 (3.0)	6 x 6 (15.2 x 15.2)
STD-S	32 (81.3)	0.95 (1.4)	10 (3.0)	Sliced 8 (20.3)
M1	32 (81.3)	1.25 (1.9)	10 (3.0)	6 x 6 (15.2 x 15.2)
M2	32 (81.3)	0.95 (1.4)	5 (1.5)	6 x 6 (15.2 x 15.2)
M3	32 (81.3)	1.25 (1.9)	5 (1.5)	6 x 6 (15.2 x 15.2)
M4	24 (61.0)	0.95 (1.4)	10 (3.0)	6 x 6 (15.2 x 15.2)
M5	24 (61.0)	0.95 (1.4)	5 (1.5)	6 x 6 (15.2 x 15.2)
M6	24 (61.0)	1.25 (1.9)	10 (3.0)	6 x 6 (15.2 x 15.2)
M7	24 (61.0)	1.25 (1.9)	5 (1.5)	6 x 6 (15.2 x 15.2)
M8	24 (61.0)	1.25 (1.9)	5 (1.5)	Offset 6 x 6 (15.2 x 15.2)

Note: STD-T = Standard ALDOT Installation Trenched; STD-S = Standard ALDOT Installation Sliced; M = Modification to Standard ALDOT Installation; 1 in. = 2.54 cm; 1 lb./ft = 1.5 kg/m; 1 ft = 0.3 m

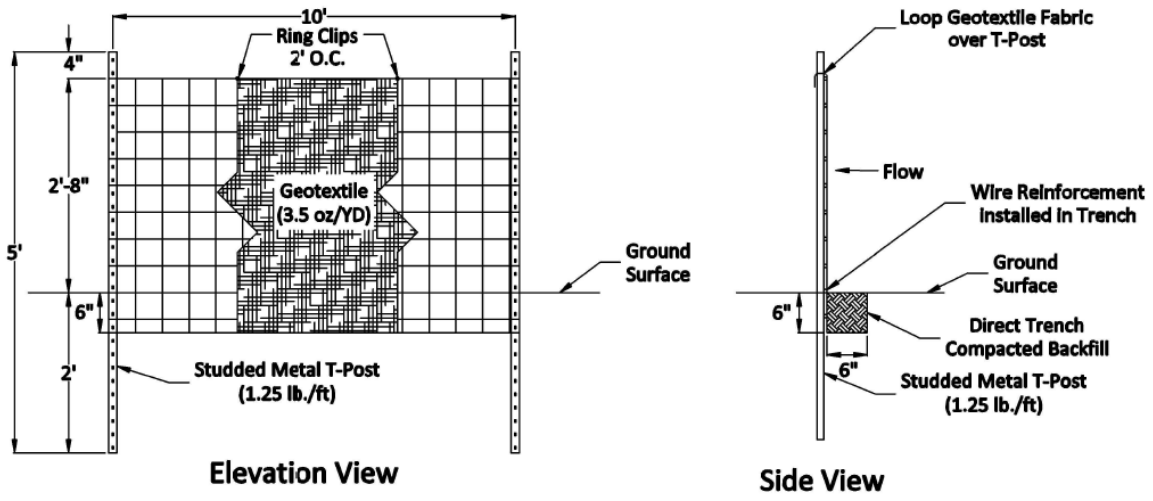

(a) modification 1

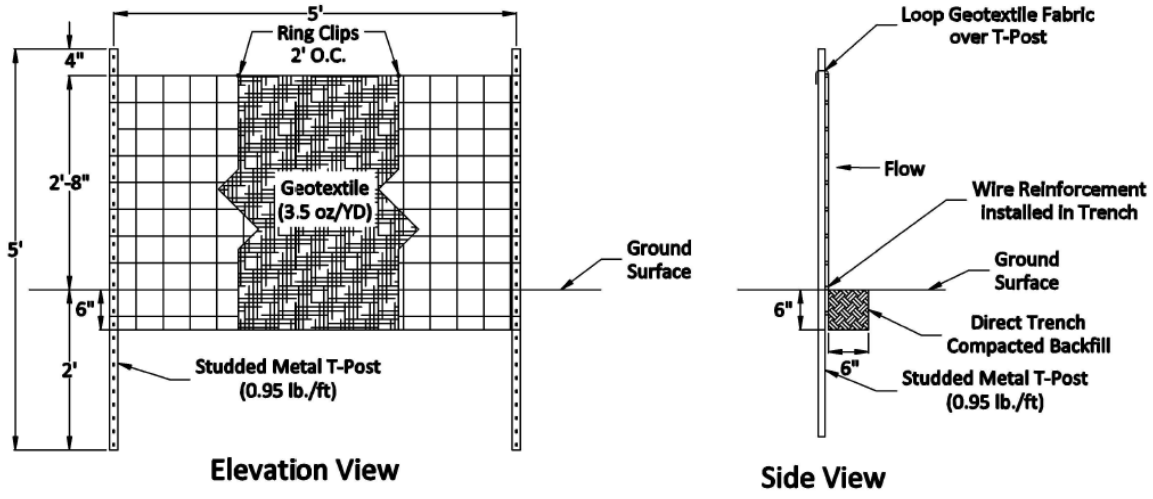

(b) modification 2

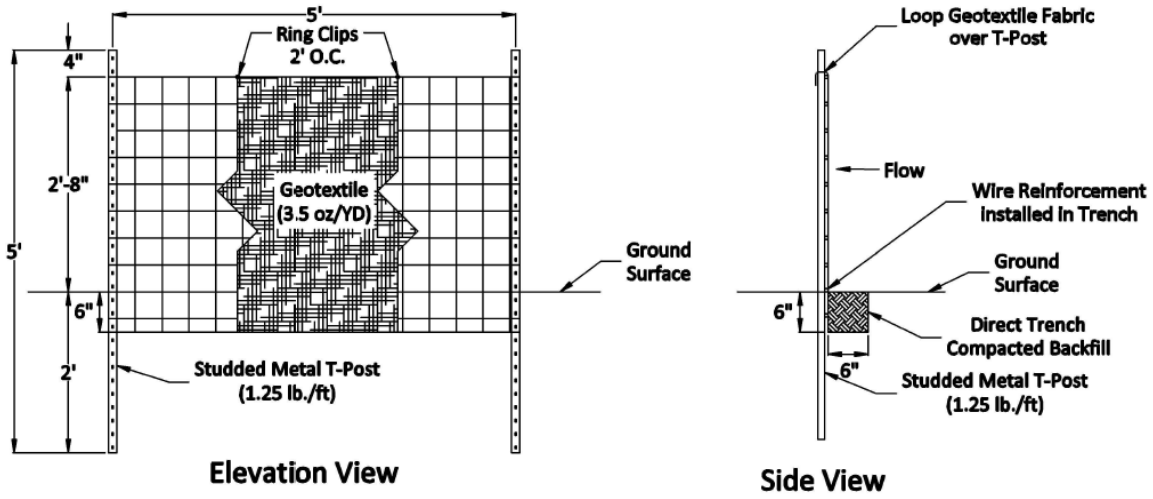

(c) modification 3

Figure 4.2. Silt fence modification details.

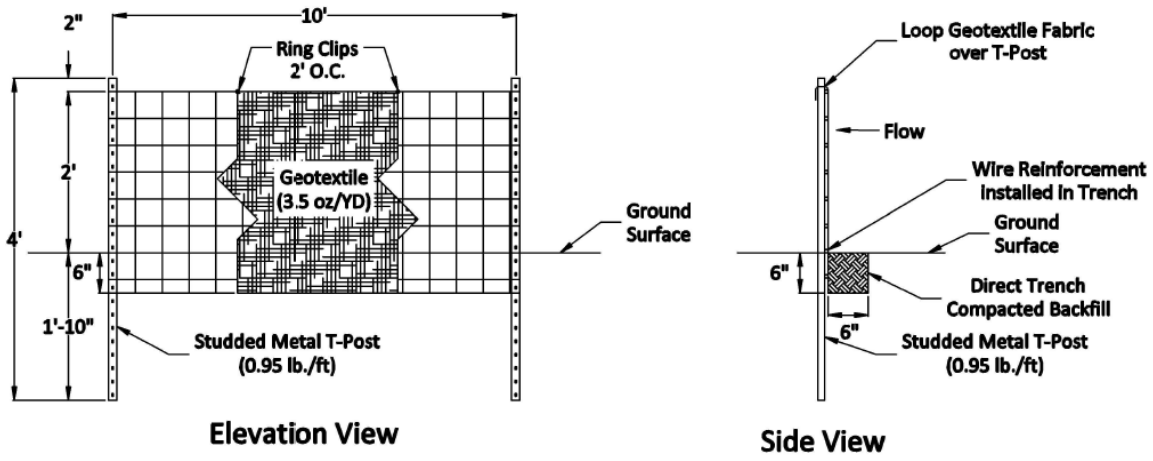

(d) modification 4

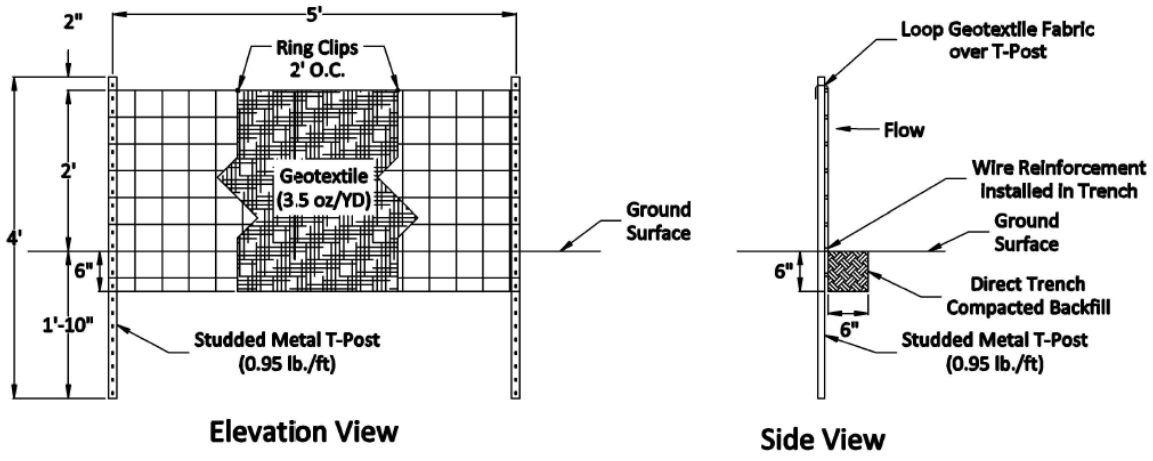

(e) modification 5

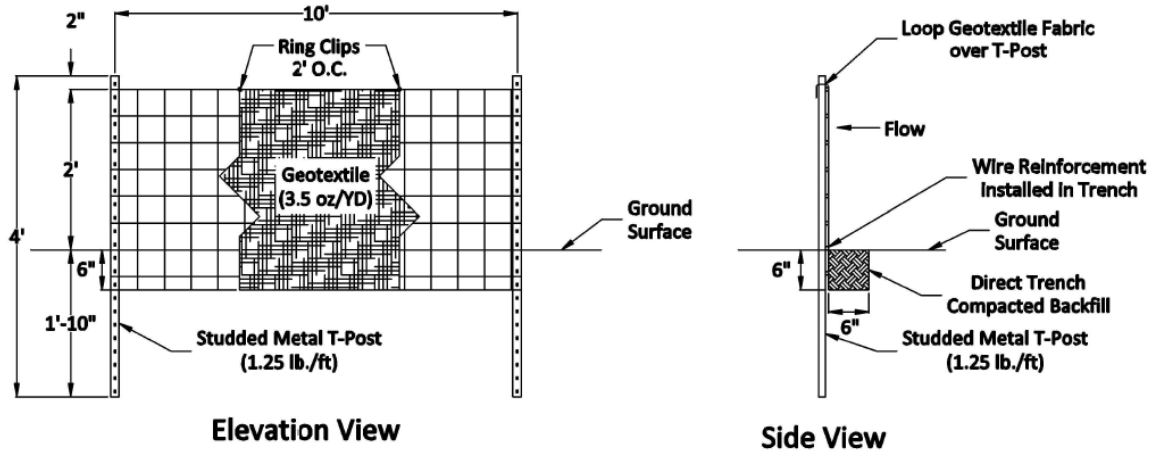

(f) modification 6

Figure 16 (cont'd). Silt fence modification details.

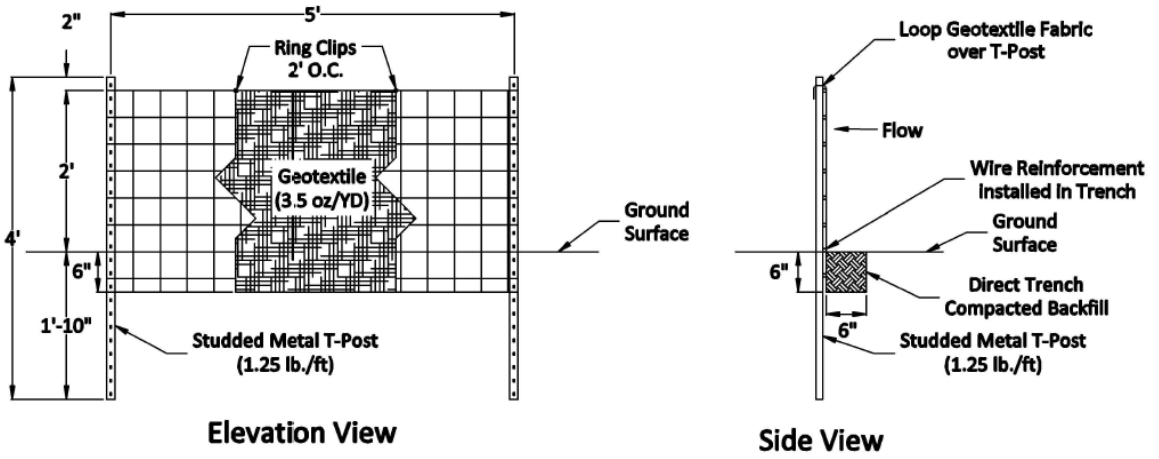

(g) modification 7

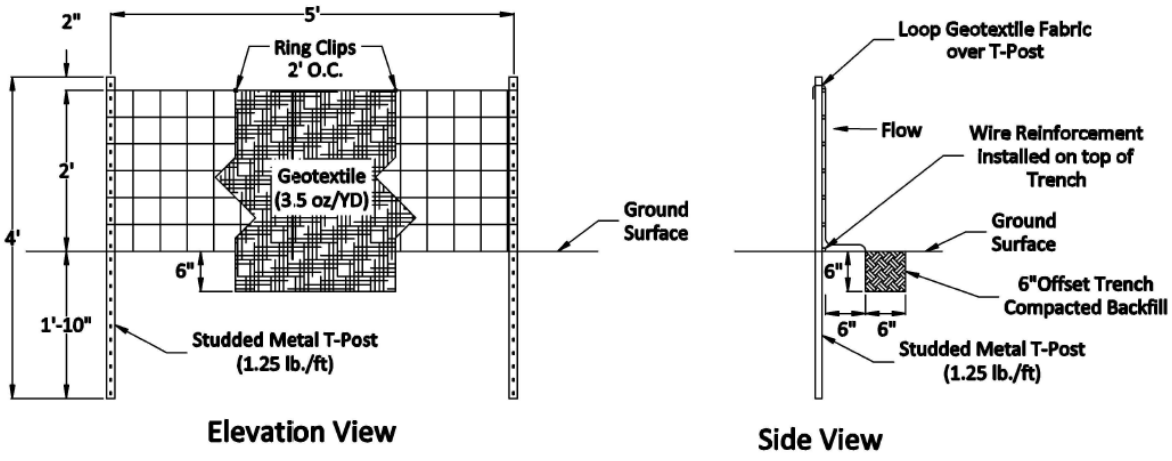

(h) modification 8

Figure 16 (cont'd). Silt fence modification details.

4.5 STATISTICAL ANALYSIS

Statistical analysis was used to evaluate the effect that each installation variable had on the performance of the silt fence installation. This was achieved by developing a traditional multiple linear regression model that was used to determine the significance of each installation variable (e.g., fence height, post weight, post spacing, and trench offset). The multiple linear regression model independently evaluates the effect each variable has on reducing T-post deflection. The magnitude of T-post deflection correlates to the structural failure of the

installation created by the fence falling backwards. Installation components were first recoded into unique binary independent variables that took values of 1 or 0, depending on whether the installation modified the component or not. The dependent variables were coded as deflection lengths, which ranged between 0.03 ft (0.01 m) and 0.72 ft (0.22 m). The objective for conducting the regression analysis was to determine the relative impact of each component on final fence deflection, independent of other components. It is important to recognize that because some installations were only evaluated once (e.g., M1, M2, M3, M4, M5, and M6), model results are not statistically significant enough to predict deflections. However, the model does provide valid quantifiable measures to support the remaining evaluation criteria described in the following section, as previously seen in work completed by Donald et al. (*2013*). Using this model, the most effective means for improving structural stability can be determined. The model equation can be written as:

$$f(x) = \beta_0 + \beta_1 x_1 + \beta_2 x_2 + \beta_3 x_3 + \beta_4 x_4 \quad \text{(Eq. 4.1)}$$

Where,

$f(x)$ = dependent variable (e.g., silt fence deflection)

β_0 = coefficient intercept

β_i = ordinary least squares coefficients

x_i = independent variables (e.g., fence height, post weight, post spacing, offset trench)

4.6 RESULTS AND DISCUSSION

The following is a summary of results and observations made over the course of nonwoven silt fence experiments. The initial phase of this investigation identified and evaluated

the performance baselines for Standard ALDOT silt fence installations. The second phase was dedicated to developing and evaluating alternative installation strategies that improved upon baseline performance data. During this phase, precedence for improvements were placed in the following order: (1) structural integrity, (2) sediment retention, and (3) water quality. The final phase of the investigation focused on the development and evaluation of an effective means for dewatering concentrated impoundment areas, upstream of a silt fence installation, while maintaining optimal performance characteristics achieved during phase two.

4.6.1 STRUCTURAL PERFORMANCE

The structural integrity of a silt fence installation is critical to achieve the desired water quality improvements of stormwater runoff prior to site discharge. As outlined previously, the ability of a silt fence installation to efficiently removing sediment is largely dependent on stormwater impoundment capabilities. To achieve desired efficiencies, two common failure modes must be addressed. First, silt fence installations should be able to structurally withstand the hydrostatic pressure imposed by stormwater that impounds upstream of the installation. Second, silt fence geotextiles should be securely entrenched as to prevent flow bypass and undermining of the installation. Figure 4.3 shows these common failure modes.

(a) overtopping (b) undermining

Figure 4.3. Common construction site silt fence structural failures.

Structural performance observations of the *Standard ALDOT Silt Fence – Trenched* installation, which will be referred to as *STD-T*, were conducted over the course of three installations. For each installation, maximum impoundment depth increased with each of the three simulated storm events due to geotextile blinding. As a result, structural failure occurred when hydrostatic forces reached the maximum allowable bending moment of the T-post. Post deflection continued until overtopped water reduced hydrostatic pressure on the installation to the point that equilibrium within the system was established. This failure mode occurred during the third simulated storm event for installation 1 and 2 (i.e., I1 and I2) but during the second simulated storm event for installation 3 (i.e., I3). The maximum horizontal T-post deflection measured during *STD-T* testing was 2.67 ft (0.81 m). Additionally, substantial fence sag was observed during evaluations. Flow overtopping occurred midway between T-post installation locations, which also corresponds to the position in which maximum fence sag occurred, as shown in Figure 4.4(a). Due to extensive fence sag between T-posts, maximum impoundments measured during testing were 0.82 ft (0.25 m), 0.90 ft (0.27 m), and 0.85 ft (0.26 m), respectively. Each of the *STD-T* installations evaluated failed in the manners identified above. Results indicate that while the *STD-T* installation can structural withstand a single 2-yr, 24-hr storm event, the installation configuration is subject to structural failure when exposed to multiple field rainfall events.

The *Standard ALDOT Silt Fence – Sliced* installation, referred to as *STD-S*, was also evaluated over the course of three installations. Observations from tests indicate that failure of each installation was due to undermining on the initial simulated storm event. Failures were similar in nature in that the entrenched geotextile dislodged from the mechanically formed

trench 8 to 12 minutes after flow introduction thus allowing flow to undermining the installations. Maximum impoundment depths measured during testing for each installation (i.e., I1, I2, and I3) were 0.37 ft (0.11 m), 0.48 ft (0.15 m), and 0.49 ft (0.15 m), respectively. The undermining failure mode observed is shown in Figure 4.4(b). Results indicate that the *STD-S* installation, as installed using the EnFencer® mechanical slicing machine, would not perform structurally when exposed to a 2-yr, 24-hr field rainfall event.

Silt fence installation methods (i.e., trenching and slicing) have typically been based on installation needs, costs, equipment, and labor availability. Slicing is considered a more efficient means of installation compared to trenching because the use of a tractor-drawn slicing implement is less labor intensive than trenching. Nonetheless, results indicate that the structural integrity of the *STD-T* installation is more reliable than that of the *STD-S* installation.

Based on the observations and evaluations of the *STD-T* installation, modifications to the standard installation were developed, tested, and assessed. Failure mechanisms observed throughout modification testing were: post deflection, fence sagging, overtopping, and undermining. The maximum and minimum post deflections for test P3 were 2.04 ft (0.62 m) (*M2*) and 0.15 ft (0.05 m) (*M8*), respectfully. Each installation using 0.95 lb./ft (1.9 kg/m) T-post and/or 10 ft (3 m) T-post spacing, experienced extensive post deflections, which resulted in overtopping (Figure 4.4(c), 4.4(d), 4.4(e), 4.4(f), and 4.4(g)). Excessive fence sag was observed in each installation using a 10 ft (3 m) T-post spacing (Figure 4.4(c), 4.4(e), and 4.4(g)). Undermining was observed at multiple T-post locations during several tests (Figure 4.4(h)). Although a definitive reason for this occurrence could not be determined, it was speculated that lack of compaction around T-posts due to their placement within the trench resulted in these failures.

(a) STD-T overtopping

(b) STD-S undermining

(c) modification 1

(d) modification 2

(e) modification 4

(f) modification 5

(g) modification 6

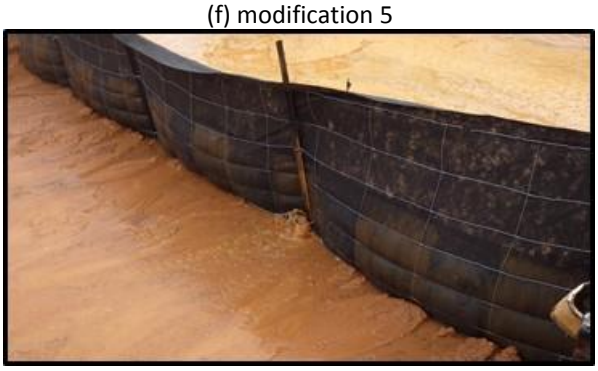

(h) undermining of modification 2

Figure 4.4. Silt fence installation configurations and failure modes.

Table 4.2 summarizes the structural performance of all nonwoven silt fence installations.

Table 4.2. Silt Fence Failure Modes

Description	Installation	Test	Overtopping Time (min:sec)	Structural Failure
STD-T	I1	P1, P2	--	No Failure
		P3	15:15	Post Deflection, Fence Sagging, Overtopping
	I2	P1,P2	--	No Failure
		P3	14:30	Post Deflection, Fence Sagging, Overtopping
	I3[a]	P1	--	No Failure
		P2	15:30	Post Deflection, Fence Sagging, Overtopping
STD-S	I1[b]	P1	--	Undermining
	I2[b]	P1	--	Undermining
	I3[b]	P1	--	Undermining
M1	I1[a]	P1	--	No Failure
		P2	18:45	Post Deflection, Overtopping, Fence Sagging, Undermining
M2	I1	P1	--	No Failure
		P2	--	Undermining
		P3	26:40	Post Deflection, Overtopping
M3	I1	P1, P2, P3	--	No Failure
M4	I1[a]	P1	--	Undermining
		P2	16:28	Post Deflection, Fence Sagging, Overtopping
M5	I1	P1	--	Undermining
		P2	--	No Failure
		P3	26:00	Post Deflection, Overtopping
M6	I1	P1, P2	--	No Failure
		P3	13:10	Post Deflection, Fence Sagging, Overtopping
M7	I1	P1, P2, P3	--	No Failure
	I2	P1, P2, P3	--	No Failure
	I3	P1, P2, P3	--	No Failure
M8	I1	P1, P2, P3	--	No Failure
	I2	P1, P2, P3	--	No Failure
	I3	P1, P2, P3	--	No Failure

Note: [a] = test P3 was not conducted due to test P2 failure; [b] = test P2 & P3 were not conducted due to test P1 failure; -- = overtopping did not occur.

In addition to increasing T-post weight and decreasing T-post spacing, improvements to the standard installation were analyzed. While conducting tests on M1, it was noted that securing the nonwoven fabric to the T-post by cutting a slit in the fabric and looping it over the T-post [Figure 4.5(a)] decreased fence sag caused by hydrostatic pressure between T-post, as shown in Figure 4.5(b) and 4.5(c). This installation method also reduced pressure applied to the c-ring fasteners [Figure 4.5(d)] along the top of the fence, which failed during the “no loop” test.

(a) T-post loop over

(b) w/o T-post loop over

(c) w/ T-post loop over

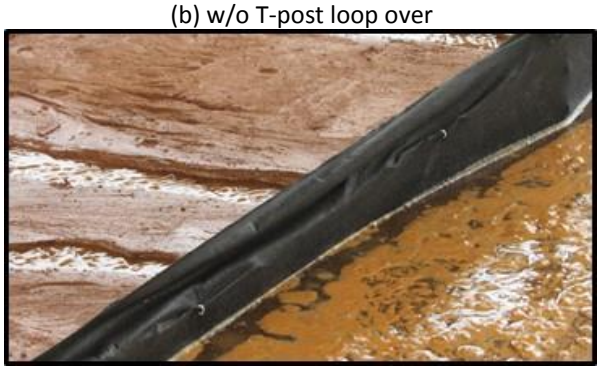

(d) c-ring fasteners

(e) offset trench

(f) offset silt fence installation

Figure 4.5. Silt fence improvement strategies.

Although scouring was not a significant factor affecting sediment retention performance for each configuration, installation improvements for reducing the reoccurrence of scouring were tested. Figure 4.5(e) and 4.5(f) show the offset trench installation implemented. Even though a justifiable metric that indicates the benefits of the offset trench in regards to scoring was not obtained, a slight increase in impoundment depth [approximately 0.12 ft (0.04 m)] was noted when compared to direct trenching method. This observation indicates that the offset trench,

which was mechanically compacted, may minimize flow under the installation as compared to direct trenching, which requires hand compaction to avoid damaging the geotextile fabric.

4.6.2 SEDIMENT RETENTION

Topographical surveys of the test area were performed using a total station to gather elevation points pre- and post-simulated events. The data points were used to develop three-dimensional surface models of sediment deposition caused by the impoundment of the silt fence installations. Pre- and post-test surfaces for each simulated event were compared and the volumetric difference between the two was calculated. These volumes, along with the volumes of soil introduced as sediment, were analyzed to determine a retained volume. Average sediment retention rates for installations that did and did not fail structurally (indicated by [a] in Table 4.3) were 78% and 95%, respectively. The sediment retention rates for each installation are shown in Table 4.3.

Table 4.3. Sediment Retention of Nonwoven Silt Fence Installations

Description	Installation	Sediment Retained
STD-T	I1	87%
	I2	87%
	I3	75%
STD-S	I1	60%
	I2	68%
	I3	73%
M1	I1	53%
M2	I1	76%
M3	I1[a]	87%
M4	I1	90%
M5	I1	95%
M6	I1	96%
M7	I1[a]	100%
	I2[a]	100%
	I3[a]	96%
M8	I1[a]	90%
	I2[a]	91%
	I3[a]	98%

Note: [a] = failure did not occur.

As shown in Table 4.3, M1 was the least effective at retaining sediment. This can be attributed to extensive undermining and fence sag between suppot posts resulting in flow bypass and overtopping. When comparing sediment retention rates for M7 and M8, it appears that M7 outperforms M8. While this could be true, it should be noted that volumetric analyses are based on topographic points collected via total station. Although survey personnel are adequately trained and protocols are in place to insure consistent data acquisition, minor elevation variations can result from slightly unleveled equipment, out-of-plumb instrument rod and prism, incorrect barometric pressure and temperature inputs, and human error. Under typical survey conditions, elevation errors of a few hundredths are negligible due to vastness of the area under evaluation; however, the area under evaluation during SB evaluations is under 320 ft^2 (29.7 m^2) with elevation changes as small as one hundredth of a foot. Thus, highly accurate data acquisition

methods for quantifying volumetric difference has proven to be challenging. In this, these results should not be taken as highly accurate retention rates (e.g., $in.^3$) but instead practical retention rates (e.g., ft^3 not $in.^3$). Nonetheless, these finding are consistent with the results reported by Donald et al. (*2016*) for sediment retention rates of silt fence used as ditch checks. The majority of particle sedimentation occurred along the impervious slope, creating a cliff like deposition as shown in Figure 4.4(f). This sediment consisted of large granular particles that settled rapidly when velocity was reduced by the impoundment. Sediment particle size gradually decreased, as well as sedimentation depth along the flow direction. Sediment not retained by the silt fence was most likely smaller than the silt fence pores, thus were discharged in the effluent.

4.6.3 WATER QUALITY

Throughout each simulated storm event, water samples were taken to evaluate the effect each installation had on water quality. Figure 4.6(a) illustrated grab sample locations. Since each installation used the same geotextile fabric, the results obtained were very similar between tests that did not experience structural failure. As shown in Figure 4.6(b), the difference in upstream-top of water (SL2) and downstream (SL4) water quality is negligible. As the test progresses, the water quality at each of these locations consistently improves (i.e., turbidity decreases). This improvement is most likely due to impoundment depth increasing as blinding of the fabric occurs along the face of the silt fence, creating a longer impoundment, resulting in a longer time period for sediment particles to fall out of suspension prior to reaching the silt fence fabric. When comparing upstream-top of water (SL2) and downstream (SL4) to upstream-bottom of water (SL3), it is further evident that impoundment depth directly affects water quality. On average, for installations that did not fail due to overtopping, a 56% reduction in turbidity was measured

between SL3 and SL4 30 minutes into each tests. Extreme variations in water quality were only observed when failures, such as overtopping or undermining, occurred.

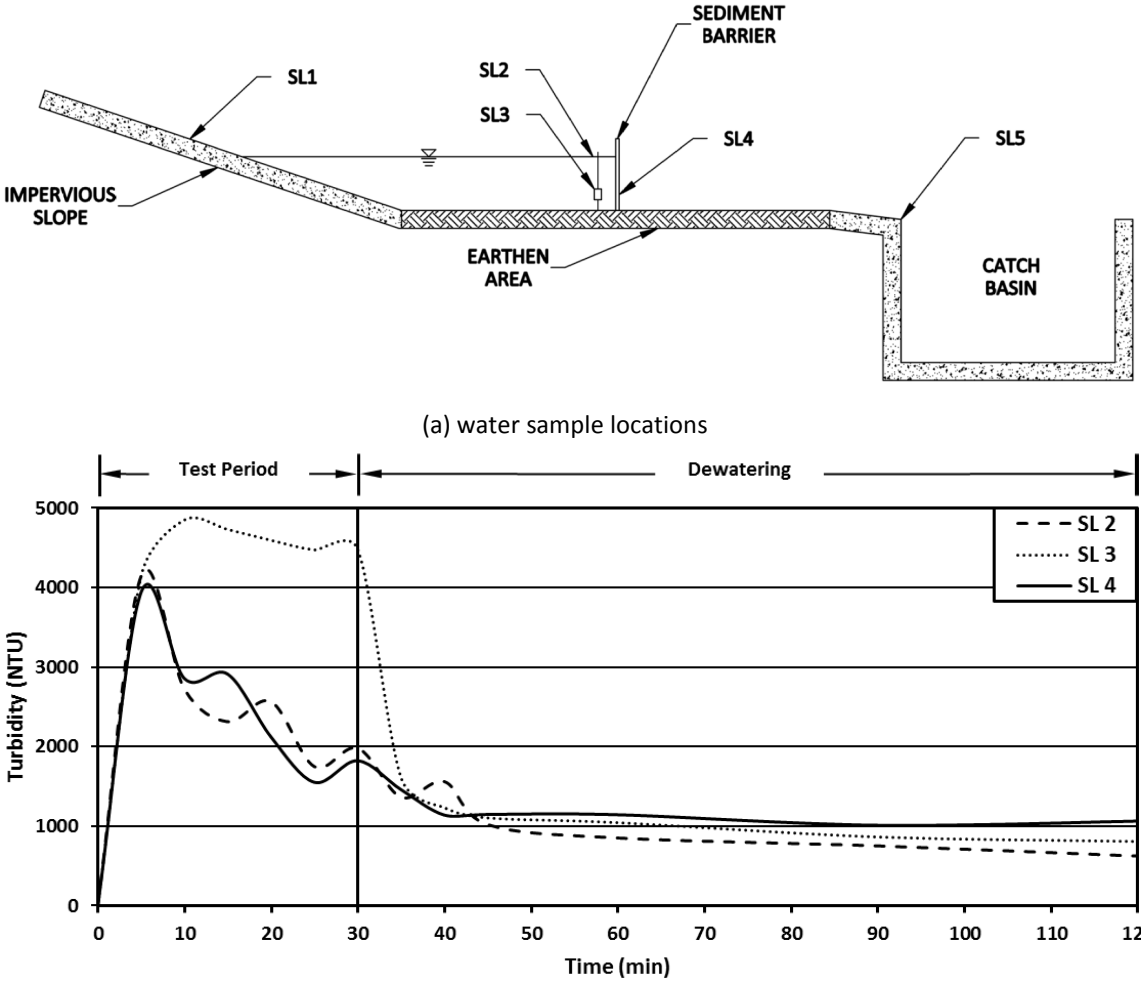

(a) water sample locations

(b) typical turbidity graph for non-woven silt fence

Figure 4.6. Water quality sample locations and representative turbidity data.

4.6.4 STATISTICAL RELEVANCE

To statistically determine the effects of different installation configurations; a multiple linear regression model was developed. Each installation had a corresponding combination of independent variables considered in the analysis: (1) fence height, (2) T-post weight, (3) T-post spacing, and (4) trench offset. For this regression model, the Standard ALDOT Installation was considered the base installation, from which each installation variation was compared. The

dependent variable selected for the analysis, which is directly affected by each independent variable, was T-post deflection. Deflections obtained from P1 tests were used within the model due to consistent initial conditions (i.e., unclogged filter fabric pores and plumb T-posts). A brief summary of T-post deflections used within the model is shown in Figure 4.7. The R^2 of the estimated model was 0.93, indicating a well-fitted linear model when compared to measured observations. Due to only conducting one evaluation for installations M2, M3, M4, M5, And M6, a confidence interval of 90% was selected for the analysis. Results, along with statistical significances, are shown in Table 4.4.

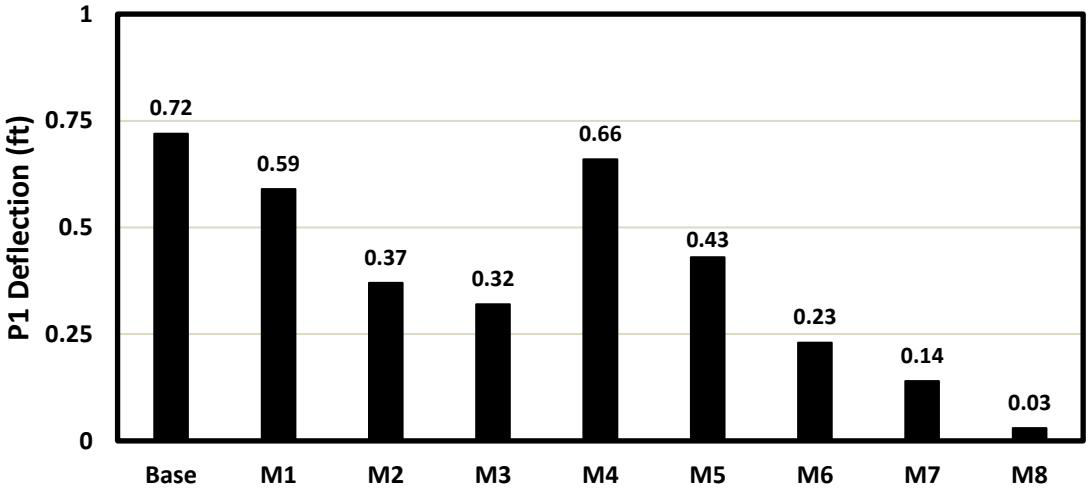

Figure 4.7. T-post deflection summary.

Table 4.4. Statistical Relationship of Installation Components

Installation Component	Statistical Significance	
	Coefficients	p-value[a]
Base (STD-T)	0.73	N/A
Fence Height	-0.13	0.024
T-Post Weight	-0.22	0.001
T-Post Spacing	-0.23	0.000
Trench Offset	-0.11	0.096

Note: [a] = comparison to effects of ALDOT Standard Silt Fence at 90% confidence interval and p-values <0.10.

Based on the statistical significance generated by the model, the following conclusions were drawn: (1) each installation component independently reduces fence deflection relative to the standard ALDOT installation, as evident by the negative coefficients (i.e., positive values indicate increased deflections, therefore negative values indicate decreased deflections), (2) each coefficient is statistically significant at a 90% confidence level, as indicated by p-values less than 0.1, thus signifying a positive effect on installation performance, (3) fence height and trench offsetting have the least effects on performance, and (4) T-post spacing and T-post weight have the greatest effects on performance. These statistical conclusions correlate to the structural failure mode observations outlined in Table 4.2, as well as sediment retention rates outlined in Table 4.3. When comparing measureable performance standards of each installation modification to the standard ALDOT installation, it is evident that each alteration facilitates a performance improvement.

4.7 SILT FENCE DEWATERING MECHANISM

During the performance evaluations of various silt fence installation modifications, a common reoccurrence was observed with each structurally sound installation. While upstream impoundment is critical to facilitate sedimentation, prolonged impoundment periods delay the drying effect once a storm event has occurred. During performance testing, impoundment periods for nonwoven silt fence installations were in excess of 24 hours from the conclusion of a simulated storm event. Due to excessive impoundment retention times, a need was identified for an effective means for discharging impounded stormwater while promoting sediment retention upstream of the installation and minimizing effluent impacts to receiving waters. Thus, an objective was set to design, construct, and evaluate a cost effective device capable of

preforming effectively when exposed to a 2 yr-24 hr design storm for the state of Alabama. Based on the knowledge obtained throughout silt fence testing and published literature, a silt fence dewatering weir was developed.

The dewatering weir was constructed out of ¾ in. (1.9 cm) plywood measuring 2 ft by 2 ft (0.6 m by 0.6 m) and supported by two 1.25 lb./ft (1.9 kg/m) steel T-post. The plywood was secured to the top and bottom of each T-post by drilling ½ in. (1.3 cm) holes in each corner of the plywood and installing heavy duty zip ties through each hole and around the T-post. A v-notch weir was cut at a 90-degree angle with a base elevation of 1.5 ft (0.46 m) from the earthen test area. Four, 1 in. (2.5 cm) holes were placed along the centerline of the plywood at elevations 0.25, 0.5, 0.75, and 1.0 ft (0.08, 0.15, 0.23, and 0.30 m) from the earthen test area. Figure 4.8(a) shows the plywood dewatering weir used during testing and Figure 4.8(b) illustrates dimensional details of the weir. Geotextile fabric was installed along the upstream face of the dewatering weir per M8 installation standards and a heavy duty staple gun was used to secure the fabric around each dewatering hole and along the v-notch weir opening. Once secured, a carpenter's knife was use to cut opening at each hole location. A 6 ft by 3 ft (1.8 m by 0.9 m) geotextile fabric underlay was installed downstream of the dewatering weir and secured using 6 in. (15.2 cm) circle top pins. Riprap was placed on top of geotextile underlay to facilitate energy dispersion as flow passed through each hole and across the weir.

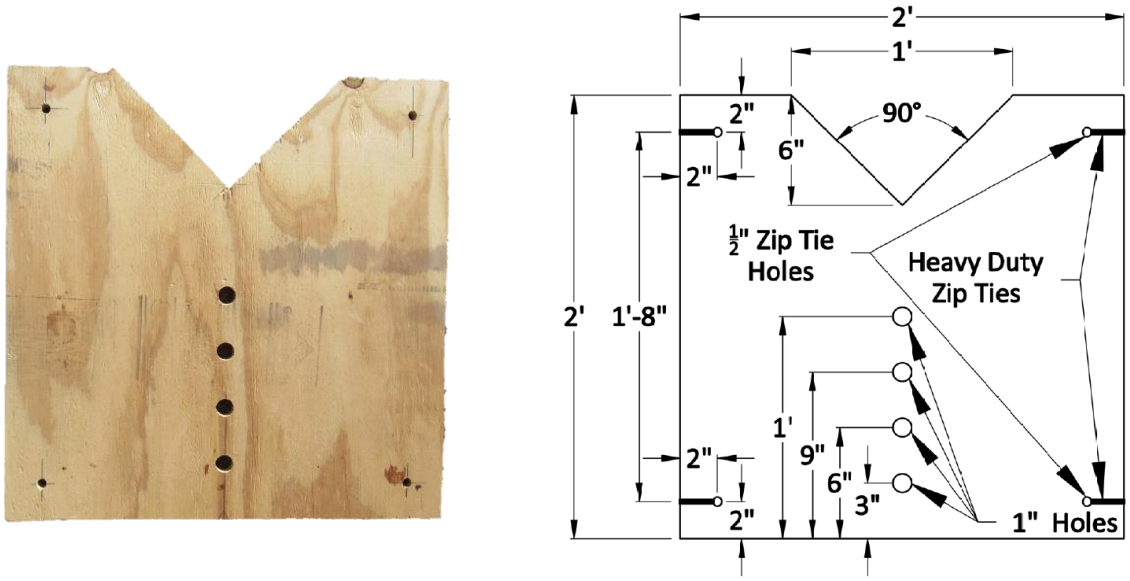

(a) plywood dewatering weir (b) weir detail

Figure 4.8. Silt fence dewatering weir details.

Performance tests were conducted on one installation of silt fence Modification 8 with the inclusion of the dewatering weir (i.e., Modification 9). In total, four performance tests were conducted on the installation. It is imperative that installers understand that in order for a dewatering weir to work effectively in field applications, the weir has to be installed in an area of concentrated impoundment, which is typically where silt fence structural failure occurs. The dewatering weir installation took minimal effort to install and proved to be a cost effective means for silt fence dewatering. Figure 4.9(a) through (d) shows the dewatering weir installation and Figure 4.10 provides installation details.

(a) upstream vantage point

(b) downstream vantage point

(c) front of weir

(d) back of weir

Figure 4.9. Dewatering weir installation.

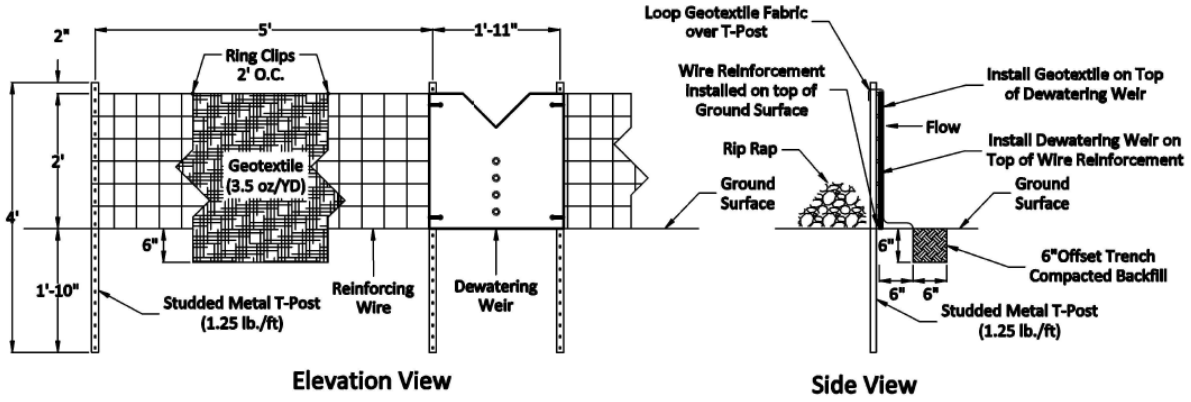

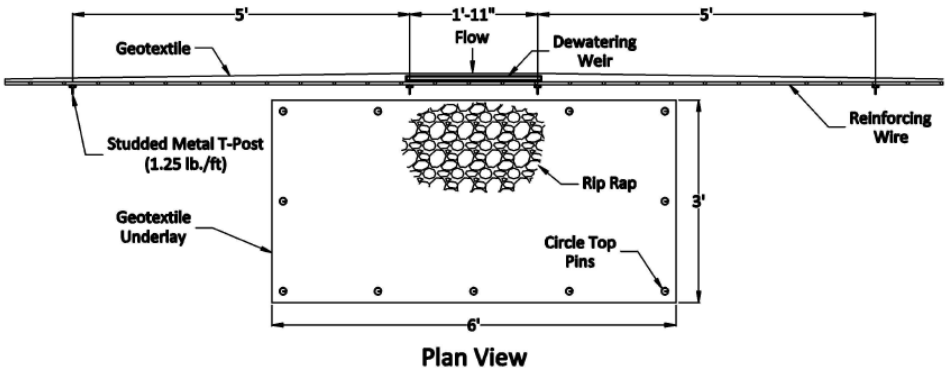

Figure 4.10. Dewatering weir installation detail.

Test results indicate that incorporating a dewatering weir into a structurally sound silt fence installation allows for a reliable and effective means for discharging impounded stormwater. Figure 4.11(a) shows sediment deposition that occurred during performance test 3 and Figure 4.11(e) shows downstream erosion resulting from three simulated storm events. When visually comparing post-test sediment deposition features of M9 (i.e., weir) to M8 (i.e., no weir), observations are consistent between tests [Figure 4.11(a) and 4.11(b)]. Due to the incorporation of a dewatering weir, effluent flow rates associated with M9 were on average 6.2 times greater than those of M8. In addition, the increased effluent flow rate is concentrated into a centralized area as opposed to being evenly distributed across the installation. This allows designers to identify areas of increased flows and implement protective practices to combat the increased erosive forces as opposed to not knowing where overtopping will occur. In order to minimize downstream erosive forces for M9, a riprap energy dissipater [Figure 4.11(c)] was installed along with a flow dispersion geotextile underlay [Figure 4.11(d)]. The implementation of these two components facilitated energy reduction in flow downstream of the dewatering weir which resulted in comparable downstream erosion rates for M9 and M8 [Figure 4.11(e) and 4.11(f)]. Soil erosion is less likely to occur in areas which vegetation has been established downstream of the dewatering weir; nonetheless, an energy dissipater should be installed to assist in soil stabilization. Figure 4.11(g) and Figure 4.11(h) show a silt fence field installation equipped with a dewatering weir.

(a) M9 sediment deposition

(b) M8 sediment deposition

(c) riprap energy dissipater

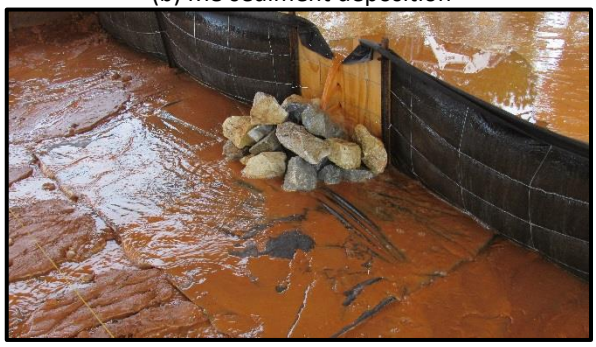

(d) geotextile flow dispersion

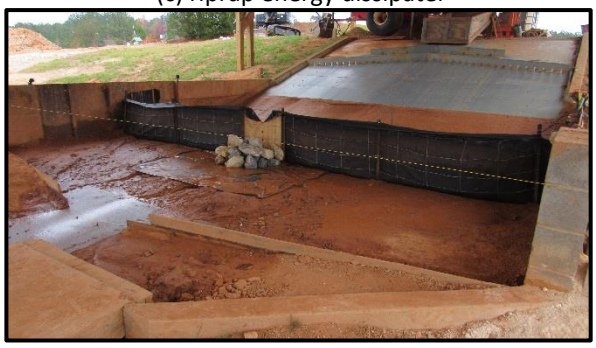

(e) M9 downstream erosion

(f) M8 downstream erosion

(g) field installation - downstream

(h) field installation - upstream

Figure 4.11. Dewatering weir performance comparison and field installation.

Sediment retention obtained during performance testing was 96% over four performance tests. This retention rate is comparable to the rates obtained from performance evaluations of

M7 and M8, which had an overall average of 96%. Nevertheless, the inherent advantage gained by incorporating a dewatering weir is time savings associated with discharging impounded stormwater. The dewatering weir installation was able to reduce dewatering time from 24+ hours (i.e., M7 and M8) to 4 hours (i.e., M9) when measured from the conclusion of the simulated storm event. Figure 4.12(a) provides an impoundment depth analysis of performance test 3 for M9 and M8. During the test period, the impoundment depth for M9 is slightly less than M8 until an impoundment of 1.5 ft (0.46 m) is achieved. Once the test period concludes and dewatering begins, the rate of depth change for M9 is considerably greater than M8. To quantify the differences between rates of change, a regression analysis was conducted to determine the theoretical time required for each to dewater completely based upon recorded impoundment depths over the dewatering period. The theoretical dewatering times for M9 and M8 were estimated at 4 hours (i.e., as observed during testing) and 2.3 days, respectively. Theoretical equations and R^2 values are shown in Table 4.5. As illustrated in Figure 4.12(b), the average discharge flow rate of M9 during dewatering was 6.2 times greater than M8. These finding indicate that M9 adequately impounds water upstream to facilitate sedimentation while also discharging flow in a time effective manner.

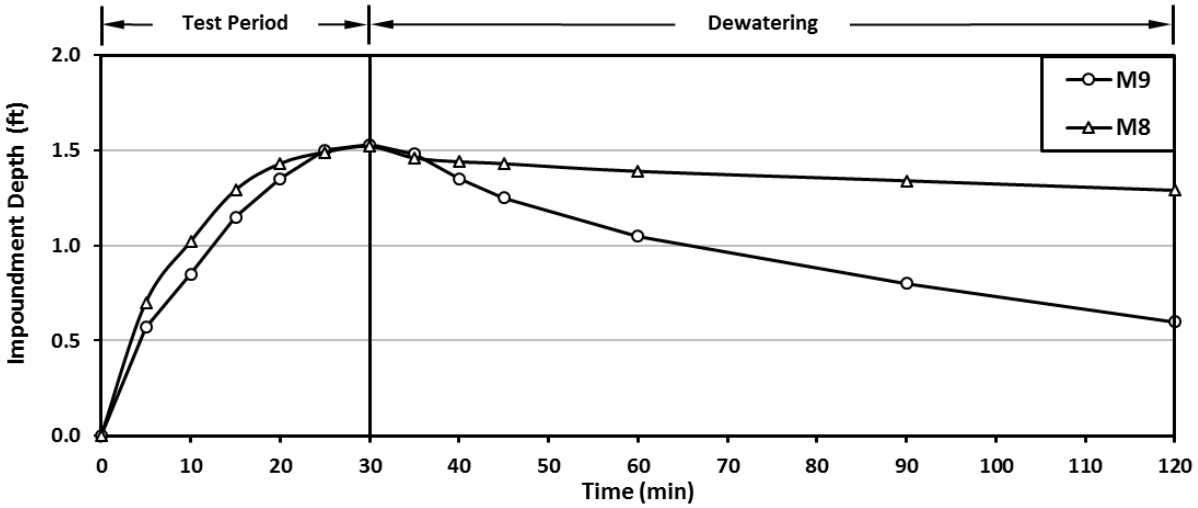

(a) impoundment analysis

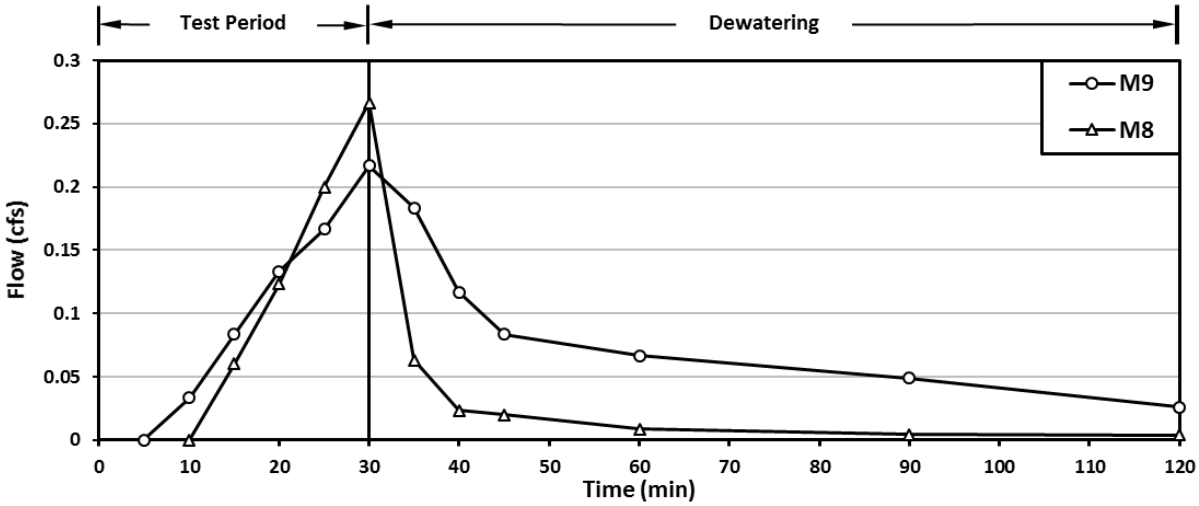

(b) flow rate analysis

Figure 4.12. Dewatering weir hydraulic comparison.

Table 4.5. Theoretical Dewatering Correlation Equations

Description	Regression Equation	R^2
M8	$y = 1635.2x^2 - 4998.6x + 3848.7$ **(Eq. 4.2)**	0.9972
M9	$y = -95.37ln(x) + 68.929$ **(Eq. 4.3)**	0.9931

Note: x = impoundment depth (ft); y = dewatering time (minutes)

To further evaluate the observed dewatering weir effluent flow rates, a theoretical effluent flow rate curve was developed based on the geometry of the orifices and v-notch weir. As shown in Figure 4.13(a), the curve provides a correlation between effluent flow and impoundment depth. Using the correlation and measured water depths, time variable

theoretical flow rates were generated and plotted along with measured time variable flow rates of M9, as shown in Figure 4.13(b). From the plot, it is evident that the peak effluent flow rate for measured flows is 32% larger than the peak theoretical flow. This difference is a result of flow passing through the geotextile fabric, which was not taken into consideration during theoretical flow calculations.

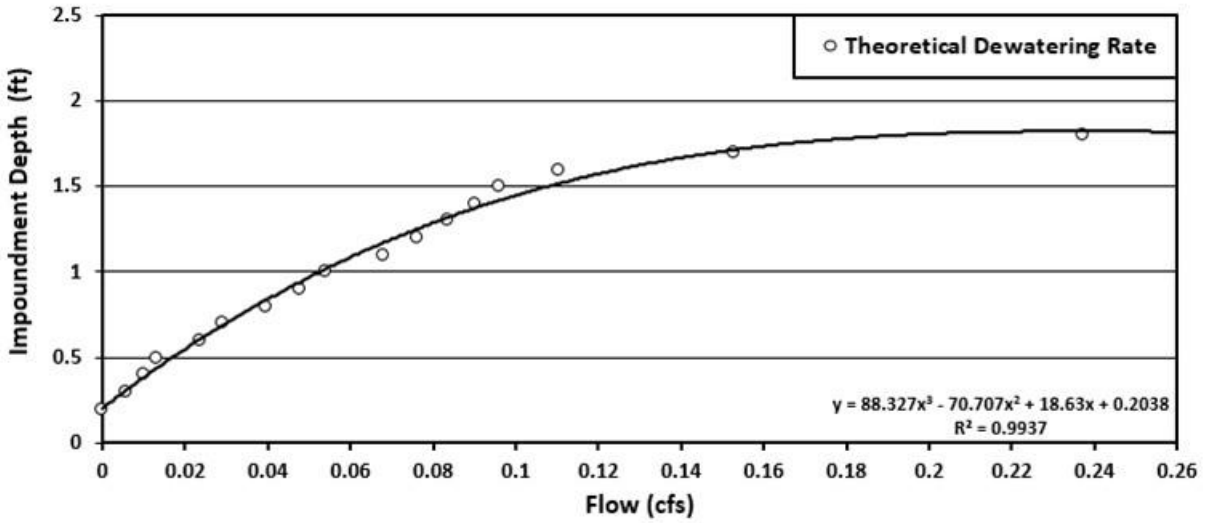

(a) theoretical dewatering curve

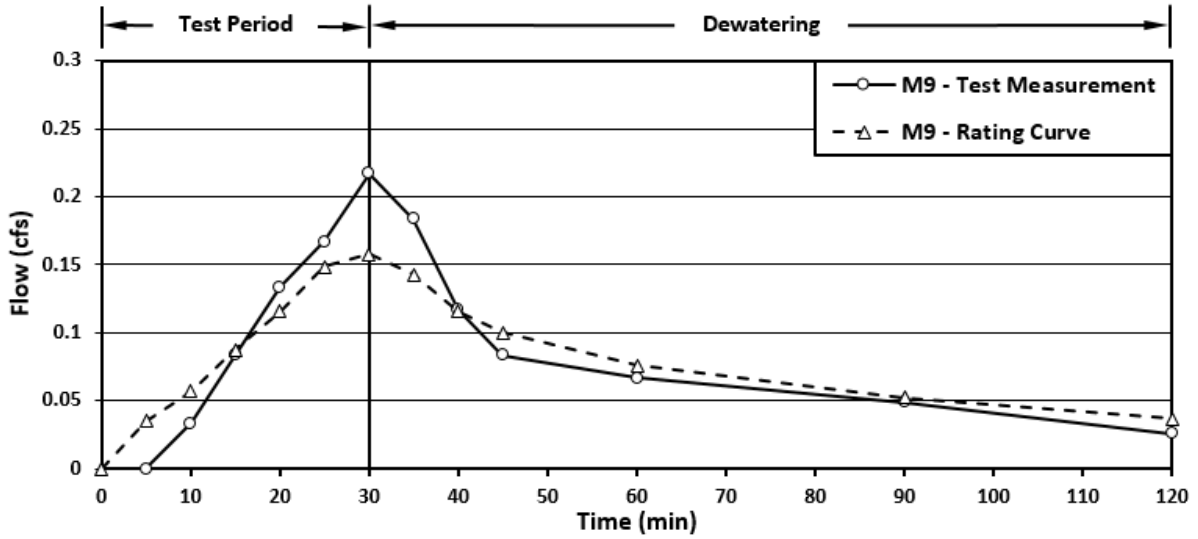

(b) theoretical flow verses measured flow

Figure 4.13. Dewatering weir theoretical flow analysis.

Figure 4.14 compares water quality from the surface of the impoundment and flow passing through the dewatering weir. The initial 5 minutes of testing consist of highly turbulent flow impoundment in which resuspension of sediment occurs. Between 5 and 10 minutes, a transition occurs in which turbulence is reduced due to increasing impoundment depth. At approximately 10 minutes, soil particle settlement within the impoundment enters a consistent state that improves slightly as impoundment increases. Once the simulated storm event concludes (i.e., 30 minutes into testing), water quality for each location quickly converge to an average of 944 NTU for the remaining samples. Overall water quality differences between the sample locations is relatively small when compared to the sediment-laden flow introduced during testing, which typical ranges between 10,000 and 15,000 NTU. Using the turbidity data obtained during the dewatering period, a water quality correlation was developed based on impoundment duration. The theoretical duration estimated to reduce turbidity to under 100 NTU by means of particle settlement was approximately 5 days. The theoretical correlation is reported as duration (min) = $2E+10^{8}x^{-2.213}$ (Eq. 4.4), where x is turbidity in NTU. R^2 is reports as 0.9674.

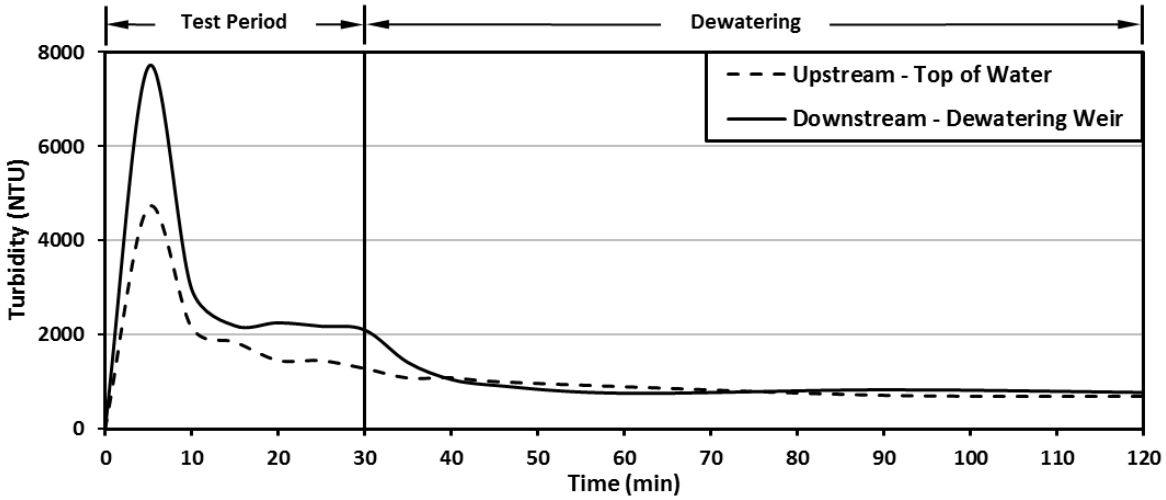

Figure 4.14. Dewatering weir water quality analysis.

4.8 SILT FENCE SUPPORT POST STRUCTURAL EVALUATION

While performance results indicate reduced T-post spacing and increased T-post weight provide enhanced structural stability to silt fence installations, conducting structural analyses on various support post types and sizes can provided additional design guidance for optimizing post selection and spacing. As shown in Table 4.6, a review was conducted to identify current silt fence design standards implemented within the southeastern region of the U.S., as well as within national design and testing standards. The review indicated that common T-post weights specified within these ESC documents range from 1.25 lb./ft (1.9 kg/m) to 1.33 lb./ft (2.0 kg/m) with post spacing ranging from 4 ft (1.2 m) to 10 ft (3.0 m).

Table 4.6. Commonly Accepted Silt Fence Design Standards

Specification Authority	T-Post Weight lb./ft (kg/m)	Yield Strength ksi (MPa)	T-Post Spacing ft (m) max	Fence Height in. (cm)	Trench Size in. by in. (cm by cm)
ALDOT	--	--	10 (3.0)	32 (81.3) min.	6 x 6 (15.2 x 15.2)
GSWCC	1.3 (1.9)	--	4 (1.2)	28 (72.1) min.	2 x 6 (5.1 x 15.2)
MDOT	1.33 (2.0)	--	10 (3.0)	26 (66.0) min.	6 x 6(15.2 x 15.2)
NC-SCC	1.25 (1.9)	--	8 (2.4)	24 (61.0) max	4 x 8 (10.2 x 20.3)
SCDOT	1.25 (1.9)	50 (345)	6 (1.8)	24 (61.0) min.	6 x 6 (15.2 x 15.2)
TNDOT	1.25 (1.9)	--	6 (1.8)	26 (66.0) min.	4 x 6 (10.2 x 15.2)
TxDOT	1.25 (1.9)	50.4 (347)	8 (2.4)	24 (61.0) min.	6 x 6 (15.2 x 15.2)
AL SWCC	1.3 (1.9)	--	10 (3.0)	32 (81.3) min.	6 x 6 (15.2 x 15.2)
TNEC	1.25 (1.9)	--	6 (1.8)	26 (66.0) min.	4 x 6 (10.2 x 15.2)
AASHTO M 288-15	1.32 (2.0)	--	4 (1.2)	29.5 –35.4 (74.9-89.9)	5.9 (15.0)[a]
ASTM A702-13	1.33 (2.0)	50 (345)	--	--	--
ASTM D6461/D6464M-16a	1.15 (1.7)	--	10 (3.0)	18–30 (45.7-73.2)	6 (15.2)[a]
ASTM D6462-03	1.3 (1.9)	--	4 (1.2)	24 (61.0) min.	4 x 8 (10.2 x 20.3)

Note: [a] = trench width not specified; -- = specification not available; 1 lb./ft = 1.49 kg/m; 1 ksi = 6.89 MPa; 1 ft = 0.3 m; 1 in. = 2.54 cm

Although these guidelines are considered proper silt fence designs by local and state compliance agencies, it is not uncommon in current practice to see silt fence installations

performing inadequately. A contributor of poor performance is the lack of structural design considerations for common in-field hydraulic loading scenarios.

To address this issue, structural analyses were performed on common silt fence support posts to provide post spacing based on maximum structural capabilities and maximum anticipated impoundment depth. Support post selected for evaluation included three steel T-post (i.e., 0.95, 1.25, & 1.33 lb./ft (1.4, 1.9, and 2.0 kg/m)) and two hardwood post (1.3 in. x 1.6 in. and 1.8 in. x 1.8 in. (3.3 cm x 4.1 cm and 4.6 cm x 4.6 cm)).

Structural load tests were conducted using a GEOTAC Sigma 1^{TM} automatic load test system outfitted with a Tinius Olsen three-point bending frame. As shown in Figure 4.15, post specimens were placed in the frame and loaded until plastic yielding or failure occurred.

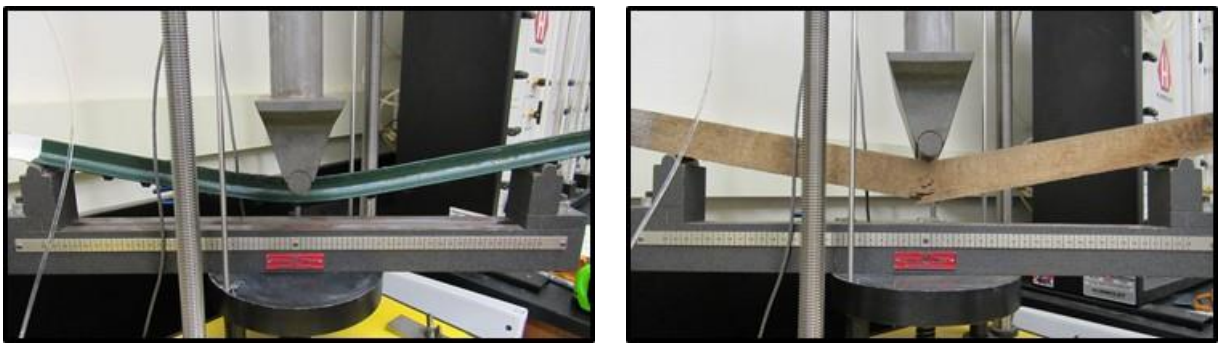

(a) steel T-post (b) hardwood post

Figure 4.15. Three point loading test.

During testing, specimens were loaded in 100 lb. (45.4 kg) increments and midpoint deflections were recorded. Five specimens were evaluated for each support post size/type and average results were plotted to identify the limit state load at which yielding or failure occurred. As shown in Figure 4.16, nonlinear yielding begun at a loading of 400, 600, and 700 lb. (181, 272, and 318 kg) for steel T-post weights of 0.95, 1.25, and 1.33 lb./ft (1.4, 1.9, and 2.0 kg/m), respectively. The limit state load for each hardwood post was 1600 lb. (726 kg), which was the

load at which failure (i.e., breaking) occurred. To use this information to identify maximum load capacity for silt fence installations, limit state moments were calculated using Equation 4.5. Calculated limit state moments for steel T-posts were 200, 300, and 350 lb.-ft (27.7, 41.5, and 48.4 kg-m), respectively, and 800 lb.-ft (110.6 kg-m) for hardwood.

$$M = \frac{PL}{4} \qquad \text{(Eq. 4.5)}$$

Where,

M = limit state moment (lb.-ft)

P = limit state load (lb.)

L = length between Tinius Olsen bending frame outer supports (i.e., 2 ft)

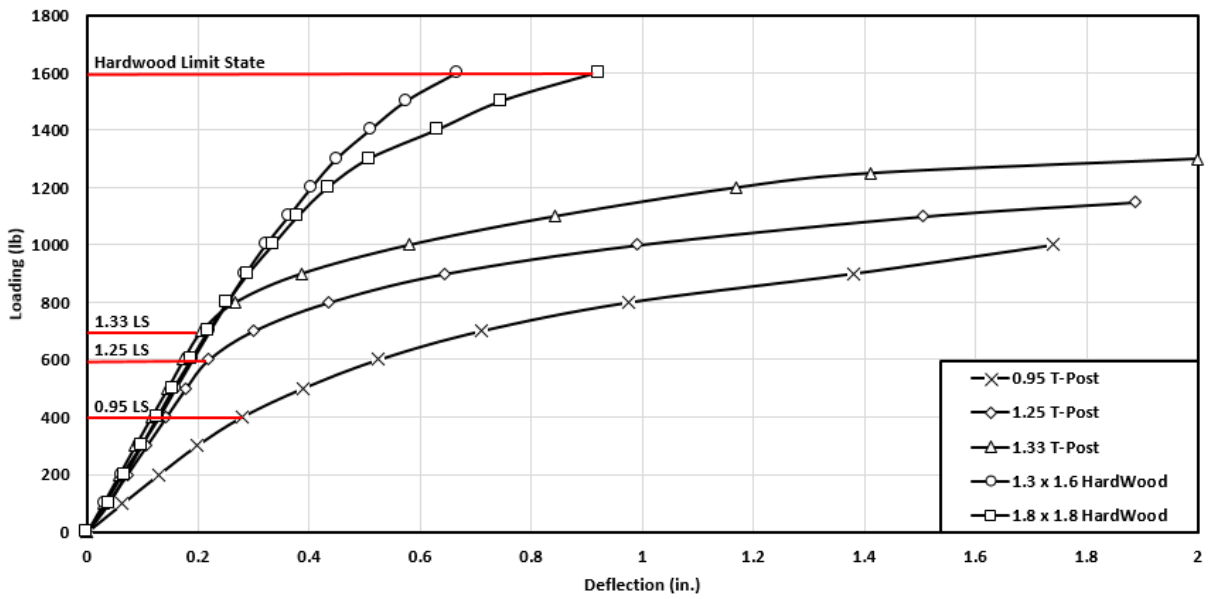

Figure 4.16. Silt fence support post limit state loading analysis.

The next step towards identifying optimum post spacing is to visualize load distribution on a silt fence installation and determine the equations needed for calculating post spacing. Figure 4.17 illustrates how hydrostatic load transfers to silt fence installations, as well as the

associated terms that represent impoundment depth (h), magnitude of the maximum distributed load (w), and distributed load width (s).

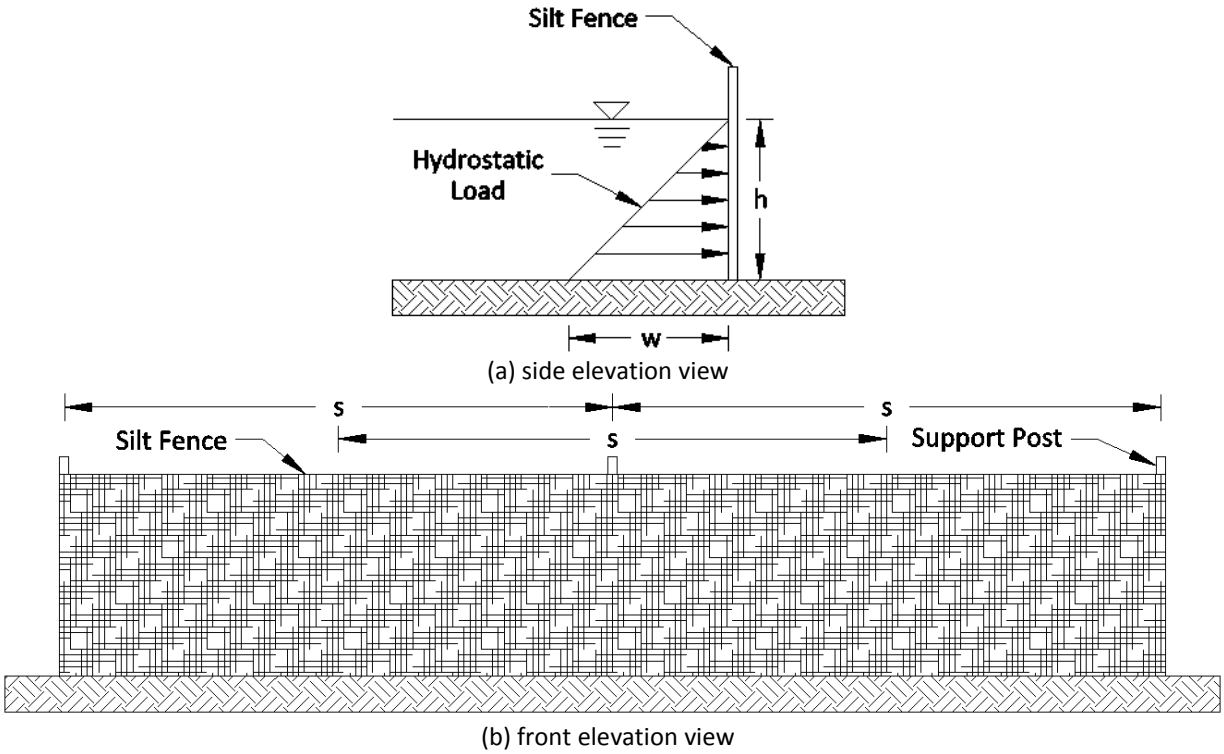

Figure 4.17. Hydraulic loading schematic.

As shown in Equation 4.6, distributed load is calculated by multiplying water density (ρ_w), impoundment depth (h), and the width of the distributed load (s). An impoundment depth of 1.5 ft (0.46 m) was selected based on the water quality evaluations that suggest impoundment depths greater than 1.5 ft (0.46 m) provide little water quality improvements. Additional discussion on the selected impoundment depth is provided in the water quality section of Chapter 5. For silt fence installations, the width of the distributed load applied to a single support post is equal to the sum of half the distance between each adjacent support post, which is also equal to the selected post spacing, as illustrated in Figure 4.17(b). This equation can then be substituted into Equation 4.7, which determines the maximum moment placed on a cantilevered

support with a triangular load distribution. Solving for post spacing (s), Equation 4.8 is obtained allowing post spacing to be calculated based on maximum moment (i.e., limit state moment), water density, and impoundment depth.

$$w = \rho_w h s \quad \text{(Eq. 4.6)}$$

$$M = \frac{\boldsymbol{wh^2}}{\boldsymbol{6}} \quad \text{(Eq. 4.7)}$$

$$s = \frac{\boldsymbol{6M}}{\boldsymbol{\rho_w h^3}} \quad \text{(Eq. 4.8)}$$

Where,

w = distributed load (lb./ft)
ρ_w = density of water (e.g., 62.4 lb./ft^3)
h = maximum impoundment depth (e.g., 1.5 ft)
s = post spacing (ft)
M = limit state moment (lb.-ft)

Using Equation 4.8 and the limit state moments determined from three-point bending tests, steel T-post spacing were calculated to be 5.7, 8.5, and 10.0 ft (1.7, 2.6, and 3.0 m) for each T-post size of 0.95, 1.25, and 1.33 lb./ft (1.4, 1.9, and 2.0 kg/m), respectively. Hardwood post spacing was considerably greater than T-post spacing at 22.8 ft (6.9 m). While these values are based on maximum load capacity prior to failure, they do not factor in soil compaction, post embedment depth (i.e., 18 in. versus 24 in.), post installation location (i.e., in the trench or 6 in. downstream of the trench), or potential fence sag between supports during hydrostatic loading. To factor in these common variations, calculated T-post spacing was reduced by 30% and hardwood posts spacing was reduced by 80%. While these reduction factors are subjectively

based on structural observations made throughout silt fence modification testing, they do provide a foundation for beginning the optimization of silt fence designs. Prior to field implementation, full-scale performance evaluations need to be conducted to verify structural integrity of these posts spacing recommendations. A summary of the results obtained from structural evaluations and recommended posts spacing are shown in Table 4.7.

Table 4.7. Support Post Structural Analysis Summary

Post Type	Size Steel (lb./ft) Wood (in. x in.)	Limit State Load (lb.)	Limit State Deflection (in.)	Limit State Moment (lb.-ft)	Calculated Post Spacing (ft)	Recommended Post Spacing (ft)
Steel T-Post	0.95	400	0.28	200	5.7	4
Steel T-Post	1.25	600	0.22	300	8.5	6
Steel T-Post	1.33	700	0.21	350	10.0	7
Hardwood	1.3 x 1.6	1600	0.67	800	22.8	5
Hardwood	1.8 x 1.8	1600	0.92	800	22.8	5

4.9 SUMMARY

Current wire-backed, nonwoven silt fence installation practices implemented by ALDOT lack the structural ability to create and sustain impoundments required to promote sedimentation. The hydrostatic loading imposed on an installation by an impoundment may cause structural failures, thus resulting in untreated sediment-laden stormwater discharges to the surrounding environment. The research team at the AU-ESCTF evaluated the structural performance of eight silt fence installation configurations and demonstrated that a structurally sound silt fence practice is achievable.

The information obtained through this study shows that increasing T-post weight and decreasing T-post spacing significantly improves the structural integrity of silt fence installations by reducing T-post deflection by 62%. Additionally, reducing fence height and implementing an offset trench can further reduce T-post deflection by 33%. From an installation standpoint, offset

trenching allows for mechanical compaction, which ultimately has the potential to reduce the occurrence of scouring and undermining. Observations made during testing suggest additional filter fabric support can be achieved by looping fabric over each T-post, which reduces the extent of fence sag between posts. The volumetric analysis conducted on retained sediment shows that structurally sound silt fence installations have a sediment retention rate of 95% as opposed to 83% for those that overtop. Water quality data indicated that as impoundment depth increased, water turbidity along the surface of the impoundment and downstream of the silt fence was reduced by 56% when compared to turbidity levels along the bottom of the impoundment. Based on all findings, modification 8 had the best overall performance characteristics of the installation variations tested. As this installation method only varies in approach and not necessarily in equipment and effort needed, this method can easily be applied in field applications with minimal training of personnel to improve silt fence structural performance. Structural performance and retention efficiency of field installations can be effectively increased by implementing routine inspections and conducting preventive maintenance by removing accumulated sediment after storm events. The incorporation of a dewatering mechanism, such as a dewatering weir, greatly reduces dewatering time while also achieving desired performance characteristics (i.e., improved sediment retention and water quality). Reduced dewatering periods facilitate soil drying, which in turn allows site operations to resume in a timely manner. Finally, analyses conducted on silt fence support posts provided a means for identifying optimum spacing based on structural capabilities of various support post types/sizes prior to nonlinear yielding or failure. Results suggest that optimum T-posts spacing range from 4 to 7 ft. (1.2 to 2.1 m), depending upon T-post weight, and 5 ft (1.5 m) post spacing for hardwood posts. The data presented in this chapter

provides enhanced silt fence design guidance, which practitioners can consider to improve upon current practice standards.

CHAPTER FIVE:
PERFORMANCE EVALUATIONS OF INNOVATIVE AND MANUFACTURED SEDIMENT BARRIER PRACTICES

5.1 INTRODUCTION

This chapter describes the design characteristics of innovative and manufactured sediment barrier (SB) practices, recommended installation guidelines, and the results of performance evaluations. Structural and material properties outlined for each SB is based on manufacturer's published product specifications. The aim for presenting this information is to provide insight into the vast array of products and materials currently available to the erosion and sediment control (ESC) industry. Installation guidelines provide guidance as to how each practice is constructed in field applications and the associated installation effort. Performance evaluations offer an unprecedented means for side-by-side comparisons of SB practices, as well as a scientifically backed approach for identifying and improving inefficiencies associated with each.

The purpose for these experimental tests are to evaluate the overall performance capabilities of innovative and manufactured SB practices. Evaluations are based on installation feasibility, structural integrity, impoundment capability, effluent flow rate, sediment retention, and filtering capability. The innovative and manufactured SB practices selected for testing were grouped into three categories: (1) manufactured silt fence systems, (2) sediment retention barriers (SRBs), and (3) manufactured SB products. The practices that fall into each of these

categories were selected for testing based on ALDOT perimeter control needs identified by the Project Advisory Committee (PAC).

5.2 MANUFACTURED SILT FENCE SYSTEMS

Though silt fence is a common practice used on construction sites, a subcategory of silt fence is what will be referred to as "manufactured silt fence systems." These two dimensional manufactured systems have fabric attached to reinforcement and support posts prior to distribution for sale. Therefore, only installation is required with no site assembly necessary. A component of this research study was to evaluate two manufactured silt fence systems. The tested practices included Georgia Type C-Polypropylene on Polypropylene (C-POP) [Figure 5.1(a)] and Silt Saver-Stage Release Silt Fence (SRSF) [Figure 5.1(b)]. The C-POP system was tested per the Georgia Soil and Water Conservation Commission (GSWCC) (*2016*) installation details for type C silt fence and the SRSF system was tested per the manufacturer's installation details and instruction. No attempts or iterations were made to improve the product's installation that would modify the design or fabrication of the systems. Currently, there are no manufactured silt fence systems approved for use as perimeter controls on ALDOT projects (*ALDOT 2018*).

(a) C-POP

(b) Silt Saver SRSF

Figure 5.1. Manufactured silt fence systems.

5.2.1 C-POP SEDIMENT BARRIER SYSTEM

The C-POP SB system [Figure 5.2(a)] is a manufactured perimeter control device assembled within a factory environment prior to site delivery. The system is comprised of woven polypropylene geotextile, polypropylene support mesh, and hardwood posts. The woven geotextile fabric is 36 in. (91.4 cm) wide with a consistent monofilament weave texture throughout and conforms to the Georgia Department of Transportation (GDOT) Type C silt fence specification, which are shown in Table 5.1. Support mesh extends the entire width of the geotextile fabric and has an apparent opening size (AOS) of 0.9 in. (2.3 cm) by 1.45 in. (3.7 cm). The reinforcement is necessary because this system is classified for sensitive applications in which the geotextile fabric may be exposed to particularly high flows or where slopes exceed 10 ft (3 m) in vertical height (*GSWCC 2016*). The system is supported by 2 in. (5.1 cm) by 2 in. (5.1 cm) hard wood posts that have a minimum length of 4 ft (1.2 m). Post are spaced 4 ft (1.2 m) on-center and attached to the geotextile fabric and support mesh via 17 gauge (1.14 mm) by 0.5 in. (1.3 cm) wire staples. Each post is required to have five wire staples supporting the geotextile fabric and mesh. Wire staple placement for each post is illustrated in Figure 5.2(b).

Table 5.1. GDOT Type C Geotextile Specifications (*GSWCC 2016*)

Property	Test Method	Requirement
Tensile Strength (lb. min.)	ASTM D4632	MD 260 XMD 180
Elongation (% max)	ASTM D4632	40
AOS (max. sieve size)	ASTM D4751	#30
Flow Rate (gal/Min./ft^2)	GDT-87	70
UV Stability (% retained @ 300 hr)	ASTM D4355	80
Bursting Strength (psi min.)	ASTM D3786	175

Note: AOS = apparent opening size; MD = machine direction, XMD = cross machine direction

Installation details shown in Figure 5.2(c) and 5.2(d) illustrate that posts should be driven a minimum of 18 in. (45.7 cm) into the ground and be exposed a minimum of 30 in. (76.2 cm) above the ground surface. The geotextile height is not specified in the details but typical systems are assembled with 28 in. (71.1 cm) of geotextile attached above the ground surface. The geotextile is secured in the ground by entrenching the fabric 6 in. (15.2 cm) deep by 2 in. (5.1 cm) horizontally and compacting the backfill material. This process minimizes the occurrence of flow bypass underneath the installation during storm events.

(a) system installation

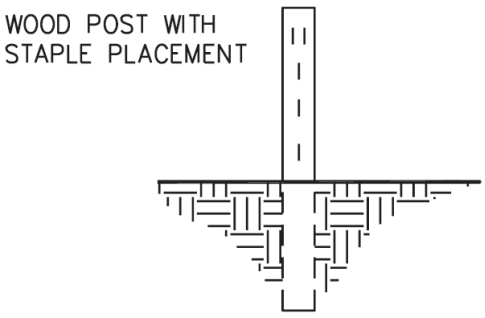

(b) staple placement

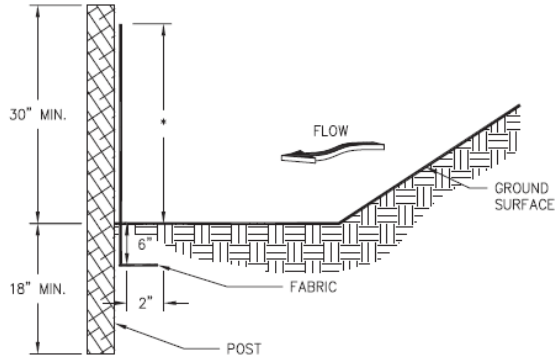

(c) side view

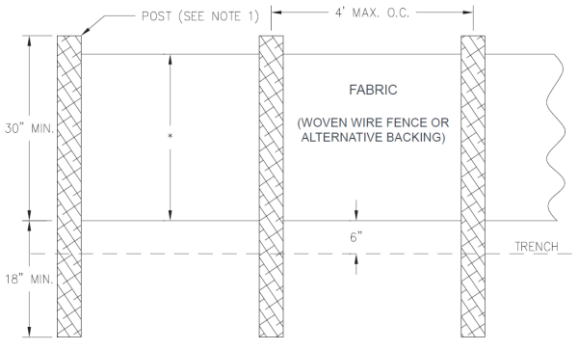

(d) front view

Figure 5.2. Georgia type C silt fence product details. (*GSWCC 2016*)

5.2.2 SILT-SAVER (SILT-SAVER®, INC.) STAGE RELEASE SILT FENCE

The Silt Saver-Stage Release Silt Fence (SRSF) is a silt fence system that allows increased flow-through capacity of stormwater runoff as impoundment depth increases upstream of the practice. This manufactured product is made of a woven monofilament geotextile that incorporates five slit-film spacing specifications in the machine direction based on horizontal regions. As shown in Figure 5.3(a), the geotextile is divided into five zones with woven reinforcement belts separating each. Zone A is the portion of geotextile that is entrenched during installation, while Zones B-E capture and impound stormwater runoff. The flow rate associated with each of the impoundment zones increases with depth, as shown in Table 5.2. Interwoven reinforcement belts (green belts) provide structural support to the systems, as the slit-film strands within the belted regions are denser than each of the zones. As with the C-POP system,

support in provided by 2 in. (5.1 cm) by 2 in. (5.1 cm) hard wood posts that have a minimum length of 4 ft (1.2 m) and spaced 4 ft (1.2 m) on center. As shown in Figure 5.3(b), the geotextile is attached to support posts using 1 in. (2.54 cm) by 1.25 in. (3.18 cm) wire staples and a wood bonding strip, which distributes the support force applied with each wire staple.

Table 5.2. Silt Saver – SRSF Geotextile Specification (*Silt Saver 2015*)

Property		Zone A	Zone B	Zone C	Zone D	Zone E
Zone Width (in.)		11.75	6.75	5.25	5.00	3.25
Tensile Strength (lb.)	MD	458	537	458	420	301
	XMD	234	254	234	238	209
AOS (US sieve size)		20	40	20	20	20
Flow Rate (gal/Min./ft^2)		210	141	210	235	324

Note: MD = machine direction; XMD = cross machine direction

The installation details for the SRSF are slightly different from that of GDOT. Figure 5.3(c) and 5.3(d) illustrate a post depth of 22 in. (55.9 cm) below ground and a post height of 26 in. (66.0 cm) above the ground surface. Geotextile height is 24 in. (61.0 cm) with an entrenchment of 8 in. (20.3 cm) deep by 4 in. (10.2 cm) horizontal with compacted backfill. Additionally, the detail specifies that the silt fence system should be installed 10 ft (3.0 m) from the toe of the upstream slope. This provides an adequate upstream impoundment pool to facilitate particle sedimentation. However, in order to compare performance results from SRSF testing with other practices, a 6 ft (1.8 m) installation distance from the toe of the impervious test slope was used.

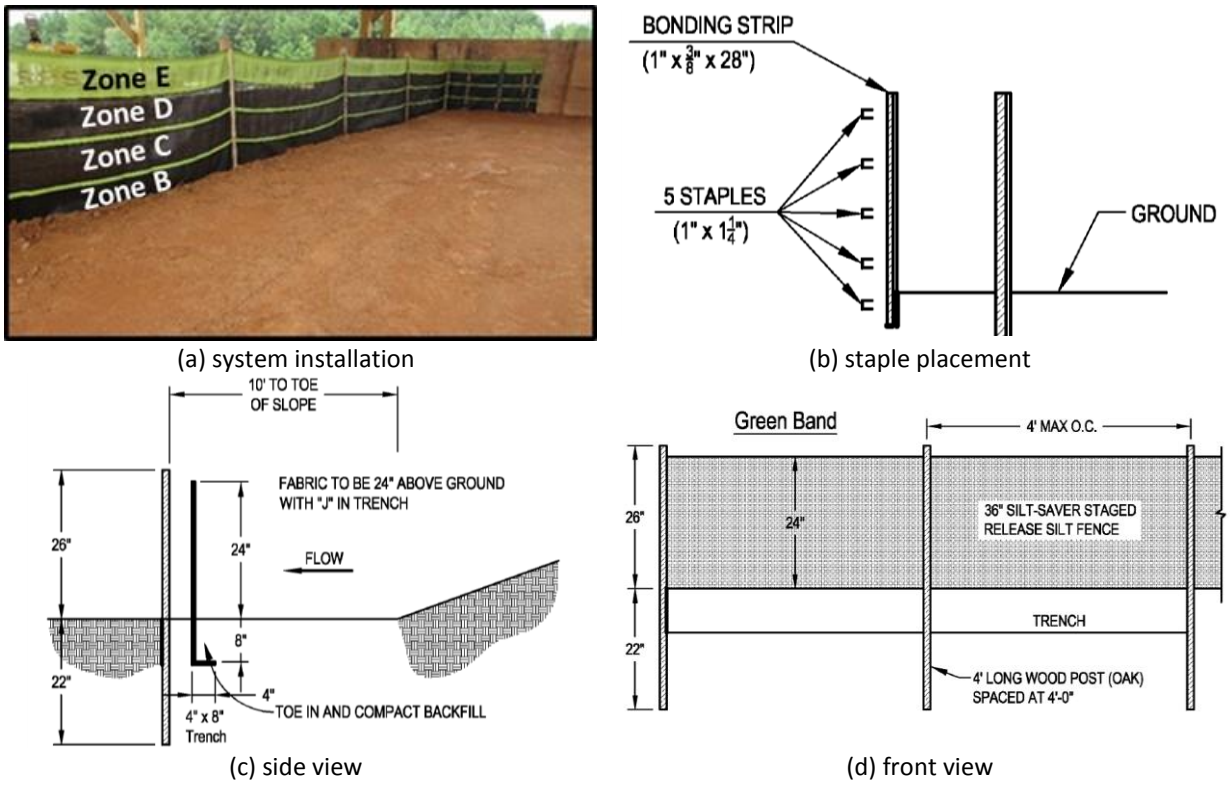

(a) system installation (b) staple placement

(c) side view (d) front view

Figure 5.3. SRSF product details. (*Silt Saver 2015*)

5.3 SEDIMENT RETENTION BARRIERS (SRB)

SRBs are designed to provide additional treatment to stormwater runoff above that of a single silt fence installation. Traditional silt fence installations treat stormwater using a single geotextile installed in a planer dimension. Once flow passes the geotextile, additional improvements to water quality are dependent on natural sediment removal processes such as vegetated buffers. SRBs apply a multi-faceted approach in which an additional dimension is incorporated to facilitate improved effluent water quality. Performance evaluations were conducted on three SRBs, which include: (1) Alabama Department of Transportation (ALDOT) SRB, (2) Alabama Handbook (AL HB) SRB without flocculant, and (3) AL HB with flocculant. Installations followed the ALDOT and AL HB design specifications and no attempts were made to enhance the installation or performance of the SRBs. Common materials used throughout testing

to construct each of the different types of SRBs are pictured in Figure 5.4(a) through (h). The nonwoven geotextile fabric [Figure 5.4(c)] was only used during ALDOT SRB testing while jute matting [Figure 5.4(d)] and polypropylene netting [Figure 5.4(e)] were only used during AL HB SBR testing.

(a) studded T-post

(b) reinforcing wire

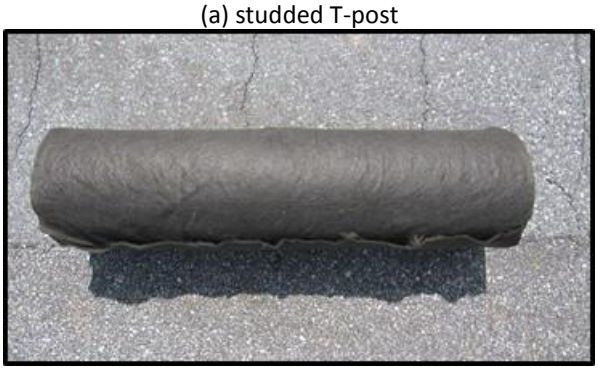

(c) nonwoven geotextile fabric

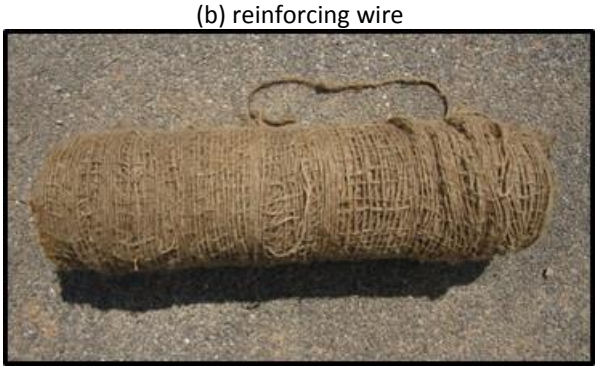

(d) jute matting

(e) polypropylene netting

(f) wheat straw bales

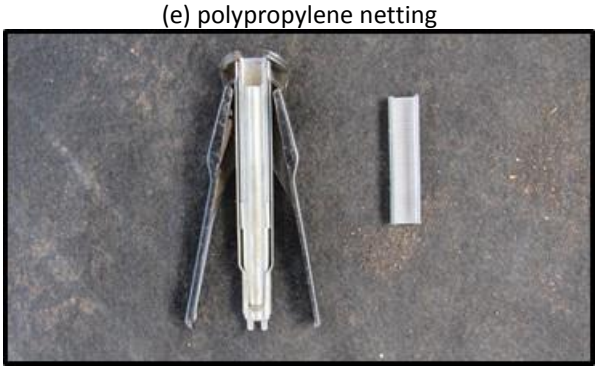

(g) c-ring clips

(h) aluminum wire ties

Figure 5.4. Common SRB installation materials.

5.3.1 ALDOT SRB

The ALDOT SRB is an alternative to the ALDOT silt fence practice, in that it can be implemented in areas down grade of newly graded fill slopes and adjacent to streams and channels where overland flow is low to moderate. The installation and details shown in Figure 5.5(a) through (c) consist of two ALDOT silt fence installations running parallel with staggered wheat straw bales placed tightly between the fences. Silt fence installation details associated with the SRB are the same as a single ALDOT silt fence installation. Each SRB silt fence is installed in a 6 by 6 in. (15.2 by 15.2 cm) trench using 0.95 lb./ft (1.4 kg/m) T-posts spaced 10 ft (3.0 m) on center and driven 24 in. (61 cm) into the ground. Reinforcing wire is placed in the trench and secured to T-posts using wire clips. The geotextile is secured to the wire reinforcement using c-ring clips spaced 24 in. (61 cm) on center. The geotextile is placed in the trench in a "J" configuration and backfilled with soil. This installation requires stormwater runoff to pass through two nonwoven silt fence installations, as well as wheat straw bales prior to site discharge.

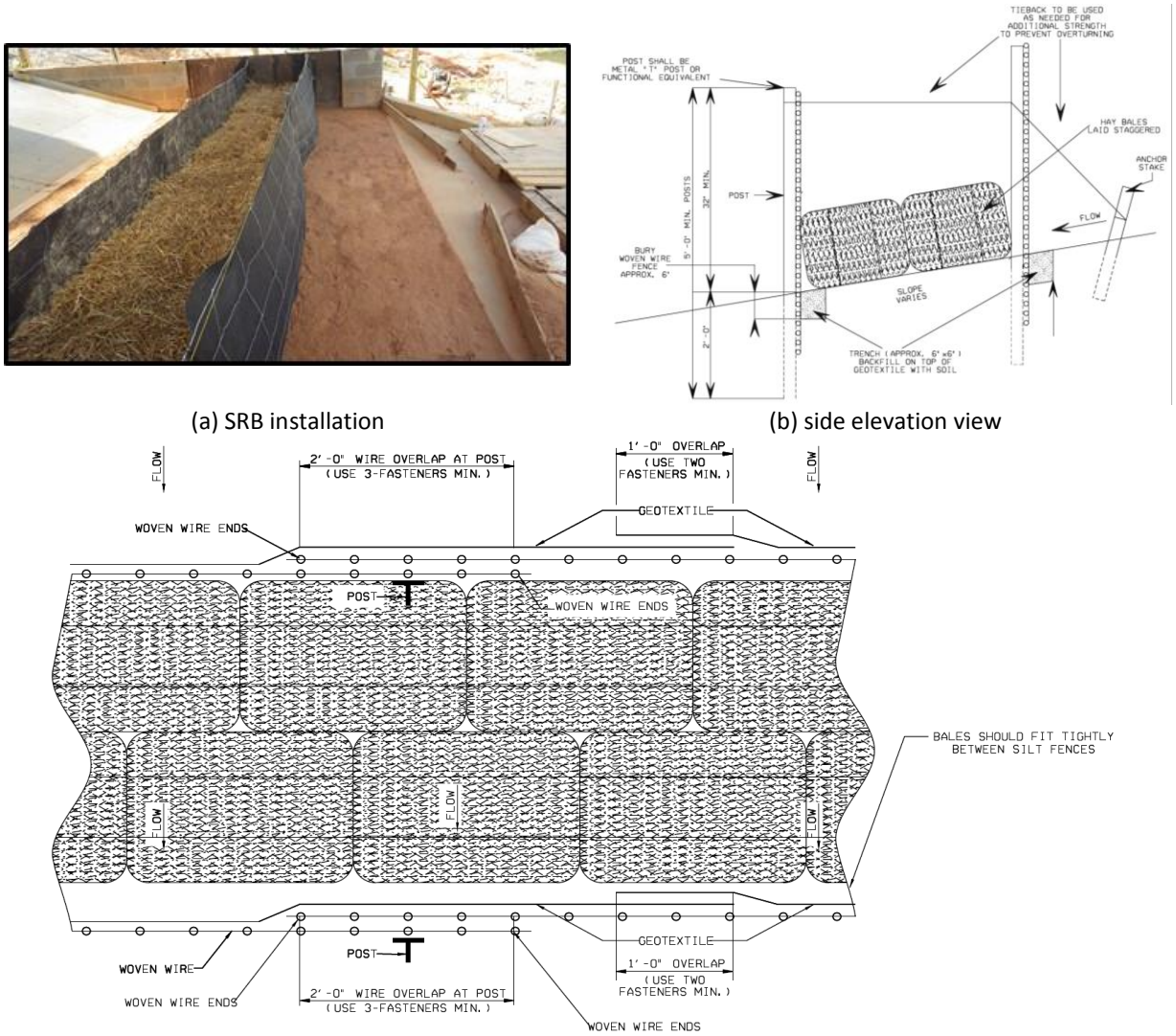

(a) SRB installation (b) side elevation view

(c) plan view

Figure 5.5. ALDOT SRB installation details. (*ALDOT 2017*)

5.3.2 ALABAMA HANDBOOK SRB

The Alabama Handbook SRB (herein referred to as the AL HB SRB) resembles a double row silt fence installation but is only intended to be used as a polishing tool to reduce turbidity in stormwater discharged to sensitive areas. It should not be used as a replacement or alternative for perimeter controls. The SRB information provided within the AL HB is limited regarding materials and installation guidelines, thus manufacturers and distributors who have experience with SRB practices were consulted to development an effective installation method. The

resulting practice consists of two parallel rows of 0.5 in. (1.3 cm) polypropylene netting supported by wire reinforcement and 0.95 lb./ft (1.4 kg/m) T-posts spaced 6 ft (1.8 m) on center. Jute matting was installed along the ground surface between the parallel rows, as well as downstream of the installation to facilitate sediment capture. Loose wheat straw was placed on top of the jute matting in 6 in. (15.2 cm) lifts between the parallel rows of netting to a depth of 24 in. (61.0 cm). Evaluations were conducted on configurations of the installation that did and did not incorporated granulated flocculant powder. When adding flocculant to the SRB, manufactures recommendations should be followed to insure proper application rates. During flocculant testing, APS 700 Series Silt Stop Powder was applied between the double rows of netting at a rate of 0.67 lb./ft (1.0 kg/m) of SRB. This granulated flocculant was anionic (i.e., negatively charged), which has not been proven to harmfully affect aquatic life (*Peng and Di 1994*, *Qian et al. 2004*, *USEPA 2005*, *Sojka et al. 2007*). Flocculant was placed in five lifts (i.e., on top of jute matting and on top of each wheat straw layer) to achieve an even distribution within the medium. Additionally, flocculant was applied on top of the jute matting downstream of the practice at a rate of 25 lb./ac (28 kg/ha). Field applications of this practice should insure an adequate perimeter control practice be installed downstream to removed flocculated sediment from the treated stormwater discharge. This system should not be used directly upstream of flow conveyance systems, such as creeks and streams, due to insufficient means of offsite sediment capture. Figure 5.6(a) through (d) illustrates the AL HB SRB installation and associated details followed during performance evaluations.

(a) SRB installation

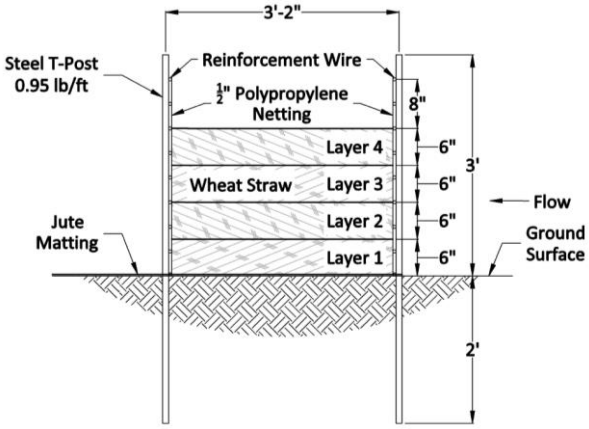

(b) side elevation view

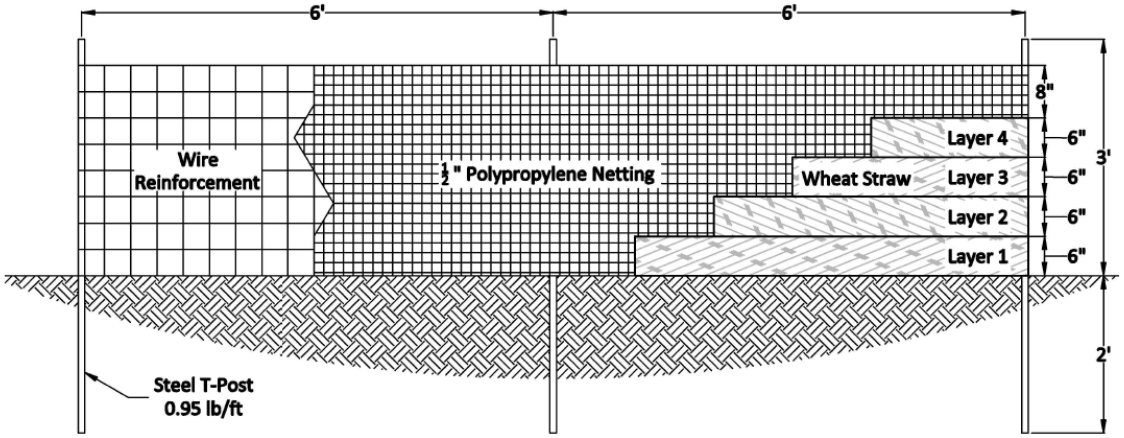

(c) front elevation view

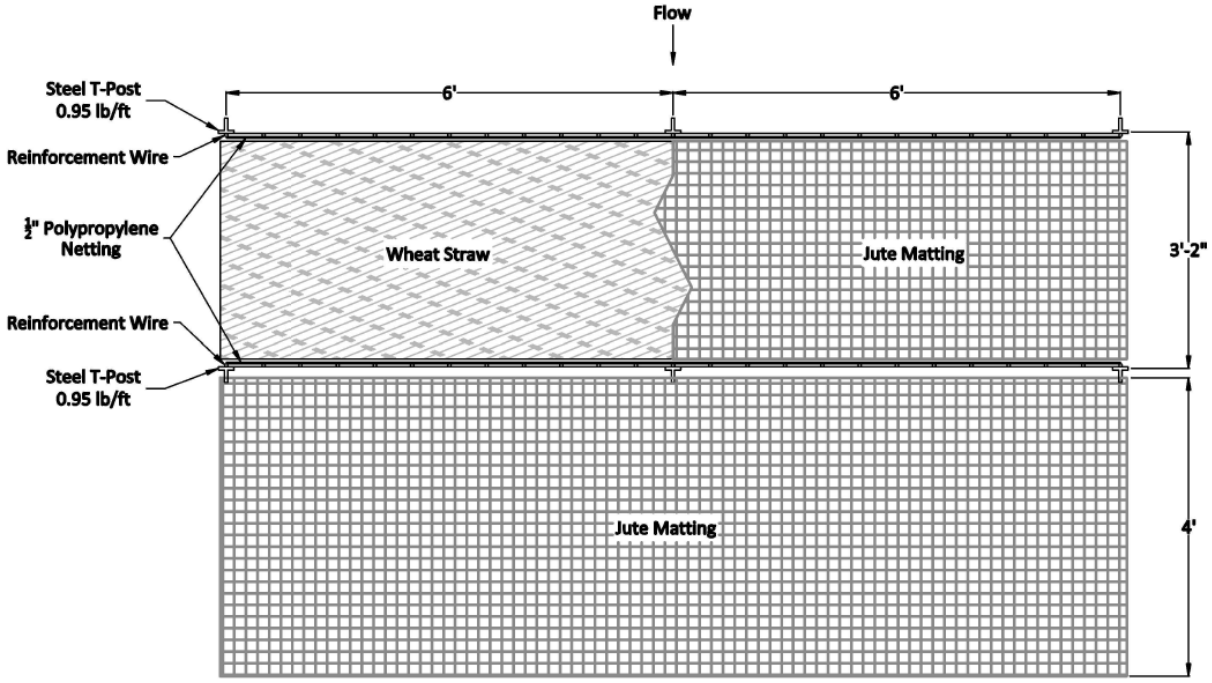

(d) plan view

Figure 5.6. Alabama Handbook SRB details.

5.4 MANUFACTURED SEDIMENT BARRIER PRODUCTS

The erosion and sediment control industry has a vast array of proprietary products that can be installed as perimeter control devices. The ALDOT Standard Drawings detail three specific perimeter control practice installations, which consist of silt fence, SRBs, and temporary brush barriers (*ALDOT 2017*). The exception to these standard drawing details is the inclusion of a 20 in. (50.8 cm) wattle, within a silt fence installation, as a water release mechanism. The ALDOT Standard Specifications for Highway Construction state that SBs installed adjacent to construction limits or along live streams may consist of silt fence, hay bales, sandbags, silt dikes, or wattles (*ALDOT 2016*). However, the ALDOT Temporary Erosion and Sediment Control Products List II-24 does not provide a section indicating approved products for perimeter control applications (*ALDOT 2018*). Due to limited guidance regarding sediment control product applicability (e.g., ditch check, inlet protection, and perimeter control), SB evaluations were conducted on three proprietary sediment control devices to determine overall performance characteristics and limitation when installed as a perimeter control. The tested products included: (1) Western Excelsior – Excel Straw Logs™, (2) Filtrexx® – SiltSoxx™, and (3) American Excelsior – Curlex® Bloc. Manufactured products were tested under modified installation details to facilitate upstream impoundment and minimize flow bypass; however, no attempts were made to improve the design or fabrication of the product itself. Currently, the Western Excelsior – EXCEL Straw Log and Filtrexx – Siltsoxx are approved wattles for use on ALDOT projects (*ALDOT 2018*) per ALDOT List II-24.

5.4.1 WESTERN EXCELSIOR – EXCEL STRAW LOGS™

Western Excelsior – Excel Straw Logs are designed to be implemented as slope interrupters, ditch checks, and inlet protection practices. Excel straw logs are available in 9, 12, 18, and 20 in. (23, 30, 46 and 51 cm) diameters and 10, 20, and 25 ft (3.0, 6.0, and 7.6 m) lengths. Manufacturing is achieved by filling a 0.5 by 0.5 in. (1.3 by 1.3 cm) tubular heavy duty synthetic net with a straw fiber matrix until the specified diameter density is achieved. Each end of the log is securely closed using hog rings clips (*Western Excelsior 2017*).

ALDOT currently does not have a standard installation detail for wattles installed as perimeter controls; however, standard installation details for wattles used as ditch checks and inlet protection are available (*ALDOT 2017*). In each of these details, wattles are installed on top of the ground surface using a teepee-staking pattern. The main difference between the two installations is the inclusion of a geotextile underlay when installed as a ditch check. The manufacturer's published perimeter guard installation detail illustrates placing the straw log in a 3 in. (7.6 cm) deep trench and backfilling (*Western Excelsior 2018*). Once compaction is achieved, wood stakes are driven through the center of the straw log and imbedded 12 in. (30.5 cm) into underlying soil. Considering each of these details as a feasible installation technique, a hybrid installation approach was developed that incorporated teepee staking and trenching [Figure 5.7(a)]. This installation procedure is shown in Figure 5.7(b) and was implemented during performance evaluations of installations I1 and I2. To evaluate an additional installation strategy, trenching was eliminated and a geotextile underlay was incorporated, as shown in the ALDOT ditch check detail, during the performance evaluation of installation I3. The manufacturer's installation details do not specify wood stake spacing; however, ALDOT required a 2 ft (0.6 m)

stake spacing. Thus, a 2 ft (0.61 m) stake spacing was implemented during performance evaluations, as shown in Figure 5.7(c).

(a) product installation

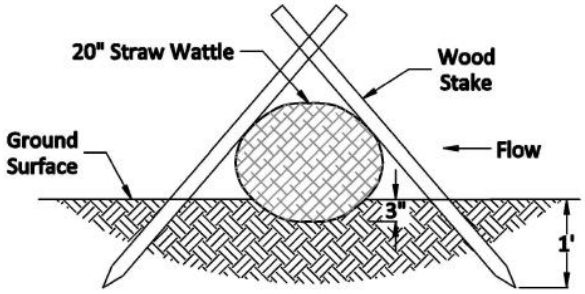

(b) side elevation view

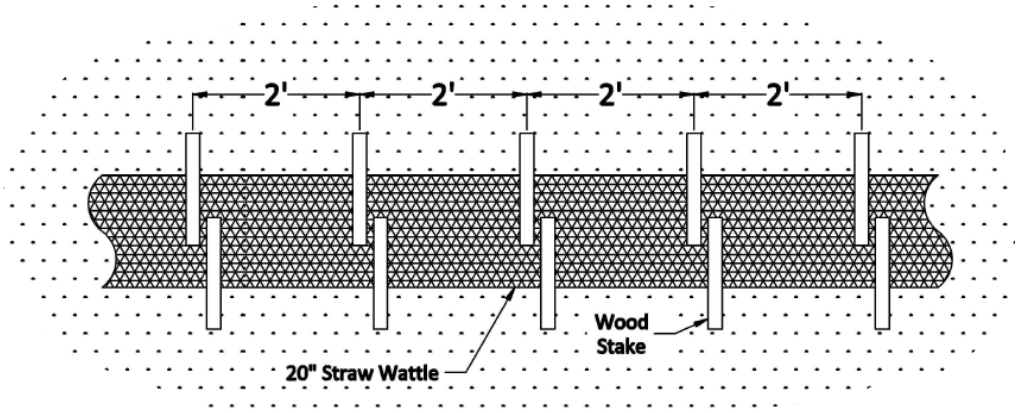

(c) plan view

Figure 5.7. Wattle installation.

5.4.2 FILTREXX® – SILTSOXX™

The SiltSoxx is a tubular manufactured sediment control product that can be implemented in a variety of stormwater treatment applications. The product is available in 5 to 32 in. (13 to 81 cm) diameters and lengths up to 200 ft (61 m). For applications requiring large diameters and/or extensive lengths, the containment system can be filled with media material on-site. Containment systems are available in a wide variety of cotton, high density polyethylene (HDPE), and multi-filament polypropylene (MFPP) materials, each having unique material specifications and applications. Media material within the containment system consist of compost that is

produced from organic matter using an aerobic composting process (*Filtrexx 2015*). When compared to similar products containing straw and excelsior fiber, this product is considerably denser per unit volume.

The Filtrexx design manual illustrates two installation details for perimeter controls. The single SiltSoxx installation calls for the product to be placed on level ground and secured using 2 in. (5 cm) wooden stakes driven through the center of the SiltSoxx every 10 ft (3 m). Alternatively, three SiltSoxxs can be installed in a pyramid fashion with two products placed on level ground, side by side, and a third placed on top. This method calls for teepee wood staking through the SiltSoxxs spaced 10 ft (3 m) on center. Tie wire is used to secure the exposed ends of the teepee stakes to promote downward pressure on the installation. Additionally, wood stakes are driven through the center of each SiltSoxx in contact with ground surface. These stakes are placed intermittently between teepee stake locations. As shown in Figure 5.8(a) through (c), the installation method implemented during performance evaluations varied slightly from the recommended pyramid installation. Teepee staking was used to secure the SiltSoxxs in place but the HDPE containment netting was not punctured. Stakes were placed 2 ft (0.6 m) on center and wood screws were used in lieu of tie wire to facilitate improved ground contact over the length of the installation.

(a) product installation

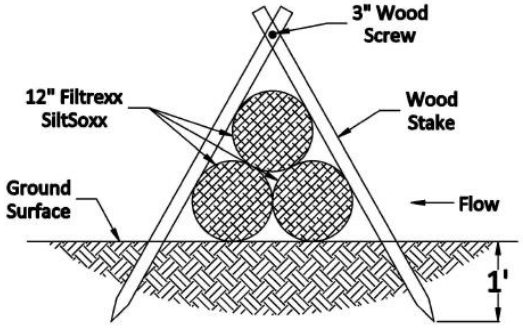

(b) side elevation view

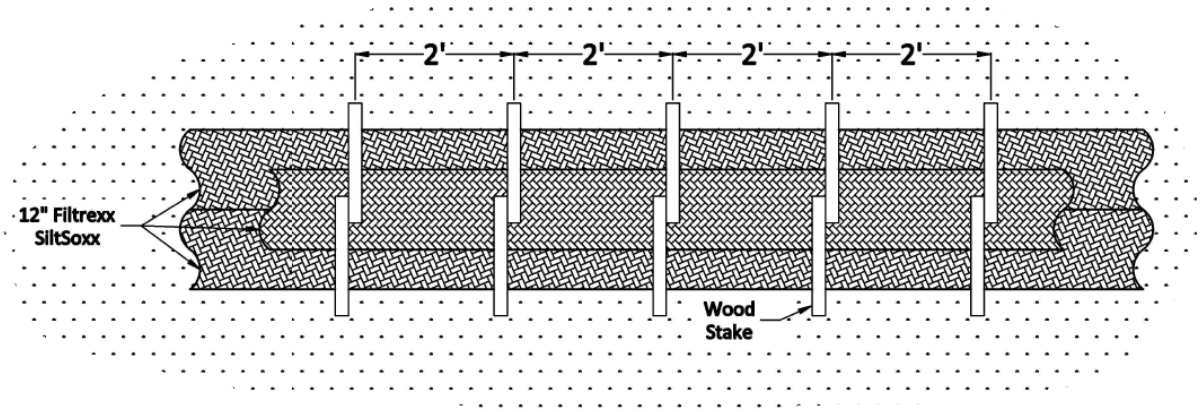

(c) plan view

Figure 5.8. SiltSoxx installation.

5.4.3 AMERICAN EXCELSIOR COMPANY® – CURLEX® BLOC

The third manufactured product evaluated was the Curlex Bloc. This product is designed for a wide variety of construction applications, as well as shoreline and streambank restoration. Curlex Blocs are composed of an excelsior fiber matrix contained within a biodegradable tubular cotton netting. The excelsior matrix is made from great lakes aspen wood that has curled, interlocking fibers with barbed edges that provide added strength and stability to the product. A unique feature of the Curlex Bloc is its rectangular cross-sectional shape and flat footprint, which promotes increased ground contact as compared to traditional tubular products. Typical nominal dimensions of the Curlex Bloc are 18 by 16 in. (46 by 41 cm) with lengths of 4 and 8 ft (1.2 and 2.4 m) (*American Excelsior Company 2018*).

The manufacturer's product installation guidelines and detail drawings indicate that the product can be installed on bare soil or over roller erosion control products. When implementing the Curlex Bloc as a perimeter control, an optional trenching installation is provided to improve sediment reduction in stormwater effluent. Each Curlex Bloc is manufactured with an extra flap of containment material attached to one end that can be pulled over an adjoining Curlex Bloc to form a seamless joint, thus creating a continuous installation. The product is secured in place using 1 by 1 in. (3 by 3 cm) wooden stakes and non-stretching rope. Stakes are driven tightly against each side of the Curlex Bloc every 2 ft (0.6 m) in an alternating pattern. Details illustrate that each stake be notched approximately 2 in. (5 cm) from the top as to provide a mean for securing the rope to the stake. Stakes are to be driven into the soil until approximately 4 in. (10 cm) of stake is remaining above the Curlex Bloc. Rope is then installed according to the details [Figure 5.9(c)] and tightly wrapped around each notch. Stakes are then driven down to tighten the rope [Figure 5.9(a) and 5.9(b)] and achieve an installation that is secured firmly to the ground.

(a) product installation

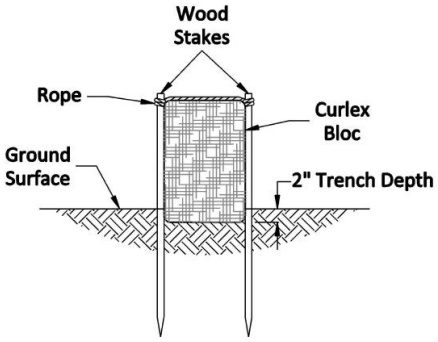

(b) side elevation view

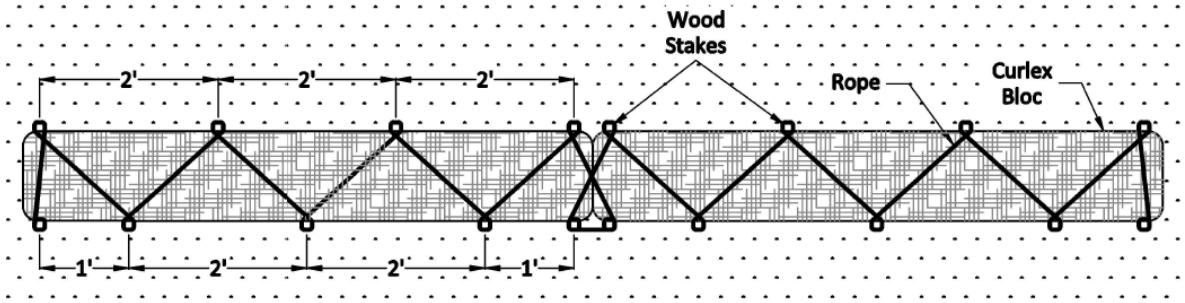

(c) plan view

Figure 5.9. Curlex Bloc installation.

5.5 RESULTS AND DISCUSSION

The evaluation of innovative and manufactured SB practice performance is based on data and observations collected throughout experimentation. Observational data gathered during testing includes still imagery and video from multiple perspectives. Physical data collected includes: impoundment length and depth, downstream catch basin depth, sediment deposition surveys, and water quality grab samples. These parameters were used to assess the overall performance of each innovative and manufactured SB practice.

5.5.1 INSTALLATION & STRUCTURAL EVALUATION

Performance results of SB practices are comparatively evaluated in three representative categories: (1) Manufactured Silt Fence Systems, (2) Sediment Retention Barriers, and (3) Manufactured Sediment Barrier Products. Evaluations were based on practices design, installation process, effectiveness, structural integrity, and testing observations.

5.5.1.1 Manufactured Silt Fence Systems

Manufactured silt fence systems are available for a range of site specific applications. The systems selected for this study are designed for 0.5 ac (0.2 ha) drainage areas with high overland flows. The installation process is similar to traditional silt fence in which the geotextile is entrenched to facilitate upstream impoundment. However, installation economics associated with manufactured silt fence systems are advantageous due to practice preassembly. In-field labor efforts for installation consist of excavating a trench, unrolling the system, driving wooded support post, backfilling the trench, and compacting the soil. Common issues associated with such installations included insufficient soil compaction during trench back filling, broken support posts [Figure 5.10(a)] and downstream post voids [Figure 5.10(b)]. Support posts can be easily damaged during installation and during construction activities. Defective support posts can affect the performance of an installation by inadequately supporting the geotextile upon hydrostatic loading, resulting in uncontrolled stormwater discharge due to overtopping. Post voids are created when support posts are driven into the bottom of an excavated trench and inadequately backfilled and compacted downstream of the installation. During C-POP testing, this proved to be a significant factor affecting the performance of the system. As shown in Figure 5.10(c), undermining occurred at a post installation due to insufficient soil compaction. To insure undermining would not reoccur during SRSF testing, extra soil was added downstream of the installation and compacted using a sledgehammer [Figure 5.10(d)]. Although this method proved effective during performance testing, in-field backfill compaction downstream of the installation is highly unlikely. A possible alternative would be to implement an offset trench installation in

which the support posts are driven into undisturbed soil 6 in. (15 cm) downstream of the trench, thus eliminating the interference posts have with trench backfill and compaction operations.

The overall structural integrity of each system proved to perform exceptionally well during longevity testing. Each system incorporates hardwood support posts spaced 4 ft (1.2 m) on center, as called for in the temporary silt fence requirement of AASHTO M 288-17 (*AASHTO 2017*). Maximum horizontal post deflections measured over the course of three simulated storm events for C-POP and Silt Saver – SRSF were each 0.13 ft (0.04 m). These measurements indicate that hardwood support posts provided adequate structural stability to the system when subjected to multiple design storms. Geotextile reinforcement for each system is unique in that C-POP incorporates polypropylene netting sown to the downstream face of the geotextile and SRSF uses high strength belts horizontally interwoven into the geotextile. Observations made during testing indicate that each of these reinforcement methods performed effectively in lieu of wire reinforcement given the design specifications (e.g., 4 ft [1.2 m] post spacing and high flow geotextile) of each system. When compared to a nonwoven fabric, the woven monofilament geotextiles used in these systems were observed to be less susceptible to pour clogging due to a larger AOS associated with the fabric. This resulted in reduced hydrostatic loading on the silt fence systems over the course of multiple simulated storm events.

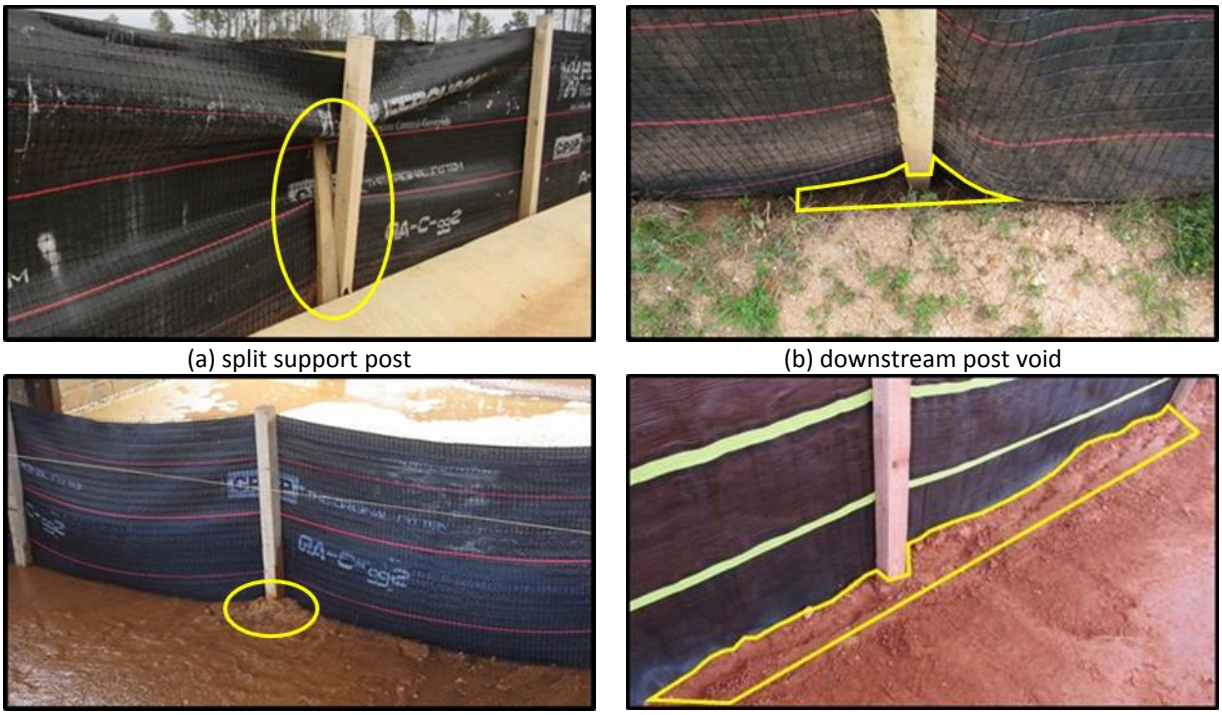

(a) split support post (b) downstream post void

(c) post undermining (d) downstream compacted backfill

Figure 5.10. Manufactured silt fence system installation evaluation.

5.5.1.2 Sediment Retention Barriers (SRBs)

The standard ALDOT SRB calls for two parallel Type A silt fence installations with bales placed tightly between each fence with staggered end abutments. Bales can consist of hay or straw with a minimum volume of 5 ft^3 (0.14 m^3), weight of 35 lb. (16 kg), and length of 3 ft (0.9 m) (*ALDOT 2016*). The concept behind this installation is not for the bales to improve water quality, but provided structural support to the upstream silt fence installation. This is accomplished by distributing and transferring the hydrostatic load placed on the upstream silt fence to the downstream silt fence via the bale media. Additionally, bales act as energy dissipaters when impounded stormwater overtops the upstream silt fence installation. The structural concept behind the load transfer design functions effectively until the resultant load placed on the downstream silt fence support posts reach their yield point and plastic deformation

begins to occur. For this scenario, resultant load is the combination of forces transferred through the bale media and the hydrostatic force of the increasing impoundment between the two silt fence installations caused by overtopping flow. As shown in Figure 5.11(a), the resultant force caused the downstream silt fence installation to deflect considerably more than the upstream silt fence installation, resulting in failure and uncontrolled discharge. Obviously, structural integrity would be improved by implementing larger support post and decreasing the associated spacing; however, an alternative strategy would be to exchange the nonwoven geotextile on the downstream silt fence installation with a woven monofilament geotextile that provides a high flow through rate, which in turn would reduce hydrostatic loading.

To capture suspended particles from SB effluent, the AL HB recommends installing a SRB as a secondary treatment practice. As shown in Figure 5.11(b), the installation process is simplistic in that flocculant-laden wheat straw is layered on top of jute matting and held in place using support posts, reinforcing wire, and polypropylene netting. The installation does not require a trenched excavation and is not designed to impound stormwater. Observations during testing indicate that the structural integrity of the AL HB SRB is more than adequate for the intended purpose and that structural materials (e.g., steel post and wire reinforcement) of the installation could be replaced with more cost effective alternatives (e.g., hardwood post and polypropylene reinforcement). Additionally, the overall height of the AL HB SRB could be reduced as flow only passes through the bottom portion (i.e., approximately 6 in. (15 cm)) of the installation.

(a) ALDOT SRB overtopping

(b) AL HB SRB support structure

Figure 5.11. SRB installation evaluation.

5.5.1.3 Manufactured Sediment Barrier Products

Installation methods for manufactured SB products are dependent upon intended application and the physical properties (e.g., size, shape, density, etc.) of the product. Each of the three SB products tested required a means for securing the product in-place so that dislodgement would not occur during flow introduction and impoundment. Wooden stakes are commonly used in industry for such purposes, and thus were implemented as the means for securement. Each product was held in place using wooden stakes; however, the methods in which the stakes were installed varied. During Excel Straw Log evaluations, wooden stakes were installed in a teepee fashion. Additionally, the product was entrenched 3 in. (8 cm) into the earthen test area in an attempt to minimize flow bypass. Test observations of this installation indicated that undermining of the product still occurred and that flow passed underneath the product as opposed to passing through the product, as shown in Figure 5.12(a). To minimize undermining of the product, a trenchless installation modification was implemented that incorporated a nonwoven geotextile undelay. As shown in Figure 5.12(b), undermining was not observed but flow passed readily between the underlay and product. The installation of sod staples to facilitate product ground contact has been shown to improve impoundment

capabilities of wattles by Donald et al. (*2013*), however were not incorporated during testing due to being excluded in ALDOT wattle standard installation details. Based on past wattle performance data when installed as a ditch check and inlet protection practice, the inclusion of sod staples during perimeter control testing would have resulted in improved performance. Throughout all evaluations of the Excel Straw Log, neither overtopping nor flow through the entire medium of the product was observed. These observations can be attributed to insufficient product ground contact and a large AOS of filler material, resulting in a high flow through rate.

Using performance observations made during Excel Straw Log testing, as well as installation guidelines provided by manufacturers, the wooden teepee installation technique was modified to facilitate downward pressure during SiltSoxx performance evaluations. This was achieved by firmly pressing each stake within a teepee configuration downward, against the tubes, and securing the tops using a wood screw, as shown in Figure 5.12(c). SiltSoxx installation also consisted of three products, installed on the ground surface in a pyramid configuration, as opposed to the singular entrenched Excel Straw Log installation. Structural observations over the course of three installation performance tests indicate that undermining occurred during installations I1 and I3. As illustrated in Figure 5.12(d), extensive undermining occurred on the upstream leading edge of the pyramid installation resulting in flow bypass, soil erosion, and stake unearthing. This failure resulted from a combination of factors including increased impoundment pressure and soil saturation. In-field failures such as this would require extensive maintenance not only to repair, but also to insure similar failures do not occur along the remaining soil interface. The incorporation of a geotextile underlay would have likely reduced the probability of such extensive undermining during testing.

When comparing manufactured SB product installation processes, the Curlex Bloc was the most labor intensive and challenging to implement. Curlex Blocs are held in place using rope that is woven stake-to-stake along the length of the installation. Installation guidelines specify that each wooden stake be notched to provide a means for rope securement. During installation, pre-notched stakes broke at notch location while being driven into the earthen soil, as illustrated in Figure 5.12(e). Because of this, an alternate rope securement method was established that called for the partial insertion of 2 in. (5 cm) wood screws into the outward facing side of each wooden stake. As shown in Figure 5.12(f), rope was looped around each stake in such a manner that each screw acted as a rope anchor when stakes were completely driven into the earthen soil. This method proved to work effectively as long as extensive shear force was not applied to the screw during rope tensioning. In rare scenarios where shear force exceeded screw capacity, failure would occur and a new screw would be installed.

Since Curlex Blocs are only available in 4 and 8 ft (1.2 and 2.4 m) lengths, three units were joined to create an installation that extended the entire width of the earthen test area. Each Bloc was firmly abutted against the adjacent Bloc and the extra flaps of containment material were securely pulled over to create seamless joints. Once the initial installation of the product was complete, voids were observed along the earthen surface at each abutment joint due to the rounded geometry of Bloc ends, as shown in Figure 5.12(g). Observations during the initial installation performance evaluation indicated that abutment voids were a means of direct flow conveyance and downstream sediment transport. Figure 5.12(h) shows sediment-laden flow rapidly passing through the abutment void and undermining the installation. Based on these observations, void fillers were installed by compacting loose excelsior fiber into each opening

using a sledgehammer. This solution proved to be ineffective in that flow was still able to pass though the void with little to no resistance or water quality improvement. During subsequent installations, rounded excelsior fiber Bloc ends were removed from the containment netting, loosened by hand, and firmly packed back into the containment material to minimize abutment voids. Additionally, a 6 in. (15 cm) soil wedge was placed and compacted along the upstream interface to minimize flow bypass underneath the product. These installation modifications facilitated increased upstream impoundment and flow through the product; however, minor undermining was still observed during testing.

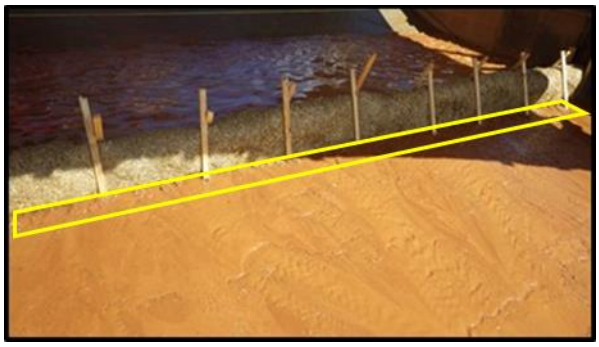

(a) undermining – trenched installation

(b) sediment-laden flow - fabric underlay installation

(c) modified teepee installation – wood screw

(d) undermining – pyramid installation

(e) rope installation - broken notched stakes

(f) rope installation – wood screw catch

(g) rounded end abutment void

(h) undermining through abutment

Figure 5.12. Manufactured product installation evaluation.

In-field applications of these manufactured SB products, when implemented as a perimeter control substitute for nonwoven silt fence installations, would require extensive labor

efforts to achieve installations capable of intercepting and effectively treating sheet flow runoff. Based on observations made during performance evaluations, the likelihood of installation failure due to undermining would be increasingly high. While these products and their associated installation guidelines implemented during these evaluations may not be structural sound, the development of innovative applications and installation strategies based on these finding may provide the necessary elements to improve reliability and performance in the future.

5.5.2 INSTALLATION & STRUCTURAL SUMMARY

As shown through testing, the major failure mode of innovative and manufactured SB practices was undermining. Consideration should be taken when specifying such products to ensure effective installation methods are implemented so that flow bypass does not occur. Installation on less erodible areas such as undisturbed vegetation may decrease undermining potential. This installation scenario was not a testing option for this project. A comprehensive summary of structural failures and associated times for each innovative and manufactured SB practice is provided in Table 5.3. Structural observations made during the Standard ALDOT silt fence testing and M8 testing are included for comparison. Recommended installation details for manufactured products are provided in Appendix C.

Table 5.3. Innovative and Manufactured SB Structural Observation

SB	Installation	Test	Failure Time (min:sec)	Failure Mode
STD-T	I1	P1, P2	--	No Failure
		P3	15:15	Post Deflection, Overtopping
	I2	P1,P2	--	No Failure
		P3	14:30	Post Deflection, Overtopping
	I3	P1	--	No Failure
		P2	15:30	Post Deflection, Overtopping
		P3	n/a	n/a
M8	I1	P1, P2, P3	--	No Failure
	I2	P1, P2, P3	--	No Failure
	I3	P1, P2, P3	--	No Failure
C-POP	I1	P1, P2, P3	--	No Failure
	I2	P1	28:00	Minor Undermining at Post
		P2, P3	--	No Failure
	I3	P1, P2	--	No Failure
		P3	25:00	Minor Undermining at Post
Silt Saver SRSF	I1	P1, P2, P3	--	No Failure
	I2	P1, P2, P3	--	No Failure
	I3	P1, P2, P3	--	No Failure
ALDOT SRB	I1	P1, P2	--	No Failure
		P3	19:30	Post Deflection, Overtopping
	I2	P1	--	No Failure
		P2	22:56	Post Deflection, Overtopping
		P3	14:00	Post Deflection, Overtopping
	I3	P1	--	No Failure
		P2	21:00	Post Deflection, Overtopping
		P3	16:11	Post Deflection, Overtopping
AL HB SRB w/o Flocculant	I1	P1, P2, P3	--	No Failure
	I2	P1, P2, P3	--	No Failure
	I3	P1, P2, P3	--	No Failure
AL HB SRB w/ Flocculant	I1	P1, P2, P3	--	No Failure
	I2	P1, P2, P3	--	No Failure
	I3	P1, P2, P3	--	No Failure
Western Excelsior Excel Straw Log	I1[a]	P1	2:20	Undermining
	I2[a]	P1	2:10	Undermining
	I3[a],[b]	P1	--	Flow Bypass
Filtrexx SiltSoxx	I1	P1	15:00	Undermining
		P2, P3	--	No Failure
	I2	P1, P2, P3	--	No Failure
	I3	P1	28:00	Undermining
		P2	5:00	Undermining
		P3	23:00	Undermining
American Excelsior Curlex Bloc	I1	P1, P2, P3	00:30	Undermining
	I2	P1, P2, P3	--	No Failure
	I3	P1	10:00	Undermining
		P2	--	No Failure
		P3	21:50	Overtopping

Notes: [a] = test P2 & P3 were not conducted; [b] = installed with a geotextile underlay; -- = failure did not occur; n/a = no test conducted

5.5.3 HYDRAULIC & SEDIMENT RETENTION EVALUATION

Measurements gathered throughout testing provide means for evaluating SB performance through direct comparisons of impoundment, effluent flow rate, and sediment capture. Performance results of SB practices will again be comparatively evaluated in three representative categories: (1) Manufactured Silt Fence Systems, (2) Sediment Retention Barriers, and (3) Manufactured Sediment Barrier Products. Hydraulic evaluations are based on water depth measurements gather thought out each experiment and sediment retention evaluations are based pre and post test surveys.

5.5.3.1 Manufactured Silt Fence Systems

Impoundment depths and effluent flow rates measured during manufactured silt fence testing indicate that on average, C-POP had a 64% increase in impoundment capability and a 13% reduction in effluent flow when compared to SRSF. These findings correspond to the design specifications of each system, in that geotextile AOS increases with height for SRSF and remains consist for C-POP. When comparing C-POP and SRSF to nonwoven geotextile properties (i.e., M8), impoundment decreases 25% and 55% while flow increases 27% and 45%, respectively. While these evaluations provide insight into how these systems relate to one another, longevity evaluations indicate how the performance of a system changes when subjected to multiple storm events. Base effluent flow rates (i.e., unclogged geotextile pores during P1 tests) for M8, C-POP, and SRSF were 0.13, 0.16, and 0.18 ft^3/s (0.004, 0.005, and 0.005 m^3/s), respectively. Measurements taken over the course of three C-POP installations (i.e., I1, I2, and I3), each subjected to three simulated storm events (i.e., P1, P2, and P3), indicate that P2 and P3 effluent flow rates were reduced by 5% and 16%, respectively, when compared to P1. Similar results were

also calculated for SRSF, where P2 and P3 were reduced by 6% and 22%, respectively. In comparison, the nonwoven silt fence installation (i.e., M8) experienced reductions of 22% and 34% in effluent flow rates, which are considerably higher than those of C-POP and SRSF. These increased reductions over time coupled with a decreased base effluent flow rate results in increased impoundments and water retention over time when compared to each of the manufactured silt fence systems. Figure 5.13(a) and (b) illustrate the change in effluent flow rates for P1 and P3 performance evaluations for each practice.

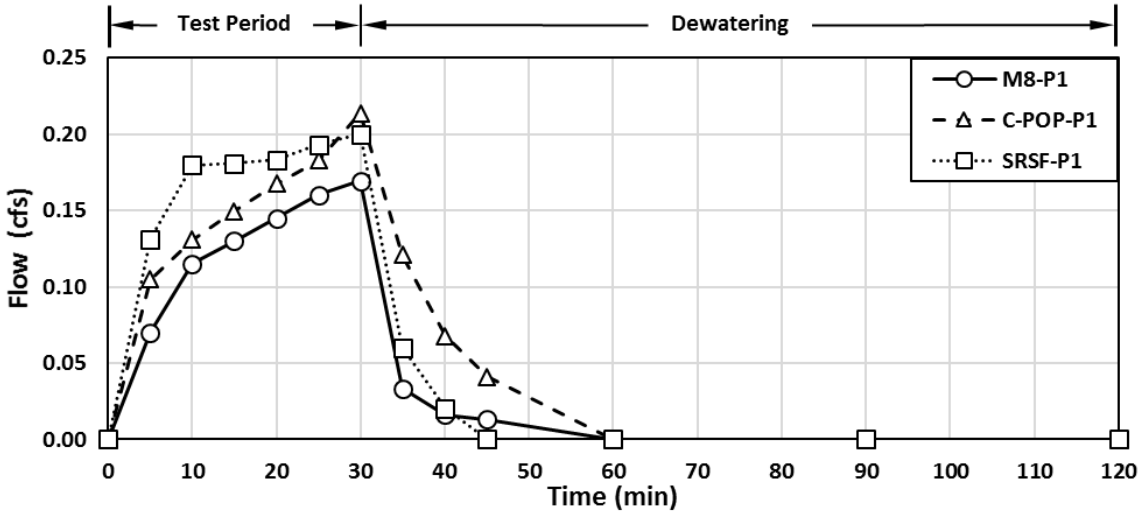

(a) P1 effluent flow

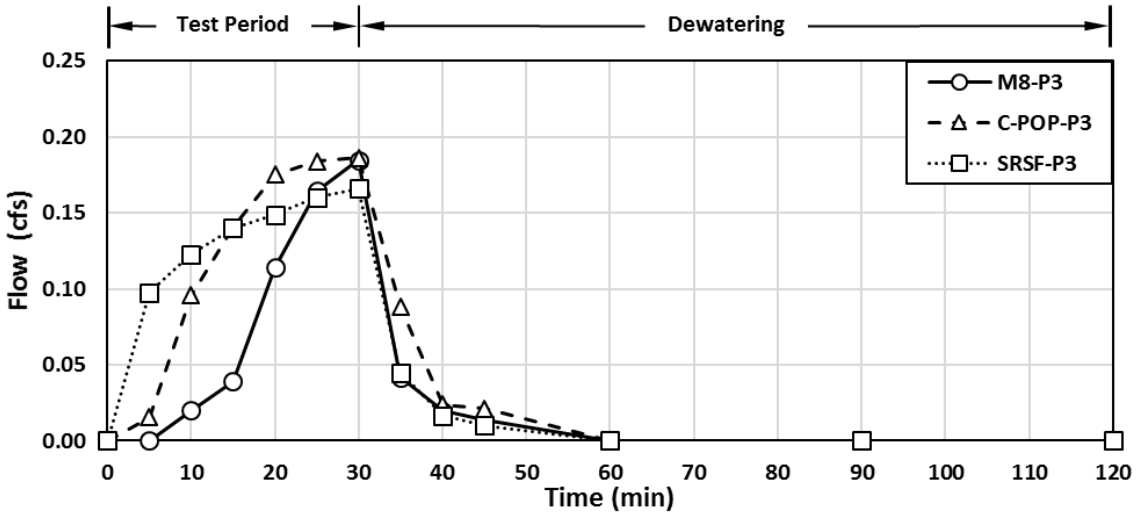

(b) P3 effluent flow

Figure 5.13. Manufactured silt fence effluent flow rate analysis.

Sediment deposition surveys indicate the volume of rapidly settable solids captured upstream of SB practices. Manufactured silt fence systems survey results indicate average sediment retention rates of 90% and 85% for C-POP and SRSF, respectively. When compared to M8 retention rates, sediment capture is reduced by 3% for C-POP and 9% for SRSF. These sediment capture differences can be attributed to the different hydraulic properties associated with each geotextile. However, results from a single factor ANOVA indicated, with a 95%

confidence level, that the differences in sediment retention rates between the two manufactured silt fence systems and M8 are not significant.

These full-scale performance evaluations provide insight into how these manufactured silt fence systems function in field applications. Side-by-side comparisons of impoundment, effluent discharge, and sediment deposition observed during testing for each manufactured silt fence system are provided in Figure 5.14(a) through (f).

(a) C-POP impoundment (b) SRSF impoundment

(c) C-POP effluent discharge (d) SRSF effluent discharge

(e) C-POP sediment deposition (f) SRSF sediment deposition

Figure 5.14. Manufactured Silt Fence System performance observations.

5.5.3.2 Sediment Retention Barriers (SRBs)

Measurements obtained during testing indicate that the ALDOT SRB achieved a maximum average impoundment depth of 1.76 ft (0.54 m), which was greater than all practice impoundment measurements obtained throughout this study. On the other hand, the calculated base effluent flow rate for the ALDOT SRB was 0.09 ft^3/s (0.003 m^3/s), which was lower than all evaluated practices. When comparing these values to those achieved during M8 testing, impoundment capability is increased 14% while base effluent flow is reduced by 31%. ALDOT SRB longevity tests indicate that effluent flow is reduced by 25% between P1 and P2 tests; however, due to structural failures and overtopping flows during P3 tests, calculated flow reductions during P3 tests are unrepresentative of that of the practice.

Each configuration of the AL HB SRB (i.e., with and without flocculant) had slightly differing impoundments and effluent flow rates. When flocculant was <u>not</u> added to the installation, the average maximum impoundment and base effluent flow rate was 0.15 ft (0.05 m) and 0.21 ft^3/s (0.006 m^3/s), respectively. In comparison, flocculant-laden installations resulted in an average maximum impoundment of 0.52 ft (0.16 m) and a base effluent flow rate of 0.20 ft^3/s (0.005 m^3/s). These slight changes in hydraulic performance can be attributed to the hydration of granulated flocculant, which creates a tacky wheat straw matrix that slightly reduces flow through capacity. Figure 5.16(a) through (d) show hydraulic performance observations made during testing for each SRB. AL HB SRB longevity testing indicated reductions in effluent flow rates for tests P2 and P3 of 2% and 3% for no flocculant installations, while flocculant-laden installations experienced reductions of 5% and 6%, respectively. As shown in Figure 5.15(a) and (b), the P1 and P3 effluent flow rates observed over time for the ALDOT SRB varies considerably

when compared to the P1 and P3 effluent flow rates for each installation configuration of the AL HB SRB. This variation in flow capacity over time is a direct result of geotextile blinding, as observed during nonwoven silt fence testing.

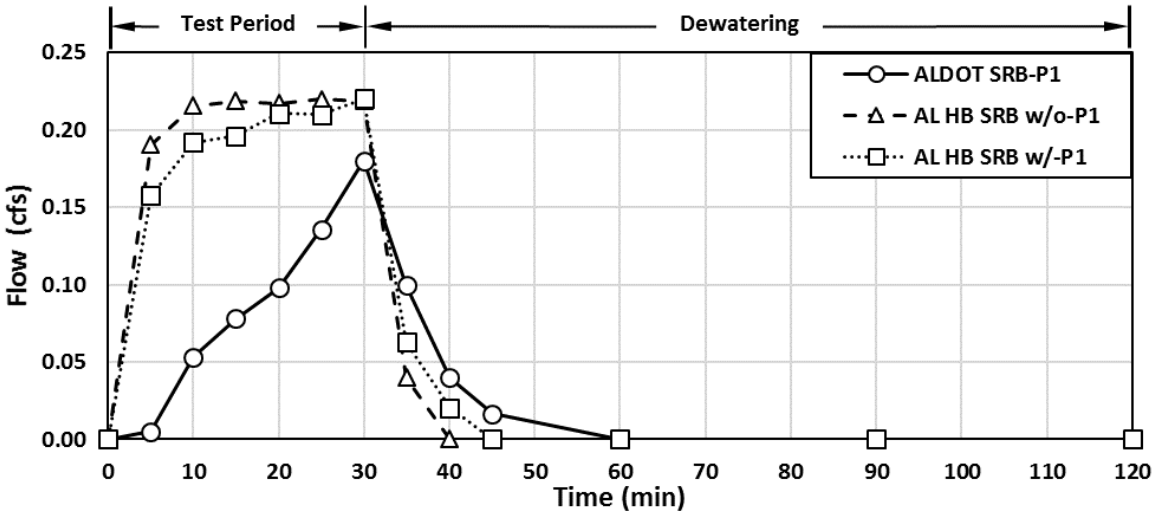

(a) P1 effluent flow

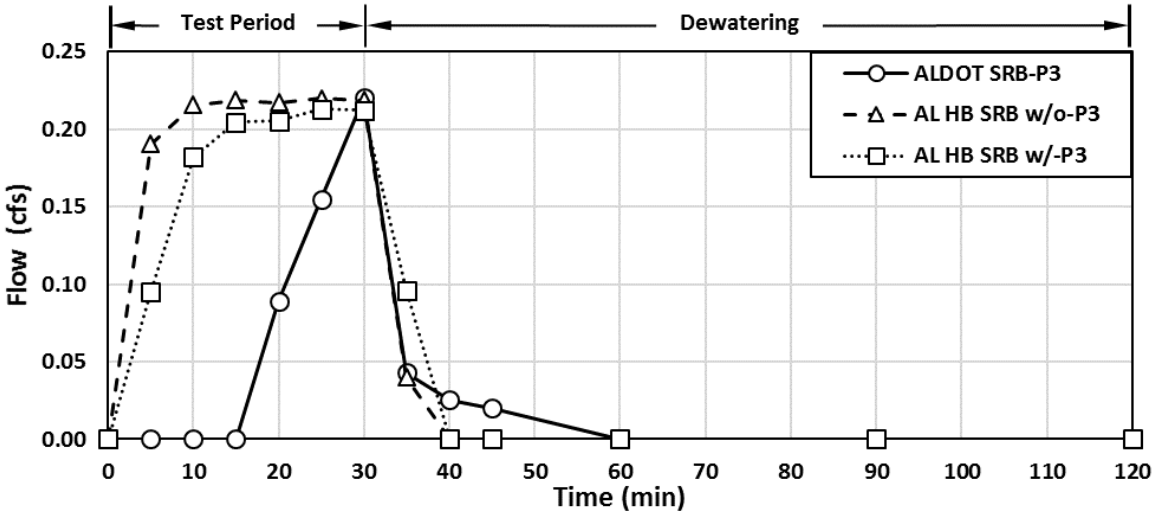

(b) P3 effluent flow

Figure 5.15. Sediment retention barrier effluent flow rate analysis.

Results from each SRB survey analysis were compiled to determine the sediment capture rates for each of the practices. On average, the ALDOT SRB retained 91% of sediment introduced, while the AL HB SRB retained 63% and 83% in the no flocculant and flocculant-laden configurations, respectively. In comparison to M8 (e.g., 93%), sediment capture for these

practices were reduced by 2% (ALDOT SRB), 32% (AL HB SRB w/o), and 11% (AL HB SRB w/). Sediment deposition observations made after testing for each SRB are shown in Figure 5.16(e) and (f).

(a) ALDOT SRB impoundment

(b) AL HB SRB impoundment

(c) ALDOT SRB discharge

(d) AL HB SRB discharge

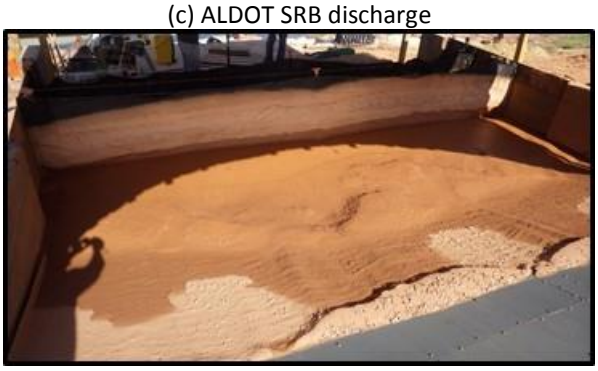

(e) ALDOT SRB sediment deposition

(f) AL HB SRB sediment deposition

Figure 5.16. SRB performance observations.

5.5.3.3 Manufactured Sediment Barrier Products

Average maximum impoundment depths measured during Excel Straw Log, SiltSoxx, and Curlex Bloc testing were 0.38, 0.51, and 0.77 ft (0.12, 0.16, 0.23 m), respectively. Figure 5.18(a)

through (c) show maximum impoundments accomplished during testing by each of these manufactured SB products. When compared to M8 (e.g., 1.54 ft), impoundment capabilities for each product were reduced by 75%, 67%, and 50%, respectively. However, overtopping did occur during Curlex Bloc testing, thus indicating maximum attainable impoundment had been achieved. Additionally, the Curlex Bloc was the only product evaluated in which stormwater was observed flowing from the downstream face of the product, as shown in Figure 5.18(d). Observations made during Excel Straw Log and SiltSoxx testing indicated that flow discharged from within the product along the earthen surface interface. These observations suggest that the majority of the three-dimensional matrix in which flow is intended to pass to obtain water quality improvement is not utilized. Base effluent flow rates for each product were similar in that the Excel Straw Log and Curlex Bloc achieved 0.20 ft^3/s (0.006 m^3/s) and the SiltSoxx achieved 0.19 ft^3/s (0.005 m^3/s). A unique observation made during SiltSoxx testing was the products ability to repel and bead water along the surface of containment material, as shown in Figure 5.18(e). This material property may be directly related to the slight decrease in effluent flow observed during testing. Longevity analyses for the SiltSoxx indicated flow reductions of 0% (P2) and 4% (P3). In comparison, flow was reduced by 15% for both P2 and P3 tests during Curlex Bloc evaluations. Due to extensive undermining during Excel Straw Log P1 evaluations, longevity tests were not conducted. Figure 5.17(a) and (b) illustrate the similarity between time variable effluent flow rates for each of the manufactured SB products for P1 and P3 evaluations.

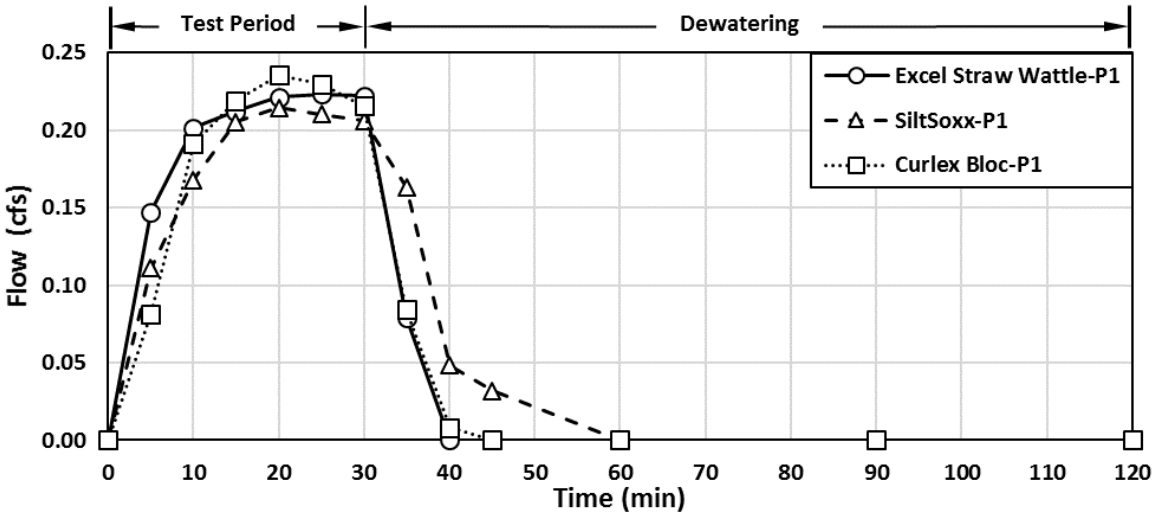

(a) P1 effluent flow

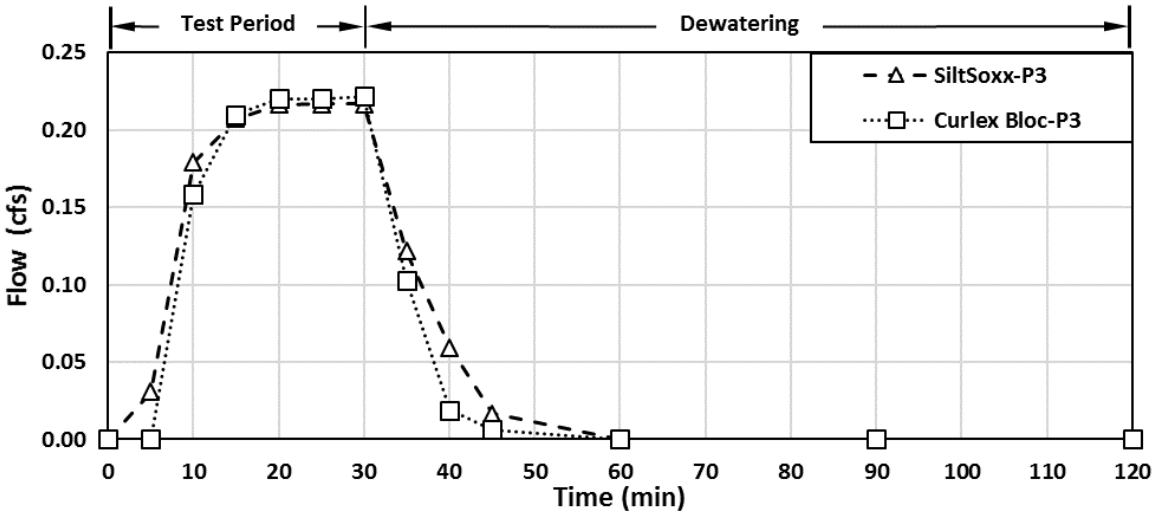

(b) P3 effluent flow

Figure 5.17. Manufactured sediment barrier product effluent flow rate analysis.

Sediment capture rates for the tested products were calculated to be 82% (Excel Straw Log), 80% (SiltSoxx), and 84% (Culex Blox). Sediment deposition observed after testing each product is shown in Figure 5.18(f) through (h). When evaluated against M8, these products have reduced retention rates by 12% (Excel Straw Log), 14% (SiltSoxx), and 10% (Curlex Bloc). Despite installation challenges and undermining incidences, these products achieve respectable retention rates during performance testing.

(a) Excel Straw Log impoundment

(b) SiltSoxx impoundment

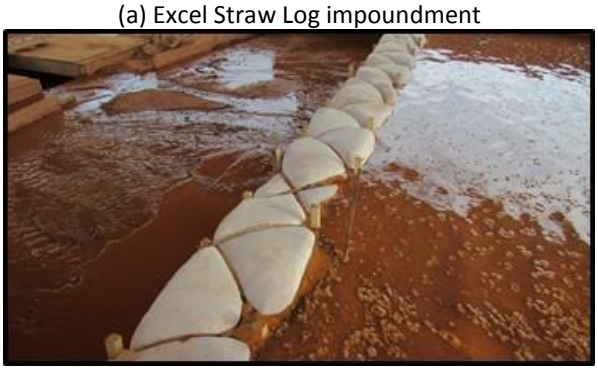

(c) Curlex Bloc impoundment

(d) Curlex Bloc discharge

(e) SiltSoxx water beads

(f) Excel Straw Log sediment deposition

(g) SiltSoxx sediment deposition

(h) Curlex Bloc sediment deposition

Figure 5.18. Sediment barrier product performance observations.

5.5.4 HYDRAULIC & SEDIMENT RETENTION SUMMARY

Performance testing has shown practices with the ability to create repeatable upstream impoundment depths greater than 1 ft (0.3 m) have consistent sediment capture rates of at least 90%. More importantly, impoundment depths greater than 1.5 ft (0.46 m) do not facilitate improved sediment capture. These observations suggest that optimized sediment capture is achieved when a SB practice has an effective upstream impoundment depth between 1 and 1.5 ft (0.3 and 0.46 m). A complete performance summary of each practice evaluated is provided in Table 5.4, as well as the results for STD silt fence and M8 testing.

Table 5.4. Innovative and Manufactured SB Performance Analysis

SB	Installation	Sediment Retained	Impoundment Depth ft (m)	Flow-Through Rate[c] ft^3/s (m^3/s)
STD-T	I1	87%	0.80 (0.24)	0.15 (0.004)
	I2	87%	0.90 (0.27)	0.16 (0.005)
	I3	75%	0.85 (0.26)	0.16 (0.005)
	Average	**83%**	**0.85 (0.26)**	**0.16 (0.005)**
M8	I1	90%	1.63 (0.50)	0.11 (0.003)
	I2	91%	1.38 (0.42)	0.11 (0.003)
	I3	98%	1.62 (0.49)	0.10 (0.003)
	Average	**93%**	**1.54 (0.47)**	**0.11 (0.003)**
C-POP	I1	90%	1.11 (0.34)	0.15 (0.004)
	I2[a]	91%	1.19 (0.36)	0.14 (0.004)
	I3[a]	90%	1.16 (0.35)	0.13 (0.004)
	Average	**90%**	**1.15 (0.35)**	**0.14 (0.004)**
Silt Saver SRSF	I1	96%	0.63 (0.19)	0.16 (0.005)
	I2	76%	0.64 (0.20)	0.17 (0.005)
	I3	82%	0.84 (0.26)	0.15 (0.004)
	Average	**85%**	**0.70 (0.22)**	**0.16 (0.005)**
ALDOT SRB	I1	90%	1.58 (0.48)	0.07 (0.002)
	I2	92%	1.75 (0.53)	0.09 (0.003)
	I3	90%	1.95 (0.59)	0.09 (0.003)
	Average	**91%**	**1.76 (0.53)**	**0.08 (0.003)**
AL HB SRB w/o Flocculant	I1	64%	0.13 (0.04)	0.21 (0.006)
	I2	63%	0.18 (0.05)	0.21 (0.006)
	I3	62%	0.15 (0.05)	0.21 (0.006)
	Average	**63%**	**0.15 (0.05)**	**0.21 (0.006)**
AL HB SRB w/ Flocculant	I1	81%	0.64 (0.20)	0.17 (0.005)
	I2	84%	0.44 (0.13)	0.18 (0.005)
	I3	85%	0.49 (0.15)	0.19 (0.005)
	Average	**83%**	**0.52 (0.16)**	**0.18 (0.005)**
Western Excelsior Excel Straw Log	I1[b]	82%	0.30 (0.09)	0.20 (0.006)
	I2[b]	84%	0.42 (0.13)	0.20 (0.006)
	I3[b]	81%	0.43 (0.13)	0.20 (0.006)
	Average	**82%**	**0.38 (0.12)**	**0.20 (0.006)**
Filtrexx SiltSoxx	I1[a]	93%	0.53 (0.16)	0.18 (0.005)
	I2	81%	0.57 (0.17)	0.18 (0.005)
	I3[b]	67%	0.43 (0.13)	0.19 (0.005)
	Average	**80%**	**0.51 (0.15)**	**0.18 (0.005)**
American Excelsior Curlex Bloc	I1[b]	67%	0.51 (0.16)	0.20 (0.006)
	I2	95%	0.91 (0.28)	0.17 (0.005)
	I3[a]	90%	0.88 (0.27)	0.17 (0.005)
	Average	**84%**	**0.77 (0.24)**	**0.18 (0.005)**

Notes: [a] minor undermining; [b] major undermining; [c] average effluent flow rate during 30 minute test period for 3 sequential storm events; n/a = not available; 1 ft = 0.3 m; 1 ft^3/s = 0.028 m^3/s

5.5.5 WATER QUALITY EVALUATION

The average turbidity results of three installations (i.e., I1, I2, and I3) were obtained from grabs samples collected at five sample locations (i.e., SL1, SL2, SL3, SL4, and SL5). In order to compare and quantify the treatment efficiency of each practice, a standardized means for water quality analysis was applied. Standardization was achieved by dividing downstream turbidity (i.e., SL4) by impoundment surface turbidity (i.e., SL2) for each sample time to determine the efficiency in turbidity reduction from upstream to downstream of the SB practice. These sample locations were chosen because water quality on the surface of the upstream impoundment is typically the least sediment-laden when compared to other upstream locations and effluent flow exiting the practice has yet to be contaminated by bare soil downstream of the installation. Points below 1.0 (shaded in green) on the generated turbidity ratio graphs indicate that there was a reduction in turbidity between upstream and downstream, while points above 1.0 (shaded in red) indicate there was an increase in turbidity. The further a point lies from 1.0 the greater the extent of the change.

5.5.5.1 Manufactured Silt Fence Systems

A comparison of P1 and P3 treatment efficiencies for M8 and each manufactured silt fence system is shown in Figure 5.19(a) and (b). From the plots, it is evident that each of the silt fence practices achieved minimal to no water quality improvements during the testing period. It was observed that turbulence reduction during the dewatering period (e.g., 30 – 120 min) does not result in significant effluent water quality improvement. The average P1 turbidity ratios for M8, C-POP, and SRSF were 1.140, 1.308, and 1.052, each of which indicates degradation in effluent water quality. Based on these evaluations SRSF out performed M8 and C-POP by

minimizing water quality degradation; however, average P3 turbidity ratios indicate that the treatment efficiency of SRSF (1.122) decreased during longevity testing where as M8 (1.051) and C-POP (1.254) improved. These changes in treatment efficiency would be difficult to correlate to long term, in-field performance expectations without additional longevity replicate tests for statistical comparison.

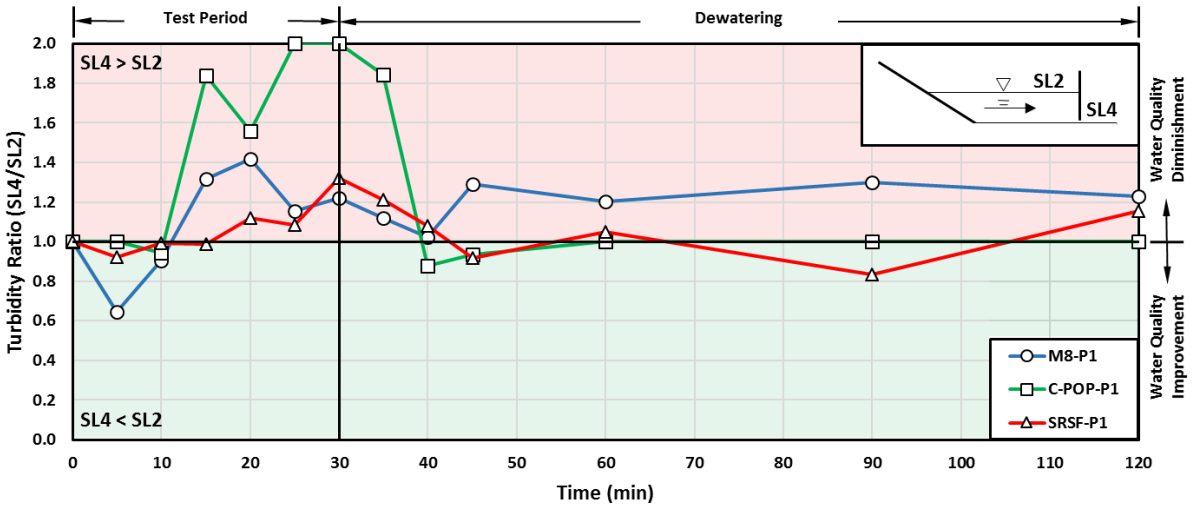

(a) P1 treatment efficiency

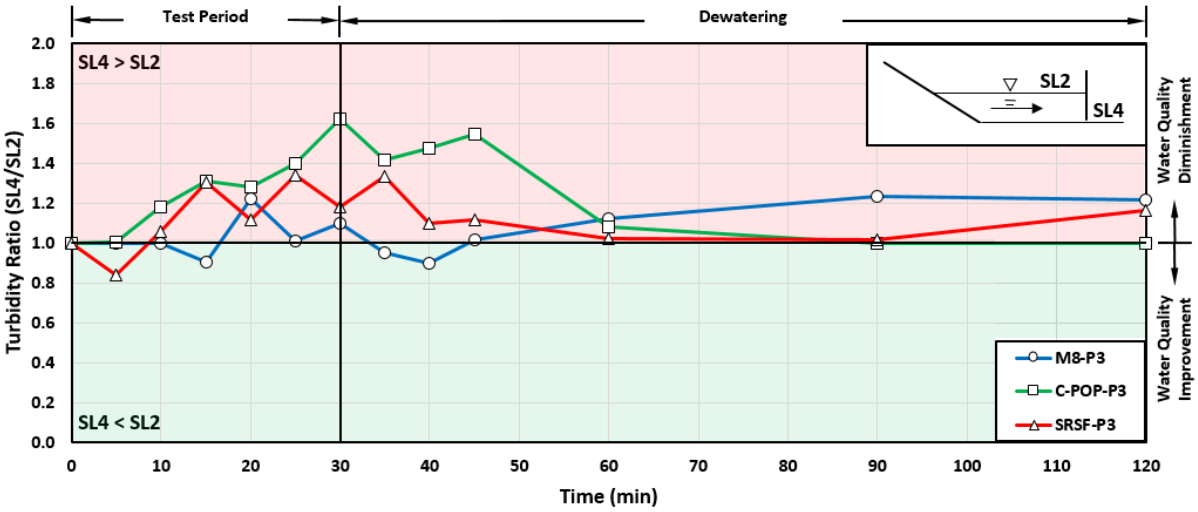

(b) P3 treatment efficiency

Figure 5.19. Manufactured silt fence system turbidity ratio comparison.

5.5.5.2 Sediment Retention Barriers (SRBs)

The P1 and P3 ratio comparisons for SRBs are shown in Figure 5.20(a) and (b). From the plots, it is evident that SRBs outperform manufactured silt fence systems. During P1 evaluations, the ALDOT SRB, AL HB SRB w/o flocculant, and AL HB SRB w/ flocculant achieved average ratios of 1.048, 0.870, and 0.546. These values indicate slight water quality degradations for the ALDOT SRB, but substantial water quality improvements for each AL HB SRB configuration. Longevity tests results show that filtering capabilities improved for the ALDOT SRB (0.922) while each AL HB SRB (0.892 w/o and 0.536 w/flocculant) remained consistent. Out of all practices evaluated, the AL HB SRB w/ flocculant was the most effective at reducing turbidity as flow passed through the medium.

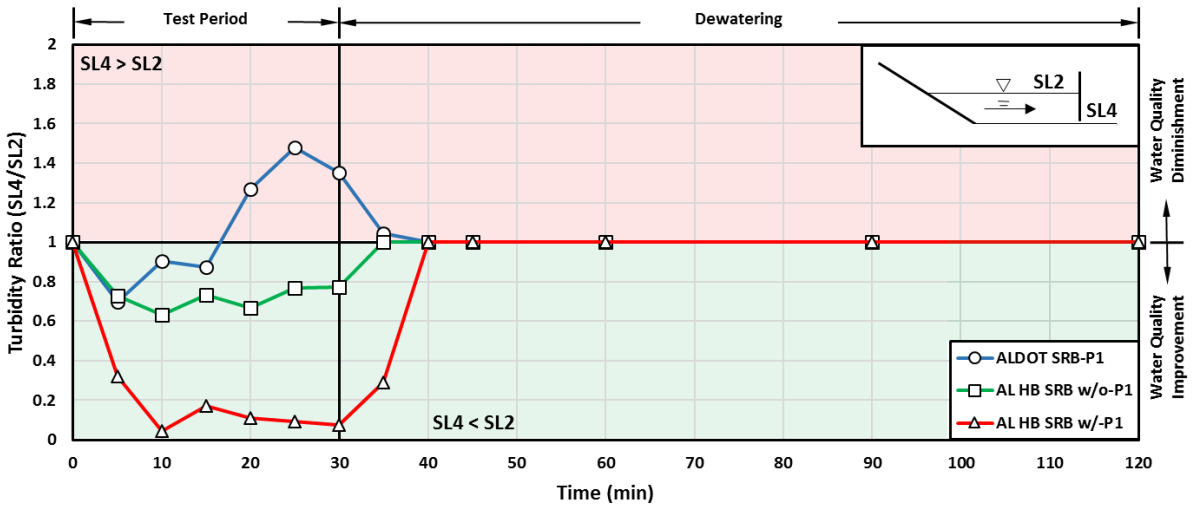

(a) P1 treatment efficiency

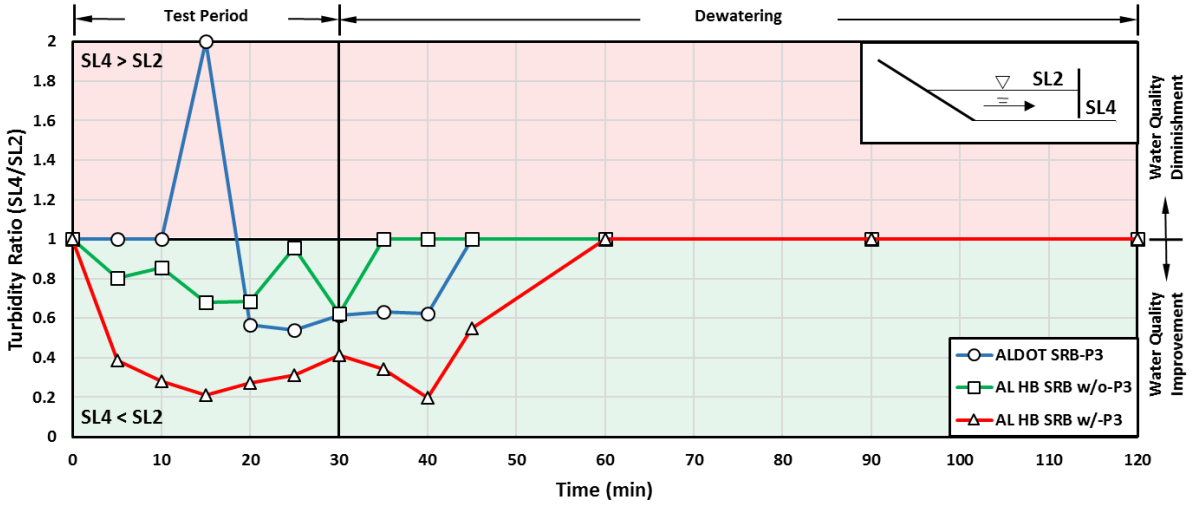

(b) P3 treatment efficiency

Figure 5.20. Sediment retention barrier turbidity ratio comparison.

5.5.5.3 Manufactured Sediment Barrier (SB) Products

Manufactured SB product turbidity ratio plots are illustrated in Figure 5.21(a) and (b). As shown in the P1 treatment efficiency plot, the Curlex Bloc outperformed the Excel Straw Log and Siltsoxx. Interestingly, the Curlex Bloc was the only product to achieve an improvement in effluent water quality. Average P1 ratios for the Excel Straw Log, SiltSoxx, and Curlex Bloc were 1.204, 1.199, and 0.894, respectively. When comparing these values to longevity P3 ratios, the diminishment associated with SiltSoxx is reduced to a ratio of 1.042 and the Curlex Bloc further

improves water quality to a turbidity ratio of 0.889. Longevity tests were not conducted on the Excel Straw Log, thus data is not available for evaluating treatment efficiency after repeated storm events. The most notable ratios from the plots is that of the Curlex Bloc during the dewatering period. When compared to all practices evaluated in this study, the Curlex Bloc was the only practice to consistently achieve an improvement in effluent water quality during dewatering. Additionally, the Curlex Bloc was the only practice that achieved noticeable improvements in treatment efficiency during longevity testing.

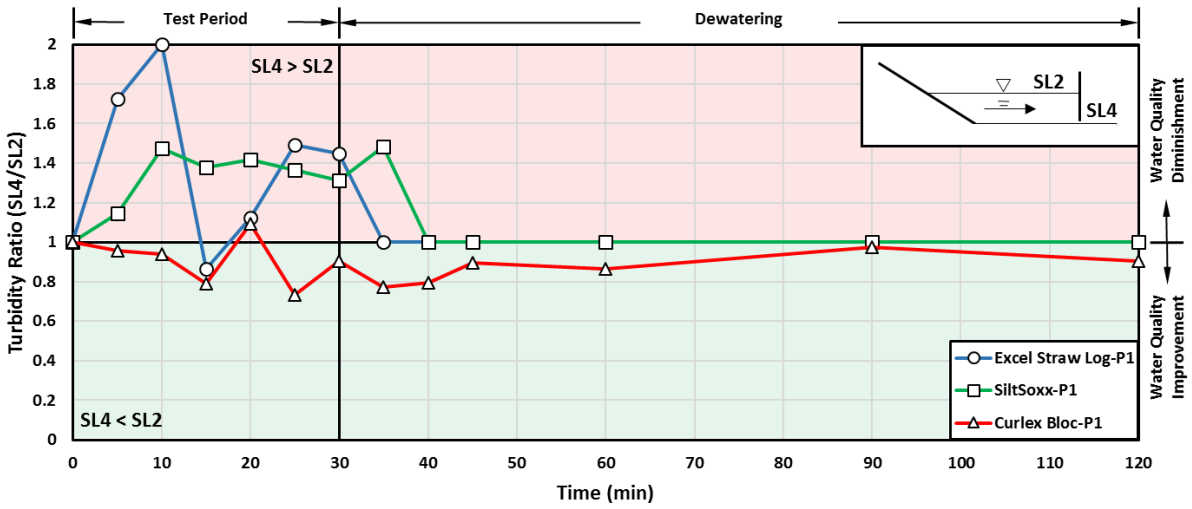

(a) P1 treatment efficiency

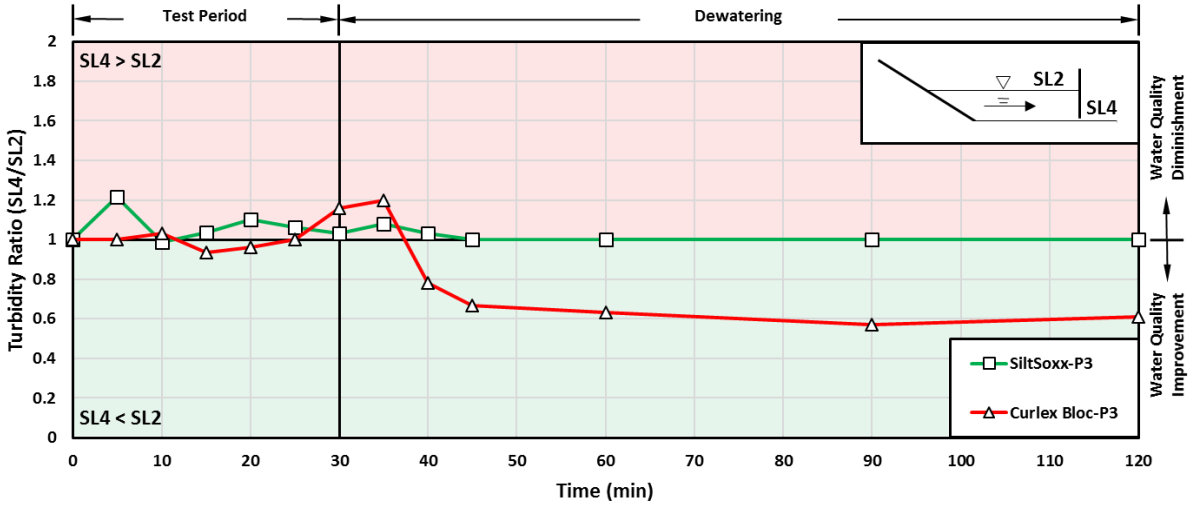

(b) P3 treatment efficiency

Figure 5.21. Manufactured sediment barrier product turbidity ratio comparison.

Time variable turbidity plots were generated for each innovative and manufactured SB practice to analyze effects on water quality based on impoundment depth. Plots indicated that turbidity along an impoundment surface (i.e., SL2) is consistently lower than turbidity along the bottom of impoundment (i.e., SL3) for most practices. This improvement in water quality is facilitated by stormwater ponding upstream of installations. Figure 5.22**Error! Reference source not found.** illustrates the time variable plots generated for M8 and SiltSoxx compost logs. When analyzing the turbidity data gathered from sample locations SL2 and SL3 during the 30 minute

test period, M8 and SiltSoxx compost logs have turbidity reductions along the surface of 60% and 34%, respectively. These reductions in turbidity can be directly linked to maximum impoundment depths achievable for each of these SB practices, which was 1.54 ft (0.47 m) and 0.51 ft (0.16 m), respectively. These findings indicate that not only upstream impoundment pools improve water quality, but the magnitude of impoundment depth also affects water quality. Analyzing the water quality plot for M8 even further, turbidity levels along the surface were only reduced by 208 nephelometric turbidity units (NTU) when transitioning from the test period to dewatering. Assuming turbidity levels observed during dewatering are the lowest achievable for the system, this observation suggest that water quality along the surface of the impoundment during the test period is almost at its lowest value at an impoundment depth of 1.54 ft (0.47 m). This observation coupled with the results obtained during structural and sediment retention analyses indicate an optimal impoundment depth range between 1.0 ft (0.30 m) and 1.5 ft (0.46 m). From a practical standpoint, this depth range would be the most effective based on hydrostatic loading, sediment capture, and water quality improvement.

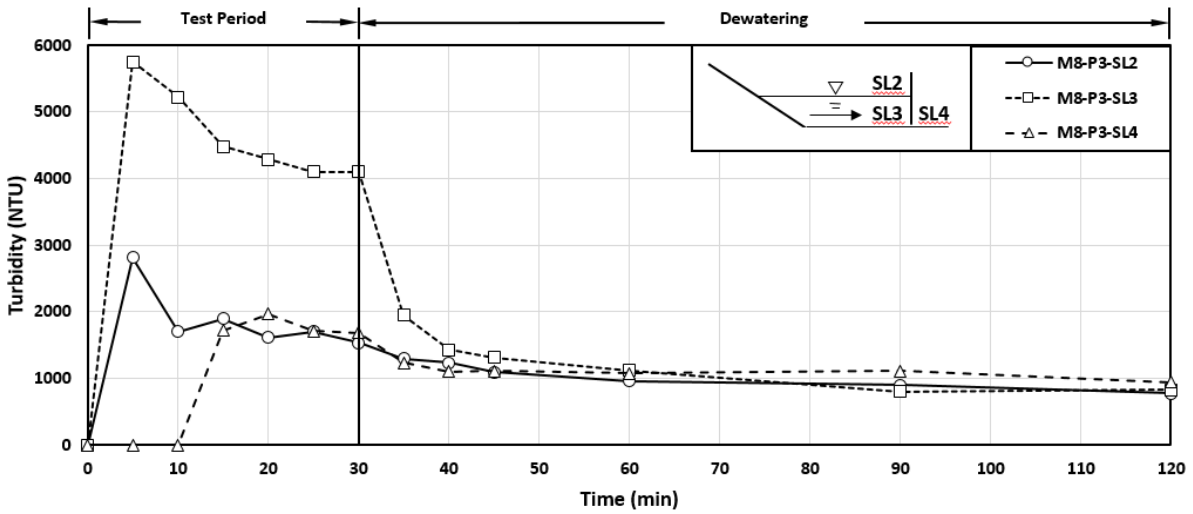

(a) M8 turbidity plot

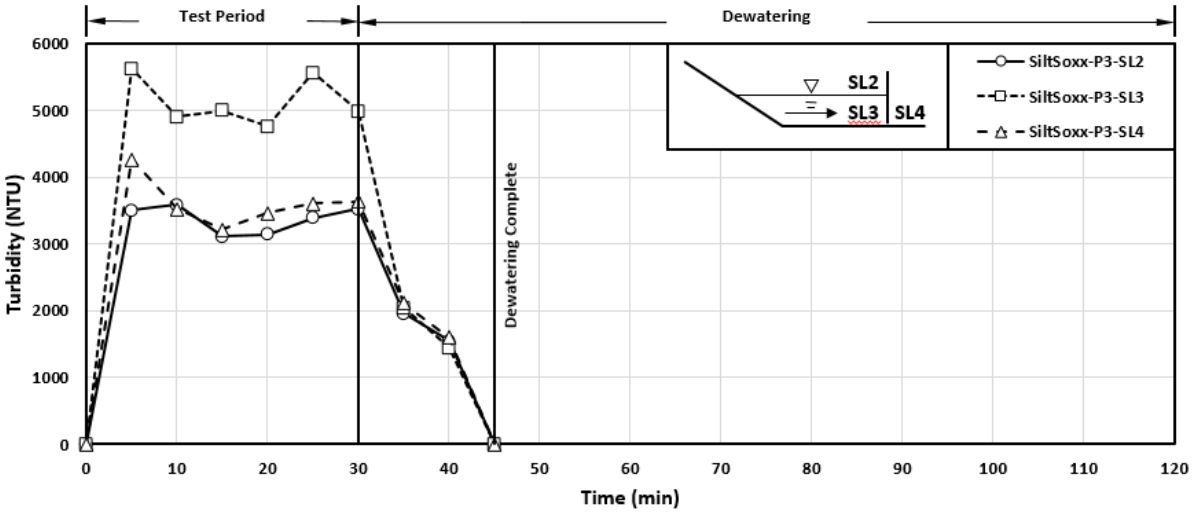

(b) SiltSoxx turbidity plot

Figure 5.22. Effects of impoundment depth capability on water quality.

5.5.6 WATER QUALITY EVALUATION SUMMARY

Performance testing has shown that the treatment efficiency of innovative and manufactured SB practices vary product to product, as well as over longevity testing. Turbidity ratio graphs do not take into consideration the extent of impoundment surface turbidity associated with each practice. For example, average impoundment surface turbidity during M8 and AL HB SRB w/o flocculant testing was 2,020 NTU and 7,470 NTU, respectively. These values are significantly different because of the impoundment depth capabilities associated with each

practice. Based on these turbidity values, a theoretical reduction of 1000 NTU would be a major achievement for M8 because turbidity would essentially be reduced by half; on the other hand, the same reduction for the AL HB SRB w/o flocculant would be considered effective but to a lesser degree. Treatment efficiency results reported provide scientifically backed filtering capabilities associated with each practice; however, it is imperative that the selection of SB practices not solely be based on treatment efficiencies. As shown through performance based testing, impoundment plays a major role in water quality improvement. When selecting a SB practice for implementation, consideration should be given to each of the performance standards evaluated within this study. Site-specific requirements should be used for selecting the most feasible practice(s) based on their capabilities identified within this study. Additional time variable turbidity results that illustrate water quality changes at sample locations SL2, SL3, and SL4 for each practice are provided in Appendix D. Furthermore, treatment efficiency plots that illustrate the changes between P1, P2, and P3 for each practices are provided in Appendix E.

5.6 SUMMARY

This study has shown the need for full-scale, reproducible SB testing methodologies to evaluate and improve current practices and to achieve greater in-field performance. The study provided full-scale performance evaluation results for two manufactured silt fence systems (C-POP and Stage Release Silt Fence), three SRBs (ALDOT SRB, AL HB SRB w/o Flocculant, and AL HB SRB w/ Flocculant), and three manufactured SB products (Excel Straw Log, SiltSoxx, and Curlex Bloc). Evaluations were conducted on installation feasibility, structural integrity, impoundment capability, effluent flow rate, sediment retention, and water quality improvement. Results from the standardized performance based testing provide researchers with a means for evaluating and

comparing new and innovative SB products emerging within industry. Results from this investigation can also be used to provide performance based installation enhancement strategies in future testing and field applications. Furthermore, these results provide designers and installers with scientifically backed performance capabilities when subjected to hydraulic and sediment loads resulting from a typical 2-yr, 24-hr storm event in the state of Alabama.

An in-depth discussion was presented identifying materials and associated properties used to manufacture and construct each of the SB practices. Recommended installation guidelines were evaluated and alternative installation strategies were developed to facilitate upstream impoundment and promote particle settlement. Installation efforts and observed deficiencies were presented to increase general knowledge and minimize reoccurrence in field applications. Observed results showed that undermining and flow bypass was a major failure mode for many practices throughout testing. Sediment capture was optimized when upstream impoundment depths were between 1 and 1.5 ft (0.3 and 0.46 m), which resulted in at least 90% retention. Impoundment depths greater than 1.5 ft (0.46 m) did not significantly improve sediment capture. Minimal to no water quality improvements were observed during manufactured silt fence system testing based upon filtration sampling directly upstream and downstream of the silt fence fabric. SRBs were the most effective practices for improving water quality as flow passed through the medium. Finally, the Curlex Bloc was the only manufactured SB product to achieve consistent water quality improvements between simulated storm events based solely upon the product's filtration capability.

Future research efforts should emanate from this project, allowing for further improvements to enhance the performance of innovative and manufactured SB practices.

Additional practices can be evaluated using the full-scale SB testing apparatus and developed test methodology to identify performance capabilities and associated limitations prior to in-field applications.

CHAPTER SIX:
SMALL-SCALE PERFORMANCE EVALUATIONS OF GEOTEXTILES USED IN SILT FENCE APPLICATIONS

6.1 INTRODUCTION

As shown in the literature review, most regulatory agencies mandate the use of silt fence as a perimeter control practice (*Toxel 2013*). Nonetheless, standard small-scale testing methodologies have failed to adequately quantify realistic filtering and sediment retention efficiencies of silt fence installations. Current small-scale testing methodologies do not address realistic stormwater runoff volumes or sediment loadings that field silt fence installations will most likely intercept during their life cycle. For example, ASTM D5141 specifies that 20 gallons (75 L) of sediment-laden water be introduced during testing in less than 10 seconds (*ASTM 2011*). This method does not mimic realistic runoff conditions for all regions of the U.S. resulting from a 2-yr, 24-hr storm event, which is stipulated in the U.S. Environmental Protection Agency's Construction General Permit as the minimum capacity requirement for all erosion and sediment control (ESC) practices (*USEPA 2017*). Cooke et al. (*2015*) identified that research regarding the efficiency of silt fence is lacking and that better science is needed to identify which factors influence the effectiveness of such devices. Thus, this study aims to improve upon current small-scale testing standards by developing an improved testing technique that addressed these issues and provides in-field performance capabilities of common geotextile fabrics used in silt fence applications.

6.2 RESEARCH OBJECTIVES

The primary objective of this study was to better understand and compare flow rates, sediment retention capabilities, and water quality impacts associated with various geotextiles commonly used in silt fence applications. Specific tasks performed to satisfy the primary objective includes: (1) design and construction of a small-scale sediment barrier (SB) testing apparatus, (2) development of a testing methodology that incorporates regionally specific design criteria that produces repeatable tests, (3) small-scale performance evaluations of various silt fence geotextiles, and (4) a proof-of-principle analysis for evaluating three-dimensional SB practices within the developed small-scale testing apparatus. Results obtained from this study can provide federal and state transportation agencies with improved geotextile performance capabilities that can enhance the design, implementation, and maintenance protocols associated with standard silt fence practices.

6.3 MEANS AND METHODS

This section describes the testing apparatus, procedures and methodology developed for small-scale testing of SB geotextiles. The testing methodology developed in this study improves upon current practices outlined within standard testing procedures and reviewed literature. The methodology aims at providing performance evaluations and analyses of geotextile fabrics while addressing limiting factors of published silt fence geotextile testing efforts. The developed testing protocol subjects SB geotextiles to typical stormwater loading conditions associated with central Alabama. The purpose of these geotextile experimental tests are to evaluate sediment retention capabilities, effluent flow rates, and water quality improvements. The geotextiles selected for testing consisted of two nonwoven fabrics (e.g., needle punched and spunbond) and

three woven fabrics with varying weave configurations. In addition, a stacked sandbag configuration was evaluated to demonstrate a proof-of-principle for evaluating three-dimensional practices using the small-scale testing apparatus and presented methodology.

6.3.1 SMALL-SCALE TEST APPARATUS DESIGN

The small-scale SB testing apparatus was designed to evaluate geotextiles installed as perimeter control practices. The apparatus is constructed out of dimensional lumber and plywood with overall dimensions of 4 ft (1.2 m) wide, 16 ft (4.9 m) long, and height of 3 ft (0.9). The profile of the apparatus consists of a 3*H*:1*V* slope that transitions to a 1% slope, which mimics typical slopes associated with highway construction projects. When evaluating geotextiles using ASTM D5141, geotextiles are installed at the toe of an 8% slope, which limits the installations stormwater storage capacity due to the close proximity to the slope. To increase storage capabilities, geotextiles were installed 6 ft (1.8 m) from the toe of the 3*H*:1*V* slope within the small-scale testing apparatus. Flow is directed into the apparatus via an 8 ft (2.4 m) plywood sheet with 2 by 6 in. (5 by 15 cm) lumber borders that transition inflow form shallow concentrated to sheet flow. Figure 6.1 shows as-built pictures and details of the small-scale SB testing apparatus.

(a) test apparatus

(b) sheet flow introduction

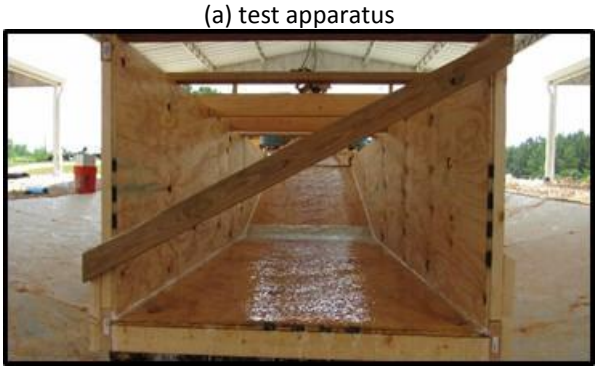

(c) downstream perspective

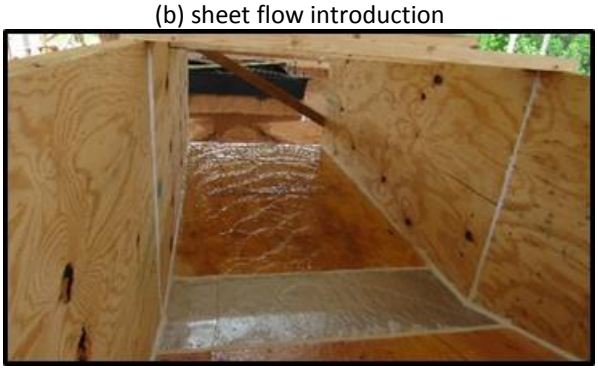

(d) upstream perspective

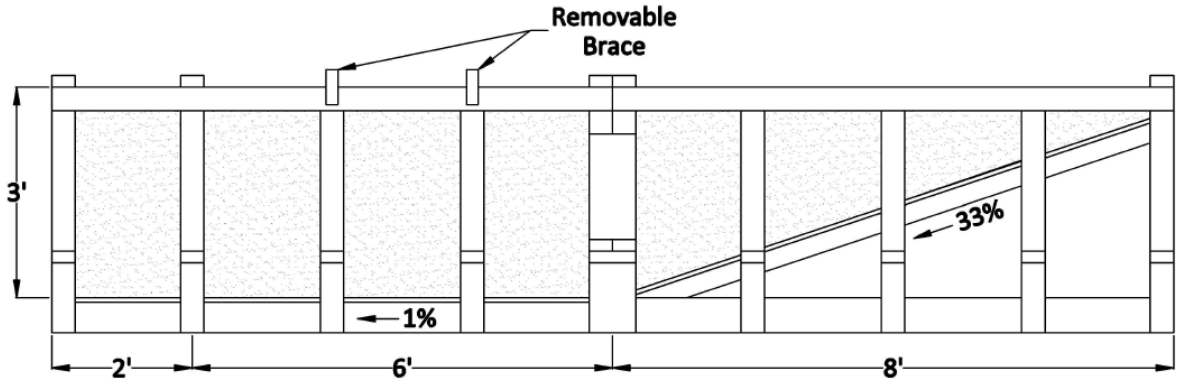

(e) elevation view detail

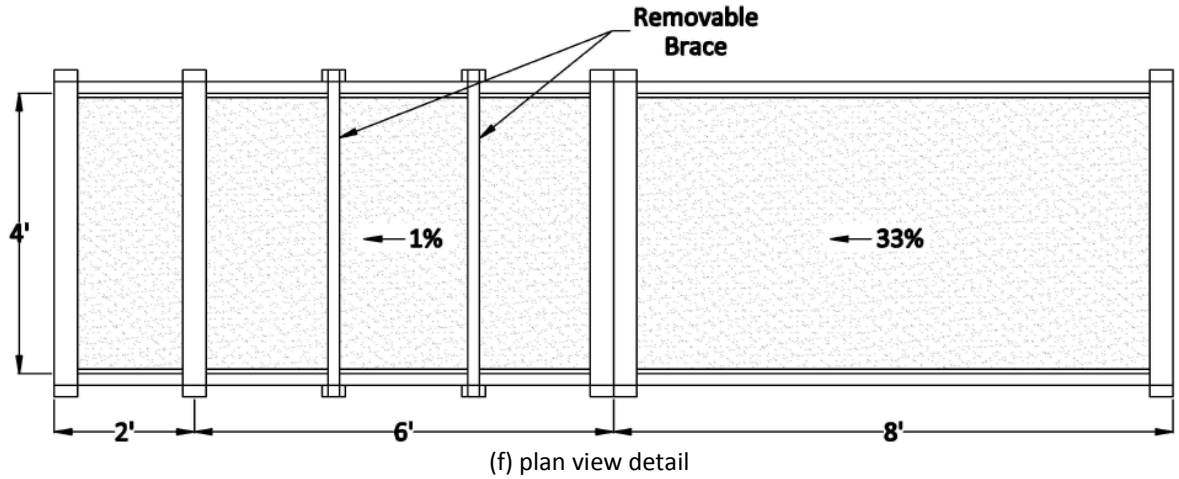

(f) plan view detail

Figure 6.1. Small-scale SB testing channel images and details.

To prevent flow from passing through joints of the small-scale apparatus during testing, a 0.006 in. (0.15 mm) thick polypropylene liner was placed inside the apparatus. Geotextiles were held in place using 2 by 4 in. (5 by 10 cm) lumber and wood screws. Flow bypass between the geotextile and polypropylene liner was prevented by sealing each installation with heavy-duty construction caulk during the installation process. After each evaluation was completed, the geotextile and dried caulk sealant were carefully removed to prevent damage to the liner. This process allowed a single liner to be used for multiple installations. However, if liner damage occurred during post-test geotextile or sediment removal, a new liner was installed. This method proved effective at preventing seepage, while also providing a means for collecting retained sediment.

6.3.2 FLOW INTRODUCTION

Water introduction into the apparatus was designed to facilitate accurate flow rate monitoring throughout testing while also providing a means for easy flow rate adjustments. To achieve the desired flow control necessary during testing, a four-stage process was implemented. The setup consisted of a submersible 2 in. (5 cm) pump [Figure 6.2(a)], a 300-gallon (1,135 L) equalizing tank [Figure 6.2(b)], a 90° v-notch discharge weir plate for controlling apparatus inflow [Figure 6.2(c)], and two 4 in. (10 cm) discharge valves for controlling flow exiting the bottom of the tank [Figure 6.2(d)]. The submersible pump transported water from the onsite supply pond into the equalizing tank located upstream of the test apparatus. As water filled the tank and began to flow across the weir plate, discharge gate valves were adjusted until the desired water level within the tank was achieved. A custom scale and pressure head tube apparatus [Figure 6.2(e)] were installed adjacent to the tank to monitor water levels. The scale provided a

correlation between water depth flowing across the weir plate and flow rate entering the apparatus. This method of water introduction and monitoring allows for a wide range of flow rates, which may vary based on regional rainfall events.

(a) submersible pump

(b) equalizing tank

(c) v-notch weir

(d) discharge gate valves

(e) flow rate monitoring

Figure 6.2. Water regulation system.

Silt fence installations are typically designed based on contributory area or maximum slope length above the installation. Within the state of Alabama, two area based design

parameters are commonly used. The first method limits contributory area to 0.25 acre (0.10 ha) per 100 ft (30.5 m) of unreinforced silt fence. This design strategy is typically implemented on small residual projects where land disturbance is minimized. The second method limits contributory area to 0.50 acre (0.20 ha) per 100 ft (30.5 m) of reinforced silt fence. This design strategy is commonly applied on projects that have large land disturbance areas, such as highway construction, and was used to develop the theoretical drainage area during full-scale testing. Appling the same principles outlined in the full-scale testing methodology, a hydrograph was created for a 0.02 acre (0.008 ha) drainage area that would be intercepted by a 4 ft (1.2 m) section of silt fence. As shown in Figure 6.3, the average flow rate for the peak 30 minutes of a 2-yr, 24-hr design storm from a drainage area of 0.02 acre (0.008 ha) was calculated to be 0.04 ft^3/s (0.0011 m^3/s). This flow rate was applied during each 30-minute small-scale test.

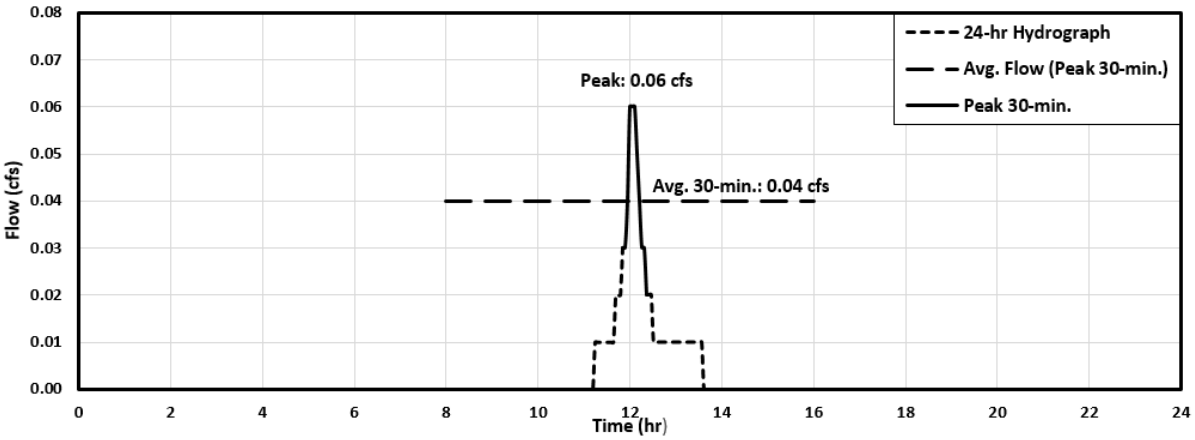

Figure 6.3. Hydrograph for 0.02 acre (0.008 ha) representative drainage area.

A summary of the drainage areas, flow rates, and runoff volumes applied during small-scale testing are shown in Table 6.1.

Table 6.1. Summary of Theoretical Flow Values for Small-Scale SB Testing

Design Drainage Area ac (ha)	Scaled-Down Drainage Area ac (ha)	Peak Flow ft^3/s (m^3/s)	Avg. Flow for 30 Min Peak ft^3/s (m^3/s)	Total Vol. 30 Min Test ft^3 (m^3)	Total Vol. 30 Min Test Gal (L)
0.50 (0.20)	0.02 (0.008)	0.06 (0.0017)	0.04 (0.0011)	72.0 (2.04)	592.4 (2,242)

Note: Average 2-year, 24-hour storm for Alabama = 4.43 inches. NRCS Type III rainfall distribution. Average CN = 88.5 for Alabama; 1 ac = 0.4 ha; 1 ft^3/s = 0.028 m^3/s; 1 ft^3 = 0.028 m^3; 1 gal = 3.79 L

6.3.3 SEDIMENT INTRODUCTION

Sediment metering was achieved by manually feeding soil into the soil/water mixing trough built on the plywood flow introduction sheet [Figure 6.4(a)]. To maintain a consistent rate throughout testing, 5-gallon (3.79 L) buckets were pre-filled with the exact amount of soil to be introduced over a 2 minutes duration. Workers would monitor a stopwatch while feeding soil from the buckets into the system so that one bucket of soil would be emptied every 2 minutes. Workers would position themselves beside the flow introduction sheet so that at the end of every 2-minute cycle, a new bucket of soil could be easily place over the mixing trough and soil feeding could continue without interruption [Figure 6.4(b)]. A mechanical means of soil introduction was available; however, soil texture caused particles to bridge together preventing soil from flowing from the hopper into the mechanical auger at a consistent rate.

(a) mixing trough (b) sediment introduction

Figure 6.4. Sediment introduction system.

While peak and 30 minute average flows associated with full and small-scale contributory areas are different, the average flow per linear foot of silt fence remains constant (e.g., 0.01

cfs/LF). Nonetheless, the modified universal soil loss equation estimations associated with each contributory area change substantially per liner foot of silt fence due to total volume and flow rate variations. To maintain consistent sediment loading parameters per linear foot between full and small-scale tests, the calculated sediment load for full-scale testing was converted into sediment load per liner foot (e.g., 1127.8 lb. (511.6 kg) of soil per 20 ft (6.1 m) of silt fence= 56.4 lb./LF (83.8 kg/LM)). Using this loading rate and the width of the small-scale testing apparatus (i.e., 4 ft (1.2 m)), total sediment load was computed to be 225.6 lb. (102.3 kg) for small-scale testing. The targeted sediment load metering rate was calculated to be 7.5 lb./min. (3.3 kg/min.) over the 30 minute test duration. Based upon the flow and sediment introduction rates, the sediment introduction concentration was calculated to be 3.1 lb./ft^3 (50,000 mg/L) as flow enters the test apparatus, which is the same concentration applied during full-scale testing. As outlined by ASTM D5141 (*2011*), soil used during testing should be site-specific or representative of the location of implementation. Thus, soil used during testing was native to central Alabama and was classified as a sandy loam according to the United State Department of Agriculture (USDA) soil classification system.

6.3.4 TESTING REGIME

To assess the performance characteristics of geotextiles used in SB applications, a multiple iteration experimental testing regime was developed for small-scale testing. The developed regime requires that each geotextile be installed and sealed inside the testing apparatus and subjected to a constant sediment-laden flow of 30 minutes. After the test period, observation and data collection continued during dewatering for an additional 90 minutes to evaluate post-test performance. In total, observational and data collection lasted 120 minutes.

To better understand performance capabilities and insure accurate reporting of geotextile properties, three installations and evaluations were conducted per geotextile. This repetitive approach provides a means for identifying inconsistencies between tests and implementing adjustments in subsequent geotextile evaluations if necessary. Figure 6.5 illustrates the small-scale testing regime implemented during geotextile evaluations.

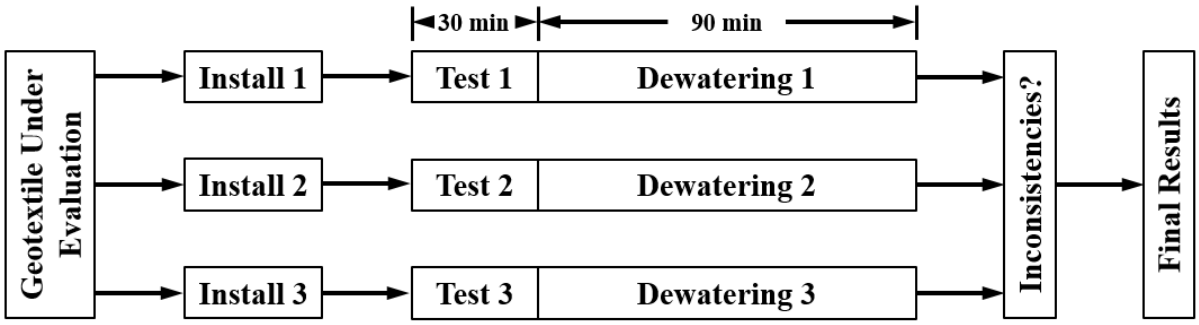

Figure 6.5. Small-scale testing regime.

6.3.5 DATA COLLECTION

Evaluations are based on observations and data collected throughout experiments. Hydraulic performance, sediment retention, and water quality data were collected for each experiment. These parameters are used to compare the performance of each geotextile tested.

6.3.5.1 Hydraulic Performance

Two Onset HOBO water level pressure transducers (U20-001-04) were deployed during testing to accurately measure impoundment depth within the apparatus throughout the duration of each experiment. One logger was installed along the floor of the test apparatus, upstream of the geotextile, to record water pressure as an impoundment formed [Figure 6.6]. The second logger was installed downstream of geotextile above the high water mark to record atmospheric pressure. Each logger was programed to take pressure and temperature measurements at 10

second intervals. Pressure data collected along the bottom of the impoundment was evaluated against atmospheric pressure data to calculate differential pressures over the course of each experiment. Using these pressures, corresponding time-variable water depths throughout each experiment were calculated using HOBO® software. Knowing the storage geometry of the test apparatus and time-variable water depth, retained time-variable flow volumes were calculated. These time-variable volumes were analyzed against the introductory flow to determine geotextile effluent flow rates.

Figure 6.6. Upstream water level logger installation location.

6.3.5.2 Sediment Retention

To accurately quantify sediment retained upstream for each experiment, dry soil weights were determined pre and post-tests. Soil used for testing was mechanically sieved to remove large rocks and organic debris then stored in a drying shed. Prior to testing, 5-gallon (3.79 L) buckets were filled with dried soil until the required weight per bucket was obtained. Soil samples were collected from several buckets and processed to determine an average moisture

content of the air dried soil. Using the moisture content results, which were typically around 9%, dry soil weight prior to testing was determined. Upon test completion, retained sediment was removed from the test apparatus and placed on polypropylene sheets to sun dry [Figure 6.7(a)]. After sun drying, retained soil was loaded in galvanized washtubs and placed in large ovens to remove residual moisture. Post-test dry soil weight was obtained from oven dried soil to calculate sediment retention [Figure 6.7(b)].

(a) sun drying (b) oven dried soil

Figure 6.7. Small-scale soil drying process.

6.3.5.3 Water Quality Sampling

Water sampling was conducted during each geotextile performance evaluation to analyze effects on water quality as flow passed through the system. Grab samples were collected in 8 oz. (236 mL) bottles by manually obtaining water samples from three locations: (1) along the surface of the upstream impoundment (i.e., SL2), (2) along the bottom of the impoundment via a sampling pump (i.e., SL3), and (3) downstream of the geotextile installation (i.e., SL4). Figure 6.8 illustrates the sample locations in relation to an installed geotextile. Over the course of each experiment, 12 grab samples were collected at each sampling location. During the initial 45 minutes of an experiment, grab samples were taken at five minutes intervals (i.e., 9 grab samples). The remaining three samples were collected at elapsed time durations of 60, 90, and

120 minutes. Grab samples were processed post-test in a laboratory to determine turbidity levels within the system oven the duration of the experiment.

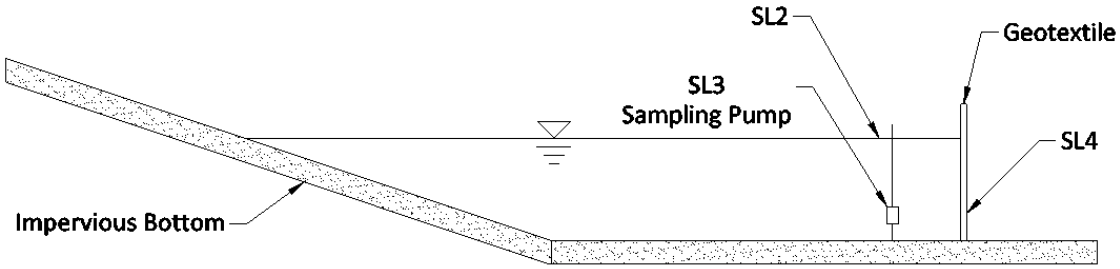

Figure 6.8. Small-scale SB grab sample locations.

6.3.6 METHODOLOGY COMPARISON

The standard method for evaluating geotextiles is outlined in ASTM D5141 *Determining Filtering Efficiency and Flow Rate of the Filtration Component of a Sediment Retention Device*. This research effort aimed to improve upon this standard test methodology be mimicking realistic runoff conditions intercepted by SB practices. The existing methodology and developed methodology are shown in Table 6.2 to provide a comparison between the methods.

Table 6.2. Comparison of ASTM D5141 and AU-ESCTF Small-Scale Testing Methodologies

Study	Focus	Design Storm	Drainage Basin ac (ha)	Flow Rate ft^3/s (m^3/s)	Sediment Load lb. (kg)	Test Duration (min)
ASTM D5141 (2011)	Filtering Efficiency and Flow Rate	N/A	N/A	0.177 (0.005)	0.33 (0.15)	0.17
AU-ESCTF Small-Scale SB Testing	Sediment Retention, Flow Rate, and Water Quality	2-yr, 24-hr	0.02 (0.008)	0.04 (0.0011)	225.6 (102.3)	30

Note: 1 ac = 0.4 ha; 1 ft^3/s = 0.028 m^3/s; 1 lb. = 0.45 kg

6.4 GEOTEXTILE MATERIALS

For this research effort, two nonwoven and three woven geotextiles were selected for evaluation. While all nonwoven geotextiles start out as a loosely connected synthetic polymer

fibers, the method in which bonding occurred varies. The most common method for bonding is by mechanically entangling staple fibers or continuous filaments using heated rollers equipped with barbed needles. Geotextiles manufactured using this needle-punch process are typically black in color and have a felt-like consistency, as shown in Figure 6.9(a). Spunbonding is another popular method for bonding synthetic fibers. Manufacturing typically consist of jetting extruding filaments onto a collection belt and passing the matrix through heated rollers to bond the fibers. Finished products are typically gray in color with a smooth finish, as shown in Figure 6.9(b). Key differences between the two method is that spunbond products typically have reduced pore size openings and increased tensile strength when compared to needle-punched products (*U.S. Fabrics 2018*).

Woven geotextiles are manufactured in two basic structures: slit film and monofilament. Slit film geotextiles are manufactured by slitting polypropylene sheets into narrow flat strands of yarn and weaving them together to from a woven sheet. These types of geotextiles work well in geotechnical applications but do not perform well in filtering applications due to low permeability and increased clogging potential. Monofilament geotextiles are manufactured by extruding strands of polypropylene yarn and weaving them together to form strong, highly permeable products that are commonly used in filtering applications (*U.S. Fabrics 2018*). Three variations of monofilament geotextiles were evaluated during this study: wide filament – constant density [Figure 6.9(c)], narrow filament – constant density [Figure 6.9(d)], and narrow filament – variable density [Figure 6.9(e)]. Each of these geotextiles are better known within industry as Blue Stripe, Red Stripe, and Green Stripe, respectively, due to the colored filaments woven into each of the

geotextiles. The physical properties and published flow capabilities associated with each of these geotextiles are summarized in Table 6.3.

(a) nonwoven - needle punched

(b) nonwoven - spunbond

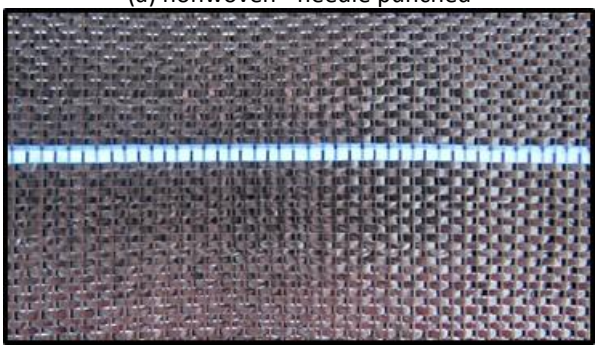

(c) woven monofilament – blue stripe
wide filament – constant density

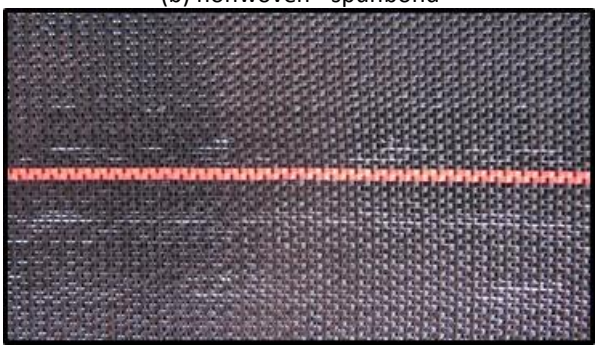

(d) woven monofilament – red stripe
narrow filament – constant density

(e) woven monofilament – greed stripe
narrow filament – variable density

Figure 6.9. Geotextile materials evaluated.

Table 6.3. Geotextile Material Properties

Geotextile	Zone	Weight (oz./yd^2)	MD Filament Width (in)	MD Density (fila./in.)	XMD Density (fila./in.)	AOS (U.S. Sieve)	Flow[a] (gpm/ft^2)
Nonwoven Needle-Punched	n/a	3.5	n/a	n/a	n/a	50	150
Nonwoven Spunbond	n/a	4.8	n/a	n/a	n/a	70	180
Woven Blue Stripe	n/a	3.3	0.055	20	14	40	93
Woven Red Stripe	n/a	5.6	0.040	28	18	30	95.5
Woven Green Stripe	E	5.2	0.030	24	20	20	324
	D	6.2	0.030	28	20	20	235
	C	6.7	0.030	32	20	20	210
	B	7.3	0.030	36	20	40	141

Note: [a] =clear water flow rates determined using ASTM D4491; n/a = not applicable; MD = Machine Direction; XMD = Cross Machine Direction; AOS = Apparent Opening Size; fila. = filament

In addition to the aforementioned geotextiles, a stacked sandbag configuration was installed and evaluated using the presented methodology. The installation consisted of stacking sandbags in alternating directions while also staggering abutment ends. These evaluations were conducted to compare the performance of a stacked sandbag configuration to various geotextiles while also demonstrating a proof-of-principle for evaluating three-dimensional products within the small-scale testing apparatus. Figure 6.10 illustrates the sandbag installation and associated schematic.

(a) upstream vantage

(b) downstream vantage

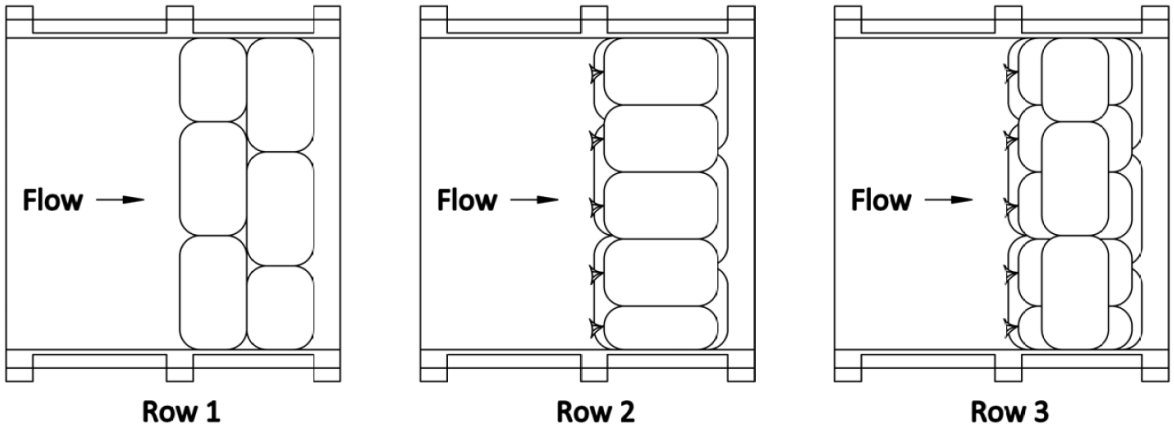

(c) installation schematic

Figure 6.10. Small-scale sandbag installation details.

6.5 RESULTS AND DISCUSSION

The following is a summary of the results and observations made from performance evaluations of five geotextile fabrics and a stacked sandbag configuration using a constant sheet flow of 0.04 cfs (0.0011 m^3/s) over a 30-minute duration.

6.5.1 HYDRAULIC EVALUATION

Hydraulic performance of the filtering component of a SB is a key parameter to determine during performance evaluations. Impoundment depth measurements obtained throughout each experiment provide a means for evaluating the hydraulic performance of each geotextile tested. Figure 6.11(a) shows average impoundment depths over three installations for each material evaluated and Figure 6.11(b) shows the calculated flow rates. From the plots, it is evident that

nonwoven geotextiles impound considerably more volume than woven geotextiles. This is expected due to nonwoven geotextiles possessing reduced apparent opening size (AOS) when compared to woven monofilament geotextiles. When comparing the two nonwoven geotextiles, spunbond creates a slightly large impoundment than needle-punched. This increased impoundment resulted in spunbond effluent flows being reduce by 30% when compared to needle-punched. Figure 6.12 shows hydraulic observations made during nonwoven geotextile testing.

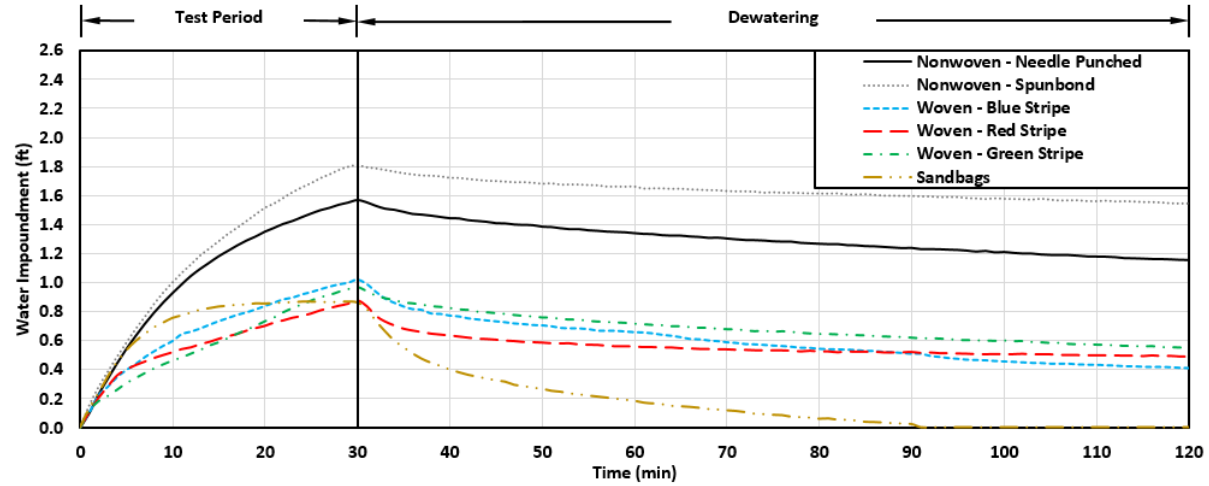

(a) measured water depths

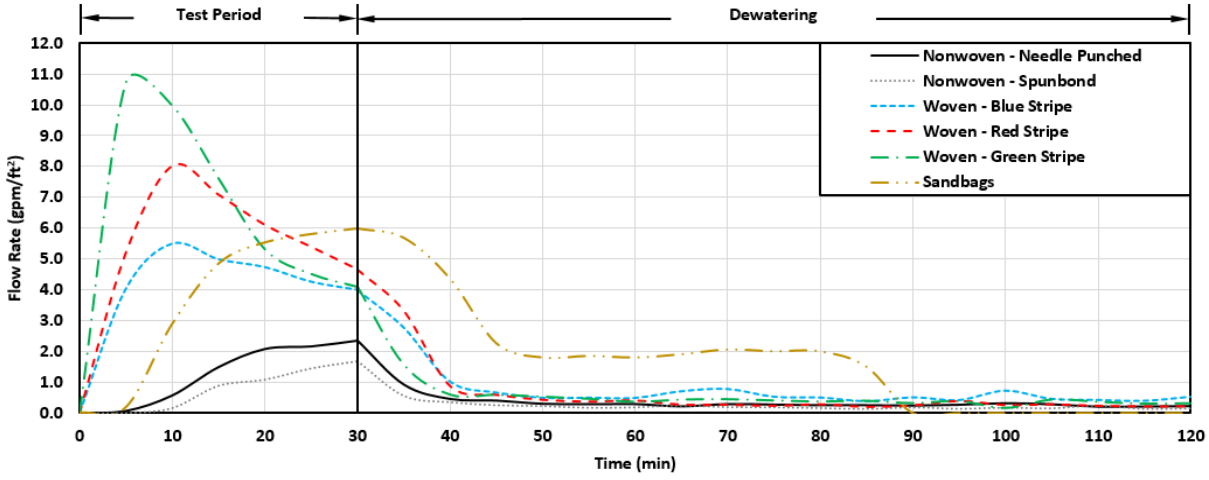

(b) calculated effluent flow rates per square foot of geotextile

Figure 6.11. Small-scale hydraulic analyses.

(a) needle punched - impoundment

(b) needle punched - effluent

(c) spunbond – impoundment

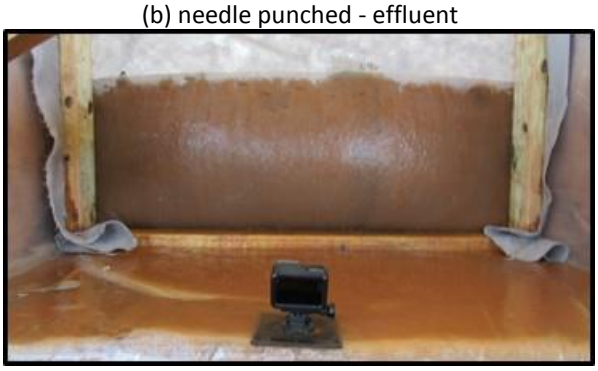

(d) spunbond - effluent

Figure 6.12. Nonwoven geotextile hydraulic observations.

As shown in Table 6.3, filament density associated with each woven geotextile varies slightly. This change in filament density affects the quantity of pore opening per unit of surface area. Based on filament densities shown, blue stripe has the least quantity of pore opening at 280 pores/in.^{2} (40 pores/cm^2), red stripe has 504 pores/in.^{2} (77 pores/cm^2), and green stripe has the most at 720 pores/in.^{2} (112 pores/cm^2). These material properties suggest that effluent flow rates would be 2.5 times higher for green stripe when compared to blue stripe. To test this hypothesis, a single factor ANOVA was conducted on average effluent flow rates calculated over the 30-minute testing period. The test failed to find a significant difference between woven geotextile flow data. This statistical analysis suggest that while each woven geotextile tested is comprised of a distinct manufacturing design to control effluent flow, no significant flow variations occurred between woven geotextiles. In addition, each geotextile emitted similar

effluent flows when subjected to sediment-laden runoff. Figure 6.13 shows the hydraulic observations made during woven geotextile testing.

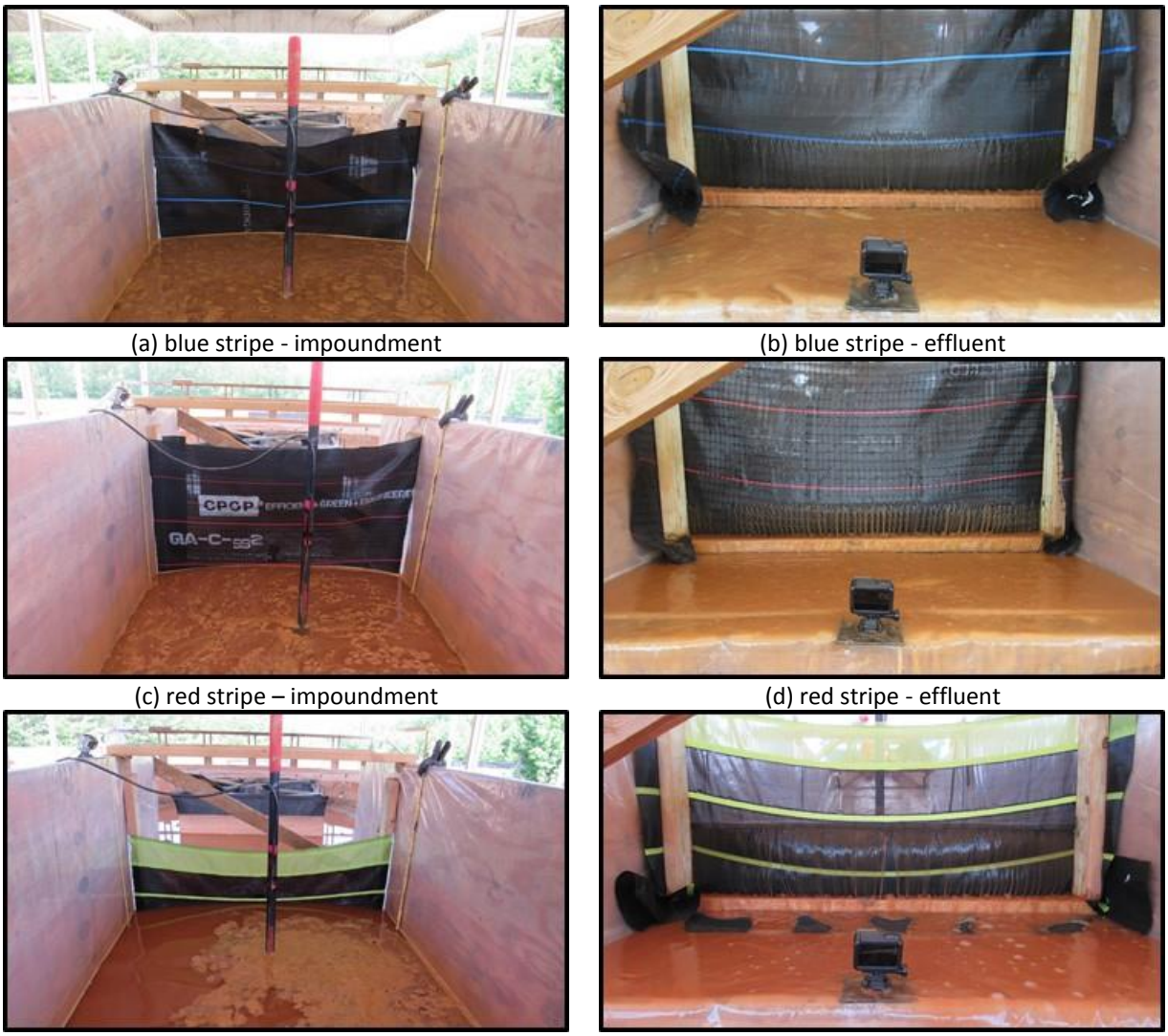

(a) blue stripe - impoundment (b) blue stripe - effluent

(c) red stripe – impoundment (d) red stripe - effluent

(e) green stripe - impoundment (f) green stripe - effluent

Figure 6.13. Woven geotextile hydraulic observations.

Sandbag barriers are commonly used in ditch check and inlet protection applications, while their uses as a construction site perimeter control is less common. The installation configuration tested, which consisted of a rotated middle row, was based on ALDOT standard drawings for ditch checks and inlet protection that provides improved friction between bags while also minimized gap voids. As shown in Table 6.4, the average maximum impoundment

achieved during evaluations was 0.87 ft (0.27 m), which was lower than all geotextiles evaluated. Hydraulic observations made during testing indicated that sandbags did not provide a tight seal and flow passed through abutment gaps with minimal to no flow passing through the sand medium, as shown in Figure 6.14(b). Sandbags were the only practices to achieve complete dewatering during the observational period, which occurred 60 minutes into dewatering.

(a) maximum impoundment (b) flow passing through abutment gaps

Figure 6.14. Sandbag hydraulic observations.

6.5.2 SEDIMENT RETENTION EVALUATION

Sediment retention indicates the percent of sediment removed from sediment-laden flow mainly through the process of sedimentation. Currently, ASTM D5141 does not specifically outline a process for differentiating the quantity of sediment removed by geotextile filtration and through the process of sedimentation. Implementation of the aforementioned small-scale sediment retention methodology has proved to an effective means for filling this evaluation gap. A complete summary of small-scale sediment retention results is provided in Table 6.4, along with maximum impoundment depths and effluent flow rates. Results obtained from needle-punched and spunbond geotextiles indicate average sediment retention rates of 97% and 98%, respectively. Of the geotextile types tested, nonwoven was the most effective and consistent at removing sediment through sedimentation. Woven geotextile results indicated that red, green,

and blue stripe fabrics had average sediment retention rates of 94%, 93%, and 87%, respectively. Of all small-scale sediment retention evaluations, sandbag were the least effective with an average retention rate of 83%. Standard deviations of sediment retention results for green stripe, blue stripe, and the sandbag installations was 4%, 6%, and 8%, respectively. These deviations were greater than both nonwoven geotextiles and the red stripe geotextile (e.g., 1%). Figure 6.15 shows sediment deposition observations for each practices evaluated.

Table 6.4. Small-Scale Performance Results

Material		Install.	Sediment Retained	Max Impoundment ft (m)	Avg. Effluent Flow			
					gpm/LF (lpm/LM)[a]		gpm/ft² (lpm/m²)[b]	
					Test Period	Dewatering	Test Period	Dewatering
Nonwoven Geotextiles	Needle Punched	I1	97%	1.54 (0.47)	1.94 (24.12)	0.54 (6.73)	1.49 (60.9)	0.48 (19.5)
		I2	96%	1.63 (0.50)	1.72 (21.34)	0.24 (2.94)	1.29 (52.4)	0.21 (8.5)
		I3	98%	1.55 (0.47)	1.96 (24.35)	0.24 (3.02)	1.59 (64.6)	0.22 (9.1)
		Avg.	**97%**	**1.57 (0.48)**	**1.88 (23.27)**	**0.34 (4.23)**	**1.46 (59.3)**	**0.30 (12.4)**
	Spunbond	I1	97%	1.85 (0.56)	1.35 (16.70)	0.31 (3.87)	0.86 (35.2)	0.18 (7.4)
		I2	98%	1.79 (0.55)	1.38 (17.16)	0.39 (4.79)	0.88 (35.8)	0.24 (9.9)
		I3	98%	1.79 (0.55)	1.29 (16.00)	0.28 (3.48)	0.87 (35.4)	0.22 (9.1)
		Avg.	**98%**	**1.81 (0.55)**	**1.34 (16.62)**	**0.33 (4.05)**	**0.87 (35.4)**	**0.22 (8.8)**
Woven Monofilament Geotextiles	Blue Stripe	I1	93%	0.97 (0.30)	3.33 (41.28)	0.49 (6.11)	5.25 (213.7)	0.96 (39.2)
		I2	86%	1.13 (0.34)	2.36 (29.22)	0.48 (5.95)	3.91 (159.2)	0.63 (25.8)
		I3	81%	0.98 (0.30)	3.07 (38.04)	0.34 (4.25)	4.57 (186.3)	0.51 (20.9)
		Avg.	**87%**	**1.03 (0.31)**	**2.92 (36.18)**	**0.44 (5.44)**	**4.57 (186.4)**	**0.70 (28.6)**
	Red Stripe	I1	93%	1.01 (0.31)	3.29 (40.82)	0.31 (3.87)	4.24 (172.8)	0.42 (17.0)
		I2	95%	0.81 (0.25)	2.69 (33.40)	0.30 (3.71)	7.19 (292.9)	0.55 (22.5)
		I3	94%	0.84 (0.26)	3.31 (41.05)	0.31 (3.79)	6.81 (277.3)	0.57 (23.2)
		Avg.	**94%**	**0.89 (0.27)**	**3.07 (38.11)**	**0.31 (3.79)**	**6.08 (247.7)**	**0.51 (20.9)**
	Green Stripe	I1	93%	1.04 (0.32)	3.16 (39.20)	0.40 (4.95)	5.61 (228.7)	0.54 (21.8)
		I2	90%	0.91 (0.28)	3.31 (41.05)	0.29 (3.63)	10.45 (425.7)	0.42 (17.0)
		I3	97%	0.98 (0.30)	3.25 (40.35)	0.31 (3.79)	4.78 (194.7)	0.38 (15.6)
		Avg.	**93%**	**0.98 (0.30)**	**3.19 (39.50)**	**0.33 (4.12)**	**6.95 (283.0)**	**0.45 (18.1)**
Sandbags		I1	74%	0.94 (0.29)	3.48 (43.14)	0.78 (9.61)	3.93 (159.9)	1.61 (65.5)
		I2	86%	0.83 (0.25)	3.61 (44.76)	0.77 (9.49)	4.52 (184.2)	2.82 (114.9)
		I3	89%	0.84 (0.26)	3.59 (44.53)	0.80 (9.87)	4.05 (164.9)	4.31 (175.6)
		Avg.	**83%**	**0.87 (0.27)**	**3.56 (44.14)**	**0.78 (9.66)**	**4.16 (169.7)**	**2.91 (118.7)**

Note: [a] = average effluent flow rate in gallon per minute per linear foot of geotextile (liter per minute per linear meter); [b] = average effluent flow rate in gallon per minute per square foot of geotextile; 1 ft = 0.3 m; 1ft² = 0.093 m²; 1 gpm = 3.78 lpm

(a) needle punched (b) spunbond

(c) blue stripe (d) red stripe

(e) green stripe (f) sandbags

Figure 6.15. Small-scale sediment deposition observations.

6.5.3 WATER QUALITY EVALUATION

Turbidity readings obtained from grab samples gathered over the duration of each experiment were used to evaluate changes in water quality as flow passed through the small-scale testing apparatus. To distinguish the extent individual mechanisms contribute to water quality improvements within the system, analyses were conducted on turbidity reductions due to sedimentation and material filtration. Water quality effects due to sedimentation were determined be comparing turbidity levels along the bottom of the impoundment (i.e., SL3) to

those along the impoundment surface (i.e., SL2) at concurrent sampling times. Figure 6.16(a) illustrates time-variable sedimentation efficiencies for each material evaluated. Water quality effects due to material filtration were determined by comparing turbidity levels along the impoundment surface (i.e., SL2) to those downstream of the material installation (i.e., SL4) at concurrent sampling times. Time-variable filtering efficiencies are shown in Figure 6.16(b). Plotted results are reported as percent increase/decrease in turbidity for each material tested over the 120-minute evaluation period. Positive percentages (i.e., shaded green) indicate water quality improvements and negative percentages (i.e., shaded red) indicate degradation of water quality between respective sampling locations.

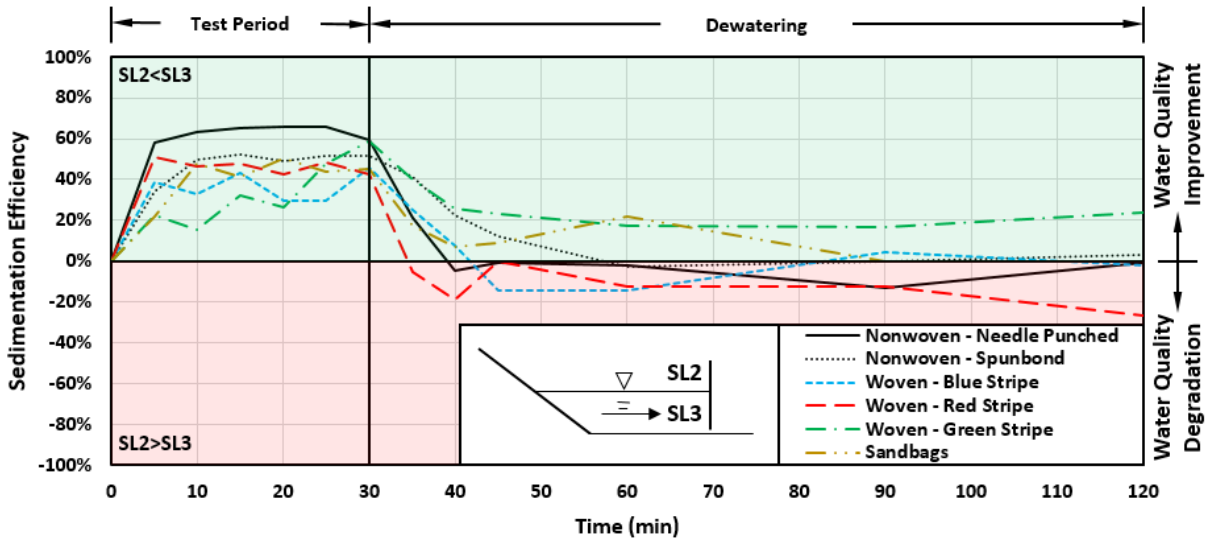

(a) effects on turbidity due to sedimentation

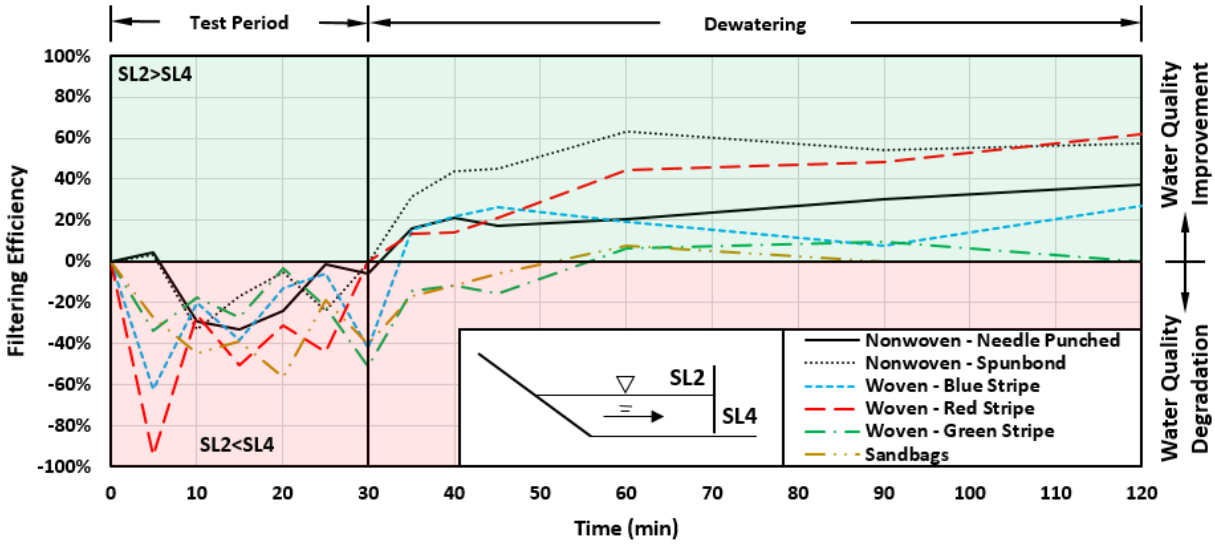

(b) effects on turbidity due to material filtration

Figure 6.16. Small-scale water quality analysis.

From the plots, it is evident that during the 30-minute test period, substantial reductions in turbidity (i.e., 34% to 63%) result from sedimentation while little to no improvements result from material filtration. Based on analyses of the sedimentation efficiency plot, nonwoven – needle punched was the most efficient by reducing turbidity an average of 63% during the test period. Green stripe was the least efficient with a 34% reduction; however, it was the most efficient during dewatering with a 24% reduction in turbidity due to sedimentation. Analyses of the filtering efficiency plot indicated that on average water quality degraded by 29%, thereby

failing to improve water quality during the 30-minute test period. However, filtering efficiencies improve on average by 19% during dewatering. While these water quality improvements are desirable, effluent flow volumes during dewatering are substantially less than flows observed during the test period. These observations are a result of pore clogging, which minimizes effluent flow and prolongs impoundment retention time.

6.6 SUMMARY

This study has shown the need to improve upon the ASTM standard for evaluating the filtering efficiency and flow rate of the filtering component of sediment retention devices. The study included the design and construction of a small-scale SB testing apparatus capable of simulating a wide range of design storm scenarios. The apparatus was designed to accommodate various manufactured geotextiles and sediment control devices. The presented methodology outlines a means for selecting appropriate flow rates and sediment loads based on regionally specific design storms data. The developed procedure lends to dedicated and controlled testing that produces replicable experimental results. The small-scale testing apparatus and presented methodology provides researchers with an improved method to evaluate innovative geotextile fabrics and material configurations in a controlled environment that allows for better understanding of performance capabilities. Results of standardized performance based testing will lead to improved design guidance for practitioners and regulatory agencies to reference when selecting geotextiles to incorporate into their SB designs.

Under the developed testing regime, performance evaluations were conducted on two nonwoven geotextiles, three woven geotextiles, and a stacked sandbag installation. Data collection included: impoundment depth, sediment retention weights, and grab samples for

water quality analyses. Each of these parameters were subsequently used to evaluate the performance capabilities of each material evaluated. Effluent flow rates observed during the test period for nonwoven geotextiles were on average 43% lower than woven materials, which resulted in extensive retention times for nonwoven materials. Sediment retention results indicated that on average nonwoven geotextiles (e.g., 97%) outperform woven geotextiles (e.g., 91%). Water quality analyses suggest that the primary means for turbidity reduction is sedimentation during the test period (e.g., 46%) and filtration during dewatering (e.g., 19%). This suggests that having adequate stormwater storage upstream of an installation is important to dissipate inflow energy, promote sedimentation, and minimize resuspension of particles. Finally, an evaluation of stacked sandbags established that performance capabilities of three-dimensional SB products can be determined using the small-scale SB testing apparatus. A comprehensive performance summary of materials evaluated as part of this study that federal and state transportation agencies can easily reference is provided in Table 6.5.

Table 6.5. Comprehensive Performance Summary

Material	Sediment Retention	Avg. Effluent Flow (gpm/LF)[a]		Avg. Sedimentation Efficiency[b]		Avg. Filtration Efficiency[b]	
		Test Period	Dewatering	Test Period	Dewatering	Test Period	Dewatering
Needle Punched	97%	1.88	0.34	63%	0%	-15%	24%
Spunbond	98%	1.34	0.33	48%	13%	-13%	49%
Blue Stripe	87%	2.92	0.44	37%	1%	-30%	19%
Red Stripe	94%	3.07	0.31	46%	-13%	-41%	34%
Green Stripe	93%	3.19	0.33	34%	24%	-26%	-4%
Sandbags	83%	3.56	0.78	46%	14%	-41%	-7%

Note: [a] = average effluent flow rate in gallons per minute per linear foot of geotextile; [b] = positive percentages indicate water quality improvement, negative percentages indicate water quality degradation

CHAPTER SEVEN:
STATISTICAL EVALUATION OF MULTIPLE TIN SURFACES CONSTRUCTED FROM UNMANNED AIRCRAFT SYSTEM IMAGERY

7.1 INTRODUCTION

Topographic surface profiles, typically used during land development activities (e.g., residential and highway construction), are generated by implementing traditional survey means (e.g., total station or global positioning system [GPS]) or remote sensing methods (e.g., Light Detection and Ranging [LiDAR]). Advancements in unmanned aircraft systems (UAS) technology and its availability commercially have facilitated the development of innovative data acquisition and processing applications. Several studies have focused on evaluating the accuracy associated with UAS derived surface models (*Draeyer and Strech 2014*, *Cryderman et al. 2014*, *Arango and Morales 2015*, & *Aquera-Vega et al. 2017*). In such studies, accuracy is an evaluation based on error between a measured data point (e.g., surface model) to that of known value (e.g., traditional survey) within photogrammetry software. While this type of accuracy information is extremely important, published studies have yet to analyze relative differences and error associated with UAS derived surface models within the computer aided design (CAD) environment. Figure 7.1 illustrates the difference between error and relative difference as it relates to surface models.

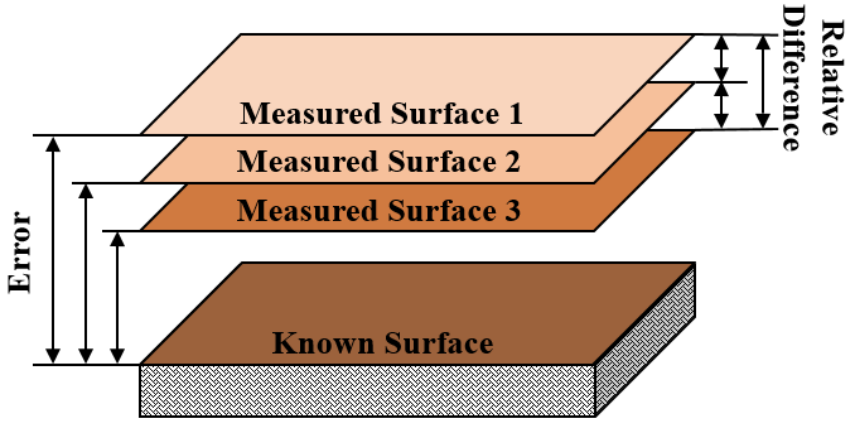

Figure 7.1. Error verses relative difference.

Currently, a need exists to scientifically evaluate CAD triangular irregular network (TIN) models to determine if they are statistically different from one another. This can be achieved by employing multiple statistical methods that apply formal methods to collect, clean, and process data. Thus, the focus of this study was to apply statistical methodologies to evaluate whether various flight factors affect the relative difference between UAS derived TIN models using elevations obtained between models and known ground positions. For this study, statistical assessments were limited to vertical accuracies, which tend to differ significantly as flight factors change (e.g., flight altitude), as opposed to horizontal accuracies that differ to a much lesser degree as long as the number of ground control points (GCPs) remain consistent, as shown by Aguera-Vega et al. (*2017*).

7.2 RESEARCH OBJECTIVES

The purpose of this study is to statistically evaluate the relative differences and error of multiple TIN surfaces, of a single study site, derived from photogrammetry software. TIN surfaces were selected for evaluation over digital surface models (DSM), digital terrain models (DTM), and point clouds due to their common use within engineering CAD workflows. A literature review is

discussed, as well as an overview of the differences between photogrammetry derived DSM and DTM. Two statistical analyses are presented that evaluate TIN surface elevations based on data collected at various flight altitudes on three different days. Finally, various flight factors that may affect model elevations are identified for further investigation.

7.3 BACKGROUND

7.3.1 UNMANNED AIRCRAFT SYSTEMS

According to the Federal Aviation Administration (FAA), a UAS is an aircraft without a human pilot onboard and controlled by an operator on the ground (*FAA 2017*). Typically, UASs are equipped with a data acquisition sensor (i.e., camera), inertial motion unit, and an onboard GPS receiver, which provides navigational assistance to the operator and georeferencing information to the data acquisition sensor. An array of companies offer small, cost-effective UAS platforms capable of autonomously navigating a preprogrammed flight trajectory while simultaneously capturing high-resolution imagery at precise intervals.

Originally, UAS development and implementation was founded on military applications such as surveillance and reconnaissance (*Remondino et al. 2011*). Over the years, advanced applications have emerged within commercial industries that provide innovative solutions in areas of data acquisition. The implementation of UASs in the fields of monitoring, volumetric analysis, and survey mapping can be attributed to the advancements in geomatics over the past few decades.

7.3.2 ACCURACY EVALUATIONS OF UAS DIGITAL MODELS

The development of photogrammetry software packages that can effectively analyze high-resolution aerial imagery and generate DSMs has inspired new and revolutionary

approaches for generating topographical surveys. Due to these new approaches, researchers have conducted various studies on UAS based DSMs. Aguera-Vega et al. (*2017*) discusses a recent study where accuracy analyses were based on the root-mean-square error (RMSE) for DSMs created using photogrammetry software. The study evaluated horizontal and vertical accuracy differences between various flight altitudes (e.g., 50, 80, 100 and 120 m), as well as the quantity of GCPs (e.g., 3, 5 and 10) referenced in each DSM. Results indicated that horizontal accuracy improved 78% as the quantity of GCPs increased from 5 to 10 and vertical accuracy improved 28% as flight altitude decreased from 120 meters (393 ft) to 50 meters (164 ft). Conclusively, the DSMs generated using 10 GCPs and imagery collected at 50 meters (164 ft) resulted in the smallest RMSE value. However, there is a lack of statistically supported data that analyzes the extent of relative precision between such models.

DSM accuracy analyses can also be accomplished through methods that are more conventional. Earthwork volumetric estimations are typically achieved by employing traditional survey instruments such as Global Navigation Satellite Systems – Real Time Kinematic (GNSS-RTK) units or total stations, and post-processing survey point data to determine volumes. However, earthwork volumetric calculations can also be achieved by analyzing DSMs derived from UAS aerial imagery. Cryderman et al. (*2014*) evaluated stockpile volumes estimated using GNSS-RTK surveying method and UAS imagery based DSMs. In addition, two flights were conducted in differing weather conditions to evaluate repeatability. Volumetric analysis indicated a 0.2% difference between flights and a 0.7% difference between the GNSS-RTK survey and first flight. Arango et al. (*2015*) also conducted a stockpile volumetric analysis where volumes from a traditional total station survey, DSM, and an engineer's estimate. When compared to the

engineer's estimate, the accuracy differences of the traditional survey and DSM were 2.88% and -0.67%, respectively. This study provided evidence that accurate volumetric calculations can be estimated using UAS imagery.

Additional methods of volumetric data acquisition, such as LiDAR survey scans, are also available on UAS platforms. Draeyer et al. (*2014*) compared stockpile DSMs generated by Pix4D™, a photogrammetry software package, to GNSS-RTK and terrestrial LiDAR surveys. When volumes from Pix4D and GNSS-RTK were compared for two sites, differences of 2% and 3% were noted. A third site compared a UAS derived DSM to a LiDAR scan and a difference of 0.1% was observed. These values were considered accurate enough to pass practical surveyor standards. Draeyer et al. (*2014*) claims that while traditional surveying is acceptable for small areas, UAS imagery based DSMs are more efficient for large areas of surveying without sacrificing accuracy.

These studies illustrate the efforts and findings of accuracy driven research articles published on UAS derived surface models. While practical in nature, these studies lack a multitude of data science analysis techniques that could provide additional support and clarity to the findings presented.

7.3.3 Applications of UAS Digital Models

Soil erosion monitoring is a potential area for UAS derived surface model applications, as erosion can be detrimental to the surrounding environment. Eltner et al. (*2013*) conducted a study monitoring soil erosion with UAS imagery and total station measurements to analyze the accuracy of the DTMs created by Pix4D™ and PhotoScan™. DTMs are typically generated from DSMs by applying a contour smoothing algorithm. Essentially, this process eliminates drastic changes in elevations caused by structures and obstacles located within the model. While both

software packages generated comparable DTMs, quantifying elevation differences between the DTMs and traditional survey proved challenging due to the inability to distinguish possible sources of error. Eltner et al. (*2013*) indicated that further analyses were necessary to draw definitive conclusions on the results. Hamshaw et al. (*2017*) conducted a study on streambank erosion and deposition where UAS photogrammetry volume estimations were within 4% of terrestrial laser scanning (TLS) and an RTK survey. Environmental applications such as these provided a glimpse as to how UAS based surface models can applied.

Construction applications in which DTMs can be applied include the estimation of cut and fill volumes. A benefit of incorporating DTM volumetric analysis into the estimating and planning phases of construction is that it provides a cost effective and time saving alternative to traditional methods currently employed within the industry. Siebert and Teizer (*2014*) conducted an analysis of a construction spoil site using a UAS derived digital elevation model (DEM). By estimating a fill volume from the DEM and using traditional production rates for personnel and equipment, a completion time for the project was estimated. By applying UAS based models to time-sensitive construction task, non-value adding activities can be minimized. Additional applications of UAS photogrammetry include forestry, agriculture, archaeology, and traffic monitoring (*Remondino et al. 2011*).

Each of the UAS derived surface model applications outlined above are innovative strategies for evaluating unique parameters. As capabilities and limitations of UAS based surface models unfold, precision and accuracy expectations for each applications will certainly be of interest to end users. Although the focus of this study is not to evaluate the accuracy associated

with all revolutionary applications, it does provide insight into precision expectations associated with UAS derived models.

7.4 METHODOLOGY

7.4.1 STUDY SITE

The study site for the vertical precision analyses was the Auburn University-Erosion and Sediment Control Test Facility located in Opelika, Alabama. The site is approximately 4.5 ac (1.8 ha) containing two water supply ponds, a multitude of surfaces (e.g., bare soil, grass, aggregate and asphalt), and multiple sheds and storage buildings. The facility has varying terrain morphology and surfaces features that are representative of heavy civil and highway construction projects. An advantage of using the facility was the ability to establish and preserve precise GCPs that can be used on future studies to identify improvements within the data acquisition and processing methodologies.

7.4.2 UNMANNED AIRCRAFT SYSTEM

To statistically evaluate the vertical precision associated with TIN surfaces derived from aerial images, a DJI™ Inspire 1 Pro quadcopter was acquired for the study. This particular UAS platform is specifically designed for professional aerial filmmaking and incorporates micro M4/3 imaging capabilities. One unique feature of the platform is the ability to interchange cameras based on user preference. For this study, a Zenmuse™ X5 camera specifically designed for aerial imagery was used. The camera operates on a 3-axis gimbal for optimal stabilization during flight and is capable of capturing video at a resolution of 3840 pixels by 2160 pixels at up to 30 frames per second and 16 megapixel still imagery. In comparison to other readily available UASs, this

platform provides exceptional image quality and enhanced safety assurances. Technical specifications associated with the DJI Inspire 1 Pro are listed in Table 7.1.

Table 7.1. Inspire 1 Pro Technical Specifications (*DJI 2017*)

Characteristic	Specification
Model:	T600
Aircraft Weight:	2.84 kg (6.27 lb.)
Max Weight:	3.50 kg (7.71 lb.)
Max Speed:	21.9 m/s (49 mph)
Max Flight Time:	Approx. 18 min
Diagonal Length:	58.1 cm (22.8 inch)
Battery Capacity:	5700mAh
Battery Voltage:	22.8 V
Battery Type:	LiPo 6S

7.4.3 CONTROL/CHECK POINTS

While the number GCPs within an observation area to accurately georeference imagery has been evaluated in published literature, a methodology for selecting and placing GCPs within an area to achieve optimal site coverage and surface projection has yet to be extensively evaluated. Thus, a need exists to evaluate GCP placement within sites to achieve optimal surface projections. Although these evaluations are beyond the scope of this research, GCPs were strategically placed within the site so that analyses could be conducted. The following criteria were used to select GCP locations: (1) various background surface materials (e.g., bare soil, grass, overgrown vegetation, gravel, asphalt), (2) differing terrain grades (e.g., 0 to 30%), and (3) various elevations. Figure 7.2(a) illustrates the locations of 10 GCPs used for model georeferencing during the study. Points were "homogeneously spread" throughout the site to ensure adequate coverage, as recommended by the image processing software. In addition to GCP locations, Figure 7.2(b) illustrates 20 check points (CPs) placed onsite to provide a means for TIN surface model vertical accuracy analysis. CPs were also placed using the GCP criteria, however spacing

between CPs was not evenly disturbed throughout the site but instead varied from dense clusters of points to single isolated points. While this method of check point placement is not recommend by the ASPRS Positional Accuracy Standards for Digital Geospatial Data (*ASPRS 2015*), this placement strategy was selected so that elevation variations between the known surface and projected model could be evaluated at various horizontal distances, as well as placement criteria, from GCPs.

(a)

(b)

Figure 7.2. GIS point location map: (a) ground control points; (b) check points.

Points were established by burying a 1 ft (0.3 m) section of 3 in. (7.6 cm) polyvinyl chloride (PVC) pipe and concreting a 1 ft (0.3 m) section of 0.5 in. (1.3 cm) rebar into the center of each pipe, leaving approximately 1 in. (2.5 cm) of rebar exposed for geolocating. Control/check points were identified in aerial imagery by centering 2 ft (0.6 m) by 2 ft (0.6 m), black and white target over each of the exposed rebar sections prior to conducting a flight. Figure 7.3 shows a control/check point and ground target, respectively. Three-dimensional coordinates (i.e., *x*, *y*,

and *z*) of each rebar cross section were recorded with a robotic total station. Existing GNSS-RTK reference points were used for total station orientation in the 1983 Alabama State Plane East coordinate system.

(a) (b)

Figure 7.3. Image georeferencing: (a) control/check point; (b) ground target.

7.4.4 FLIGHT PLANNING

To investigate the effects various flight altitudes have on TIN surface model precision, flights were conducted at three elevations above ground level (AGL). Additionally, flights at each elevation were replicated three times to evaluate precision repeatability. To minimize error, flights were executed by implementing replicable autonomous flight trajectories, ground speeds, vertical camera angle with respect to the UAS (i.e., 80°), image overlaps (i.e. 80% front; 60% side), and camera orientation with respect to the UAS (i.e., facing the direction of flight). The camera angle setting was at the maximum allowable angle and image overlap settings were based on the minimums recommended by the software manufacturer. Autonomous flight trajectories and associated flight/camera settings were controlled using the Pix4Dmapper™ application installed on a UAS remote controller tablet. Table 7.2 shows the implemented image acquisition flight plans and associated weather conditions for each of the nine flights conducted.

Table 7.2. Image Acquisition Flight Plans and Weather Conditions

Elevation AGL (ft)	Ground Sample Distance (in./px)	Repetition	Flight Date	Temperature (°F)	Wind Speed (mph)
100	0.30	R1	10/04/2017	73	9
		R2	10/06/2017	74	7
		R3	10/18/2017	60	8
200	0.61	R1	10/04/2017	73	9
		R2	10/06/2017	74	7
		R3	10/18/2017	60	8
300	0.91	R1	10/04/2017	73	9
		R2	10/06/2017	74	7
		R3	10/06/2017	60	8

Note: R = Repetition; 1 ft = 0.3 m; 1 in/px = 2.54 cm/px; 1 mph = 1.6 kph.

7.4.5 DATA PROCESSING

Post-processing was achieved using Pix4D version 3.3.29, a software package that applies a photogrammetry algorithm to develop a point cloud and 3D textured mesh from geolocated aerial imagery. Once image processing is complete, a site mosaic and DSM are generated for analysis. For sites that contain objects (e.g., trees, sheds, buildings, etc.) that obstruct the ground surface, a DTM can be developed. This process applies a surface smoothing algorithm to the DSM that identifies regions that have abrupt elevation changes and replaces them with interpreted values based on the surrounding contours. DTM generation results in reduced model resolution when compared to the DSM due to the smoothing nature associated with the algorithm. Figure 7.4 shows the site mosaic, DSM, and DTM generated by Pix4D for one data acquisition flight. When visually comparing the DSM to the DTM, it is evident that resolution diminishes due to the degradation of definable features within the models.

(a)

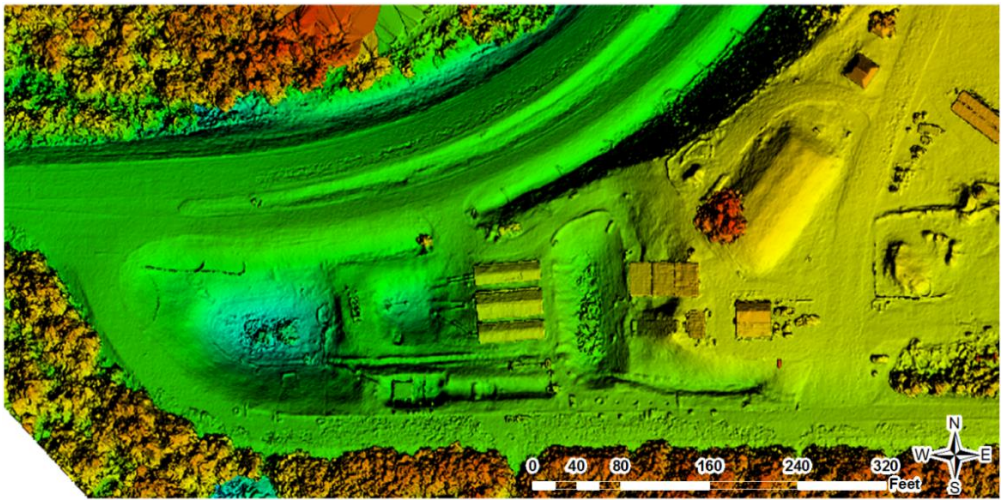

(b)

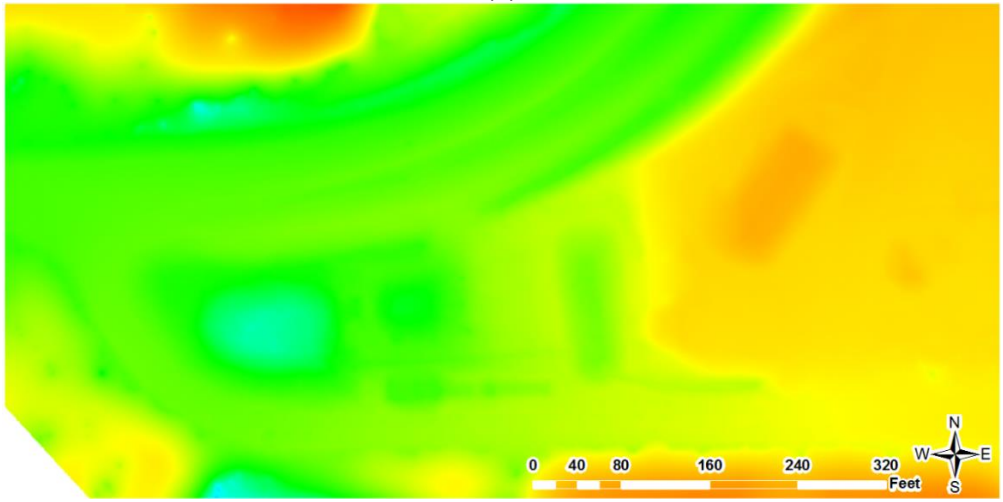

(c)

Figure 7.4. Pix4D generated output models: (a) site mosaic; (b) DSM; (c) DTM.

Model processing is essentially a six-step process that includes: (1) initial processing, (2) point cloud densification, (3) 3D texture mesh generation, (4) DSM generation, (5) orthomosaic generation, and (6) contour line generation. Processing time for this study ranged between 1.5 hours for flights at altitudes of 300 ft (132 images) to 9.5 hours for flight altitudes at 100 ft (882 images). Once processing and model generation was complete, a quality report was displayed indicating the easting, northing, and elevation errors, as well as the RMSE for each coordinate. This information provides insight into model accuracy and assists in identifying inconsistences within the model prior to application.

For this study, TIN surface models were selected for evaluation due to their wide implementation and versatility within the areas of land surveying and site design. To create a photogrammetry derived TIN surface, DSM generated within the image processing software were exported in SHP file formats. Files were then imported into AutoCAD® Civil 3D® and developed into TIN surface models that can be used on a variety of land development projects. Figure 7.5(a) shows a contour map of a TIN surface created within CAD that was derived from a UAS based DSM and Figure 7.5(b) shows the associated contour map derived from a UAS based DTM. Contours intervals were set to 2 ft (0.6 m) for each map.

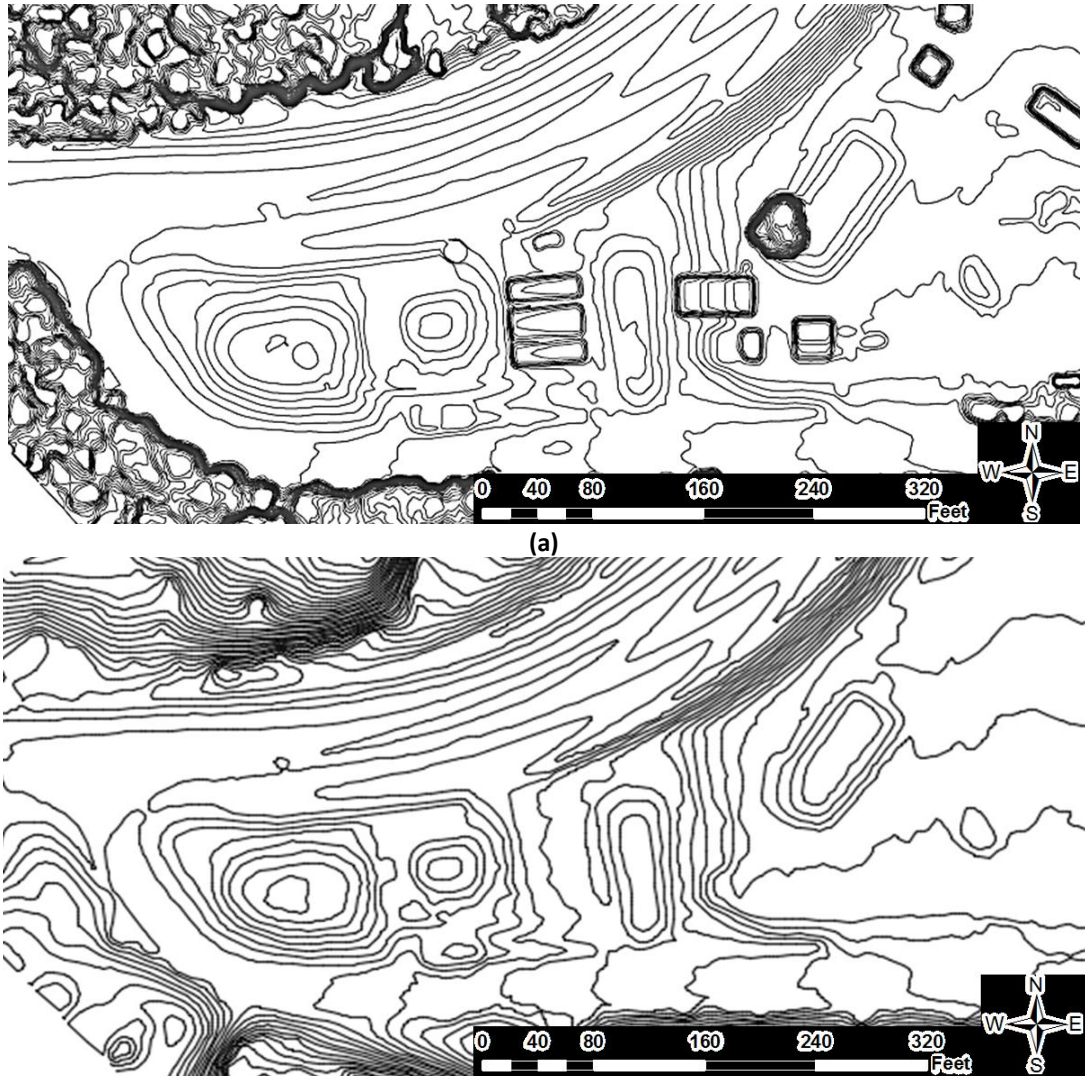

Figure 7.5. Contour maps of CAD TIN models derived from: (a) DSM; (b) DTM.

7.4.6 OUTLIER DETECTION

Outlier detection is critical in statistical analysis due to potential calculation variations of analytic coefficients, which may result in a large residual and/or leverage. Outlier detection is the process of identifying one or more observations within a sample that are not typical of the data sample and are located away from the main body of data. Several detection methods (e.g., Standard Deviation, Z-Score, Modified Z-Score, Boxplot, etc.) can be applied to a sample to determine the presence of outliers. The modified Z-score method was selected for this study

because it uses the median value under consideration ($\tilde{x}$) and the absolute deviation of the median (MAD) to identify outliers (Jeffrey and Menches 1993). This method is the most applicable for small data sets because more common methods use mean and standard deviation values which are sensitive to extreme values, which could result in outlier masking (*Seo 2006*). Sample data evaluated include elevation variations between each TIN surface model and CPs within the model; thus, 180 observation (i.e., 9 TIN surfaces x 20 CPs = 180 observations) were represented in the analysis. To capture each of these observations, CPs were characterized by a mean elevation variation determined from corresponding CP elevation variations of each TIN surface model. From these values, modified Z-scores were determined. Figure 7.6 illustrates the modified Z-scores for each CP, as well as the upper and lower outlier limits recommend by Iglewica and Hoaglin (*Jeffrey and Menches 1993*). From the plot, no outliers were present within the sample.

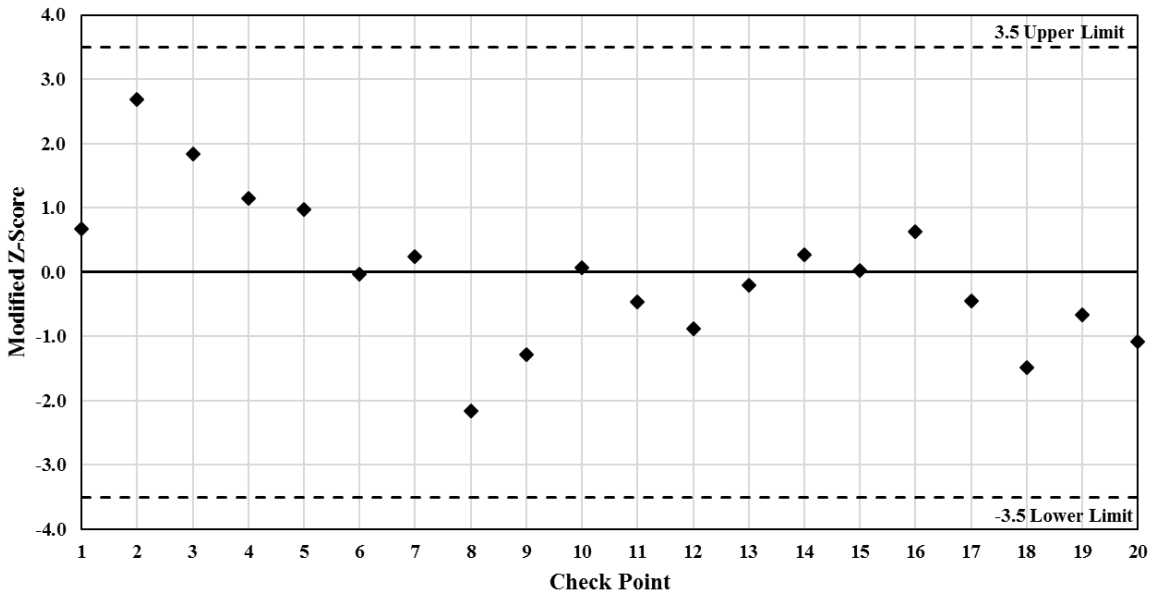

Figure 7.6. Check point outlier analysis.

7.4.7 ANALYSIS OF VARIANCE

The first analysis was to determine whether the vertical precision associated with TIN surface models are influenced by flight day (of 3), flight altitude (of 3), or some combinations of the two. The analysis of variance (ANOVA): two factor with replication is the most appropriate method to analyze these factors because it is an equality test that associates sources of variation based on total variability in a set of observations. Variability is measured by component sums of squares associated with each sources of variation. In essence, the ANOVA identifies if groups have equal means or if at least one group has a mean that is statistically different from the others. Observation independency, factor normality, and homogeneity of variances within groups are conditions that must be met in order to perform an ANOVA. Null and alternative hypotheses for ANOVA analyses can be written as:

$$\boldsymbol{H_0}: \boldsymbol{\mu_1 = \mu_2 = \mu_3} \quad \text{(Eq. 7.1)}$$

$$\boldsymbol{H_1}: \boldsymbol{\mu_1 \neq \mu_2 \neq \mu_3} \quad \text{(Eq. 7.2)}$$

Where,

μ_i = treatment effect

For this study, the treatment effects were flight day and flight altitude. The two hypotheses tested are: (1) is there a significant difference in relative elevation difference between flight days at a 95% confidence level and (2) is there a significant difference in relative elevation difference between flight altitudes at a 95% confidence level.

7.4.8 MULTIPLE LINEAR REGRESSION

The second analysis was to determine the relative impact each flight factor has on TIN surface precision, independent of other factors. Multiple linear regression techniques can be applied to an array of data sets to build empirical models that analyze multiple regression factors independently. Each flight plan has a corresponding combination of independent regression factors considered in the analysis. The dependent variables selected for the analysis, which are affected by each independent factor, were vertical accuracy RMSE values associated with each flight. RMSE values indicate a measure of accuracy magnitude within each TIN surface model. Each flight factor combination (i.e., independent variable) was recoded into a unique binary independent variable that took values of 1 or 0, depending on whether the flight incorporated the factor or not and the dependent variables were coded as RMSE values corresponding models. The model equation can be written as:

$$f(x) = \beta_0 + \beta_1 x_1 + \beta_2 x_2 + \beta_3 x_3 + \beta_4 x_4 \quad \text{(Eq. 7.3)}$$

Where,

$f(x)$ = dependent variable (e.g., RMSE)

β_0 = coefficient intercept

β_i = ordinary least squares coefficients

x_i = independent variables (e.g., flight altitude, flight day)

7.5 ANALYSIS AND RESULTS

The following is a summary of the results and interpretations of two statistical evaluations of nine TIN surface models derived from aerial imagery acquired from the flight plans described

above. For each flight plan, independent variables (e.g., flight altitude and flight day) were altered systematically. To minimize TIN surface inconsistences, pre-flight camera parameters (e.g., front overlap, side overlap, camera angle, camera orientation) were consistent between all flights. Additionally, flight trajectories (e.g., flight paths) associated with each flight altitude were kept consistent. Due to UAS flight time limitations, flight altitudes 100, 200, and 300 ft (30.5, 60.7, and 91.4 m) had flight groupings (i.e., number of flights to encompass the entire site) of 4, 2, and 1, respectively. Flight grouping variations are directly associated with image ground sample distance (GSD), which increases as altitude increases. Throughout the investigation, precedence for flight consistency and repeatability was of most importance. The assurance of static pre-flight variables facilitated unbiased statistical analyses of elevation variations associated with each TIN surface model developed. Statistical methods implemented for elevation variation analysis include analysis of variance and multiple liner regression.

7.5.1 DATA SUMMARY

Vertical differences associated with each surface model were determined by evaluating the change between known ground positions and the projected TIN surface model positions. Results of the analysis are expressed in terms of RMSE. Vertical elevation differences, means, standard deviations, and RMSE calculated for each TIN surface models, as well as the mean check point elevation difference used for outlier detection, are shown in Table 7.3. These values represent the sub-dataset used to evaluate each of the TIN surface models.

Table 7.3. Vertical Elevation Deviation Sub-Dataset

Check Point	Difference between know CP and TIN surface (ft)									Mean CP Elevation Differences
	Altitude 100 ft			Altitude 200 ft			Altitude 300 ft			
	Day 1	Day 2	Day 3	Day 1	Day 2	Day 3	Day 1	Day 2	Day 3	
	Model 1	Model 2	Model 3	Model 4	Model 5	Model 6	Model 7	Model 8	Model 9	
1	0.445	0.333	0.225	0.218	0.021	0.085	0.435	0.612	0.487	0.318
2	0.695	0.692	0.724	0.764	0.730	0.728	0.737	1.573	1.512	0.906
3	0.301	0.352	0.6	0.743	0.561	0.781	0.776	0.855	0.954	0.658
4	0.385	0.404	0.433	0.451	0.233	0.388	0.55	0.536	0.71	0.454
5	0.455	0.463	0.432	0.344	0.096	0.229	0.48	0.473	0.659	0.403
6	0.483	0.341	0.115	0.037	-0.334	-0.155	0.096	0.133	0.281	0.111
7	0.637	0.433	0.19	0.064	-0.282	-0.114	0.191	0.186	0.383	0.188
8	0.357	0.31	-0.62	-0.645	-1.497	-0.665	-0.621	-0.622	-0.647	-0.517
9	0.247	0.073	-0.224	-0.366	-0.767	-0.608	-0.243	-0.362	-0.074	-0.258
10	-0.055	0.015	0.238	0.095	0.188	0.104	0.108	0.478	0.082	0.139
11	-0.099	-0.147	0.014	0.046	0.032	-0.054	-0.095	0.039	0.122	-0.016
12	-0.279	-0.286	-0.108	-0.175	-0.134	-0.161	-0.162	0.025	0.027	-0.139
13	-0.095	0.042	0.182	0.024	-0.038	-0.06	0.019	0.18	0.279	0.059
14	-0.27	0.241	0.218	0.26	0.257	0.247	0.257	0.255	0.311	0.197
15	-0.002	0.05	0.19	0.184	0.074	0.168	0.093	0.11	0.274	0.127
16	0.151	0.231	0.353	0.376	0.224	0.377	0.278	0.24	0.492	0.302
17	-0.14	-0.029	0.026	0.106	-0.039	0.054	-0.058	-0.094	0.048	-0.014
18	-0.031	-0.177	-0.276	-0.179	-0.319	-0.436	-0.477	-0.481	-0.478	-0.317
19	0.21	0.39	-0.54	0.046	0.033	-0.058	0.022	-0.362	-0.446	-0.078
20	-0.169	-0.16	-0.245	-0.199	-0.378	-0.317	-0.141	-0.145	-0.023	-0.197
Mean	0.161	0.179	0.096	0.110	-0.067	0.027	0.112	0.181	0.248	
SD	0.301	0.260	0.351	0.339	0.474	0.381	0.367	0.502	0.499	
RMSE	0.335	0.310	0.356	0.349	0.467	0.372	0.375	0.522	0.546	

Note: 1 ft = 0.3 m

7.5.2 ANALYSIS OF VARIANCE

Shown in Table 7.4, a two factor ANOVA with replication was conducted to compare the effect of flight day and flight altitude on TIN surface model precision. Based on the ANOVA factor evaluation, the following conclusions were drawn. Flight Day did not have a significant effect on TIN surface precision at the 95% confidence level. While close, flight altitude did not have a significant effect on TIN surface precision at the 95% confidence level. Finally, flight Day and flight Altitude interaction was also statistically insignificant at the 95% confidence level. These conclusions are evident by each factor having $F_{Critical}$ values greater than $F_{Calculated}$ values, as well as p-values greater than the confidence interval (α). Taken together, these results suggest that

the day in which a flight is conducted and the altitude at which these images were collected do not have a significant effect on the relative differences of TIN surface models. Essentially, each of the projected surface models do not differ from one another and can be considered statistically equivalent.

Table 7.4. ANOVA Factor Evaluation

Source of Variation	$F_{Critical}$	$F_{Calculated}$	p-value[a]
Day	3.05	0.10	0.90
Altitude	3.05	2.63	0.08
Interaction	2.42	0.49	0.49

Note: [a] = comparison between Flight Days and Flight Altitudes at 95% confidence interval and α = 0.05.

7.5.3 Multiple Linear Regression

Multiple linear regression analysis was used to develop a model for predicting changes in RMSE of TIN surface models based on flight day and flight altitude. For the regression model generated, flight Day 1 and Altitude 100 ft were considered the base flight factors, from which each successive flight was compared. Results of the analysis, along with statistical significances, are shown in Table 7.5. The R^2 of the model was 0.76, indicating a positive, moderately strong, linear correlation when compared to measured observations. The regression model predicted that RMSE is equal to 0.28 + 0.08(Day 2) + 0.07(Day 3) + 0.06(Altitude 200 ft) + 0.15(Altitude 300 ft), where each flight factor (i.e., Day 2, Day 3, Altitude 200, and Altitude 300) was coded as 1 or 0, depending on whether or not it was implemented. An evaluation of the regression model yielded the following conclusions. TIN surface model RMSE increased 0.08 and 0.07 beyond the constant for flight Day 2 and Day 3, respectively. RMSE increased 0.06 and 0.15 beyond the constant for flight Altitudes 200 ft and 300 ft, respectfully. These increases in RMSE are evident by the positive coefficients (i.e., negative coefficients would reduce RMSE). Changes associated

with each flight Day and Altitude 200 ft were not significant at the 95% confidence level because corresponding p-values were greater than the confidence interval ($\alpha = 0.05$). However, the RMSE change associated with Altitude 300 ft was significant at the 95% confidence level. These results indicate that flight factors Day 2, Day 3, and Altitude 200 ft have no significant effects on the base RMSE value. On the other hand, flight factor Altitude 300 ft does significantly change the base RMSE value. Essentially, these findings show that model error is significantly affected by increasing flight altitude from 100 ft (30.6 m) to 300 ft (91.4 m) but does not change significantly based on the day images are collected or by increasing flight altitude form 100 ft (30.6 m) to 200 ft (61.0 m).

Table 7.5. Flight Plan Factor Regression Analysis

Flight Factor	Statistical Significance	
	Coefficients	p-value[a]
Constant	0.28	0.00
Day (Base: Day 1)		
Day 2.	0.08	0.18
Day 3	0.07	0.22
Altitude (Base: 100 ft)		
Altitude 200 ft	0.06	0.27
Altitude 300 ft	0.15	0.04

Note: [a] = comparison to effects of Day 1 and Altitude 100 ft at 95% confidence interval and $\alpha = 0.05$.

7.6 SUMMARY

This study statistically analyzed the vertical precision and accuracy of nine TIN surface models generated from aerial imagery obtained via a UAS. For this study, measured differences between known CPs and projected points ranged between -0.62 ft (-0.19 m) and +0.72 ft (+0.22 m) at an altitude of 100 feet and -0.65 ft (-0.20 m) and +1.57 ft (+0.48 m) at an altitude of 300 feet. The ANOVA assessment for each flight factor indicated that the relative difference between models was not statistically significant at the 95% confidence level, indicating adequate precision

between the models. The multiple linear regression model indicated that the day in which images are collected does not significantly affect the RMSE of the model when compared to the base day. This conclusion is expected as each of the days had favorable and consistent weather conditions. Additionally, evaluations indicate that lower flight altitudes yield the most accurate models based on RMSE values, as shown by Aguera-Vega (*2015*). However, a statistically significant change in RMSE was only observed when increasing the base flight altitude from 100 ft (30.6 m) to 300 feet (91.4 m). These finding indicate that reliable UAS data acquisition can be achieved over time, as well as at flight altitudes of 200 ft (61.0 m) or below without significant degradation of vertical accuracy. This elevation threshold is likely dependent topographical conditions at the analyzed site. The ability to collect imagery at higher altitudes reduces the quantity of images and computing time needed for DSM construction. These results can assist government agencies (e.g., FHWA and State DOTs) and construction professionals when developing the most feasible and effective method for UAS data acquisition, as well as provide elevation error expectations within the CAD environment.

CHAPTER EIGHT:
CONCLUSIONS & RECOMMENDATION

8.1 INTRODUCTION

The US Environmental Protection Agency (USEPA) construction general permit (CGP) mandates that erosion and sediment control (ESC) practices achieve equivalent sediment load reduction to that of a 50 ft (15 m) natural buffer when earth-disturbing activities are within 50 ft (15 m) of a water of the U.S. and a natural buffer cannot be maintained (*USEPA 2017*). In order for practitioners to select appropriate practices to meet this requirement, performance capabilities of various sediment barrier (SB) practices need to be available. This research effort was undertaken to provide a comprehensive understanding of SB capabilities and improve their overall performance. The research presented in this dissertation outlines the design, development, and implementation of a full-scale testing apparatus and methodology to quantifiably evaluate SB practices, explore improvements in the design and installation of wire-backed nonwoven silt fence installations, assesse overall effectiveness and applicability of common innovative and manufactured SB practices employed within the construction industry, analyze treatment effectiveness of geotextiles used in silt fence applications, and investigate the vertical accuracy of TIN surface models derived from UAS imagery.

8.2 CONCLUSIONS

This section summarizes the conclusions of each research objective investigated in this dissertation. This work will ultimately provide improved SB practices that are designed, implemented, and installed correctly on construction sites. Ultimately, this study will assist in minimizing the amount of sediment discharged from construction sites and reaching surface waters, thus protecting the nation's water resources.

8.2.1 SEDIMENT BARRIER TEST APPARATUS DESIGN AND TESTING METHODOLOGY

The first objective of this research was achieved through the design and construction of a scientifically sound SB testing apparatus that allowed performance-based testing of different SB practices, products, and installation strategies. The experimental setup was repeatable, created conditions that allowed for direct comparisons, and were conducive of field-like conditions. A literature review of past and current SB testing experiments and standards was conducted to facilitate an effective design and testing methodology that would be suitable for the prescribed experimental needs. Furthermore, water and sediment introduction systems were constructed and calibrated to achieve the desired introduction rates that were determined appropriate through hydrologic and soil loss analysis for the state of Alabama. Data collection procedures and analysis were developed to evaluate installation tactics, structural integrity, hydraulic performance, sediment retention, and effects on water quality.

8.2.2 PERFORMANCE EVALUATIONS OF SILT FENCE INSTALLATIONS

The second research objective was to evaluate the standard Alabama Department of Transportation (ALDOT) silt fence installation, identify structural deficiencies, and provide improvements to assure a structurally sound nonwoven, wire-backed silt fence installation. This

objective was achieved by developing and testing eight alternative installation configurations that individually and jointly varied the standard silt fence height, T-post weight, T-post spacing, and geotextile entrenchment location. Variations to the standard parameters include (1) reducing fence height from 32 in. (81.3 cm) to 24 in. (61.0 cm), (2) increasing minimum T-post weight from 0.95 lb./ft (1.4 kg/m) to 1.25 lb./ft (1.9 kg/m), (3) reducing T-post maximum spacing from 10 ft (3.0 m) to 5 ft (1.5 m), and (4) trench offsetting. Ultimately, the offset 24 in. (61.0 cm) fence with 1.25 lb./ft (1.9 kg/m) T-post spaced 5 ft (1.5 m) on-center resulted in the best overall improvement, retaining an average of 93% of sediment and deflecting only 0.18 ft (0.05 m) over the course of three simulated storm events. Additionally, the implementation of a dewatering mechanism within a silt fence installation proved to be an effective means for controlled dewatering. Effluent flow rates calculated from the dewatering board installation were 6.2 times greater than flows calculated for installations without a dewatering board. Increased effluent flows reduced dewatering time from +24 hours (i.e., w/o dewatering board) to 4 hours (i.e., w/ dewatering board). Water quality analyses indicated that the inclusion of the dewatering board had little to no effect on water turbidity.

8.2.3 Performance Evaluations of Innovative and Manufactured Sediment Barrier Practices

The third objective was to conduct performance-based direct comparisons between various innovative and manufactured SB practices. This objective was satisfied by conducting full-scale experiments on common innovative and manufactured SB practices used within the construction industry following the developed protocols and testing regime. Tests were conducted on two manufactured silt fence systems [(1) C-POP and (2) SRSF], three sediment retention barriers (SRBs) [(1) ALDOT SRB, (2) AL HB SRB w/o Flocculant, and (3) AL HB SRB w/

Flocculant], and three manufactured SB products [(1) Excel Straw Log, (2) SiltSoxx, (3) Curlex Bloc]. Installation details were analyzed and amendments were made to promote stormwater impoundment and minimize flow bypass. Test observations indicated that a major failure mode of manufactured SB practices was undermining. Performance based comparisons of sediment retention rates, maximum impoundment heights, effluent flow rates, and treatment efficiencies were determined for each practice. Longevity tests were conducted to evaluate how each of these parameters changed over multiple storm events. Overall performance evaluations indicate that practices which achieve impoundment depths between 1 and 1.5 ft (0.3 and 0.46 m) achieve sediment capture rates of at least 90% and reduce impoundment surface turbidity up to 60% when compared to turbidity along the bottom of the impoundment.

8.2.4 Small-Scale Performance Evaluations of Geotextiles used in Silt Fence Applications

The forth objective of this dissertation was achieved through the design, construction, methodology development, and testing of common geotextile filter fabrics used in perimeter control applications. Testing was performed on five geotextile filter fabrics and a stacked sandbag configuration within the small-scale test apparatus. Observations and data collected during experiments were used to evaluate effluent flow rates and efficiencies associated with sediment retention and water quality improvements. Test results indicated that effluent flow rates observed during the test period for nonwoven geotextiles were on average 43% lower than woven materials. Sediment retention evaluations indicated that on average nonwoven geotextiles (i.e., 97% retention) outperform woven geotextiles (i.e., 91% retention). Water quality analyses suggest that the primary means for turbidity reduction is sedimentation during the test period (i.e., 46% reduction) and filtration during dewatering (i.e., 19% reduction).

8.2.5 Statistical Evaluation of Multiple TIN Surfaces Constructed from Unmanned Aircraft System Imagery

The final objective was fulfilled by conducting elevation analyses on triangular irregular networks (TIN) surface models of a single site derived from unmanned aircraft systems (UAS) imagery taken at various altitudes over multiple days. Evaluations showed that measured differences between known control points (CPs) and projected points range between -0.62 ft (-0.19 m) and +0.72 ft (+0.22 m) at an altitude of 100 feet and -0.65 ft (-0.20 m) and +1.57 ft (+0.48 m) at an altitude of 300 feet. Findings also indicate that reliable UAS data acquisition can be achieved over time, as well as at flight altitudes of 200 ft (61.0 m) or below without significant degradation of vertical accuracy.

8.3 SEDIMENT BARRIER RECOMMENDATIONS

8.3.1 Design Guidelines

Optimizing ESC practices on construction sites has been the focus of this research study for ALDOT. Currently, ALDOT does not provide specific design criteria for SBs other than installation details shown in ALDOT standard drawings. The 2018 edition of the ALDOT Standard Specifications states “SBs shall be constructed at the locations shown on the plans, the accepted stormwater management plan (SWMP) or where directed by the Engineer to intercept sheet flow runoff and to treat concrete washout wastewater” (*ALDOT 2018*). To insure consistency between SWMPs, ALDOT Standard Specifications could adopt silt fence design criteria outlined within the current edition of the Alabama Handbook (AL HB) for Erosion Control, Sediment Control and Stormwater Management on Construction Sites and Urban Areas or reference the criteria within the Standard Specifications. The criteria indicate maximum drainage area up-slope of silt fence

installations, as well as maximum slope length above silt fence installations. Additionally, the 2018 edition of the Alabama Handbook incorporates many of the silt fence installation improvements identified through this study.

8.3.2 ALDOT Standard Drawing Details

A lack of scientific knowledge has resulted in an industry need for performance-based testing of SBs in a controlled, full-scale environment. Existing ASTM International (ASTM) standard test methods have limitations; not allowing for full-scale installations, and failing to expose practices to typical flow conditions experienced in field applications. The results of this study show how full-scale testing was conducted to improve current standard silt fence installation designs. Installation improvements identified through this research provided structural enhancements to silt fence installations so that failures are less likely to occur up to design storm events. The improved silt fence installation was designed to maximize impoundment depth and provide efficient dewatering. Based on the performance observations and analyses conducted during this study, the following recommendation for revision are made for ALDOT Standard Drawing Details for Silt Fence Installations and SRBs:

(a) Reduce minimum fence height to 24 in.(61.0 cm),

(b) Specify a minimum T-post weight of 1.25 lb./ft (1.9 kg/m),

(c) Reduce geotextile ring fastener spacing to 1 ft (0.3 m) on-center,

(d) Indicate geotextile fabric be looped over the T-posts,

(e) Reduce maximum T-post spacing to 5 ft (1.5 m) in areas where impoundment will be concentrated,

(f) Incorporate a dewatering weir in areas experiencing a concentrated impoundment,

(g) Indicate silt fence installations be installed a minimum of 6 ft (1.8 m) from the toe of the slope to allow for adequate storage volume,

(h) Implement a 6 in. (15.2 cm) offset trench/slice, and

(i) Indicate maintenance be conducted when sediment accumulation reaches ½ the height of the silt fence installation

8.3.3 INNOVATIVE SEDIMENT BARRIER PRACTICES

The results of this research identified performance capabilities of innovative and manufactured SB practices when implemented as perimeter controls. Currently, the ALDOT Temporary Erosion and Sediment Control Products List II-24 does not provide a category for manufactured SB practices. As a result of this research effort, the research team recommends that ALDOT revise List II-24 to include a SB category with representative sub-categories (e.g., wattles, silt fence, etc.). An example List II-24 revision is provided in Appendix F. It is recommended that all future SB products seeking ALDOT Product Evaluation Board (PEB) approval and inclusion on List II-24 be evaluated to determine associated installation feasibility, structural integrity, impoundment capability, effluent flow rate, sediment retention, and effect on water quality using the performance criteria methodology developed during this study. Lastly, we recommend comparing performance capabilities of products seeking approval to the capabilities of practices evaluated and presented in this report to determine in-field feasibility.

8.4 LIMITATIONS AND RECOMMENDED FURTHER RESEARCH

The following section describes general limitations of the research performed and explores avenues by which the knowledge base can be expanded by performing additional studies and investigations.

8.4.1 Full-Scale Performance Evaluations of Silt Fence Installations Configurations

Tests were performed on various full-scale silt fence installations. While the evaluations indicated increased T-post weights and reduced T-post spacing were key components to improving structural stability, evaluations were limited to only two T-post weights and two T-post spacing scenarios. While the silt fence support post structural analyses provides recommended post spacing based on size/type, full-scale performance evaluations of the installations recommendations would provide further justification for the optimized designs. Further enhancements to the designs would be to evaluate the effects of post embedment depths and installation methods. These parameters would be helpful in maximizing the structural integrity of the silt fence while minimizing materials required for an effective installation.

The behavior of each silt fence installation configuration was evaluated using the same brand and weight nonwoven geotextile fabric. The results and finding from the silt fence evaluations are limited to the physical properties of the selected geotextile fabric. Further research could be conducted to gain a better understanding of structural performance when implementing woven geotextile fabrics.

The SB testing apparatus and protocols used in this study had the advantage of evaluating performance within a controlled environment (i.e., flow rate, soil loading, sheet flow conditions, etc.). In-field investigations could be conducted to assess the capabilities of the silt fence design improvements on active construction projects, which are susceptible to unforeseen and uncontrollable variables. A field study could provide further insight on the performance of the installation across a wide range of rainfall, sediment loading, and topographical scenarios.

Furthermore, a field study many highlight the importance of proper installation to achieve desired performance.

8.4.2 Full-Scale Performance Evaluations of Innovative Sediment Barrier Practices

The full-scale testing efforts on innovative SB practices mainly focused on evaluating the performance capabilities of the practices. While determining performance capabilities was the main objective, iterative attempts at improving the baseline performance capabilities associated with each practice were not conducted. A study could be performed to systematically vary installations components (e.g., trenching, pinning, staking, underlay, etc.) to improve treatment capabilities associated with each practice. Furthermore, filter materials used in manufacture products (e.g., geotextile, casement netting, filler materials, etc.) could also be evaluated. These results could be useful in the development of revolutionary products, as well as aid designers in selecting practices and products with improved installation methods that provide optimum water quality improvements.

8.4.3 Small-Scale Performance Evaluations of SB Filtration Components

As demonstrated in this research, the small-scale test apparatus can be used to evaluate the performance of a wide range of SB practices. Although it does not provide a means for identifying installation improvement strategies, it does allow SB practices to be evaluated under realistic loading conditions typically observed on construction sites. Future research should focus on evaluating innovative and manufactured products within the small-scale apparatus. This will provide comparative data that is not affected by structural failures or in-situ soil conditions. Researchers should also investigate effects of geotextiles installed in series and spacing between

the installations. A multifaceted geotextile installation may provide enhanced performance that can be used to protect sensitive areas at points of discharge.

8.4.4 Statistical Evaluation of Multiple TIN Surfaces Constructed from Unmanned Aircraft System Imagery

The TIN surface models generated during this research were based on digital surface model (DSM) constructed from UAS imagery. Future research should determine if accuracies and precisions associated with DTM models are equivalent to those of digital terrain models (DTM). Researchers should also investigate the accuracy differences of TIN surface model generated from DTM contours files and DTM point cloud files. Accuracies associated with each method will most likely improve as photogrammetry software advancements emerge within industry. Further research should focus on developing a method for identifying optimal reference point placement beyond traditional methodologies that focus on practical site parameters that facilitate enhanced model accuracy. This will provide uses with practical guidelines for identifying optimal locations and placing reference points across the site. Furthermore, research is needed to evaluate accuracy expectations in differing climate and weather conditions as these variables can change substantially over the course of complex projects.

8.5 ACKNOWLEDGEMENTS

This research is based on a study sponsored by Alabama Department of Transportation. The author greatly acknowledges the financial support. The findings, opinions, and conclusions expressed in this report are those of the author and do not necessarily reflect the view of the sponsor.

REFERENCES

AASHTO Standard M 288-17. (2017). "Standard Specification for Geotextile Specification for Highway Applications." West Conshohocken, PA.

Aguera-Vega, F., Carvajal-Ramírez, F., Martínez-Carricondo, P. (2017). "Accuracy of Digital Surface Models and Orthophotos Derived from Unmanned Aerial Vehicle Photogrammetry." *ASCE J. Surv. Eng.* Vol. 143, No. 2, 04016025.

Alabama Department of Environmental Management (ADEM). (2016). *National pollutant discharge elimination system permit*, General Permit, Montgomery, AL.

Alabama Department of Transportation (ALDOT). (2016). "Standard specifications for highway construction." *2016 Edition, Section 665*, Montgomery, AL

Alabama Department of Transportation (ALDOT). (2018). "Standard specifications for highway construction." *2018 Edition, Section 665*, Montgomery, AL

Alabama Department of Transportation (ALDOT). (2017). "*Standard Drawing ESC-200 (Sheet 4).*" Montgomery, AL.

Alabama Department of Transportation (ALDOT). (2018). "Approved Materials List II-24: Temporary Erosion and Sediment Control Products." Montgomery, AL.

Alabama Soil and Water Conservation Committee (AL-SWCC). (2014). *Alabama handbook for erosion control, sediment control and stormwater management on construction sites and urban areas.* Vol. 1, Montgomery, AL.

American Excelsior Company (2018). *Material Specifications – Curlex Bloc.* Arlington, TX. <https://americanexcelsior.com/wp-content/uploads/2017/05/Curlex-Bloc-MSMC-1.pdf>

Arango, C., Morales. C.A. (2015). "Comparison between Multicopter UAV and Total Station for Estimating Stockpile Volumes." *International Archives of the Photogrammetry, Remote Sensing and Spatial Information Sciences,* Vol. XL-1/W4.

Arkansas State Highway and Transportation Department (AHTD). (2009). *2009 erosion and sediment control design and construction manual*." Little Rock, AR.

ASPRS (2015) "Position Accuracy Standards for Digital Geospatial Data." *Photogrammetric Engineering & Remote Sensing.* Vol. 81, No. 3, A1-A26.

ASTM International. (2008). “Standard Practice for Silt Fence Installation.” *ASTM D6462-03.* West Conshohocken, PA.

ASTM International. (2011). “Standard test method for determining filtering efficiency and flow rate of the filtration component for a sediment retention device.” *ASTM D5141 - 11*, West Conshohocken, PA.

ASTM International. (2013). “Standard test method for determination of sediment retention device effectiveness in sheet flow applications.” *ASTM D7351 - 13*. West Conshohocken, PA.

ASTM International. (2013). “Standard Specification for Steel Fence Posts, Hot Wrought.” *ASTM A702-13*. West Conshohocken, PA.

ASTM International. (2017). “Standard Specifications for Silt Fence Materials.” *ASTM D6461/D6461M-16a.* West Conshohocken, PA.

Barrett, M. E., Kearney, J. E., McCoy, T. G., and Malina, J. F. (1995). “An Evaluation of the use and Effectiveness of Temporary Sediment Controls.” *Center for Research in Water Resources.* Technical Report 261. University of Texas at Austin, Austin, TX.

Barrett, M. E., Malina, J. F., Jr., and Charbeneau, R. J. (1998). “An Evaluation of Geotextiles for Temporary Sediment Control.” *Water Environment Research*, Vol. 70, No. 3, 283-290.

Britton, S. L., Robinson, K. M., Barfield, B. J., and Kadavy, K. C. (2000). “Silt fence performance testing.” Presented at the July 2000 ASAE Annual International Meeting, Paper 00-2162. ASAE, St. Joseph, MI.

Bugg, R. A., Donald, W. N., Zech, W. C., and Perez, M. A. (2017). “Performance Evaluation of Three Silt Fence Installations Using a Full-Scale Testing Apparatus.” *Water*, Vol. 9, No. 502.

Bugg, R. A., Donald, W. N., Zech, W. C., and Perez, M. A. (2017). “Improvements in Standardized Testing for Evaluating Sediment Barrier Performance: Design of a Full-Scale Testing Apparatus.” *J. Irrig. Drain Eng.,* Vol. 143, No. 8.

Chapman, J. M., Proulx, C. L., Veilleux, M. A. N., Levert, C., Bliss, S., Andre, M., Lapointe, N. W. R., Cooke, S. J. (2014). “Clear as mud: a meta-analysis on the effects of sedimentation on freshwater fish and the effectiveness of sediment-control measures.” *Water Research*, Vol. 56, 190-202.

City of Madison. (2018). “Example of Erosion Control Practices: The Good, Bad and OK.” Engineering. Madison, MI.

Cooke, S. J., Chapman, J. M., and Vermaire, J. C. (2015). “On the apparent failure of silt fences to protect freshwater ecosystems from sedimentation: A call for improvements in science,

technology, training and compliance monitoring." *Journal of Environmental Management*, Vol. 164, 67-73.

Crebbin, C. (1988). Laboratory Evaluations of Geotextile Performance in Silt Fence Applications Using Subsoil of Glacial Origin. MS Thesis. University of Washington, Seattle.

Cryderman, C., Mah, S., Shufletoski, A. (2014). "Evaluation of UAV Photogrammetric Accuracy for Mapping and Earthworks Computations." *Geomatica,* Vol. 68, No. 4, 309-317.

DJI Innovation. (2017). "Inspire 1 User Manual V2.2." http://www.dji.com/inspire-1/info.

Donald, W., Zech, W., Perez, M., and Fang, X. (2013). "Ditch Check Installation Evalautions of Wheat Straw Wattles Used for Velocity Reduction." *Transportation Research Record: Journal of the Transportation Research Board,* No. 2358, 69-78.

Donald, W., Zech, W., Perez, M., and Fang, X. (2016). "Evaluation and Modification of Wire-Backed, Nonwoven Geotextile Silt Fence for use as a Ditch Check." *J. Irrig. Drain Eng.*, Vol. 142, No. 2.

Draeyer, B., Strecha, C. (2014). "How accurate is UAV surveying? Testing stockpile volumetrics to get your answer. A comparison between Pix4D UAV photogrammetry software and GNSS/ terrestrial LIDAR scan surveys." *Pix4D White Paper.*

Dubinsky, G. S. (2014). *Performance evaluation of two silt fence geosynthetic fabrics during and after rainfall event*, thesis, presented to University of Central Florida, Orlando, FL.

Eltner, A., Mulsow, C., Maas, H.G. (2013). "Quantitative Measurement of Soil Erosion from TLS and UAV Data." *International Archives of the Photogrammetry, Remote Sensing and Spatial Information Sciences,* Vol. XL-1/W2. UAV-g2013, 4-6.

Federal Aviation Administration (2017). Unmanned Aircraft Systems. Washington, D.C.: U.S.

Filtrexx (2015) *Standard Specifications and Design Manual for Erosion, Sediment, Pollution Control and Stormwater Management.* Version 10.0. Akron, OH.

Fisher, L. S., and Jarrett, A. R. (1984). "Sediment retention efficiency of synthetic filter fabrics." Trans. ASAE, Vol. 60, No. 2, 429-436.

Florida Department of Transportation (FDOT) and Florida Department of Environmental Protection (FDEP). (2013). *State of Florida erosion and sediment control designer and reviewer manual,* State Erosion and Sediment Control Task Force, Tallahassee, FL.

Georgia Soil and Water Conservation Commission (GSWCC). (2016). *Manual for erosion and sediment control in Georgia 2016 edition*, Athens, GA.

Gogo-Abite, I., and Chopra, M. (2013). “Performance evaluation of two silt fence geotextiles using a tilting test-bed with simulated rainfall.” *Geotextiles and Geomembranes*, Vol. 39, 30-38.

Haan, C. T., Barfield, B. J., and Hayes, J. C. (1994).“*Design Hydrology and Sedimentology for Small Catchments.*” *Academic Press, San Diego, CA.*

Hamshaw, S., Bryce, T., Dunne, J., Rizzo, D., Frolik, J., Engel, T., Dewoolkar, M. (2017). “Quantifying Streambank Erosion Using Unmanned Aerial Systems at Site-Specific and River Network Scales.” *Geotechnical Frontiers*, GSP 278 499-508.

Harbor, J. (1999). “Engineering geomorphology at the cutting edge of land disturbance: erosion and sediment control on construction sites.” *Geomorphology*, Vol. 31, 247-263.

Henry, K. S., and Hunnewell, S. T. (1995). “Silt Fence Testing for Eagle River Flats Dredging.” Special Report 95-27 U.S. Army Corps of Engineers Cold Regions Research & Engineering Laboratory. NTIS, Springfiled, Virginia 22161.

Jeffrey, J., and Menches, C. (1993). “How to detect and handle outliers.” ASQC Quality Press, Wisconsin.

Kaufman, H. M. (2000). “Erosion Control at Construction Sites: The Science – Policy Gap.” Environmental Management, Vol. 26, No. 1, 89-97.

Keener, H. M., Faucette, L. B., and Klingman, M. H. (2007). “Flow-Through Rates and the Evaluation of Solids Separation of Compost Filter Socks versus Silt Fence in Sediment Control Applications.” *Journal of Environmental Quality.* Vol. 36, No. 3, 742-752.

Kouwen, N. (1990). Silt Fences to Control Sediment Movement on Construction Sites. Report MAT-90-03. Research Development Branch Ontario Ministry of Transportation, Downsview, Ontario, Canada.

Louisiana Department of Transportation and Development (LA DOTD) (2007). “EC-01 Temporary Erosion Control Details.” *Sheet 2 of 2*, Baton Rouge, LA.

McLaughlin, R. A., Rajbhandari, N., Hunt, W. F., Line, D. E., Sheffield, R. E., and White, N. M. (2001). “The Sediment and Erosion Control Research and Education Facility at North Carolina State University.” *Soil Erosion Research for the 21st Century, Proc. Int. Symp.* Honolulu, HI.

Mississippi Department of Environmental Quality (MDEQ). (2011). *Erosion control, sediment control and stormwater management on construction sites and urban areas, vol. 1, erosion and sediment control*, Jackson, MS.

Mississippi Department of Transportation (MDOT). (2017). “Mississippi Standard Specifications for Road and Bridge Construction.” *Standard Specifications – Section 234 Silt Fence.* Jackson, MS.

North Carolina Sedimentation Control Commission (NC-SCC), Department of Environmental and Natural Resources (DNER), and North Carolina Agricultural Extension Service (NC-AES). (2013). *Erosion and sediment control design manual*, Raleigh, NC.

Peng, F. F., and Di, P. (1994). "Effect of Multivalents Salts - Calcium and Aluminum on the Flocculation of Kaolin Suspension with Anionic Polyacrylamide." *Journal of Colloid and Interface Science*, 164.

Perez, M. A., Zech, W. C., Donald, W. N., and Fang, X. (2015). "Installation Enhancements to Common Inlet Protection Practices Using Large-Scale Testing Techniques." *Transportation Research Record: Journal of the Transportation Research Board.* No. 2521, 151-161.

Perez, M. A., Zech, W. C., Donald, W. N., and Fang, X. (2015). "Methodology for Evaluating Inlet Protection Practices Using Large-Scale Testing Techniques." *Journal of Hydrologic Engineering*, 101061/(ASCE)HE.1943-5584.0001019.

Perez, M. A., Zech, W. C., Fang, X., and Vasconcelos, J. G. (2016). "Methodology and Development of a Large-Scale Sediment Basin for Performance Testing." *J. Irrig. Drain Eng.*, Vol. 142, No. 10.

Pitt, R. E., Clark, S. E., and Lake, D. W. (2007). *Construction site erosion and sediment controls: planning, design, and performance*, DEStech Publications, Inc., Lancaster, PA., Vol. 3, 186-192.

Qian, J. W., Xiang, X. J., Yang, W. Y., Wang, M., and Zheng, B. Q. (2004). "Flocculation Performance of Different Polyacrylamide and the Relation between Optimal Dose and Critical Concentration." *European Polymer Journal*, 40.

Remondino, F., Barazzetti, L., Nex, F., Scaioni, M., Sarazzi, D. (2011). "UAV Photogrammetry for mapping and 3D modeling – current status and future perspectives." *Int. Arch. Photogramm. Remote Sens. Spatial Inf. Sci.,* Vol. 38(1/C22), 25-31.

Richardson, G. N., and Middlebrooks, P. (1991). "A simplified design method for silt fences." *Proceedings of Geosynthetics '91*, IFAI, Atlanta, GA, 879-888.

Risse, L. M., Thompson, S. A., Governo, J. and Harris, K. (2008). "Testing of new silt fence materials: a case study of a belted strand retention fence." *Journal of Soil and Water Conservation,* Vol. 63, No. 5, 265-273.

Robichaud, P. R., McCool, D. K., Pannkuk, C. D., Brown, R. E., and Mutch, P. W. (2001). "Trap Efficiency of Silt Fence Used in Hillslope Erosion Studies." *Soil Research for the 21 Century,* Proc. Int. Symp. January 3-5, Honolulu, HI, 541-543.

Schueler, T. R., and Holland, H. K. (1997). "Impacts of Suspended and Deposited Sediment." Article 14 in *The Practices of Watershed Protection,* pp. 64-65, Center for Watershed Protection, Ellicott City, MD.

Seo, S. (2006). “A review and comparison of methods for detecting outliers in univariate data sets.” Dissertation. University of Pittsburgh, PA.

Siebert, S., Teizer, J. (2014). “Mobile 3D mapping for surveying earthwork projects using an Unmanned Aerial Vehicle (UAV) system.” *Automation in Construction,* Vol. 41, 1-14.

Silt-Saver (2015). “Product Details: Staged-Release, 4 – Stage Specifications.” https://siltsaver.com/products/silt-fence/srsf-4-stage/. (April 9, 2018).

Sojka, R. E., Bjorneberg, D. L., Entry, J. A., Lentz, R. D., and Orts, W. J. (2007). "Polyacrylamide in Agriculture and Environmental Land Management." *Advances in Agronomy*, 92.

South Carolina Department of Transportation (SCDOT). (2014). *SCDOT stormwater quality design manual*, Columbia, SC.

Sprague, C. J. (2006). “Laboratory testing of sediment retention devices.” *37th Conference of the International Erosion Control Association 2006: EC 06 Environmental Connection*, International Erosion Control Association, Steamboat Springs, CO, 201-210.

Sprague, C. J. (2007). *“Large-Scale Sediment Retention Device Testing (ASTM D 7351) of a Heavyweight™ Wattle on Sandy Loam.”* World Textile and Bag, Inc.

Sprague, C. J. and Sprague, J. E. (2012). *“BMP Testing for Erosion and Sediment Control.”* Georgia Soil and Water Conservation Commission, Final Report, Contract No. 480-12-ESC-4008.

State of Tennessee Department of Transportation (TNDOT). (2012). “Standard Drawing EC-STR-3B – Silt Fence.”

Stevens, E., Yeri, S., Barfield, B., Gasem, K., and Matlock, M. (2004). “On and Off Site Sediment Control Using Silt Fence.” *World Water Congress.* Critical Transitions in Water and Environment Resource Management.

Tennessee Department of Environment and Conservation (TNEC). (2012). *Tennessee erosion and sediment control handbook, 4th edition*, Nashville, TN.

Texas Department of Transportation (TxDOT). (2012). *Storm water management guidelines for construction activities,* Austin, TX.

Toxel, C. F., (2013). “Life Cycle Analysis of Sediment Control Devices.” *Thesis,* Master of Civil Engineering. Georgia Institute of Technology, Atlanta, GA.

U.S. Congress. (1972). “Clean Water Act.”. Federal Water Pollution Control Act, 33 U.S.C. §1251 et seq., Washington D.C.

U.S. Congress (1987). “Water Quality Act of 1987.” Public Law 100-4. Washington, D.C.

U.S. Department of Agriculture (USDA). (2006). “Soil quality – urban technical note No.1, erosion and sedimentation on construction sites.” Natural Resources Conservation Service, Auburn, AL.

U.S. Environmental Protection Agency (USEPA). (2001). “Storm water phase II final: construction rainfall erosivity waiver.” *EPA 833-F-00-014*, Fact Sheet 3.1, Washington, DC.

U.S. Environmental Protection Agency (2005). "National Management Measures to Control Nonpoint Source Pollution from Urban Areas." Washington, DC.

U.S. Environmental Protection Agency (USEPA). (2007). “Developing your stormwater pollution prevention plan: a guide for construction site.” *EPA-833-R-06-004*, Washington, DC.

U.S. Environmental Protection Agency (USEPA). (2012). “Stormwater best management best practices; silt fences.” *EPA 833-F-11-008*, Washington, DC.

U.S. Environmental Protection Agency (USEPA). (2017). Construction General Permit. Office of Water, Washington, DC.

U.S. Fabrics (2018). Nonwoven Geotextiles. Cincinnati, OH. < https://www.usfabricsinc.com/products/nonwoven?gclid=EAIaIQobChMIk4f58crH3AIVlIKzCh2_MQG5EAAYASAAEgJNw_D_BwE>

Western Excelsior (2017). *Excel Straw Logs – Material Properties and Dimensions.* Product Specifications, Evansville, ID.<http://www.westernexcelsior.com/products/documentation/WE_EXCEL_ESL_SPEC.pdf>

Western Excelsior (2018). *Log and Wattle Installation Instructions.* Evansville, ID. <http://www.westernexcelsior.com/products/documentation/WE_EXCEL_ESL_INL.pdf>

Willet, G. (1980). “Urban erosion.” *National Conference on Urban Erosion and Sediment Control: Institutions and Technology*, EPA 905/9-80-002, U.S. Environmental Protection Agency, 51-56.

Williams, J. R., and Berndt, H. D. (1977). “Sediment yield prediction based on watershed hydrology.” *Trans. ASAE,* Vol. 20, No. 6, 1100-1104.

Wyant, D. C. (1981). “Evaluation of Filter Fabrics for use as Silt Fence.” Transportation Research Record: Journal of the Transportation Research Board, No. 832, 6-12.

APPENDICES

Appendix A: ALDOT Standard Highway Drawing for Erosion and Sediment Controls

Appendix B: Example Experimental Results (Test Data Log)

Appendix C: Manufacturer's Installations Details

Appendix D: Water Quality Analysis Graphs

Appendix E: Sediment Barrier Practice Treatments

Appendix F: ALDOT List II-24 Modifications

APPENDIX A

ALDOT STANDARD HIGHWAY DRAWING FOR

EROSION AND SEDIMENT CONTROL

REFERENCE PROJECT NO	FISCAL YEAR	SHEET NO

NOTES:

1. "J-HOOK" CONFIGURATION SILT FENCE APPLICATIONS ARE TO BE USED IN CONJUNCTION WITH PERIMETER SILT FENCE WHEN STORMWATER RUNOFF IS IN TWO DIRECTIONS (DOWN A FILL SLOPE AND DOWN GRADIENT ALONG THE RIGHT-OF-WAY).
2. "SMILE CONFIGURATION" APPLICATIONS ARE TO BE USED AS PERIMETER SILT FENCE WHEN THERE IS ONE-DIRECTIONAL FLOW DOWN A SLOPE.
3. SAND BAGS CAN BE USED AS DIVERSION BERMS TO PREVENT SEDIMENT FROM BEING WASHED ONTO OR ACROSS HARD SURFACES, OR TO HELP SLOW SHEET FLOW VELOCITY WHEN DRAINING AWAY FROM HARD SURFACES.
4. FOR SHORTER SLOPES AND/OR SLOPES THAT ARE LESS STEEP, DIVERSION BERMS CAN BE USED TO SAFELY CONVEY STORMWATER AWAY FROM OR AROUND A DENUDED AREA. THEY CAN BE CONSTRUCTED USING A MANUFACTURED SILT DIKE OR BY CONSTRUCTING A TEMPORARY EARTH BERM AND TRENCH WITH GEOTEXTILE OR POLYETHYLENE SHEETING PROTECTION.
5. TEMPORARY DEWATERING STRUCTURES CAN BE USED DURING CULVERT CONSTRUCTION, STREAM DIVERSIONS, OR OTHER CONSTRUCTION ACTIVITIES WHERE TURBID WATERS NEED TO BE CLARIFIED BEFORE RELEASE. SEE SPECIAL DRAWING NO ESC-503 FOR INSTALLATION DETAILS.
6. ROLLED OR HYDRAULIC EROSION CONTROL PRODUCTS MAY BE USED FOR EROSION PROTECTION AND VEGETATION ESTABLISHMENT ON 2H:1V OR STEEPER SOIL SLOPES WITH SLOPE LENGTH MORE THAN 15 FEET OR IN SENSITIVE AREAS WHEN DIRECTED. ROLLED EROSION CONTROL PRODUCTS MAY ALSO BE UTILIZED IN CHANNELS WHEN DIRECTED. SEE PLANS FOR SPECIFIC REQUIREMENTS AND SPECIAL DRAWING NUMBER ESC-509 FOR INSTALLATION DETAILS.
7. THE ABUTMENT SLOPE TOE BERM SHALL BE A MINIMUM OF 18 INCHES TALL. THE BERM MAY BE CONSTRUCTED WITH ROCK IN ACCORDANCE WITH REQUIREMENTS FOR ROCK DITCH CHECKS ON SP-DWG ESC-300 OR WITH SOIL IN ACCORDANCE WITH ESC-200-2.
8. MATERIAL STOCKPILES THAT ARE TO REMAIN IN PLACE AFTER PROJECT COMPLETION SHALL BE PERMANENTLY SEEDED. FINAL SHAPING SHALL BE SUBSIDIARY TO UNCLASSIFIED EXCAVATION AND/OR TOPSOIL WORK.

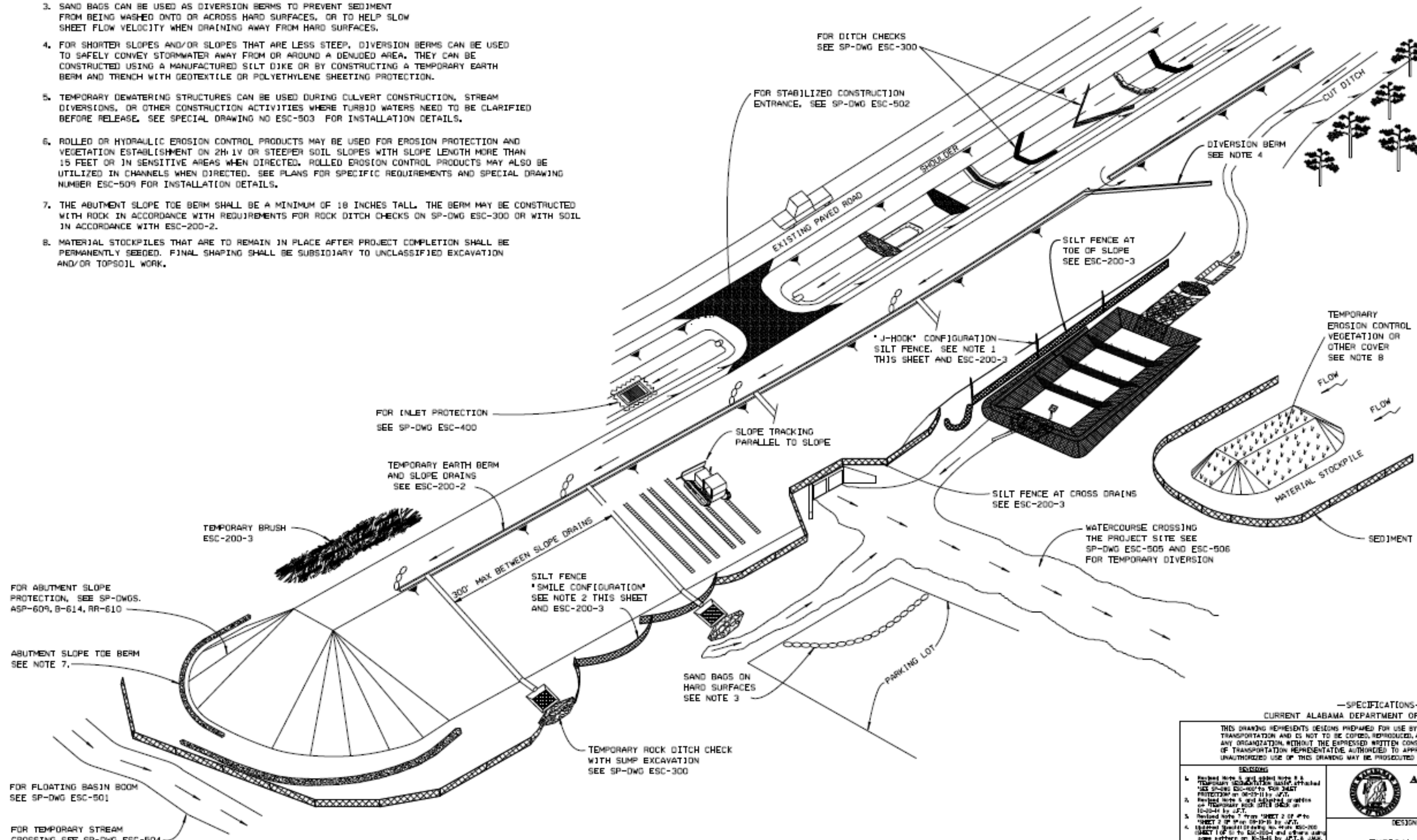

—SPECIFICATIONS—
CURRENT ALABAMA DEPARTMENT OF TRANSPORTATION

REVISIONS

ALABAMA DEPARTMENT OF TRANSPORTATION
1409 COLISEUM BOULEVARD
MONTGOMERY, AL 36130-3050

DESIGN BUREAU SPECIAL DRAWING

TYPICAL TEMPORARY EROSION/
SEDIMENT CONTROL APPLICATIONS

Bureau Std Engr: L.V.S.
DRAWN BY: ______ DATE DRAWN: 2006

SPECIAL DRAWING NO: ESC-200-1

INDEX NO: 1161

NOT TO SCALE

REFERENCE PROJECT NO	FISCAL YEAR	SHEET NO

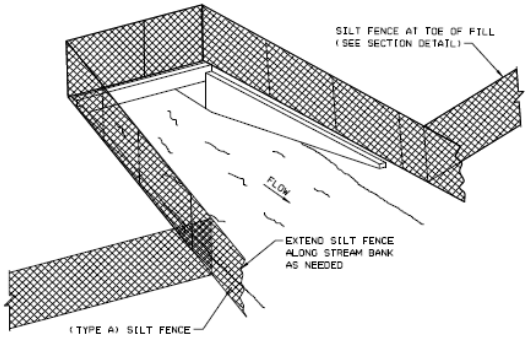

SEDIMENT BARRIER AT CROSS DRAIN

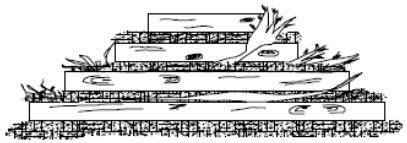

REAR ELEVATION

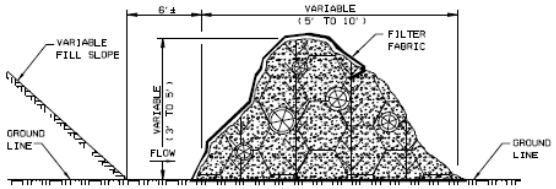

SIDE ELEVATION

TEMPORARY BRUSH BARRIER

NOTES:
1. BRUSH BARRIER MAY BE USED WHERE NATURAL GROUND IS LEVEL OR SLOPING AWAY FROM PROJECT.
2. PLACE BRUSH, LOG AND TREE LAPS APPROXIMATELY PARALLEL TO TOE OF FILL SLOPE WITH SOME OF THE HEAVIER MATERIALS BEING PLACED ON TOP TO PROPERLY SECURE THE BARRIER AS DETAILED AT LOCATIONS SHOWN ON PLANS OR AS DIRECTED OR PERMITTED BY THE ENGINEER.
3. TO ALLOW WATER TO SEEP THROUGH BRUSH BARRIER, INTERMINGLE THE BRUSH, LOG AND TREE LAPS SO AS NOT TO FORM A SOLID DAM.
4. THE BRUSH BARRIER SHALL BE CHOKED WITH FILTER FABRIC.

NOTE:
1. ANCHOR AND INSTALL SILT FENCE PER DETAILS SHOWN ON SPECIAL DRAWING No. ESC-200-4.

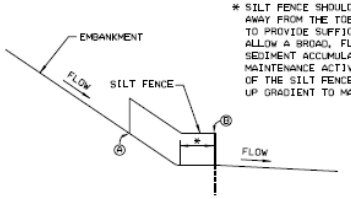

* SILT FENCE SHOULD BE LOCATED AWAY FROM THE TOE OF THE SLOPE TO PROVIDE SUFFICIENT SPACE TO ALLOW A BROAD, FLAT AREA FOR SEDIMENT ACCUMULATION AND MAINTENANCE ACTIVITIES. THE ENDS OF THE SILT FENCE SHOULD BE TURNED UP GRADIENT TO MAXIMIZE STORAGE.

SILT FENCE SECTION AT TOE OF FILL

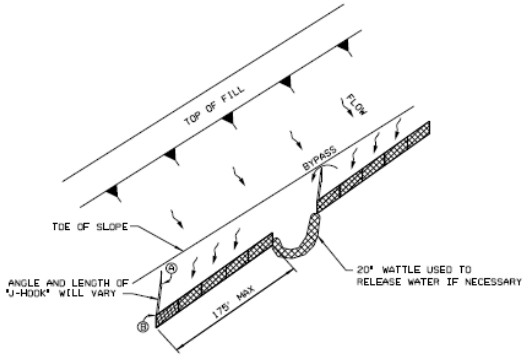

"J-HOOK" SILT FENCE APPLICATION

THE ELEVATION AT THE BOTTOM OF THE DISTANT END OF THE "J-HOOK" Ⓐ SHOULD BE THE SAME AS THE LOWEST POINT ALONG THE TOP OF SILT FENCE Ⓑ.

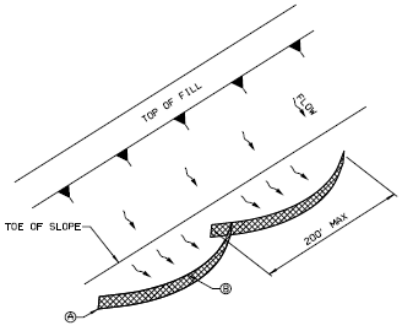

"SMILE-CONFIGURATION" SILT FENCE APPLICATION

NOTE:
1. EL Ⓐ = EL Ⓑ TO MAXIMIZE STORAGE.

—SPECIFICATIONS—
CURRENT ALABAMA DEPARTMENT OF TRANSPORTATION

REVISIONS
1. Revised "SIDE ELEVATION" to show Geotextile Filter and Under-branch. Edited and reconstructed text on drawing by JJTA.
2. Updated Special Drawing No. from ESC-200-3 (Sheet 3 of 3) to ESC-200-3 on 10-16-15 by JJTA & JAMH.

ALABAMA DEPARTMENT OF TRANSPORTATION
1409 COLISEUM BOULEVARD
MONTGOMERY, AL 36130-3050

DESIGN BUREAU SPECIAL DRAWING

DETAILS OF SEDIMENT BARRIER APPLICATIONS

Bureau Std Engr.
DRAWN BY: DATE DRAWN: 2006

SPECIAL DRAWING NO: ESC-200-3

INDEX NO: 1161-B

NOT TO SCALE

REFERENCE PROJECT NO	FISCAL YEAR	SHEET NO

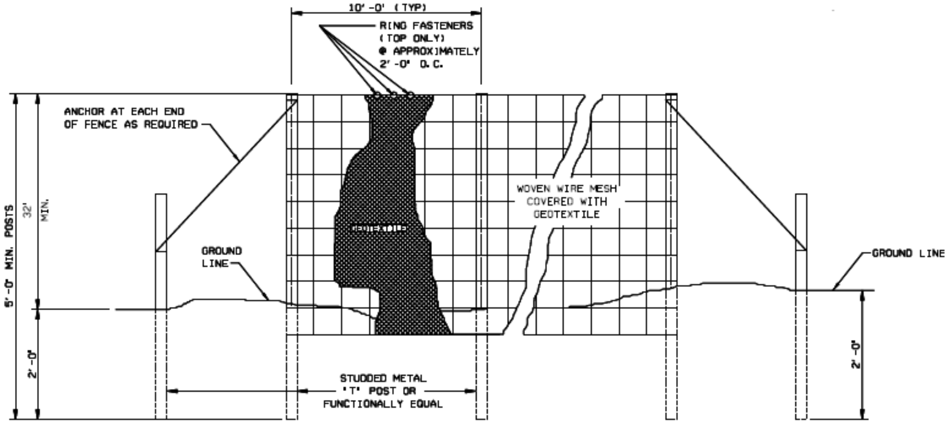

ELEVATION VIEW

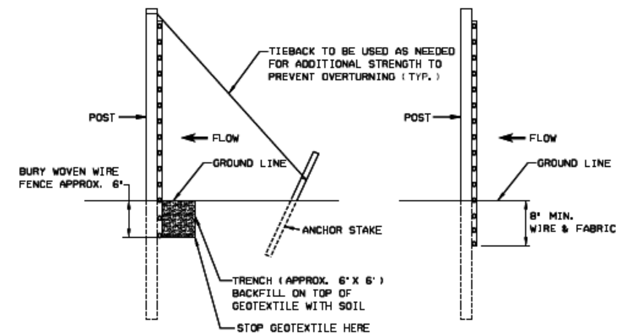

SIDE VIEW

NOTES:
1. METHOD II FENCE INSTALLATION ALSO TO INCLUDE ANCHORS AND TIEBACKS AS REQUIRED.
2. SILT FENCE SHALL BE USED IN AREAS WHERE FLOW IS LOW TO MODERATE OR AS DIRECTED BY THE ENGINEER.
3. SILT FENCES ARE TEMPORARY SEDIMENT CONTROL ITEMS THAT SHALL BE ERECTED DOWN GRADE OF ERODIBLE AREAS SUCH AS NEWLY GRADED FILL SLOPES AND ADJACENT TO STREAMS AND CHANNELS.
4. SILT FENCE SHOULD BE PLACED WELL INSIDE RIGHT-OF-WAY AND ALONG EDGE OF CLEARING LIMITS. THIS WILL ALLOW ROOM FOR ADDITIONAL BEST MANAGEMENT PRACTICES SUCH AS VEGETATED BUFFERS.
5. WHEREVER POSSIBLE SILT FENCES SHALL BE CONSTRUCTED ACROSS A LEVEL AREA IN THE SHAPE OF A SMILE. THIS AIDS IN PONDING OF RUNOFF AND FACILITATES SEDIMENTATION.
6. THE CONTRACTOR MAY ELECT TO USE EITHER INSTALLATION METHOD I OR METHOD II.
7. METHOD II INSTALLATION SHALL BE ACCOMPLISHED USING AN IMPLEMENT THAT IS MANUFACTURED FOR THE APPLICATION AND PROVIDES A CONFIGURATION MEETING THE REQUIREMENTS OF THE DETAIL.
8. SEE ALDOT LIST II-3 FOR APPROVED SILT FENCE GEOTEXTILES.

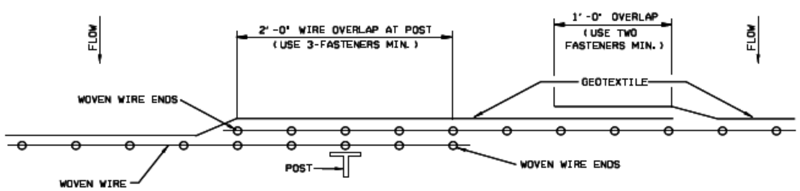

PLAN VIEW

REQUIRED LAPPING

—SPECIFICATIONS—
CURRENT ALABAMA DEPARTMENT OF TRANSPORTATION

REVISIONS

ALABAMA DEPARTMENT OF TRANSPORTATION
1409 COLISEUM BOULEVARD
MONTGOMERY, AL 36130-3050

DESIGN BUREAU SPECIAL DRAWING

DETAILS OF SILT FENCE INSTALLATION

Bureau Std Engr: LVS
DRAWN BY: ______ DATE DRAWN: 2006

SPECIAL DRAWING NO: ESC-200-4
INDEX NO: 1161-C

NOT TO SCALE

REFERENCE PROJECT NO	FISCAL YEAR	SHEET NO

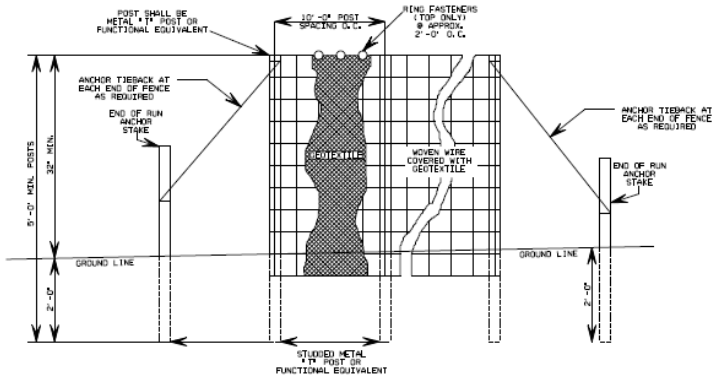

ELEVATION VIEW

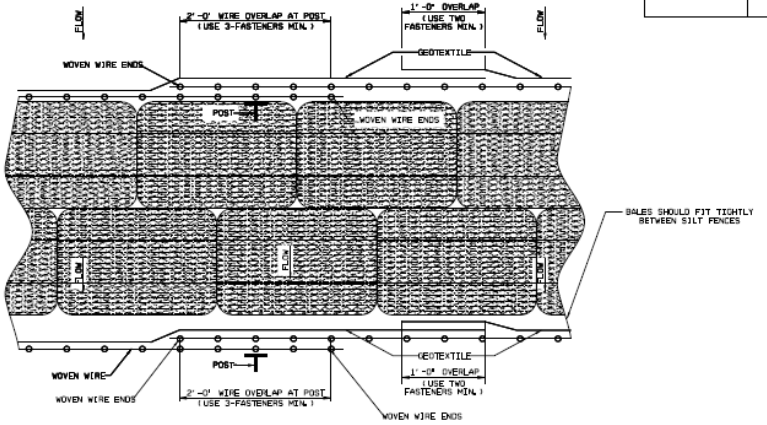

PLAN VIEW
REQUIRED LAPPING

NOTES:
1. METHOD II FENCE INSTALLATION ALSO TO INCLUDE ANCHORS AND TIEBACKS AS REQUIRED.
2. SEDIMENT RETENTION BARRIER SHALL BE USED IN AREAS WHERE FLOW IS LOW TO MODERATE OR AS DIRECTED BY THE ENGINEER.
3. SEDIMENT RETENTION BARRIERS ARE TEMPORARY SEDIMENT CONTROL ITEMS THAT SHALL BE ERECTED DOWN GRADE OF ERODIBLE AREAS SUCH AS NEWLY GRADED FILL SLOPES AND ADJACENT TO STREAMS AND CHANNELS.
4. SEDIMENT RETENTION BARRIERS SHOULD BE PLACED WELL INSIDE RIGHT-OF-WAY AND ALONG EDGE OF CLEARING LIMITS IF POSSIBLE. THIS WILL ALLOW ROOM FOR ADDITIONAL BEST MANAGEMENT PRACTICES SUCH AS VEGETATED BUFFERS.
5. WHEREVER POSSIBLE SEDIMENT RETENTION BARRIERS SHALL BE CONSTRUCTED ALONG A CONTOUR WITH THE ENDS TURNED. THIS AIDS IN PONDING OF RUNOFF AND FACILITATES SEDIMENTATION.
6. THE CONTRACTOR MAY ELECT TO USE EITHER INSTALLATION METHOD I OR METHOD II.
7. METHOD II INSTALLATION SHALL BE ACCOMPLISHED USING AN IMPLEMENT THAT IS MANUFACTURED FOR THE APPLICATION AND PROVIDES A CONFIGURATION MEETING THE REQUIREMENTS OF THE DETAIL.
8. SEE ALDOT LIST 11-3 FOR APPROVED SILT FENCE GEOTEXTILES.

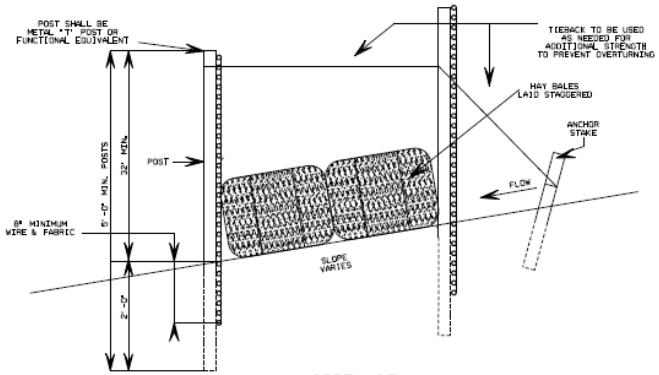

SIDE VIEW
SECTION A-A
METHOD II
MECHANICAL INSTALLATION

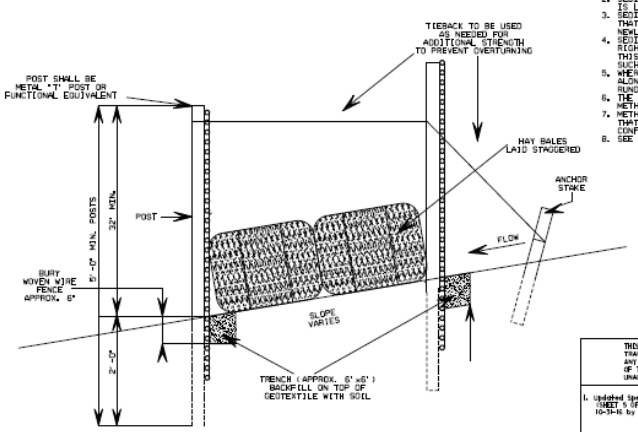

SIDE VIEW
SECTION A-A
METHOD I

—SPECIFICATIONS—
CURRENT ALABAMA DEPARTMENT OF TRANSPORTATION

REVISIONS
1. Updated Special Drawing No. ESC-200 (SHEET 5 OF 5) to ESC-200-5 on 10-31-16 by A.F.T. & J.M.M.

ALABAMA DEPARTMENT OF TRANSPORTATION
1409 COLISEUM BOULEVARD
MONTGOMERY, AL 36130-3050

DESIGN BUREAU SPECIAL DRAWING

DETAILS OF SEDIMENT RETENTION BARRIER

Bureau SM Engr. LVS
DRAWN BY: MDH DATE DRAWN: 09-22-15

SPECIAL DRAWING NO: ESC-200-5

INDEX NO: 1161-D

NOT TO SCALE

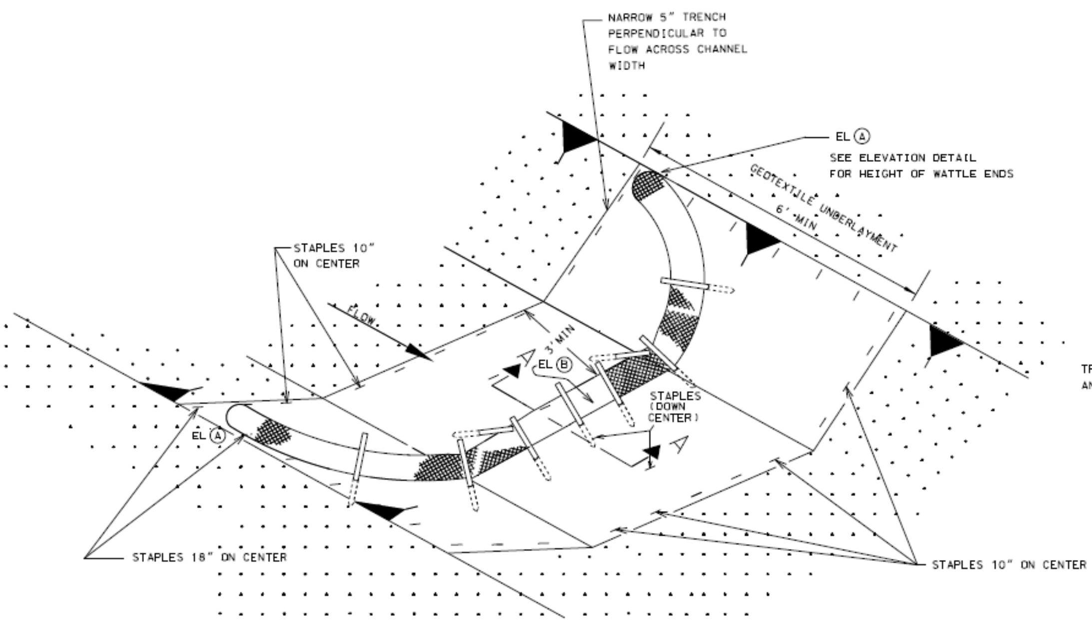

DETAIL (DITCH CHECK)

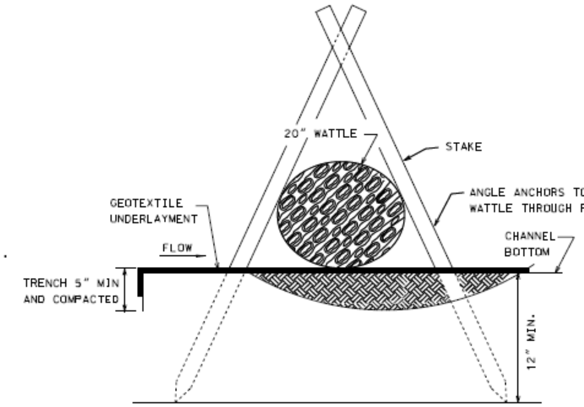

SECTION A-A

NOTES:

1. MINIMUM RECOMMENDED PLACEMENT INTERVAL BETWEEN WATTLE DITCH CHECK IS 100 FEET UNLESS SHOWN OTHERWISE ON THE PLANS OR APPROVED BY THE ENGINEER. SEE SPACING GUIDANCE ON ESC-300-1.
2. ANCHORING STAKES SHALL BE SIZED, SPACED, DRIVEN, AND BE OF A MATERIAL THAT EFFECTIVELY SECURES THE CHECK. STAKE SPACING SHALL BE A MAXIMUM OF TWO FEET.
3. WATTLES SHOULD NOT BE USED IN HARD BOTTOM CHANNELS.
4. STAPLES SPACED 18 INCHES APART, ALONG THE CHANNEL EDGES AND DOWN THE CENTER OF THE CHANNEL. STAPLES SPACED 10 INCHES APART, ACROSS THE UPSTREAM AND DOWNSTREAM EDGES.

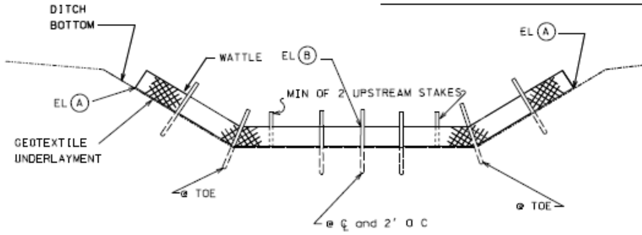

ELEVATION DETAIL

NOTE: END POINTS (A) MUST BE HIGHER THAN FLOWLINE POINT (B)

WATTLE DITCH CHECK SELECTION GUIDELINES

WATTLE DITCH CHECKS ARE APPROPRIATE FOR VELOCITY REDUCTION AND CONTROL OF SEDIMENT TRANSPORT UNDER LOW TO MEDIUM FLOW CONDITIONS NOT EXCEEDING 1.0 CU FT/SEC.

REFERENCE PROJECT NO	FISCAL YEAR	SHEET NO

—SPECIFICATIONS—
CURRENT ALABAMA DEPARTMENT OF TRANSPORTATION

ALABAMA DEPARTMENT OF TRANSPORTATION
1409 COLISEUM BOULEVARD
MONTGOMERY, AL 36130-3050

DESIGN BUREAU SPECIAL DRAWING

DETAILS OF EROSION CONTROL
WATTLE DITCH CHECK

SPECIAL DRAWING NO ESC-300-4
INDEX NO 1162-C

DATE DRAWN 2006

NOT TO SCALE

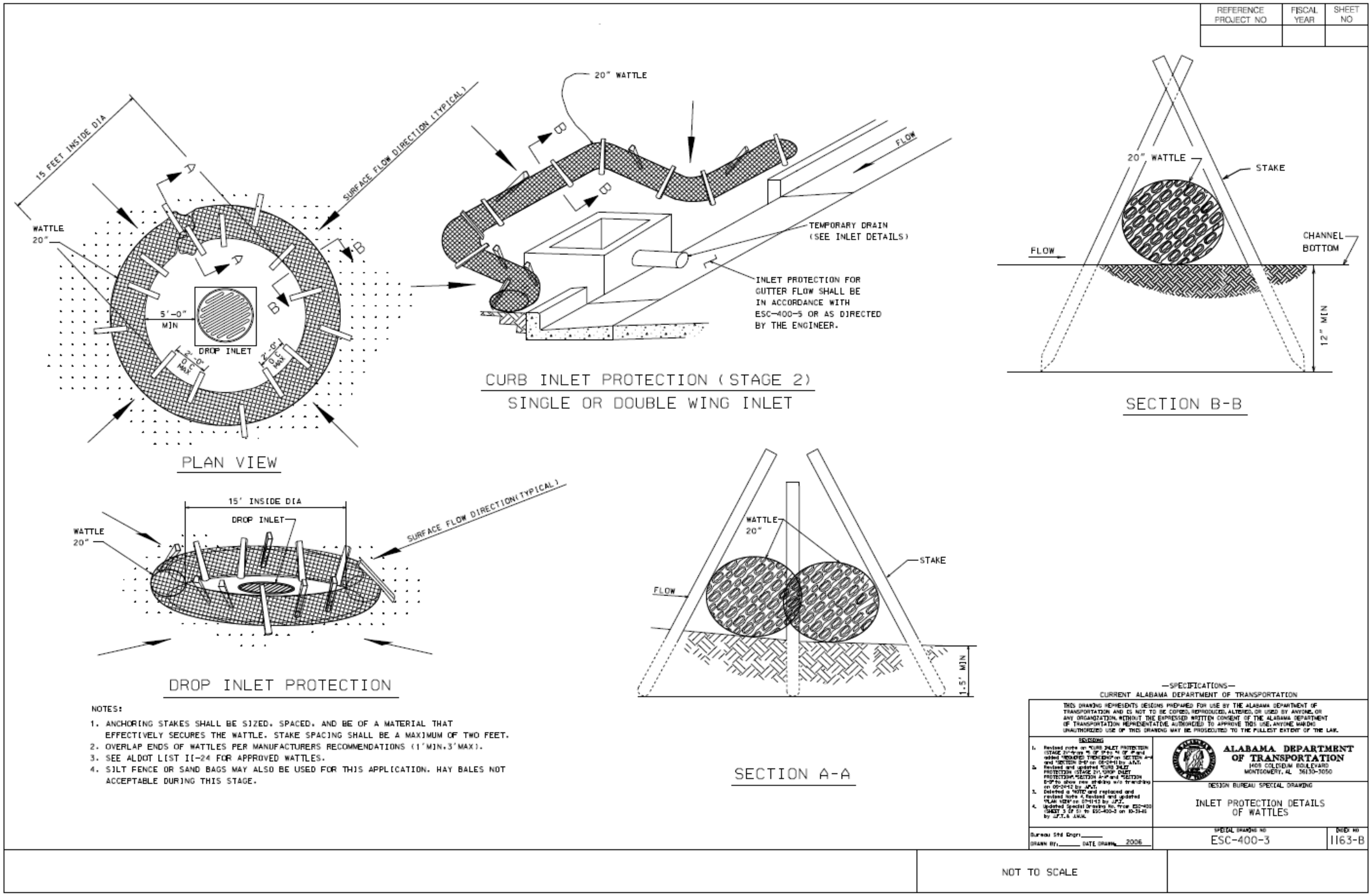
REFERENCE PROJECT NO
FISCAL YEAR
SHEET NO
15 FEET INSIDE DIA
SURFACE FLOW DIRECTION (TYPICAL)
WATTLE 20"
5'-0" MIN
DROP INLET
2'-0" MAX
PLAN VIEW
20" WATTLE
FLOW
TEMPORARY DRAIN (SEE INLET DETAILS)
INLET PROTECTION FOR GUTTER FLOW SHALL BE IN ACCORDANCE WITH ESC-400-5 OR AS DIRECTED BY THE ENGINEER.
CURB INLET PROTECTION (STAGE 2)
SINGLE OR DOUBLE WING INLET
20" WATTLE
STAKE
FLOW
CHANNEL BOTTOM
12" MIN
SECTION B-B
15' INSIDE DIA
DROP INLET
WATTLE 20"
SURFACE FLOW DIRECTION(TYPICAL)
DROP INLET PROTECTION
WATTLE 20"
STAKE
FLOW
1.5' MIN
SECTION A-A
NOTES:
1. ANCHORING STAKES SHALL BE SIZED, SPACED, AND BE OF A MATERIAL THAT EFFECTIVELY SECURES THE WATTLE. STAKE SPACING SHALL BE A MAXIMUM OF TWO FEET.
2. OVERLAP ENDS OF WATTLES PER MANUFACTURERS RECOMMENDATIONS (1'MIN,3'MAX).
3. SEE ALDOT LIST II-24 FOR APPROVED WATTLES.
4. SILT FENCE OR SAND BAGS MAY ALSO BE USED FOR THIS APPLICATION. HAY BALES NOT ACCEPTABLE DURING THIS STAGE.
—SPECIFICATIONS—
CURRENT ALABAMA DEPARTMENT OF TRANSPORTATION
THIS DRAWING REPRESENTS DESIGNS PREPARED FOR USE BY THE ALABAMA DEPARTMENT OF TRANSPORTATION AND IS NOT TO BE COPIED, REPRODUCED, ALTERED, OR USED BY ANYONE, OR ANY ORGANIZATION, WITHOUT THE EXPRESSED WRITTEN CONSENT OF THE ALABAMA DEPARTMENT OF TRANSPORTATION REPRESENTATIVE AUTHORIZED TO APPROVE THIS USE. ANYONE MAKING UNAUTHORIZED USE OF THIS DRAWING MAY BE PROSECUTED TO THE FULLEST EXTENT OF THE LAW.
REVISIONS
ALABAMA DEPARTMENT OF TRANSPORTATION
1409 COLISEUM BOULEVARD
MONTGOMERY, AL 36130-3050
DESIGN BUREAU SPECIAL DRAWING
INLET PROTECTION DETAILS OF WATTLES
Bureau Std Engr.
DRAWN BY
DATE DRAWN 2006
SPECIAL DRAWING NO
ESC-400-3
INDEX NO
1163-B
NOT TO SCALE

APPENDIX B

EXAMPLE EXPERIMENTAL RESULTS

(TEST DATA LOG)

SEDIMENT BARRIER TEST LOG

Table 1: Test Overview	
Test ID:	SB-01-M9-I1-P4
Date:	11/30/2017
SB Installation:	M8 w/ Dewatering Weir
Techs:	Whitman, Savage
Test Type:	Performance

Start Time:	8:05
End Time:	10:05
Flow Rate (ft^3/s):	0.22
Sediment Load Rate (lb/min):	37.2

Figure 1: Sediment Barrier Installation

Installation Description: ALDOT Standard Reinforced Silt Fence was installed and evaluated. Installation configuration was modified from the ALDOT Standard Drawing ESC-200 (Sheet 3 & 4). The modification reduced fence height from 32 inches to 24 inches, increased T-Post size from 0.95 lb/ft to 1.25 lb/ft, decreased T-Post spacing from 10 feet to 5 feet and offset trench 0.5 feet from T-Post. A v-notch weir/orifice board was installed in the center of the installation to promote controlled dewatering. Soil density tests indicated average moisture content and dry unit weight of 9.27% (15.0% optimal) and 113.61 lbs/ft^3 (max 113.1 lbs/ft^3); respectfully, in the earthen test area.

Table 2: Hydraulic Observations	
Overtopping Time (min):	N/A
Max. Impoundment (ft):	1.54
Upstream Ponding (ft):	10.80
Dewatering (hrs.):	4.0

Test Notes: During Performance Test 4 (P4), end T-Posts were tied with wire to anchor T-Post outside of the test area. The anchor T-Post were located 4 feet from the end T-Post, on 20-degree angles uphill.

Figure 2: Impoundment

Figure 3: Deposition / Erosion

Test Observations: Overtopping did not occur during the second performance test on this installation.

PRE-TEST PHOTO DOCUMENTATION

Location 1

Location 2

Location 3

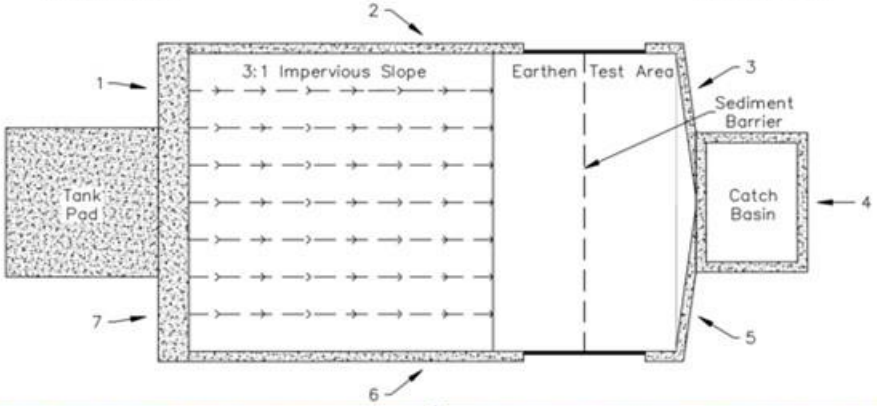

Location 4

Location 7

Location 6

Location 5

DURING TEST PHOTO DOCUMENTATION

Location 1

Location 2

Location 3

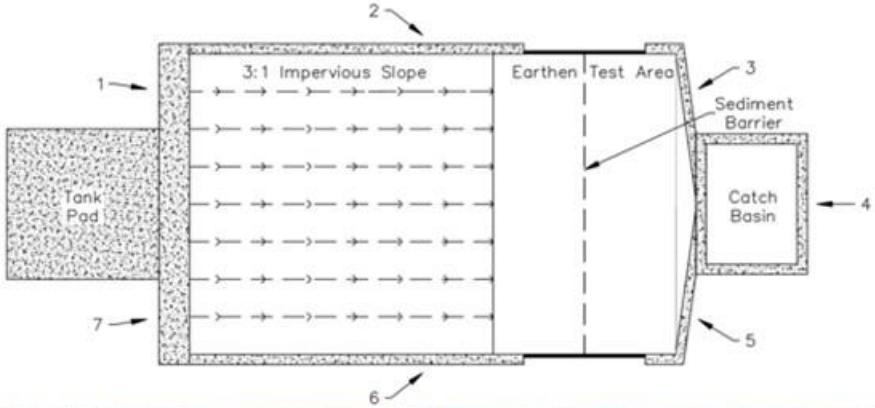

Location 4

Location 7

Location 6

Location 5

POST-TEST PHOTO DOCUMENTATION

Location 1

Location 2

Location 3

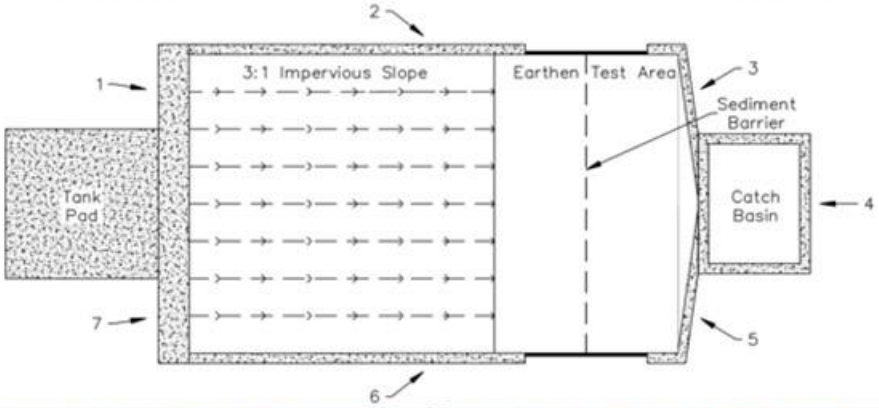

Location 4

Location 7

Location 6

Location 5

Deposition/Erosion Survey

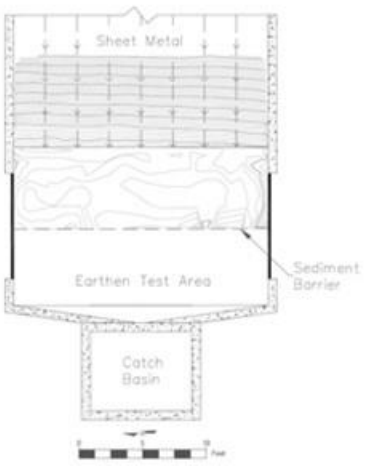

Figure 4: Pre-Test Survey

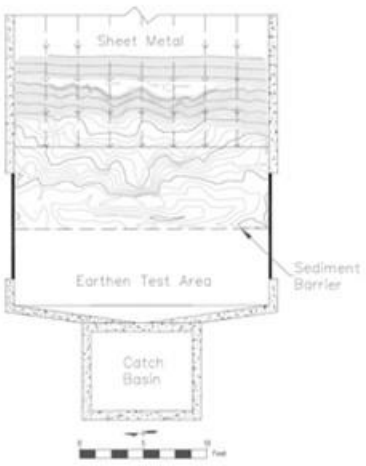

Figure 5: Post-Test Survey

Figure 6: Pre-Test Deposition / Erosion

Figure 7: Post-Test Deposition / Erosion

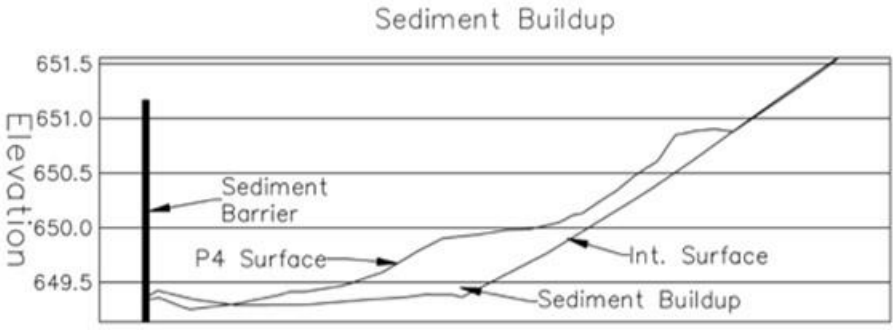

Figure 8: Cross Section

Table 3: Sediment Transport	
Sediment Introduced (yd^3):	1.45
Sediment Retained (yd^3):	1.40
% Sediment Retained:	96%

Water Quality

Table 4: Turbidity & Total Suspended Solids (TSS)										
Time	Turbidity (NTU)					TSS (mg/L)				
(min)	Imp. Slope	U/S Top Water	U/S Bot. Water	D/S SB	Dis. Into Tank	Imp. Slope	U/S Top Water	U/S Bot. Water	D/S SB	Dis. Into Tank
5	9,344	4,712	6,344	7,696	5,712	9,344	2,976	6,048	5,696	4,768
10	9,328	2,168	5,192	2,984	4,240	9,328	608	4,768	2,000	4,032
15	9,872	1,856	3,872	2,200	3,172	9,872	704	4,128	1,536	2,832
20	12,832	1,464	3,288	2,264	2,852	12,832	608	3,424	1,664	2,656
25	7,600	1,458	3,216	2,188	3,124	7,600	808	2,976	2,336	3,424
30	7,904	1,292	3,044	2,112	3,144	7,904	720	2,848	1,696	3,312
35	No Data	1,090	2,564	1,420	1,900	No Data	536	2,288	976	1,840
40		1,096	1,308	1,060	1,252		528	1,056	560	912
45		1,016	1,024	934	1,156		408	608	416	768
60		906	1,516	766	1,008		424	1,056	352	592
90		722	962	840	866		360	512	344	440
120		700	961	783	710		328	396	332	336

Note: Imp. = Impervious, U/S = Upstream, D/S = Downstream, Bot. = Bottom, SB = Sediment Barrier, Dis. = Discharge

Table 5: Turbidity & TSS Statistics (During Test)								
	Avg.		Min.		Max.		Std. Dev.	
	NTU	TSS	NTU	TSS	NTU	TSS	NTU	TSS
Imp. Slope	9,480	824	7,600	658	12,832	1,116	1,868	163
U/S Top	2,158	1,071	1,292	608	4,712	2,976	1,291	936
U/S Bot.	4,159	4,032	3,044	2,848	6,344	6,048	1,328	1,225
D/S of SB	3,241	2,488	2,112	1,536	7,696	5,696	2,206	1,598
Discharge	3,707	3,504	2,852	2,656	5,712	4,768	1,093	786

Note: averages are across test duration (i.e., 0-30 min)

Table 6: Turbidity & TSS Statistics (Post-Test)								
	Avg.		Min.		Max.		Std. Dev.	
	NTU	TSS	NTU	TSS	NTU	TSS	NTU	TSS
U/S Top	922	431	700	328	1,096	536	177	86
U/S Bot.	1,389	986	961	961	2,564	2,288	617	696
D/S of SB	967	497	766	332	1,420	976	247	250
Discharge	1,149	815	710	336	1,900	1,840	416	544

Note: averages are across post-test duration (i.e., 31-120 min)

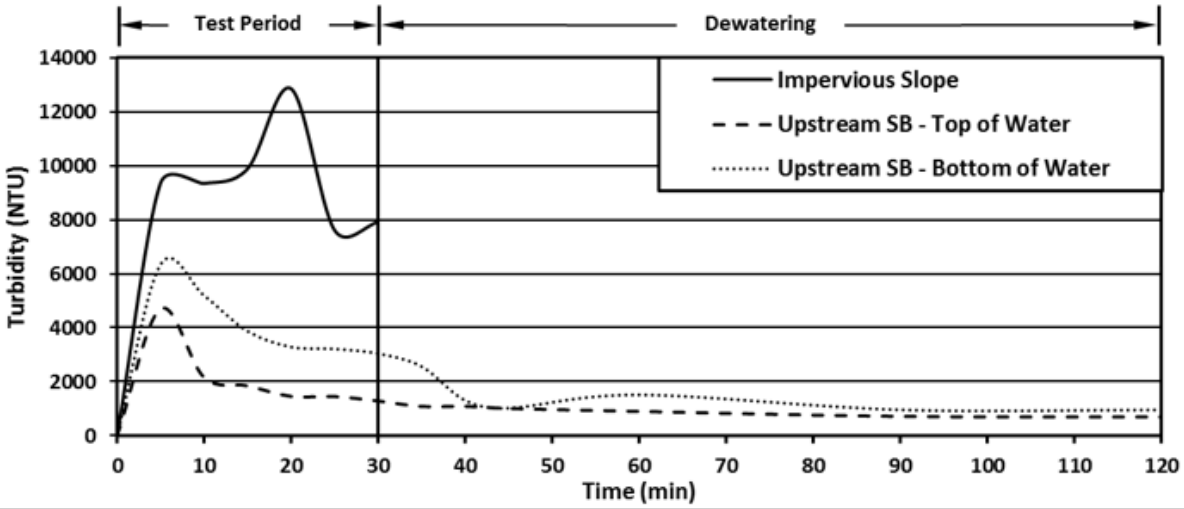

Figure 7: Turbidity Data Plot – Upstream of Sediment Barrier

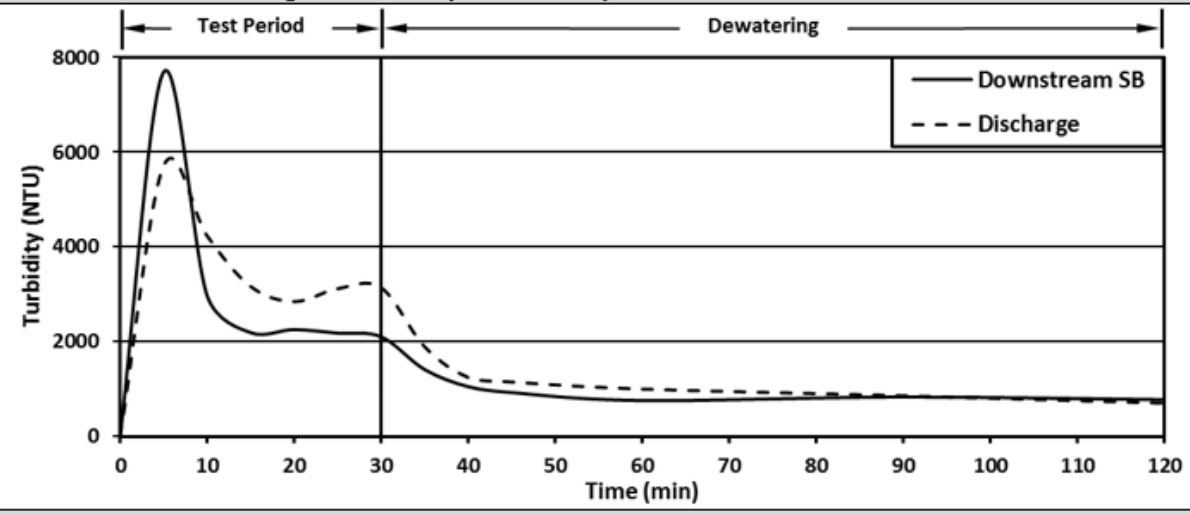

Figure 8: Turbidity Data Plot – Downstream of Sediment Barrier

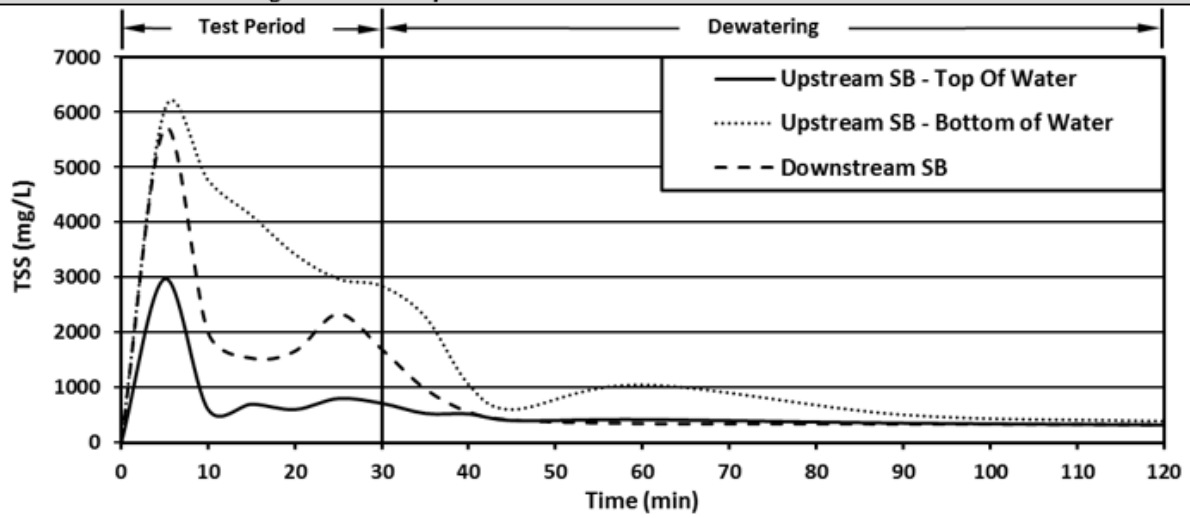

Figure 9: Total Suspended Solids Data Plot – Directly Upstream vs. Directly Downstream of Sediment Barrier

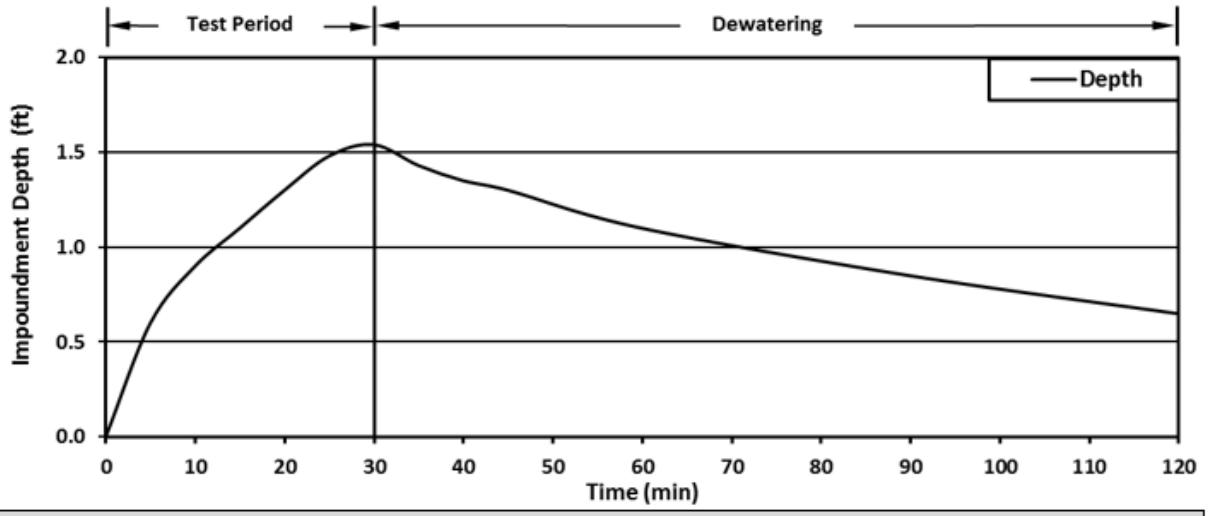

Figure 10: Sediment Barrier Impoundment Depth

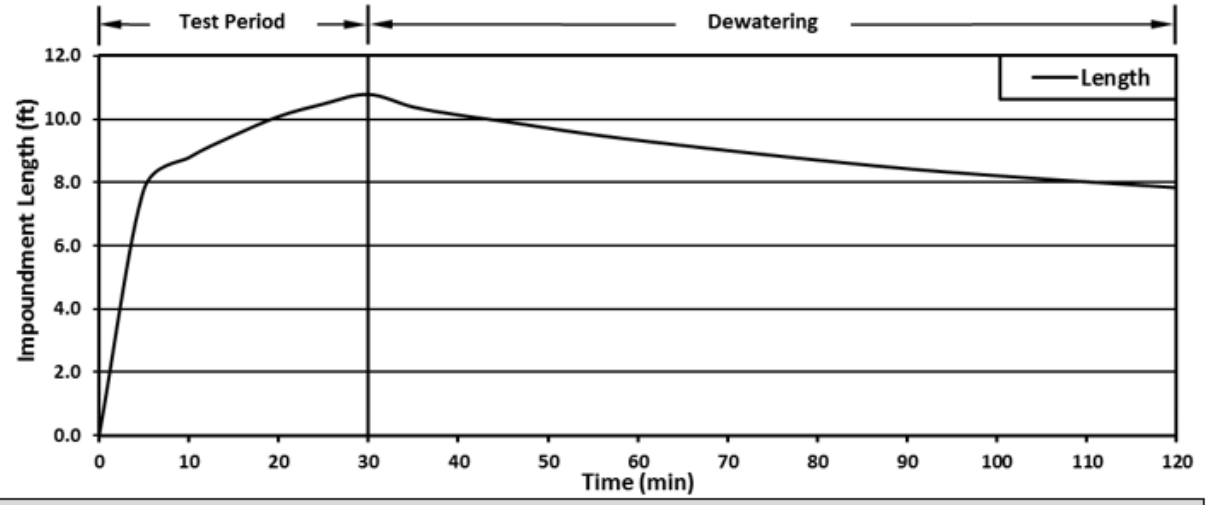

Figure 11: Sediment Barrier Impoundment Length

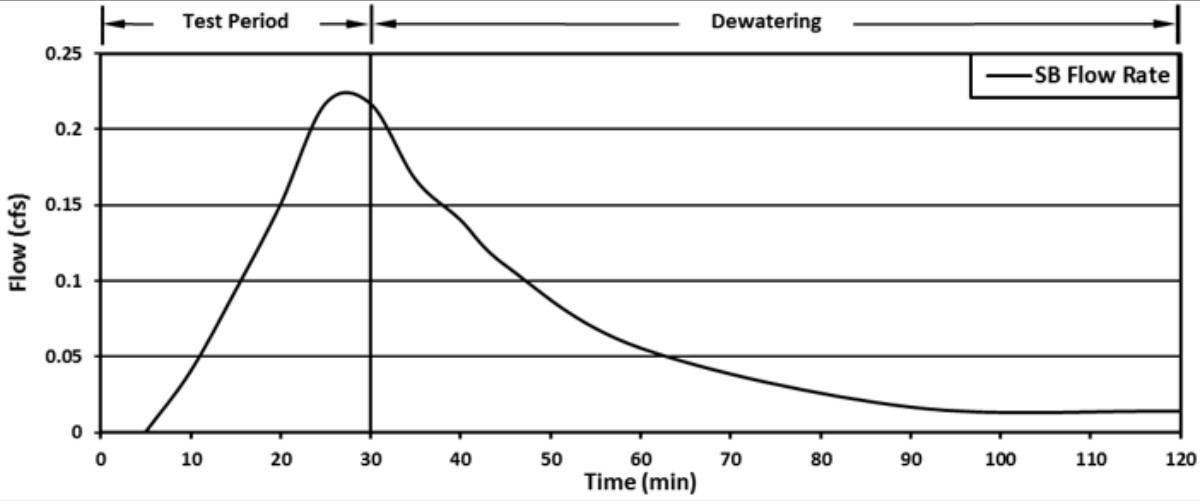

Figure 12: Flow Rate Through Sediment Barrier

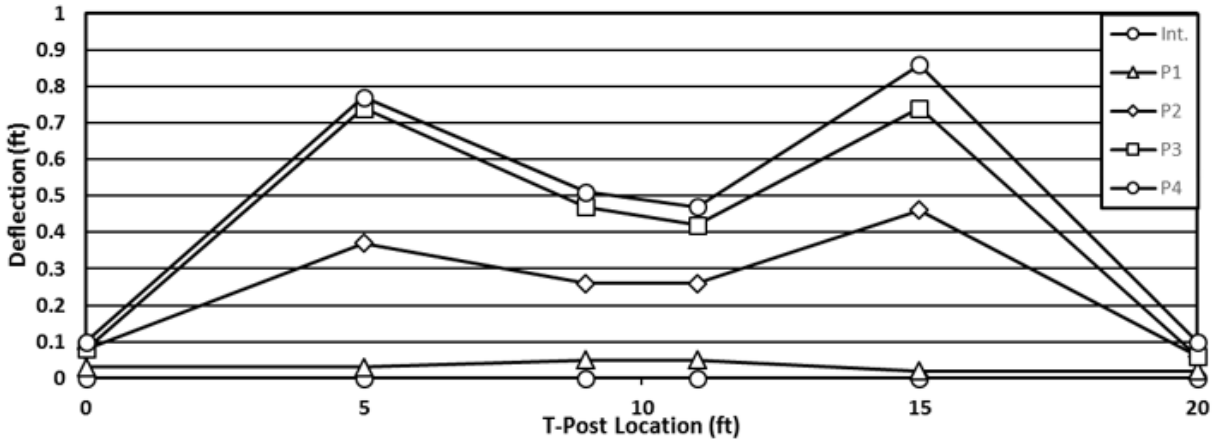

Figure 13: T-Post Deflection

APPENDIX C

MANUFACTURER'S INSTALLATION DETAILS

SILT - SAVER

EROSION AND SEDIMENT CONTROL PRODUCTS

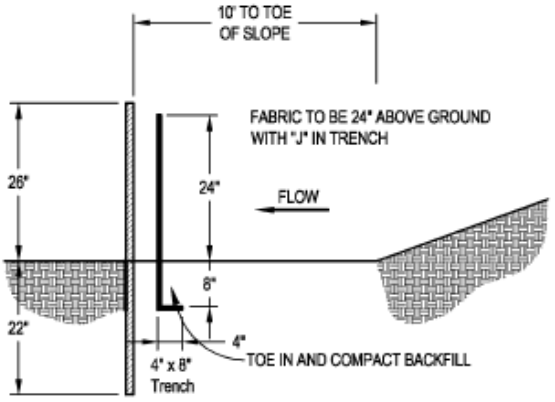

SIDE VIEW

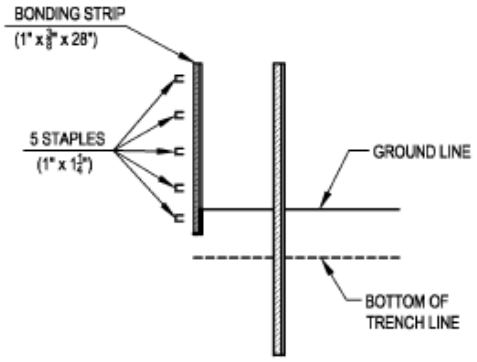

POST (OAK)

(1 3/4" x 1 1/4" x 48")

(OR EQUAL DENSITY)

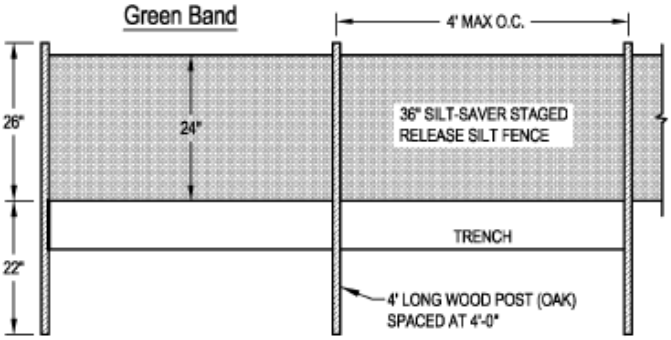

FRONT ELEVATION

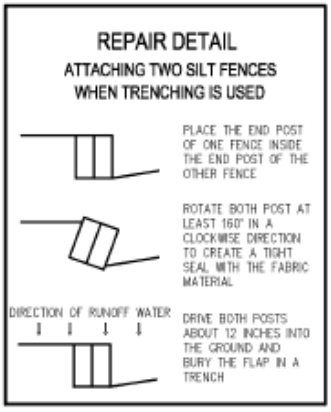

PLAN VIEW

STAGED RELEASE SILT FENCE

FRAME MATERIAL: OAK OR SIMILAR
FILTER FABRIC MATERIAL: REFER TO SPEC
SCALE: NOT TO SCALE
LAST UPDATED: FEBRUARY 2015

SILT-SAVER, INC. 1094 CULPEPPER DRIVE, CONYERS, GA 30094 PHONE: (770) 388-7818 FAX: (770) 388-7640 TOLL FREE: 1-888-382-SILT (7458) www.siltsaver.com

Installation Instructions
Logs and Wattles

Step 1 - Site Preparation

Prepare site to design profile and grade. Remove debris, rocks, clods, etc.. Ground surface should be smooth prior to installation to ensure log remains in contact with slope.

Step 2 - Staple Selection

At a minimum, 1 in. by 1 in. by 24 in., stakes are to be used to secure the log to the ground surface. Installation in rocky, sandy or other loose soil may require longer stakes.

Slope Installation

Place RECP along slope to provide upstream apron for log. Secure RECP according to standard slope installation instructions including upstream anchor trench. Secure log to blanket, ensuring log remains in intimate contact with the RECP over the length of the installation. A minimum of one foot upstream apron and two foot downstream apron are required for installation. Subsequent, downslope rows of logs should be spaced appropriately for site conditions to minimize acceleration of flow. Further, log seams are to be offset to ensure continuous filtration. Figure A presents a schematic of a slope installation in profile view.

Channel Installation

Place RECP along channel to provide upstream and downstream apron for log identically to slope installation. Secure log to blanket, ensuring log remains in intimate contact with the RECP over the length of the installation. A minimum of one foot upstream apron and two foot downstream apron are required for installation. Subsequent, downslope rows of logs should be spaced appropriately for site conditions to minimize acceleration of flow. Further, log seams are to be offset to ensure continuous filtration. Figure A / Figure C presents a schematic of a channel installation.

Drain Filter Installation

Surround drain inlet to be protected with log, ensuring seams are overlapping to minimize flow circumventing log. Secure logs to ground surface ensuring the log remains in intimate contact with the ground surface over the entire installation. Provide RECP apron secured to the ground surface between drain and log.

Please contact Western Excelsior Technical Support Division at 800-967-4009 with specific questions or for further information.

Slope/Channel Installation

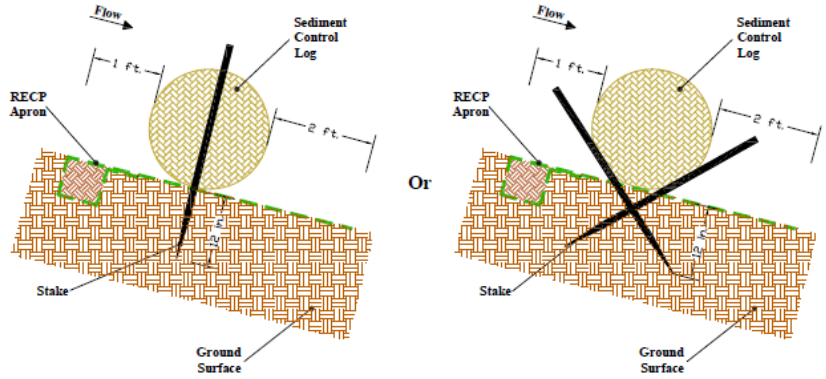

Figure A - Profile View

Flat Ground (Perimeter Guard) Installation

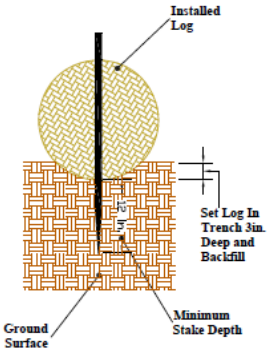

Figure B - Profile View

Channel Installation

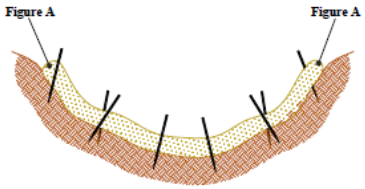

Minimum stake in ground, 12 in.

Do not allow flow to overtop installation.

Figure C - Cross-Section View

Drain Filter

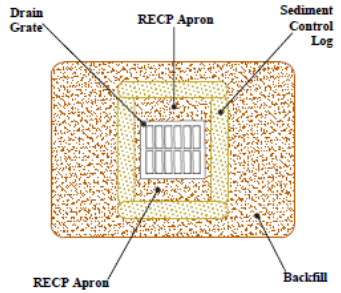

Figure D - Cross-Section View

Curbside Installation

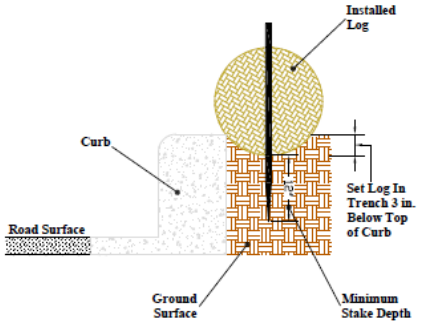

Figure E - Cross-Section View

Document # WE_EXCEL_LOG_II

Figure 1.1. Engineering Design Drawing for Perimeter Control

FILTREXX® SILT SOXX™

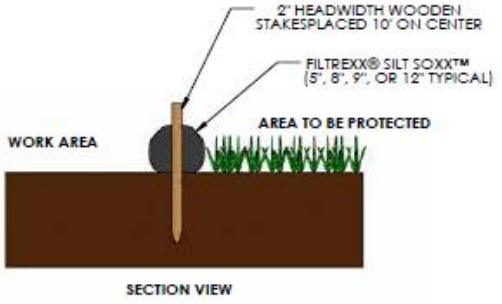

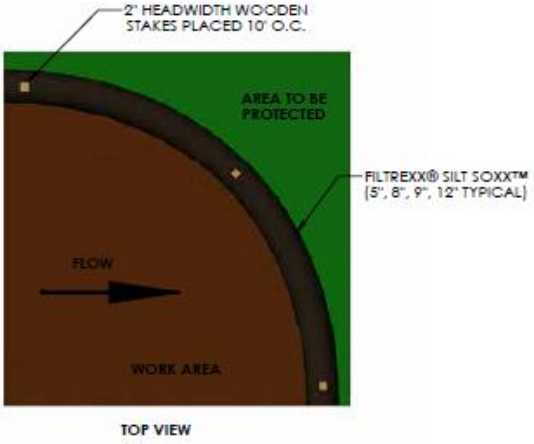

COMPOST SOCK CONNECTION/ATTACHMENT DETAIL

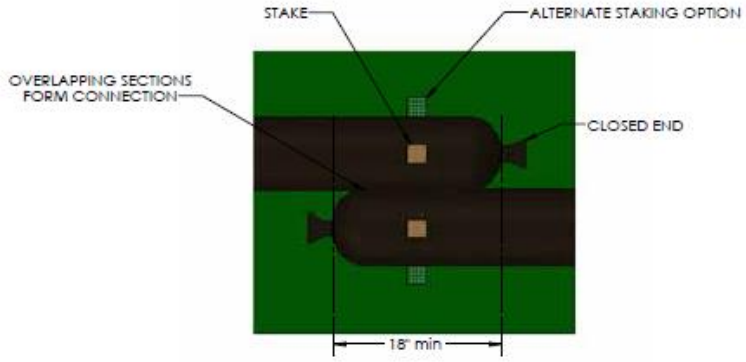

FILTREXX® PYRAMID STAKING DETAIL

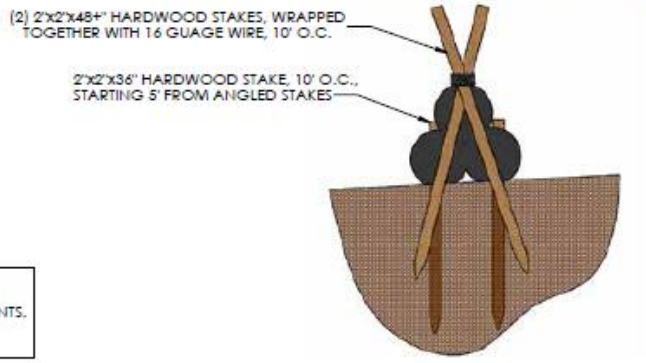

NOTES:
1. ALL MATERIAL TO MEET FILTREXX® SPECIFICATIONS.
2. SILT SOXX™ FILL TO MEET APPLICATION REQUIREMENTS.
3. COMPOST MATERIAL TO BE DISPERSED ON SITE, AS DETERMINED BY ENGINEER.

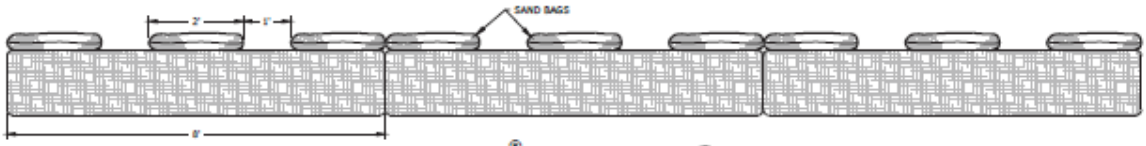

CURLEX® BLOC SAND BAG DETAIL 1/31
NO SCALE

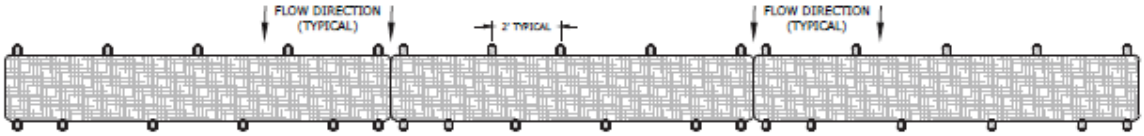

CURLEX® BLOC STAKING DETAIL 2/31
NO SCALE

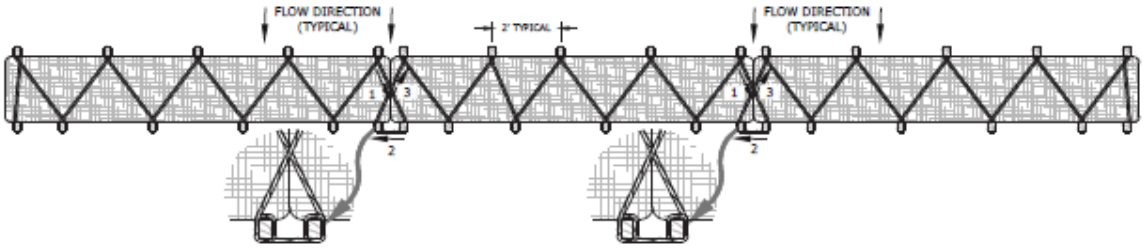

CURLEX® BLOC STAKING AND ROPING DETAIL 3/31
NO SCALE

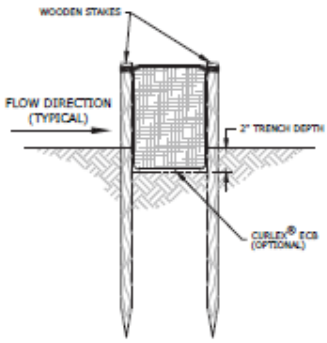

CURLEX® BLOC TRENCH OPTION (FLAT GROUND) 4/31
NO SCALE

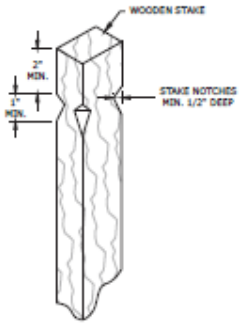

STAKE NOTCHING DETAIL 5/31
NO SCALE

INSTALLATION NOTES:
1) NON-STRETCHING ROPE WHEN WET.
2) 1½" x 1½" x 48" WOODEN STAKES ARE RECOMMENDED.
3) POUND STAKES TIGHTLY NEXT TO CURLEX® BLOC LEAVING APPROXIMATELY 4" OF STAKE ABOVE SURFACE OF CURLEX® BLOC.
4) INSTALL ROPE ACCORDING TO DRAWING (ENSURE ROPE IS WRAPPED TIGHTLY IN STAKE NOTCHES).
5) KNOT OFF ROPE TO STAKE AT LEAST EVERY 25 FEET OF ROPE.
6) POUND DOWN STAKES FLUSH WITH SURFACE OF CURLEX® BLOC AFTER ALL IS INSTALLED TO TIGHTEN ROPES.
7) ABUT ADJOINING CURLEX® BLOCS TIGHTLY AND SECURE WITH STAKES AND ROPE ACCORDING TO DRAWING.
8) 8' LONG CURLEX® BLOC SHOWN. ADJUST STAKING AND ROPING PATTERN ACCORDINGLY IF USING 4' LONG CURLEX® BLOCS.

NOTE:
1) TRENCHING OF CURLEX® BLOC IS OPTIONAL FOR INLET OR OUTLET PROTECTION, PERIMETER CONTROL, RUNOFF DIVERSION AND FILTERING APPLICATIONS.
2) INSTALL ON BARE SOIL & ECB
3) USE ON HARD SURFACE (CONCRETE, FROZEN GROUND, ETC.)
4) SAND BAG SIZE 14" x 24", 60lb. MIN.

American Excelsior Company®
Earth Science Division

AMERICAN EXCELSIOR COMPANY ARLINGTON, TEXAS	SHEET DESCRIPTION: CURLEX® BLOC ANCHORING TECHNIQUES DETAIL	DATE 3/27/17	DRAWN BY	
		SCALE: NONE	PROJECT NO.	SHEET NO. 31

APPENDIX D

WATER QUALITY ANALYSIS GRAPHS

WATER SAMPLE LOCATIONS

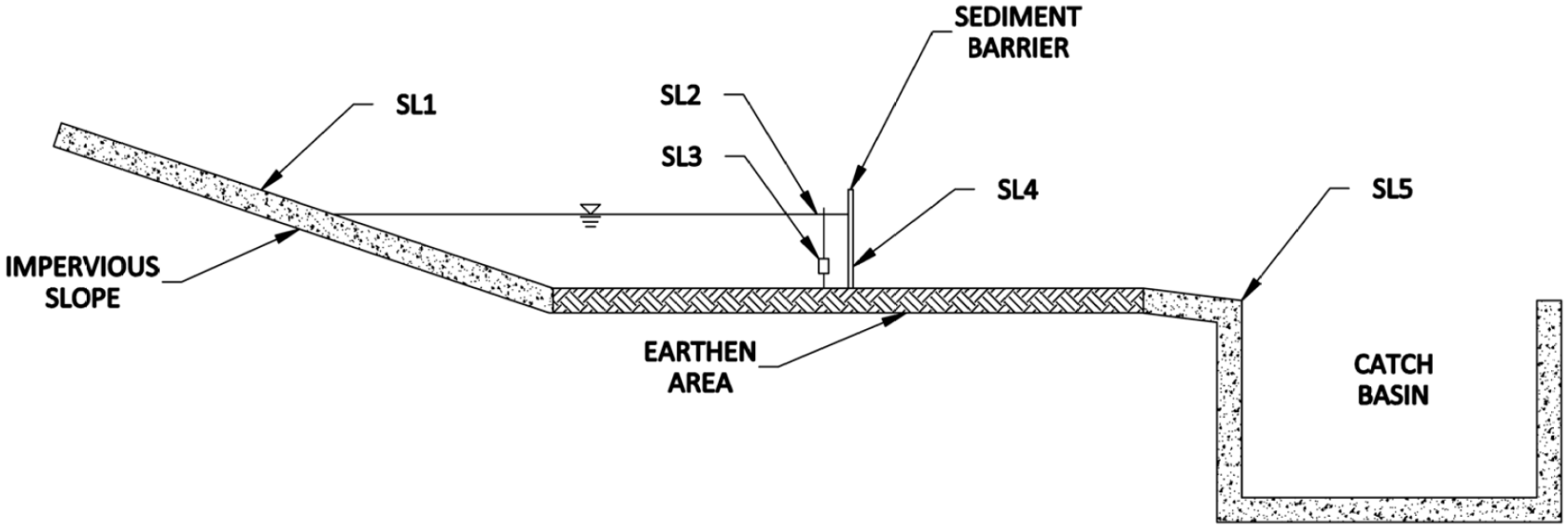

M8

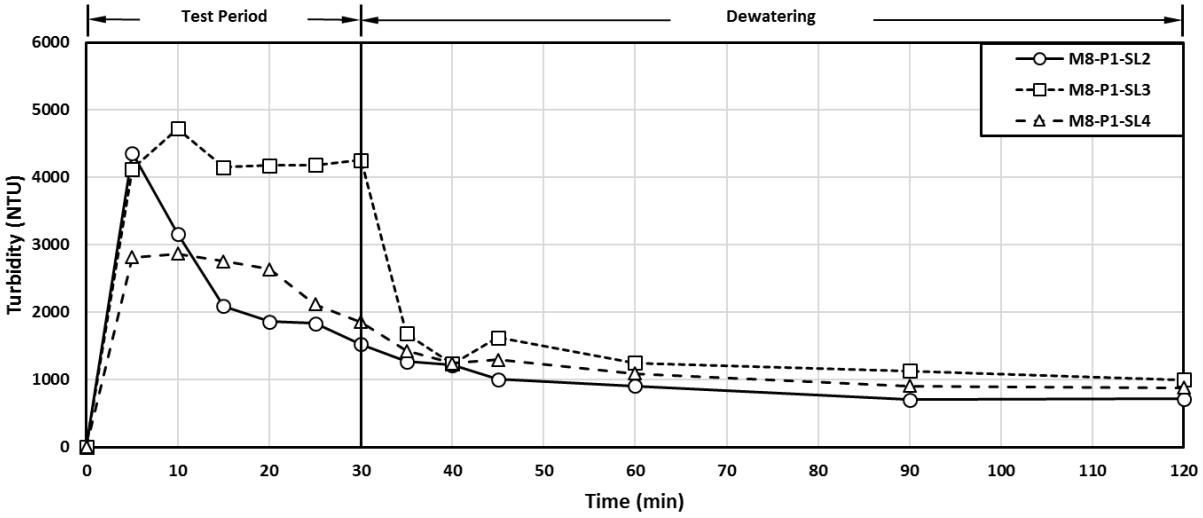
Test Period
Dewatering
M8-P1-SL2
M8-P1-SL3
M8-P1-SL4
Turbidity (NTU)
Time (min)

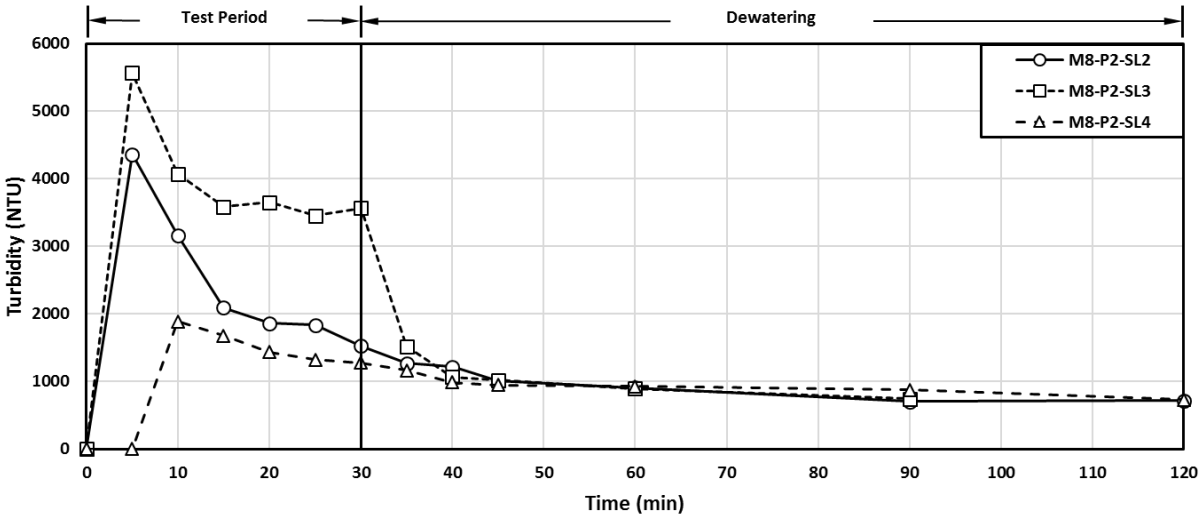
Test Period
Dewatering
M8-P2-SL2
M8-P2-SL3
M8-P2-SL4
Turbidity (NTU)
Time (min)

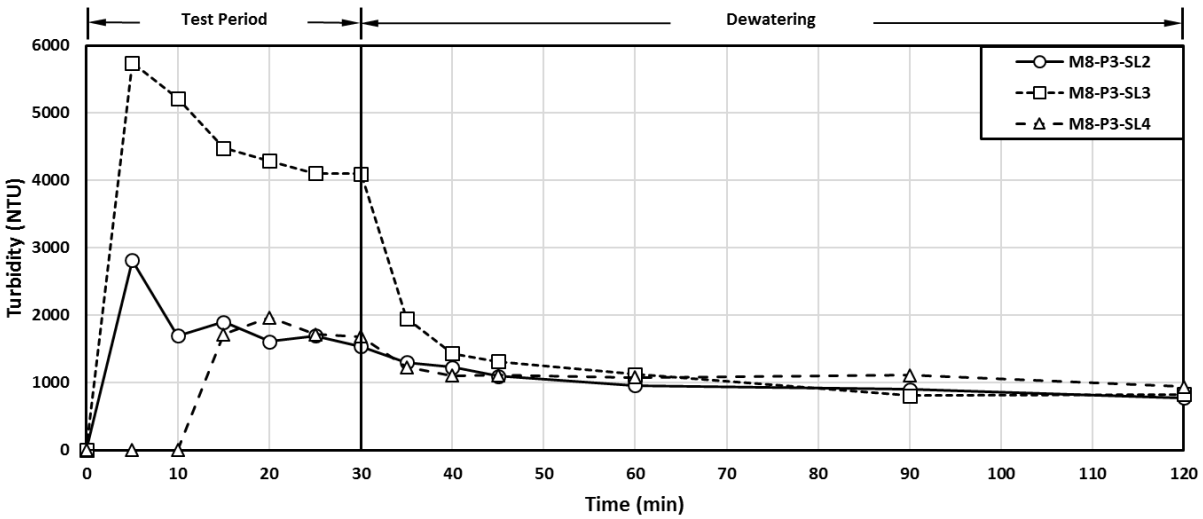
Test Period
Dewatering
M8-P3-SL2
M8-P3-SL3
M8-P3-SL4
Turbidity (NTU)
Time (min)

C-POP

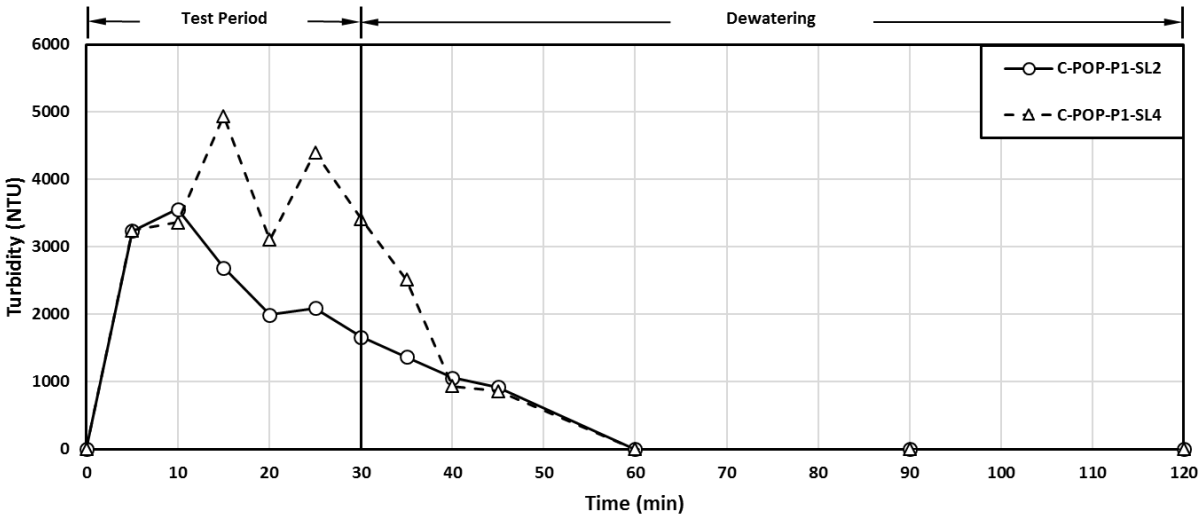
Test Period
Dewatering
C-POP-P1-SL2
C-POP-P1-SL4
Turbidity (NTU)
Time (min)

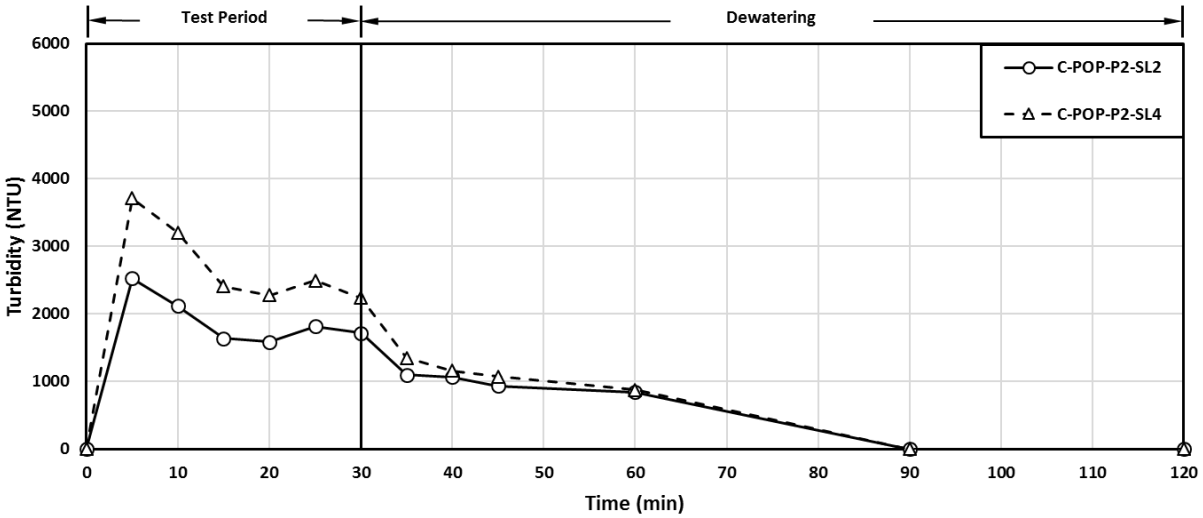
Test Period
Dewatering
C-POP-P2-SL2
C-POP-P2-SL4
Turbidity (NTU)
Time (min)

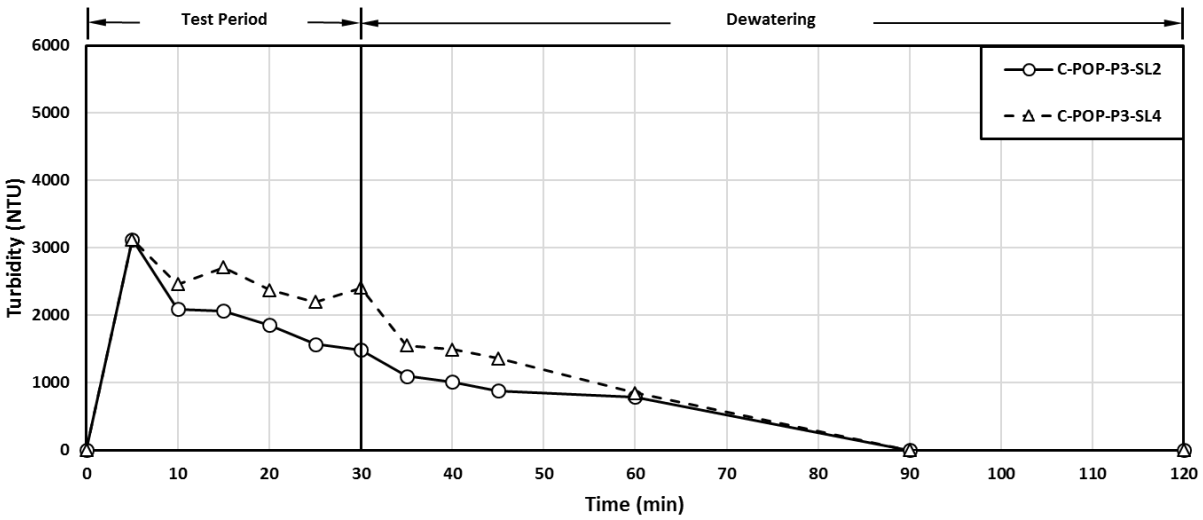
Test Period
Dewatering
C-POP-P3-SL2
C-POP-P3-SL4
Turbidity (NTU)
Time (min)

SRSF

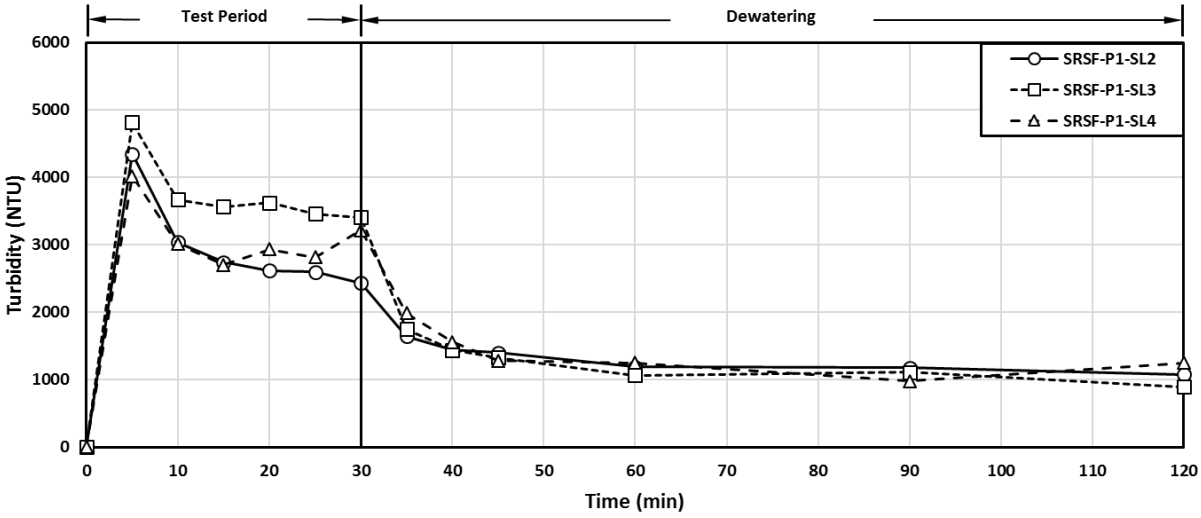
Test Period
Dewatering
SRSF-P1-SL2
SRSF-P1-SL3
SRSF-P1-SL4
Turbidity (NTU)
Time (min)

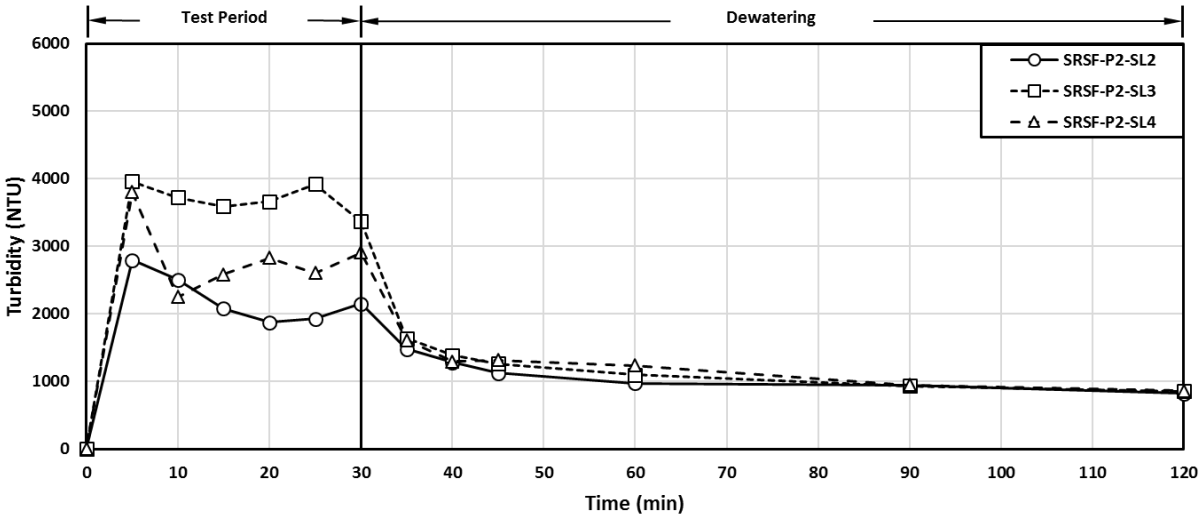
Test Period
Dewatering
SRSF-P2-SL2
SRSF-P2-SL3
SRSF-P2-SL4
Turbidity (NTU)
Time (min)

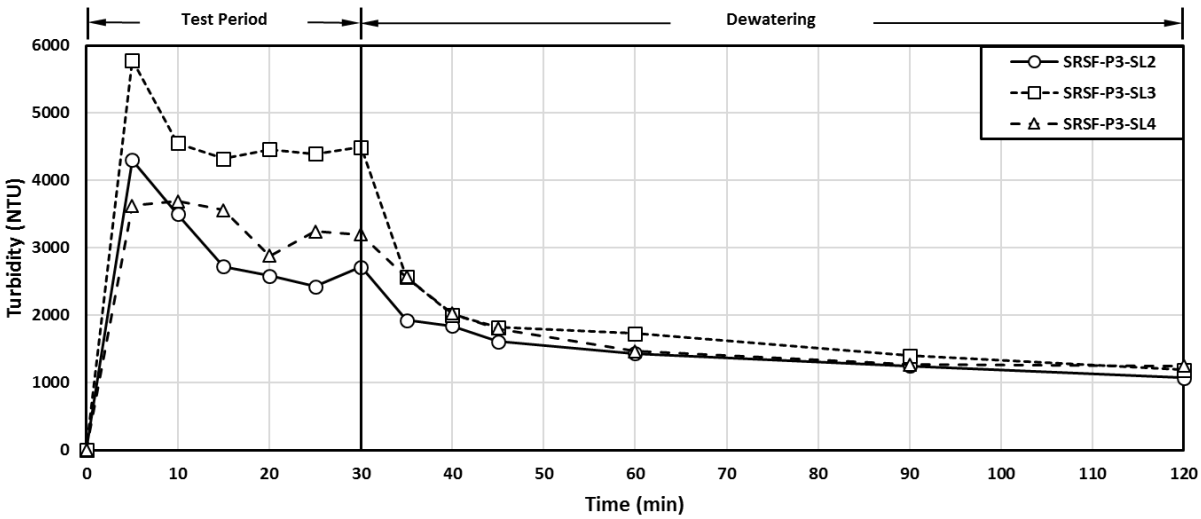
Test Period
Dewatering
SRSF-P3-SL2
SRSF-P3-SL3
SRSF-P3-SL4
Turbidity (NTU)
Time (min)

ALDOT SRB

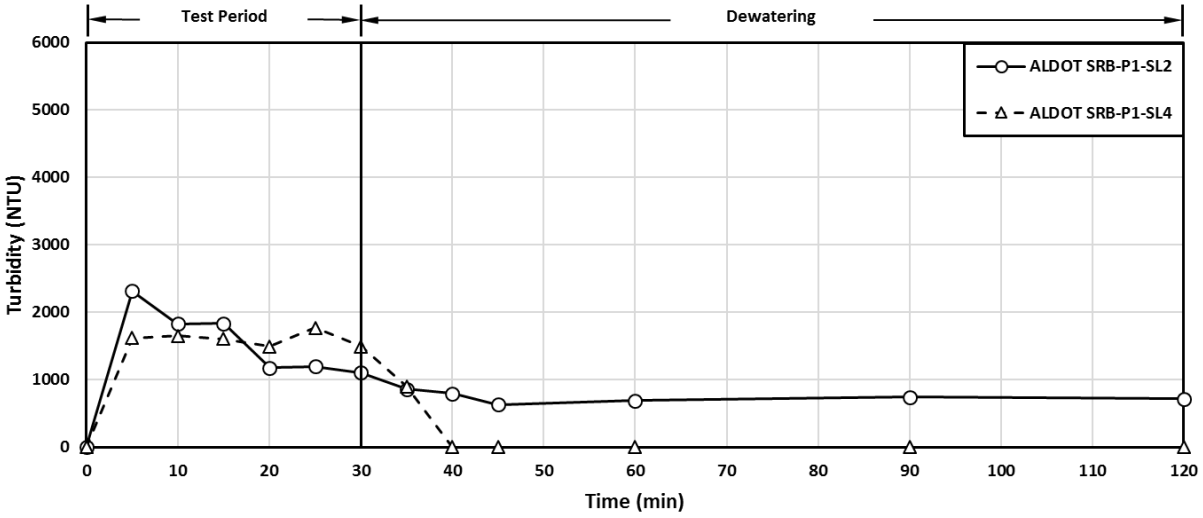
Test Period
Dewatering
ALDOT SRB-P1-SL2
ALDOT SRB-P1-SL4
Turbidity (NTU)
Time (min)

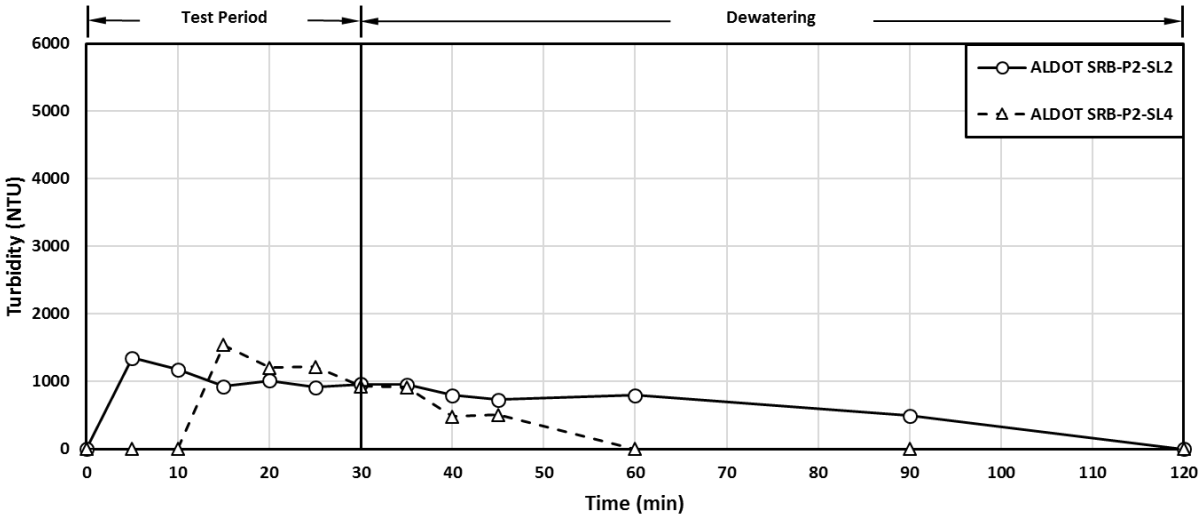
Test Period
Dewatering
ALDOT SRB-P2-SL2
ALDOT SRB-P2-SL4
Turbidity (NTU)
Time (min)

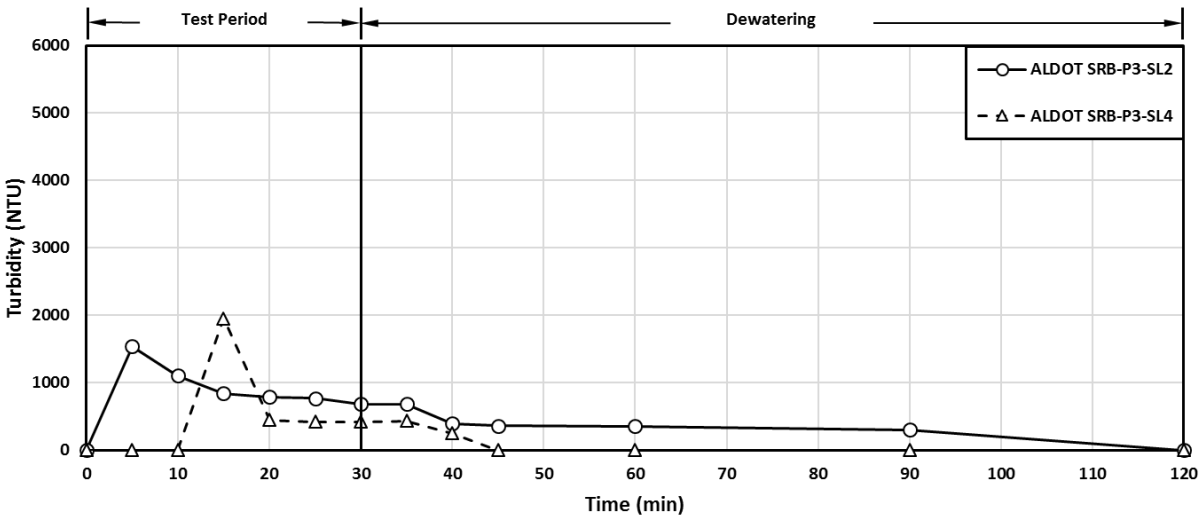
Test Period
Dewatering
ALDOT SRB-P3-SL2
ALDOT SRB-P3-SL4
Turbidity (NTU)
Time (min)

AL HB SRB w/o Flocculant

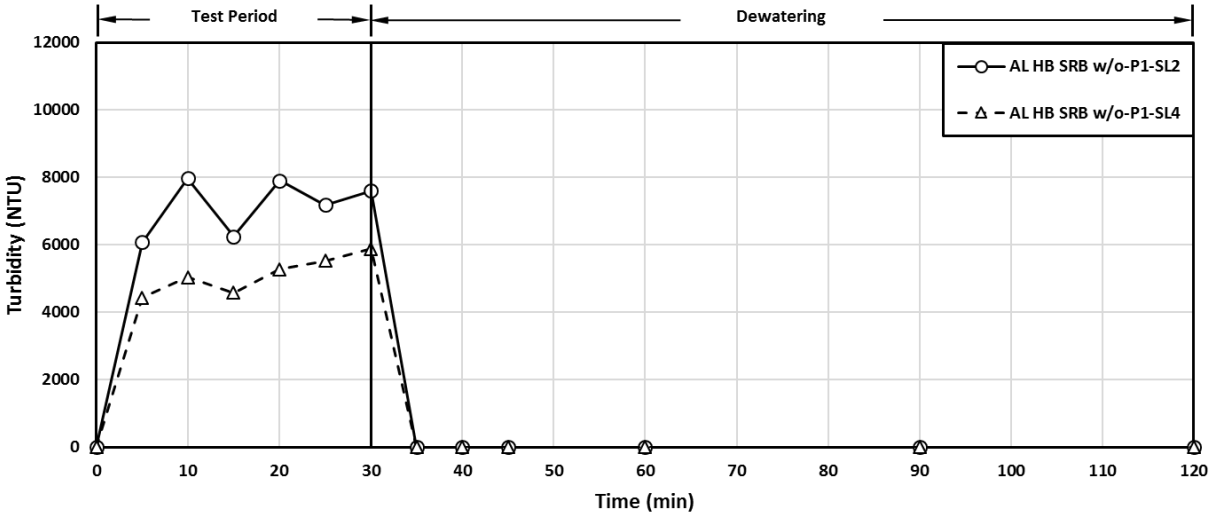

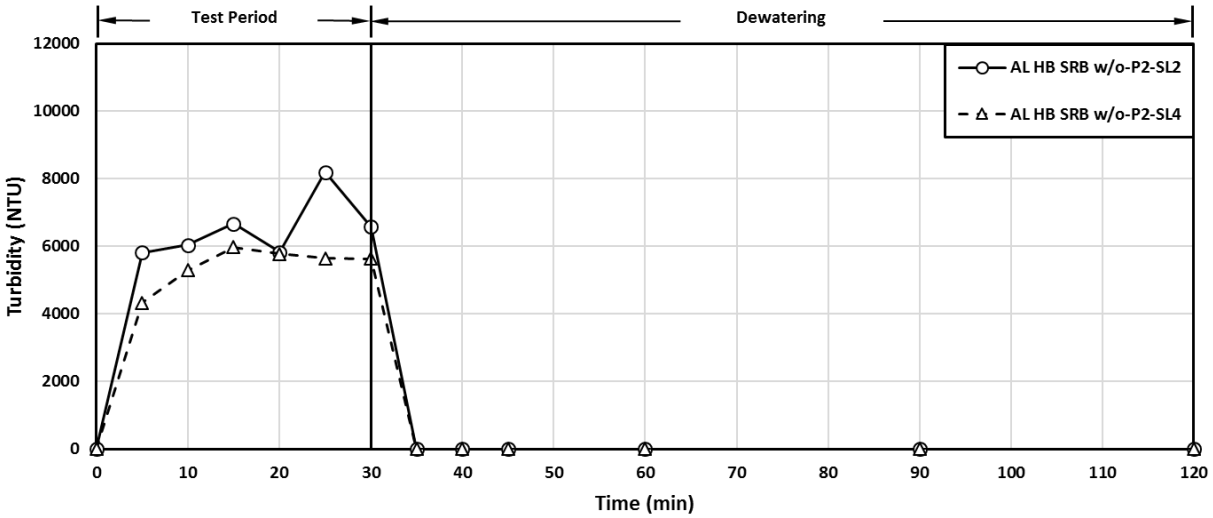

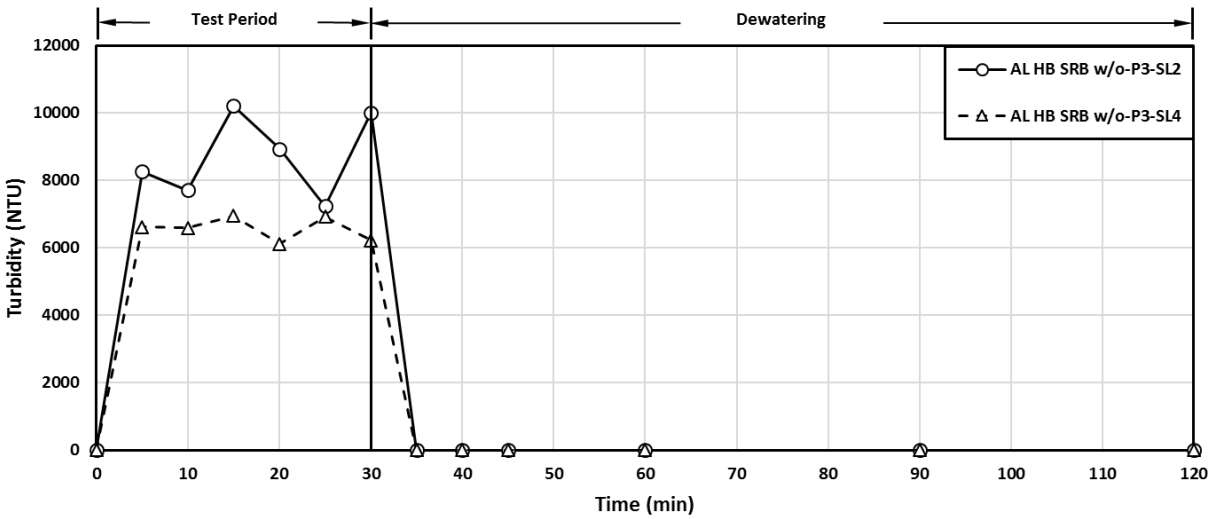

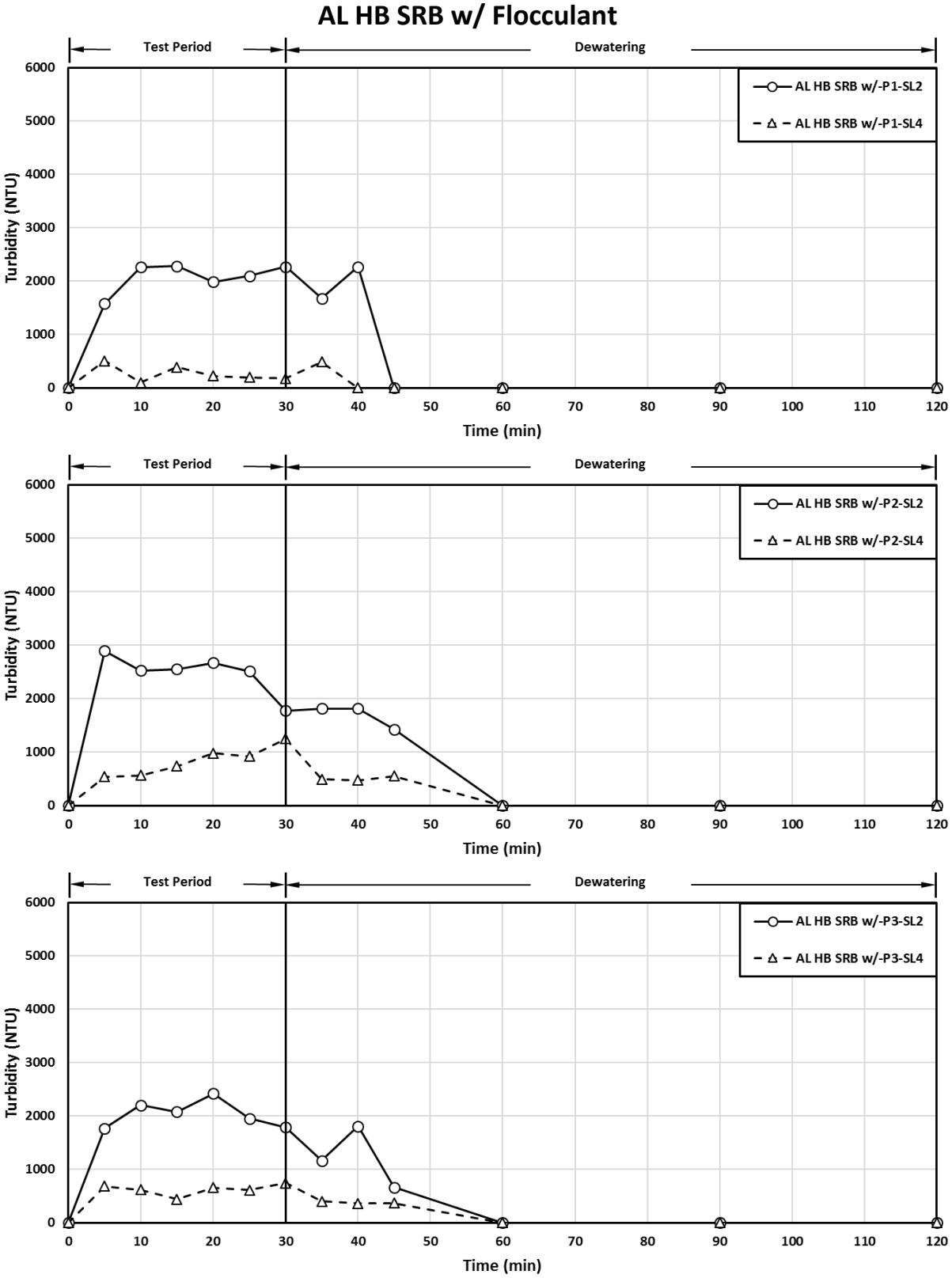
AL HB SRB w/ Flocculant
Test Period
Dewatering
AL HB SRB w/-P1-SL2
AL HB SRB w/-P1-SL4
Turbidity (NTU)
Time (min)
Test Period
Dewatering
AL HB SRB w/-P2-SL2
AL HB SRB w/-P2-SL4
Turbidity (NTU)
Time (min)
Test Period
Dewatering
AL HB SRB w/-P3-SL2
AL HB SRB w/-P3-SL4
Turbidity (NTU)
Time (min)

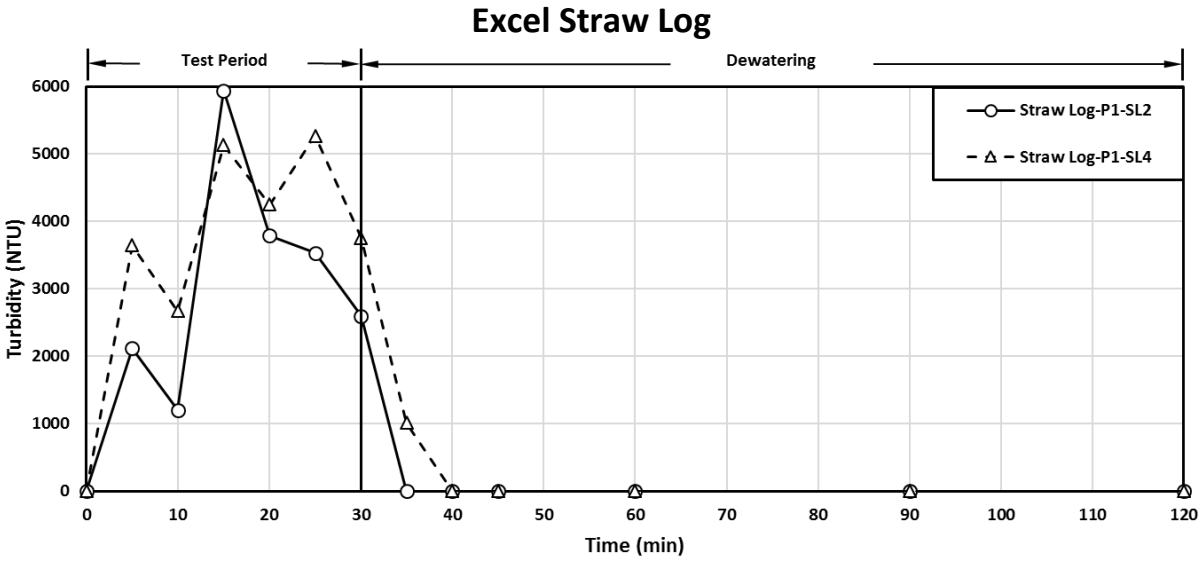
Excel Straw Log
Test Period
Dewatering
Straw Log-P1-SL2
Straw Log-P1-SL4
Turbidity (NTU)
Time (min)
0
1000
2000
3000
4000
5000
6000
0
10
20
30
40
50
60
70
80
90
100
110
120

SiltSoxx

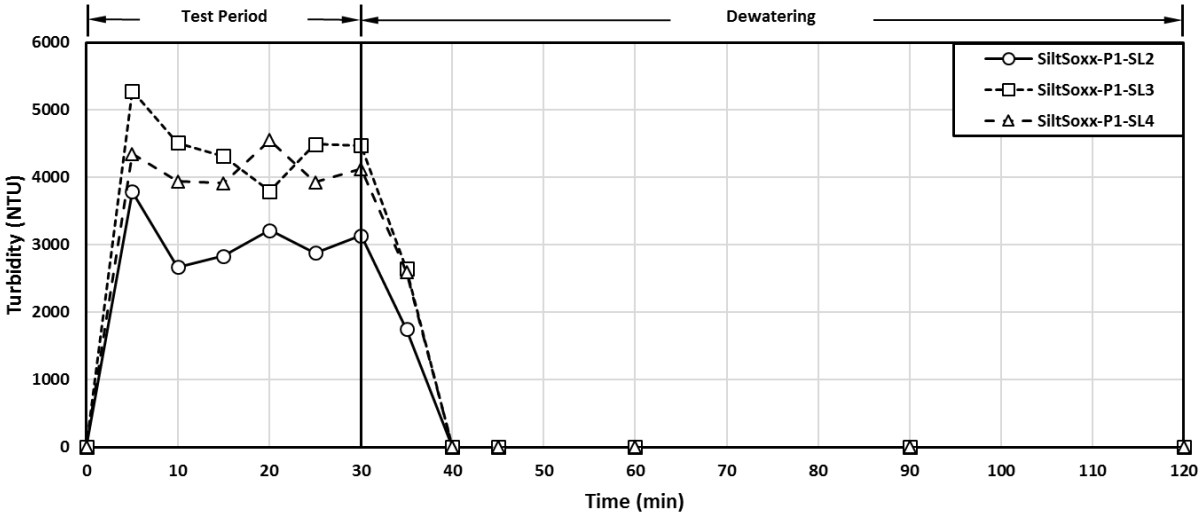
Test Period
Dewatering
SiltSoxx-P1-SL2
SiltSoxx-P1-SL3
SiltSoxx-P1-SL4
Turbidity (NTU)
Time (min)

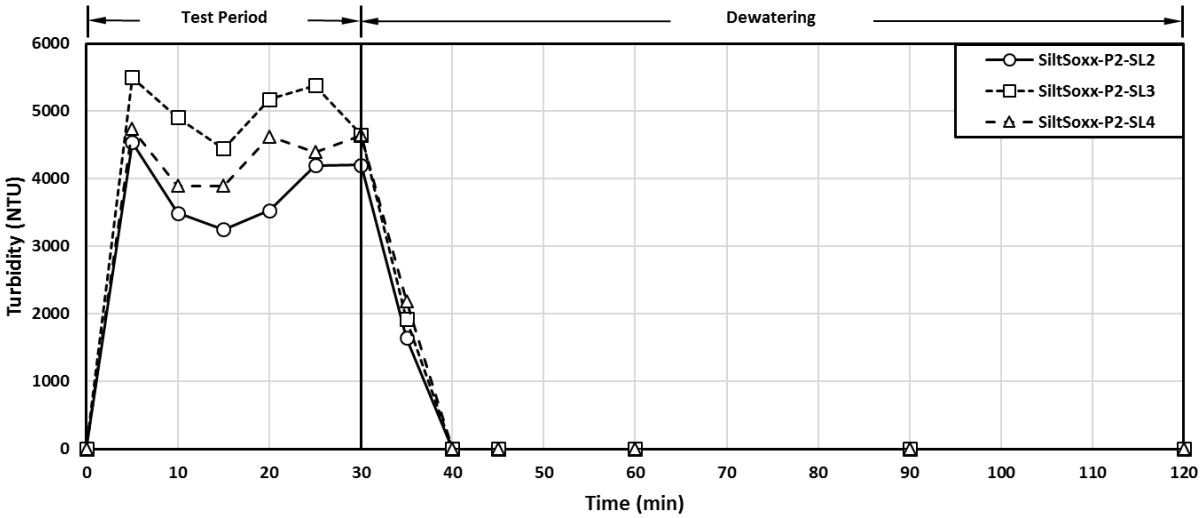
Test Period
Dewatering
SiltSoxx-P2-SL2
SiltSoxx-P2-SL3
SiltSoxx-P2-SL4
Turbidity (NTU)
Time (min)

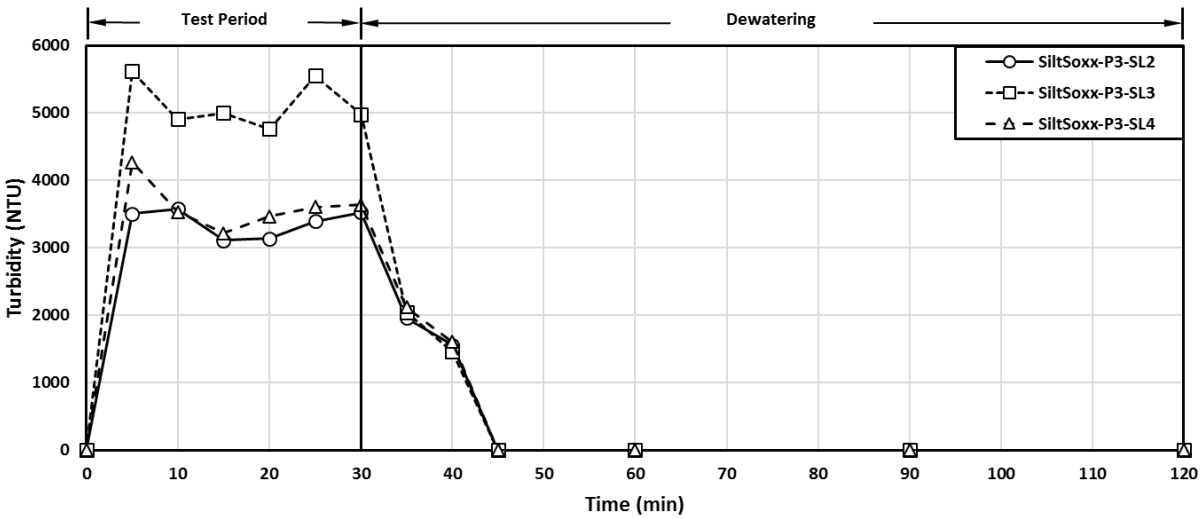
Test Period
Dewatering
SiltSoxx-P3-SL2
SiltSoxx-P3-SL3
SiltSoxx-P3-SL4
Turbidity (NTU)
Time (min)

Curlex Bloc

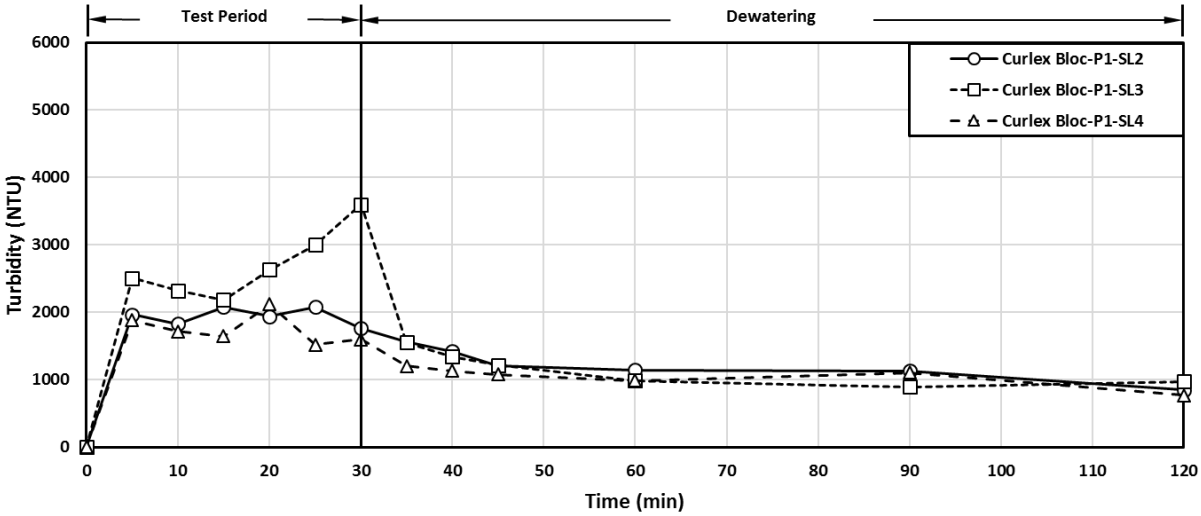
Test Period
Dewatering
Curlex Bloc-P1-SL2
Curlex Bloc-P1-SL3
Curlex Bloc-P1-SL4
Turbidity (NTU)
Time (min)

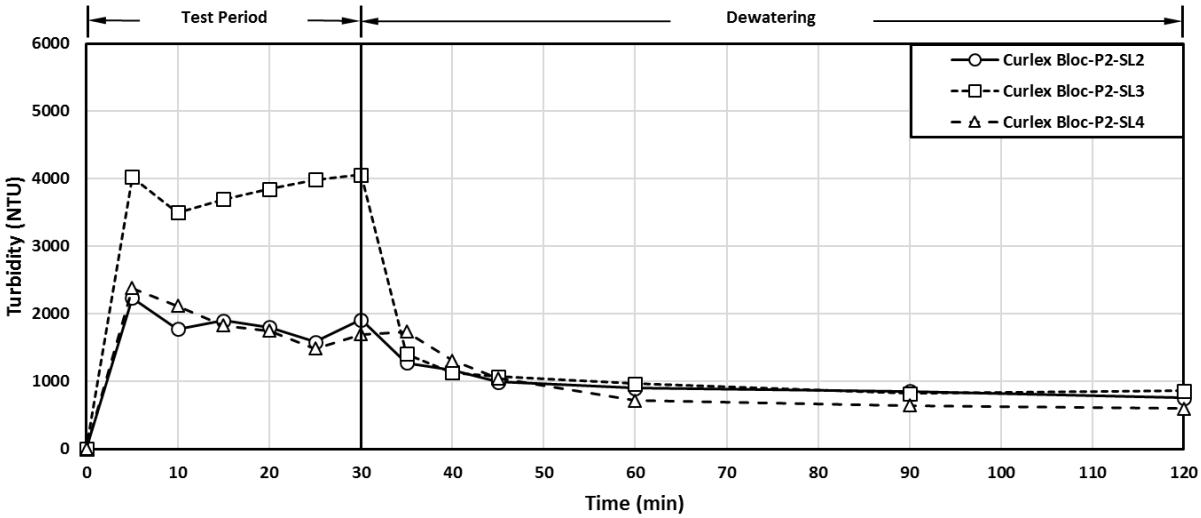
Test Period
Dewatering
Curlex Bloc-P2-SL2
Curlex Bloc-P2-SL3
Curlex Bloc-P2-SL4
Turbidity (NTU)
Time (min)

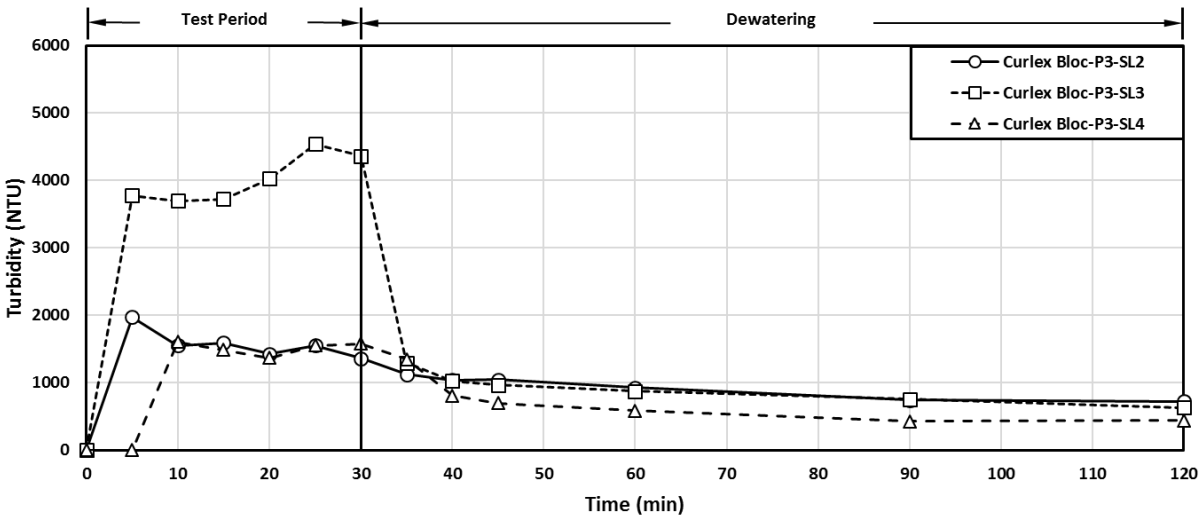
Test Period
Dewatering
Curlex Bloc-P3-SL2
Curlex Bloc-P3-SL3
Curlex Bloc-P3-SL4
Turbidity (NTU)
Time (min)

APPENDIX E

Sediment Barrier Practice Treatment Efficiency

M8

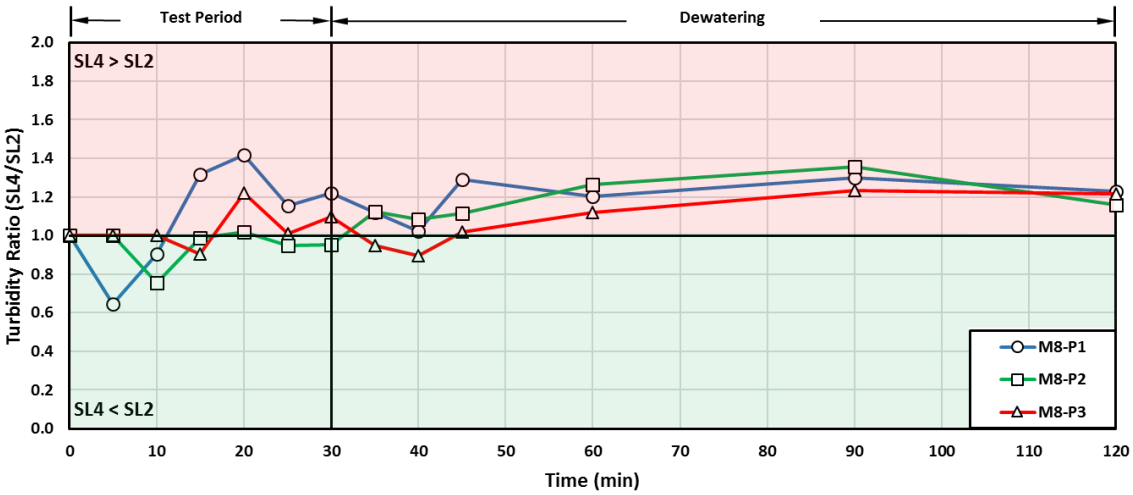
Test Period
Dewatering
SL4 > SL2
SL4 < SL2
Turbidity Ratio (SL4/SL2)
Time (min)
M8-P1
M8-P2
M8-P3

C-POP

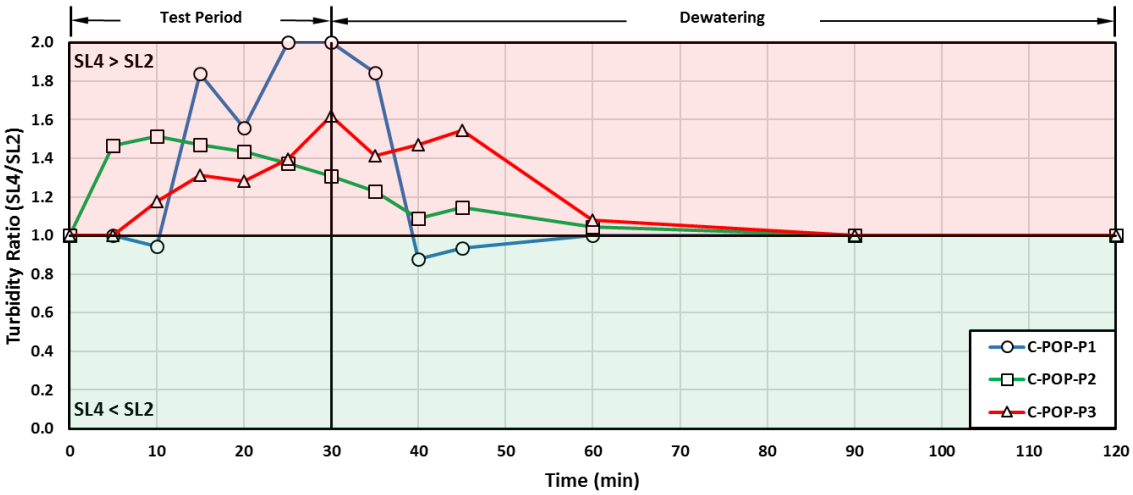
Test Period
Dewatering
SL4 > SL2
SL4 < SL2
Turbidity Ratio (SL4/SL2)
Time (min)
C-POP-P1
C-POP-P2
C-POP-P3

SRSF

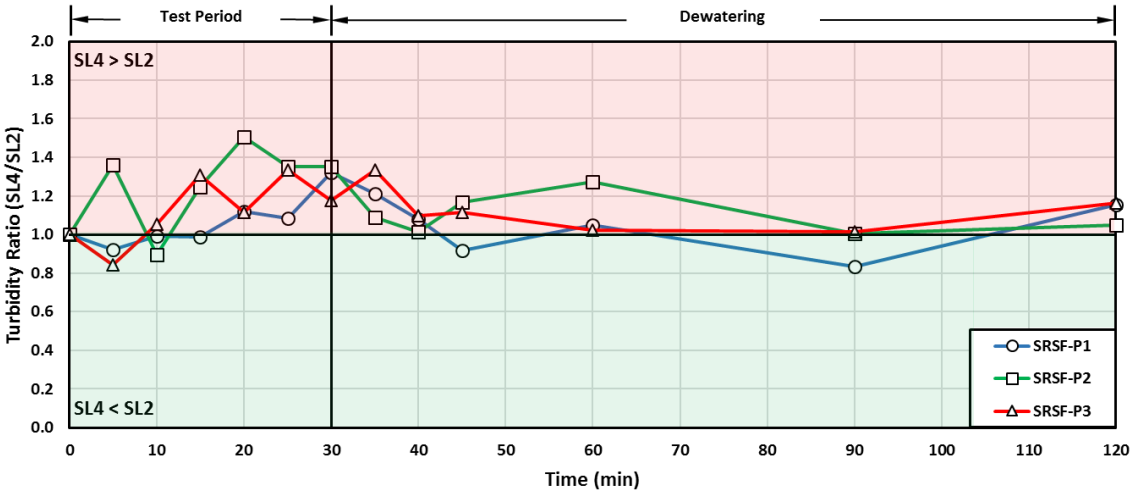
Test Period
Dewatering
SL4 > SL2
SL4 < SL2
Turbidity Ratio (SL4/SL2)
Time (min)
SRSF-P1
SRSF-P2
SRSF-P3

ALDOT SRB

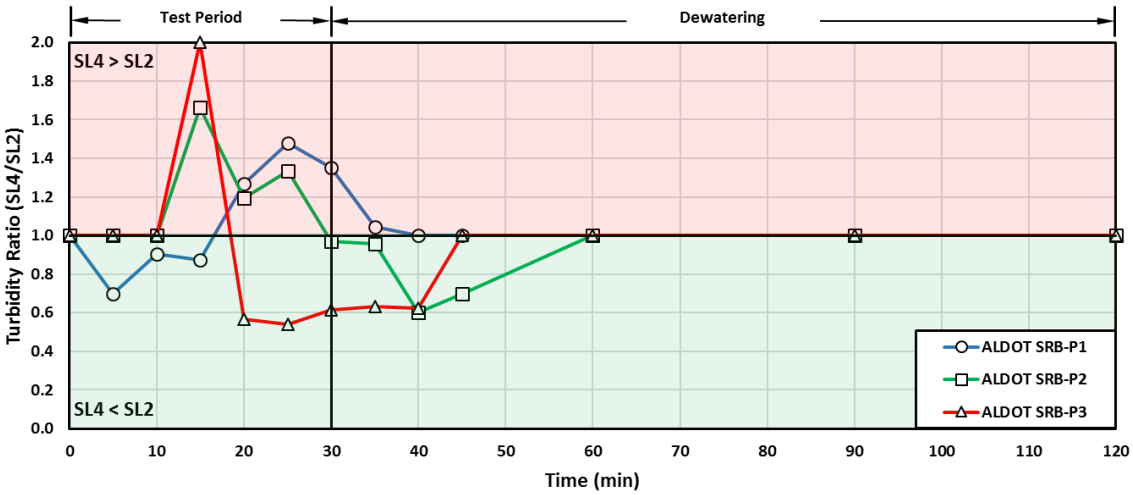

AL HB SRB w/o FLOCCULANT

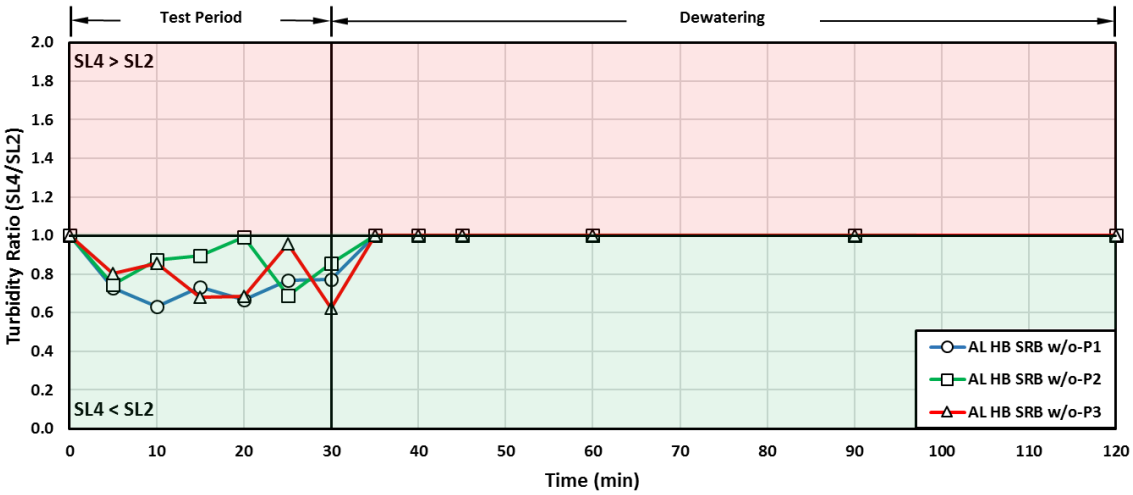

AL HB SRB w/ FLOCCULANT

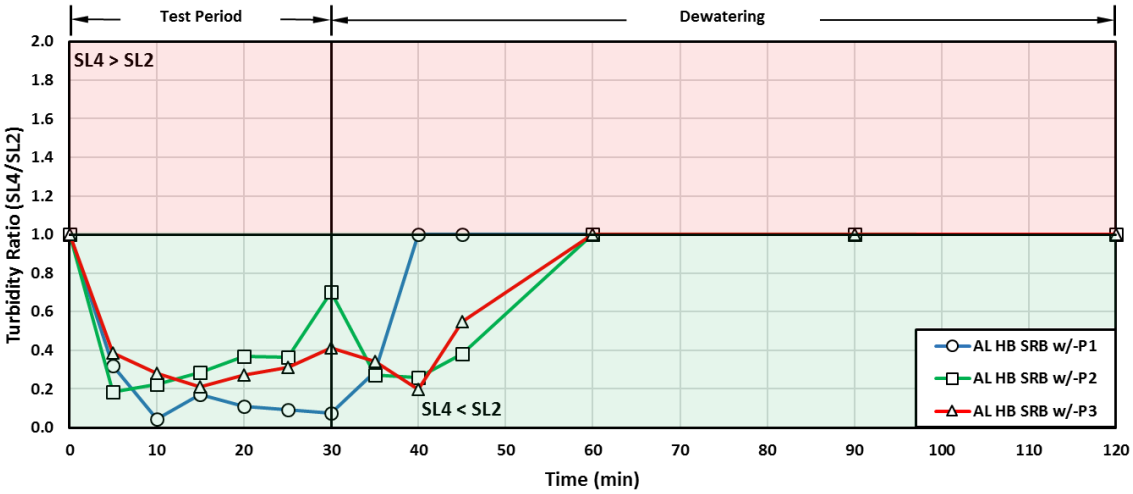

EXCEL STRAW LOG

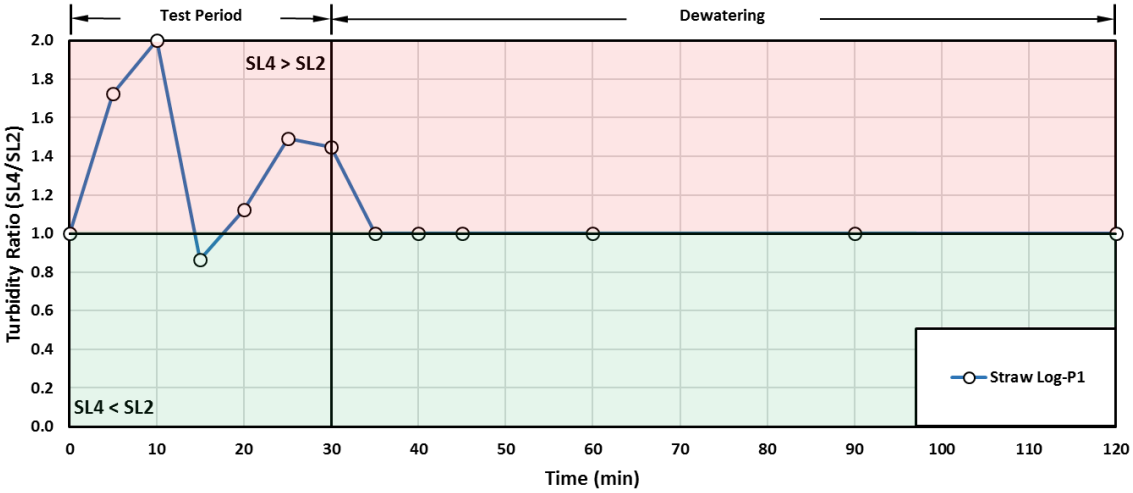

SILTSOXX

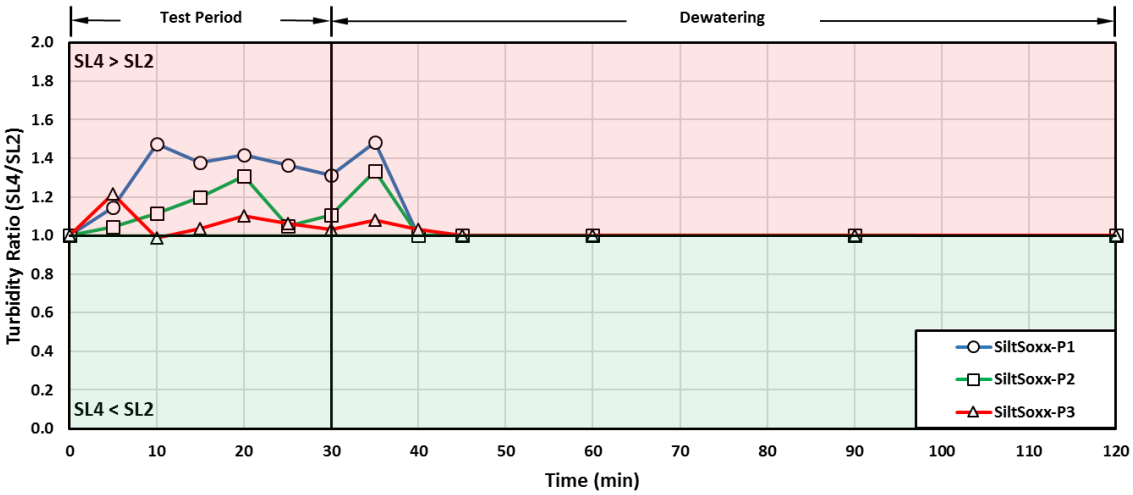

CURLEX BLOC

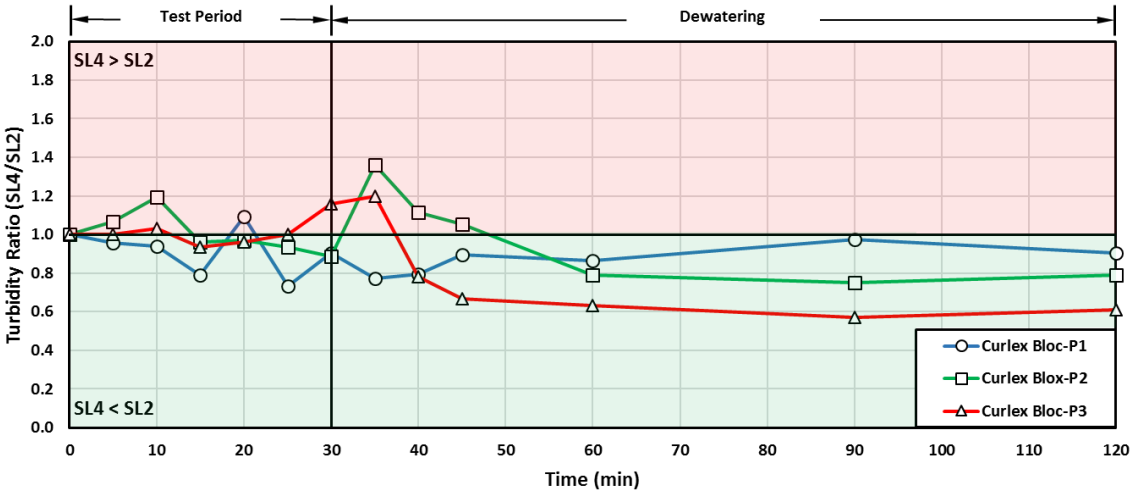

APPENDIX F

ALDOT List II-24 Modification

TEMPORARY EROSION and SEDIMENT CONTROL PRODUCTS

(for SILT FENCE see List II-3 GEOTEXTILES)

	PEB#	Product Name	Approved Manufacture	Approval Date
FLOW BAFFLES	2590	EC-7y Coir Mat	East Coast Erosion - Bernville, PA	08/01/11
	3013	Coir Mat 700 grams	Hanes Geo Components - Winston Salem, NC	01/07/13
	4590	KoirMat 700	Nedia Enterprises, Inc. - Ashburn, VA	11/07/16
TURBIDIMETERS	2599	2100Q with USB+Power Module	Hach Company - Loveland, CO	08/01/11
	4041	HI 98703	Hanna Instruments - Woonsocket, RI	05/06/13
	4473	2020we	LaMotte Company – Chestertown, MD	033/07/16
FLOCCULANT* **POWDERS**	1264	APS 700 Series Silt Stop Powder (705, 712, 730, 740)	Applied Polymer Systems - Woodstock, GA	
	1232	EnviroPam (Granular)	Innovative Turf Solutions - Cincinnati, OH	04/02/12
BLOCKS	1264	APS 700 Series Floc Log (703d, 703#d, 706b)	Applied Polymer Systems - Woodstock, GA	
SOCKS	2362/2363	StormKlear DBP-2100 FS & Gel Floc (System)	HaloSource, Inc. - Bothell, WA	08/01/11

**For use with 2012 Standard Specifications and GASP12-0399*

FLOCCULANTS**	1264	APS 700 Series	Applied Polymer Systems - Woodstock, GA	
	1232	EnviroPam (Granular)	Innovative Turf Solutions - Cincinnati, OH	04/02/12
	2907	FLOC	Innovative Turf Solutions - Cincinnati, OH	05/06/13
	4018	HaloKlear/StormKlear DBP-2100 & Gel Floc (System)	HaloSource, Inc. - Bothell, WA	05/06/13
	4549	Tigerfloc	Floc Systems, Inc. - Surrey (Province) B.C. Canada	02/06/17

***For use with GASP 12-0399(3) and 12-0575, Section 672 – Stormwater Turbidity Control.*

Basin Dewatering Devices	2996	IAS Water Quality Skimmer	Innovative Applied Solutions - Jamestown, NC	01/06/14
	4140	ESC Skimmer	Erosion Supply Company - Raleigh, NC	01/06/14
	4182	Faircloth Skimmer Surface Drain	J.W. Faircloth & Son, Inc. - Hillsborough, NC	04/07/14
	4246	Marlee Float Skimmer (#1, #2, #3)	SW FeeSaver - Greenville, SC	05/04/15

		PEB#	Product Name	Max Flow	Approved Manufacture	Installation Method	Approval Date
DITCH CHECK	WATTLES (SINGLE-20 IN.)	1397	Curlex Sediment Log	1.875 cfs	American Excelsior - Arlington, TX	ALDOT STD. DETAIL	05/03/04
		1597	Aspen Excelsior Logs	1.875 cfs	Western Excelsior - Mancos, CO	ALDOT STD. DETAIL	12/06/04
		1758	EXCEL Straw Logs	1.25 cfs	Western Excelsior - Mancos, CO	ALDOT STD. DETAIL	06/06/06
		1851	ECWattles 100% Agricultural Straw	1.25 cfs	East Coast Erosion - Bernville, PA	ALDOT STD. DETAIL	03/05/07
		1866	Wheat Straw Sediment Logs	1.25 cfs	Erosion Tech - Juliette, GA	ALDOT STD. DETAIL	06/05/07
		2114	AEC Premier Straw Wattles	1.25 cfs	American Excelsior - Arlington, TX	ALDOT STD. DETAIL	09/14/09
		2008	GeoWattle	1.25 cfs	GeoHay - Spartanburg, SC	ALDOT STD. DETAIL	11/02/09
		1994	Straw Wattle	1.25 cfs	US Erosion Control Products - Pearson, GA	ALDOT STD. DETAIL	03/03/14
	WATTLES (STACKED)	1849	Erosion Eel	1.25 cfs	Friendly Environmental - Shelbyville, TN	ALDOT STD. DETAIL	08/13/07
		1649	Filtrexx Filter Soxx	1.25 cfs	Filtrexx International – Grafton,OH	ALDOT STD. DETAIL	11/05/07
		4500	RocSoxx Gabion Soxx	1.875 cfs	RocSoxx – Defuniak Springs, FL	MANF. DETAIL	02/06/17
	SILT FENCE		Check-Pop System	1.875 cfs	C-Pop Systems	MANF. DETAIL	
	BAG TYPE		GRS VersaShield	1.875 cfs	Guardian Retention Systems	MANF. DETAIL	
	OTHER		Triangular Silt Dike	1.875 cfs	Triangular Silt Dike Company	MANF. DETAIL	
INLET	WATTLES	1397	Curlex Sediment Log		American Excelsior - Arlington, TX	ALDOT STD. DETAIL	05/03/04

	1597	Aspen Excelsior Logs	Western Excelsior - Mancos, CO	ALDOT STD. DETAIL	12/06/04
	1758	EXCEL Straw Logs	Western Excelsior - Mancos, CO	ALDOT STD. DETAIL	06/06/06
	1851	ECWattles 100% Agricultural Straw	East Coast Erosion - Bernville, PA	ALDOT STD. DETAIL	03/05/07
	1866	Wheat Straw Sediment Logs	Erosion Tech - Juliette, GA	ALDOT STD. DETAIL	06/05/07
	2114	AEC Premier Straw Wattles	American Excelsior - Arlington, TX	ALDOT STD. DETAIL	09/14/09
	2008	GeoWattle	GeoHay - Spartanburg, SC	ALDOT STD. DETAIL	11/02/09
	1994	Straw Wattle	US Erosion Control Products - Pearson, GA	ALDOT STD. DETAIL	03/03/14
WATTLES (STACKED)	1849	Erosion Eel	Friendly Environmental - Shelbyville, TN	ALDOT STD. DETAIL	08/13/07
	1649	Filtrexx Filter Soxx	Filtrexx International – Grafton,OH	ALDOT STD. DETAIL	11/05/07
	4500	RocSoxx Gabion Soxx	RocSoxx – Defuniak Springs, FL	MANF. DETAIL	02/06/17
SILT FENCE		Check-Pop System	C-Pop Systems	MANF. DETAIL	
BAG TYPE		GRS VersaShield	Guardian Retention Systems	MANF. DETAIL	
DOME TYPE	1323	SS-100A or SS-200A (w/ DOT Filter)	Silt Saver - Conyers, GA	MANF. DETAIL	02/17/03
OTHER	1905	GeoBale	GeoHay - Spartanburg, SC	MANF. DETAIL	11/02/09

PEB#	Product Name	Approved Manufacture	Installation Method	Approval Date

SEDIMENT BARRIERS	WATTLES (SINGLE)	1397	Curlex Sediment Log	American Excelsior - Arlington, TX	ALDOT STD. DETAIL	05/03/04
		1597	Aspen Excelsior Logs	Western Excelsior - Mancos, CO	ALDOT STD. DETAIL	12/06/04
		1758	EXCEL Straw Logs	Western Excelsior - Mancos, CO	ALDOT STD. DETAIL	06/06/06
		1851	ECWattles 100% Agricultural Straw	East Coast Erosion - Bernville, PA	ALDOT STD. DETAIL	03/05/07
		1866	Wheat Straw Sediment Logs	Erosion Tech - Juliette, GA	ALDOT STD. DETAIL	06/05/07
		2114	AEC Premier Straw Wattles	American Excelsior - Arlington, TX	ALDOT STD. DETAIL	09/14/09
		2008	GeoWattle	GeoHay - Spartanburg, SC	ALDOT STD. DETAIL	11/02/09
		1994	Straw Wattle	US Erosion Control Products - Pearson, GA	ALDOT STD. DETAIL	03/03/14
	WATTLES (STACKED)	1849	Erosion Eel	Friendly Environmental - Shelbyville, TN	ALDOT STD. DETAIL	08/13/07
		1649	Filtrexx Filter Soxx	Filtrexx International – Grafton,OH	ALDOT STD. DETAIL	11/05/07
		4500	RocSoxx Gabion Soxx	RocSoxx – Defuniak Springs, FL	MANF. DETAIL	02/06/17
	SILT FENCE		C-Pop	C-Pop Systems	MANF. DETAIL	
	BAG TYPE		GRS FlexiShield	Guardian Retention Systems	MANF. DETAIL	
	OTHER					